

Ivan Rodolfo Pereira Garcia de Galvão

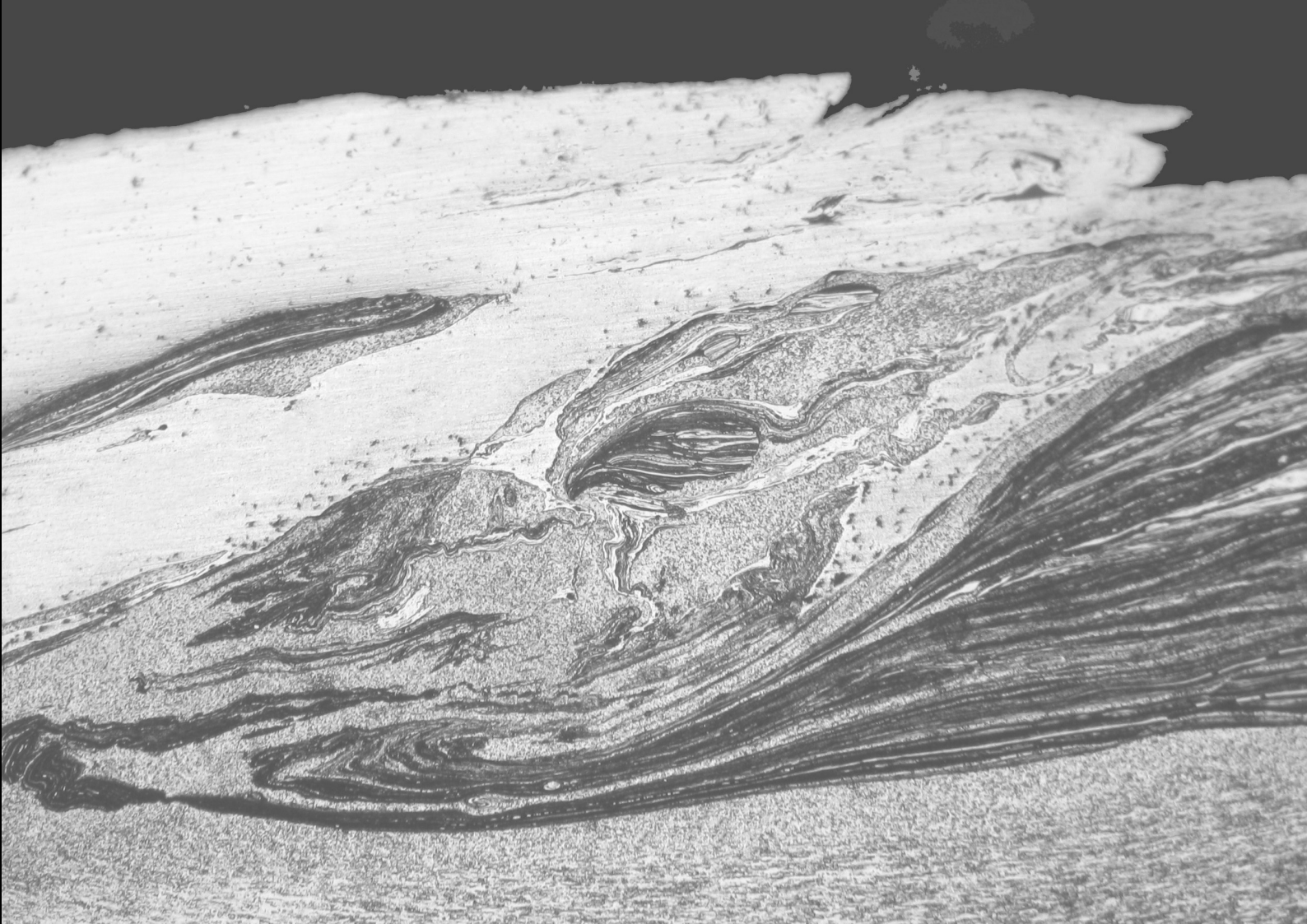
ANALYSIS OF FRICTION STIR WELDABILITY OF ALUMINIUM TO COPPER

Doctor of Philosophy Thesis in Mechanical Engineering, specialisation in Production Technology, supervised by Professor Altino de Jesus Roque Loureiro and Professor Dulce Maria Esteves Rodrigues and submitted to the Mechanical Engineering Department of the Faculty of Sciences and Technology of the University of Coimbra.

2014



UNIVERSIDADE DE COIMBRA



Ivan Rodolfo Pereira Garcia de Galvão

ANALYSIS OF FRICTION STIR WELDABILITY OF ALUMINIUM TO COPPER

Doctor of Philosophy Thesis in Mechanical Engineering, specialisation in Production Technology, supervised by Professor Altino de Jesus Roque Loureiro and Professor Dulce Maria Esteves Rodrigues and submitted to the Mechanical Engineering Department of the Faculty of Sciences and Technology of the University of Coimbra.

2014



UNIVERSIDADE DE COIMBRA

PhD studentship SFRH/BD/60545/2009

FCT Fundação para a Ciência e a Tecnologia

MINISTÉRIO DA EDUCAÇÃO E CIÊNCIA



ACKNOWLEDGEMENTS

Much more than the product of five years of research, this PhD thesis was a challenging journey of work and an unforgettable experience of learning and growth. Many people and several institutions have contributed in many ways to the success of this study, providing their support, guidance and encouragement. I would like to take the opportunity to express my sincere gratitude to all of them.

Above all, I want to thank my supervisors, Professor Altino Roque Loureiro and Professor Dulce Esteves Rodrigues, for their continuous support of my PhD research. It is difficult to overstate my gratitude to them for their valuable advices, constructive criticisms and extensive discussions around the work. Their patience, flexibility, motivation, enthusiasm and immense knowledge were crucial to the success of this journey of my personal and academic life. I am also extremely indebted to them for providing the necessary infrastructures and resources to accomplish my research work.

I would like to acknowledge the financial, academic and technical support of the research group in which this work was conducted, the *Centro de Engenharia Mecânica da Universidade de Coimbra* (CEMUC). I am deeply grateful to CEMUC's current and previous Presidents, Professor Valdemar Fernandes and Professor Luís Filipe Menezes, respectively, as well as to all the professors, researchers, students and collaborators of this research group. A special thanks to those who had a direct contribution to my PhD work.

I am also particularly indebted to the *Fundação para a Ciência e a Tecnologia* (FCT) for the financial support provided through the PhD studentship SFRH/BD/60545/2009.

My sincere gratitude to the *Instituto Superior Técnico* and to the *Centro Tecnológico AIMEN* for providing the friction stir welding equipments used in the production of the

welds studied in this work. A special thanks to the company *Thyssen Portugal - Aços e Serviços Lda.* for providing the heat treatments for the welding tools.

To the publishers, the copyright holders and the scientific journals, my acknowledgement for providing the licenses allowing the print and electronic reuse of the papers published under the scope of this research.

Lastly, I wish to thank my friends and, especially, my family. To my parents, grandparents and great-grandmother, who, unfortunately, only witnessed the initial stage of this journey, my heartfelt acknowledgement for their unconditional support, encouragement and presence.

ACRONYMS AND SYMBOLS

Al - Aluminium

Al-Al - Aluminium-Aluminium

Al/Cu - Aluminium/Copper (interfacial and transition zones)

Al-Cu - Aluminium-Copper

Al-Fe - Aluminium-Steel

Al-Ti - Aluminium-Titanium

BM - Base Material

CEMUC - Centro de Engenharia Mecânica da Universidade de Coimbra

Cu - Copper

Cu-Cu - Copper-Copper

Copper-DHP - Deoxidised High-Phosphorous Copper

EBSD - Electron Backscatter Diffraction

EHF - Effective Heat of Formation

FCT - Fundação para a Ciência e a Tecnologia

FSP - Friction Stir Processing

FSW - Friction Stir Welding

HAZ - Heat-Affected Zone

NR - Non-Referred

NT - Non-Tested

O-free - Oxygen-free

TEM - Transmission Electron Microscopy

TMAZ - Thermomechanically-Affected Zone

TWI - The Welding Institute

v - Traverse Speed

ω - Rotation Speed

ω/v - Rotation to Traverse Speed Ratio

ω^2/v - Rotation's Square to Traverse Speed Ratio

ABSTRACT

Friction stir welding (FSW) is a solid-state welding technology with increased potential for joining dissimilar materials with strong differences in physical and mechanical properties, as well as high chemical affinity, such as aluminium and copper (Al-Cu). Nevertheless, although Al-Cu FSW has high scientific, technical and economic interest, very scarce research had been conducted in this field until a few years ago, and so, most of the core issues on Al-Cu friction stir weldability remained largely unexplored. This way, current work, conducted from September 2009 to June 2014, in the *Centro de Engenharia Mecânica da Universidade de Coimbra*, had the purpose of analysing the friction stir weldability of aluminium to copper. Large number of Al-Cu butt and lap welds, produced using a wide range of welding conditions and three distinct base materials (AA 5083-H111 and AA 6082-T6 aluminium alloys and deoxidised high phosphorous copper), were subjected to a broad spectrum of experimental analyses, aiming their structural, morphological and mechanical characterisation.

The characterisation of the material flow mechanisms occurring during welding evidenced that both the base materials mixing and the material deposition, at the rear of the tool, are strongly influenced by the shoulder geometry and the relative positioning of the base material plates, seriously impacting on the structure and morphology of the welds. From the study of the intermetallic phases' formation and distribution, it was found that the formation of the intermetallic phases is governed by a thermomechanically induced solid-state diffusion phenomenon occurring inside the shoulder and pin-governed mixing volumes. The structural and morphological characterisation of the welds revealed that the morphology and the intermetallic content of the weld surface, which was concluded to be the key factor affecting the surface finishing of the welds, are strongly dependent on the shoulder geometry, but insensitive to the tool rotation and traverse speeds. On the other hand, the morphology and the intermetallic content of the weld nugget were found to be strongly influenced by both the shoulder geometry and the tool rotation and traverse speeds. Moreover, the study of the spindle torque evolution in Al-Cu FSW revealed that this physical quantity is highly

sensitive to the formation of intermetallic phases and to the volume of material dragged by the tool at each revolution. However, the impact of each factor on the spindle torque was found to depend on the relative positioning of the base material plates.

The analysis of the effect of the tool offset towards the aluminium alloy side on the structural, morphological and mechanical properties of the welds evidenced that this strategy significantly reduces base materials mixing, providing the production of welds with lower intermetallic content, both at the surface and nugget. So, tool offset revealed to be very suitable to achieve excellent surface finished Al-Cu welds. Nevertheless, it was not found to be effective to improve Al-Cu friction stir weldability, since welds with desirable strength were not achieved. A strong influence of the aluminium alloy type on Al-Cu friction stir weldability was also observed in current work. Important differences in the structural, morphological and mechanical properties of AA 5083/copper and AA 6082/copper friction stir welds, produced under similar conditions, were noticed. The mechanical behaviour of the aluminium alloys, under the extreme conditions of temperature and plastic deformation occurring during welding, was found to have strong influence on the welding results. Additionally, an impressive hardness increase was noticed in the nugget of the AA 5083/copper welds, which was inferred to result from the formation of a nano-structured aluminium region in this zone.

Keywords: Friction stir weldability; Aluminium; Copper; Intermetallic phases.

RESUMO

Friction stir welding (FSW) é uma tecnologia de soldadura no estado sólido com grande potencial para realizar ligações heterogêneas entre materiais com propriedades físicas e mecânicas muito distintas e com elevada afinidade química, sendo exemplo a ligação de alumínio a cobre (Al-Cu). Não obstante o elevado interesse científico, económico e técnico da ligação Al-Cu por FSW, a investigação nesta área, até há alguns anos, era praticamente inexistente, pelo que a maioria das questões relacionadas com a soldabilidade de ambos os metais por esta técnica permanecia quase totalmente inexplorada. Neste sentido, o presente trabalho, desenvolvido entre Setembro de 2009 e Junho de 2014, no Centro de Engenharia Mecânica da Universidade de Coimbra, teve como principal objectivo analisar a soldabilidade do alumínio ao cobre por FSW. Um número substancial de soldaduras Al-Cu, produzidas em juntas de topo e sobreposta, usando uma larga gama de condições de soldadura e três materiais base distintos (ligas de alumínio AA 5083-H111 e AA 6082-T6 e cobre desoxidado com elevado teor em fósforo), foi submetido a um amplo espectro de análises experimentais, por forma a caracterizar as suas propriedades estruturais, morfológicas e mecânicas.

A caracterização dos mecanismos de fluxo do material durante a soldadura evidenciou que a mistura dos materiais base, assim como a deposição do material na parte de trás da ferramenta, na sequência do seu movimento de translação, são fortemente influenciados pela geometria da base da ferramenta e pelo posicionamento relativo dos materiais base, tendo forte impacto na estrutura e morfologia das soldaduras. Ao estudar-se a formação e distribuição das fases intermetálicas nas soldaduras, inferiu-se que a sua formação é resultado de um fenómeno de difusão no estado sólido, induzido térmica e mecanicamente, que ocorre nos volumes de mistura gerados pela acção da base e do pino da ferramenta. A caracterização estrutural e morfológica das soldaduras revelou ainda que tanto a morfologia como o conteúdo intermetálico das superfícies de soldadura, factor com influência preponderante no seu acabamento superficial, são fortemente dependentes da geometria da base da ferramenta, mas independentes das suas velocidades de rotação e de avanço. Por outro

lado, a morfologia e o conteúdo intermetálico do *nugget* mostraram ser dependentes quer da geometria da ferramenta, quer das velocidades de rotação e de avanço. Adicionalmente, o estudo da evolução do binário imposto na ferramenta, durante o processo de soldadura, revelou que esta grandeza física é sensível à formação de fases intermetálicas, bem como ao volume de material arrastado pela ferramenta em cada rotação. Todavia, verificou-se que o impacto de cada factor no binário registado durante o processo depende do posicionamento relativo dos materiais base.

Ao analisar-se o efeito do desvio da ferramenta, relativamente à linha de interface dos materiais a ligar, para o lado da liga de alumínio, nas propriedades estruturais, morfológicas e mecânicas das soldaduras, verificou-se que esta estratégia proporciona uma redução significativa da mistura dos materiais base, levando à produção de soldaduras com menor conteúdo intermetálico, tanto à superfície como no *nugget*. Assim, concluiu-se que o desvio da ferramenta é uma estratégia de grande eficácia na obtenção de soldaduras Al-Cu com excelente acabamento superficial. Porém, não apresenta qualquer mais-valia no que respeita à melhoria da soldabilidade Al-Cu por FSW, uma vez que origina soldaduras com resistência mecânica insuficiente. O estudo permitiu ainda verificar que o tipo de liga de alumínio tem forte influência na soldabilidade Al-Cu por FSW. Efectivamente, soldaduras AA 5083/cobre e AA 6082/cobre, produzidas sob as mesmas condições de soldadura, apresentaram propriedades estruturais, morfológicas e mecânicas bastante distintas. Concluiu-se, assim, que o comportamento mecânico das ligas de alumínio, sob as extremas condições de temperatura e deformação plástica experienciadas durante a operação de soldadura, tem grande influência nos resultados finais obtidos. É ainda de realçar que um aumento de dureza assinalável foi observado no *nugget* das soldaduras AA 5083/cobre, sendo resultado da formação de uma região de alumínio nanoestruturada nesta zona.

Palavras-chave: Soldabilidade por FSW; Alumínio; Cobre; Fases intermetálicas.

CONTENTS	pp.
1 - INTRODUCTION.....	19
2 - INVESTIGATION OVERVIEW.....	23
2.1 - MATERIAL FLOW IN HETEROGENEOUS FRICTION STIR WELDING OF ALUMINIUM AND COPPER THIN SHEETS.....	24
2.2 - FORMATION AND DISTRIBUTION OF BRITTLE STRUCTURES IN FRICTION STIR WELDING OF ALUMINIUM AND COPPER: INFLUENCE OF PROCESS PARAMETERS.....	28
2.3 - FORMATION AND DISTRIBUTION OF BRITTLE STRUCTURES IN FRICTION STIR WELDING OF ALUMINIUM AND COPPER: INFLUENCE OF SHOULDER GEOMETRY.....	32
2.4 - STUDY OF THE WELDING CONDITIONS DURING SIMILAR AND DISSIMILAR ALUMINIUM AND COPPER WELDING BASED ON TORQUE SENSITIVITY ANALYSIS.....	36
2.5 - INFLUENCE OF TOOL OFFSETTING ON THE STRUCTURE AND MORPHOLOGY OF DISSIMILAR ALUMINIUM TO COPPER FRICTION-STIR WELDS.....	40
2.6 - INFLUENCE OF ALUMINIUM ALLOY TYPE ON DISSIMILAR FRICTION STIR LAP WELDING OF ALUMINIUM TO COPPER.....	44
3 - SCIENTIFIC EVIDENCE ON ALUMINIUM-TO-COPPER FRICTION STIR WELDING.....	49
3.1 - WELD MACROSTRUCTURE.....	49

3.1.1 - Tool rotation and traverse speeds.....	49
3.1.2 - Base Materials Positioning.....	53
3.1.3 - Tool Offset.....	56
3.1.4 - Tool Geometry.....	58
3.1.5 - Base Materials.....	59
<i>Overall remarks on weld macrostructure.....</i>	<i>60</i>
3.2 - WELD DEFECTS.....	61
<i>Overall remarks on weld defects.....</i>	<i>64</i>
3.3 - WELDING CONDITIONS' PHYSICAL INDICATORS.....	64
3.3.1 - Welding Temperature.....	64
3.3.2 - Welding Torque.....	67
<i>Overall remarks on welding conditions' physical indicators.....</i>	<i>68</i>
3.4 - WELD MICROSTRUCTURE.....	68
3.4.1 - Weld Microstructural Zones.....	68
3.4.2 - Al-Cu Interaction Patterns.....	69
3.4.3 - Al/Cu Interface.....	75
<i>Overall remarks on weld microstructure.....</i>	<i>77</i>
3.5 - ALUMINIUM-COPPER PHASES' FORMATION PHENOMENON	77
3.5.1 - Al-Cu Phase System.....	77
3.5.2 - Intermetallic Phases' Formation Mechanisms in Al-Cu FSW.....	79
3.5.3 - Weld's Intermetallic Content and Phases' Kinetics of Growth...	81
<i>Overall remarks on aluminium-copper phases' formation phenomenon.....</i>	<i>84</i>
3.6 - WELD HARDNESS.....	84
<i>Overall remarks on weld hardness.....</i>	<i>87</i>

3.7 - WELD MECHANICAL STRENGTH AND DUCTILITY.....	87
<i>Overall remarks on weld mechanical strength and ductility.....</i>	<i>90</i>
4 - INVESTIGATION OUTPUTS AND FUTURE RESEARCH.....	91
4.1 - INVESTIGATION OUTPUTS.....	91
4.2 - FUTURE RESEARCH.....	94

REFERENCES

ANNEXES

- ANNEX I** - Galvão, I.; Leal, R. M.; Loureiro, A.; Rodrigues, D. M. Material flow in heterogeneous friction stir welding of aluminium and copper thin sheets. *Sci. Technol. Weld. Joining* **2010**, *15* (8), 654–660.
- ANNEX II** - Galvão, I.; Oliveira, J. C.; Loureiro, A.; Rodrigues, D. M. Formation and distribution of brittle structures in friction stir welding of aluminium and copper: influence of process parameters. *Sci. Technol. Weld. Joining* **2011**, *16* (8), 681–689.
- ANNEX III** - Galvão, I.; Oliveira, J. C.; Loureiro, A.; Rodrigues, D. M. Formation and distribution of brittle structures in friction stir welding of aluminium and copper: Influence of shoulder geometry. *Intermetallics* **2012a**, *22*, 122–128.
- ANNEX IV** - Galvão, I.; Leitão, C.; Loureiro, A.; Rodrigues, D. M. Study of the welding conditions during similar and dissimilar aluminium and copper welding based on torque sensitivity analysis. *Mater. Des.* **2012b**, *42*, 259–264.
- ANNEX V** - Galvão, I.; Loureiro, A.; Verdera, D.; Gesto, D.; Rodrigues, D. M. Influence of tool offsetting on

the structure and morphology of dissimilar aluminum to copper friction-stir welds. *Metall. Mater. Trans. A* **2012c**, *43* (13), 5096–5105.

ANNEX VI - Galvão, I.; Verdera, D.; Gesto, D.; Loureiro, A.; Rodrigues, D. M. Influence of aluminium alloy type on dissimilar friction stir lap welding of aluminium to copper. *J. Mater. Process. Technol.* **2013**, *213* (11), 1920–1928.

FIGURES	pp.
Figure 1 - Influence of shoulder geometry (a, b) and base materials positioning (c, d) on the material flow mechanisms during Al-Cu FSW (adapted from Galvão et al., 2010).....	27
Figure 2 - Influence of rotation and traverse speeds on the formation and distribution of intermetallic phases in the surface (a, b) and nugget (c, d) of Al-Cu friction stir welds (adapted from Galvão et al., 2011).....	31
Figure 3 - Influence of the shoulder geometry on the formation and distribution of intermetallic phases in the surface (a, b) and nugget (c, d) of Al-Cu friction stir welds (adapted from Galvão et al., 2012a).....	35
Figure 4 - Average (a) and instantaneous (b) torque evolution in Al-Al, Cu-Cu and Al-Cu FSW (adapted from Galvão et al., 2012b).....	39
Figure 5 - Influence of tool offset on the structural/morphological (a, b, c) and mechanical (d, e, f) properties of Al-Cu friction stir welds (adapted from Galvão et al., 2012c).....	43
Figure 6 - Influence of the aluminium alloy type on the structural/morphological properties of the surface (a, b) and nugget (c, d) of Al-Cu friction stir lap welds (adapted from Galvão et al., 2013).....	47
Figure 7 - Internal discontinuities formed in AA 6061/copper friction stir lap welds (adapted from Firouzdor and Kou, 2012).....	61
Figure 8 - Cracking in AA 5083/copper friction stir butt welds (adapted from Galvão et al., 2011).....	62

Figure 9 - Poor surface finishing in AA 6082/copper friction stir butt welding (adapted from Galvão et al., 2012c).....	62
Figure 10 - Lamellar intercalated structure formed in the nugget of AA 6061-T6/copper friction stir welds (adapted from Murr et al., 1998b).....	71
Figure 11 - Homogeneous mixture formed in the nugget of AA 5083/copper friction stir welds (adapted from Galvão et al., 2012a).....	72
Figure 12 - Composite-like structure formed in the nugget of AA 1060/copper friction stir welds (adapted from Xue et al., 2010).....	73
Figure 13 - Intermetallic phases distribution over the nugget of AA 6061/pure copper friction stir welds (adapted from Ouyang et al., 2006).....	73
Figure 14 - Base materials interface. (a) Single intermetallic layer-type microstructure noticed in AA 1060/pure copper friction stir welds (adapted from Xue et al., 2010). (b) Multiple layers-type microstructure noticed in AA 6082/copper-DHP friction stir welds (adapted from Galvão et al., 2012c).....	76
Figure 15 - Al-Cu phase diagram (adapted from Kouters et al., 2013).....	78

TABLES	pp.
Table 1 - Papers published, under the scope of current work, in <i>Science Citation Index</i> journals.....	23
Table 2 - Studies addressing the effect of the rotation speed on Al-Cu weld macrostructure.....	51
Table 3 - Studies addressing the effect of the traverse speed on Al-Cu weld macrostructure.....	52
Table 4 - Studies addressing the effect of the rotation to traverse speeds ratio on Al-Cu weld macrostructure.....	53
Table 5 - Studies addressing the effect of the base materials positioning on Al-Cu butt weld macrostructure.....	55
Table 6 - Study addressing the effect of the base materials positioning on Al-Cu lap weld macrostructure.....	55
Table 7 - Studies addressing the effect of tool offset on Al-Cu butt weld macrostructure.....	58
Table 8 - Studies addressing the effect of the tool geometry on Al-Cu weld macrostructure.....	59
Table 9 - Study addressing the effect of the base materials on Al-Cu weld macrostructure.....	60
Table 10 - Literature-based overview of the most reported defects in Al-Cu FSW and the causes promoting their formation.....	63
Table 11 - Welding temperature reported in Al-Cu FSW literature.....	66
Table 12 - Study addressing the welding conditions in Al-Cu FSW by torque sensitivity analysis.....	67

Table 13 -	Nugget interaction features noticed in Al-Cu FSW literature.....	74
Table 14 -	Microstructural properties of base materials interface reported in Al-Cu FSW literature.....	76
Table 15 -	Effective heat of formation of the Al-Cu equilibrium phases.....	79
Table 16 -	Studies addressing intermetallic phases' formation phenomenon in Al-Cu FSW.....	81
Table 17 -	Studies addressing phases' kinetics of growth in Al-Cu FSW.....	83
Table 18 -	TMAZ hardness peaks in Al-Cu FSW literature.....	86
Table 19 -	Literature-based overview of tensile and bending testing in Al-Cu FSW.....	89

1 - INTRODUCTION

Friction stir welding (FSW) was developed by *The Welding Institute* (TWI), at the beginning of the 90's, with the main aim of joining thick aluminium plates. Over the years, as a consequence of its proven capabilities in aluminium welding, the field of application of this process has widened expressively, comprising many other materials and materials combinations, for a large range of thicknesses and varied joint geometries (Nandan et al., 2008; Çam, 2011). Effectively, being a solid-state technology, FSW has high potential to be used in similar welding of several materials hardly weldable by the traditional fusion welding processes as well as in dissimilar joining of materials with strong differences in physical/mechanical properties and high chemical affinity. Specifically, dissimilar welding of these materials became a subject of intense research at both the academic and industrial level (DebRoy and Bhadeshia, 2010).

The aluminium to copper (Al-Cu) dissimilar joining system, in particular, has great interest to many industrial sectors, such as power generation, electronics and transportation, where it is expected that enables to develop new engineering solutions combining the improved mechanical, thermal and electrical properties of the copper with the low specific weight and cost of the aluminium. In addition to its industrial interest, the Al-Cu system has also important research interest. Actually, some of the main concerns regarding the Al-Cu weldability in FSW are common to other dissimilar materials systems, such as the Al-Ti (aluminium-titanium) and the Al-Fe (aluminium-steel). In this way, research in Al-Cu FSW is expected to provide not only global knowledge on dissimilar materials friction stir weldability, but also some general guidelines for dissimilar materials FSW, helpful to the development of optimised techniques for harder materials joining. In fact, since Al-Cu FSW does not require the use, for research purposes, of the very expensive high-strength tool materials necessary to weld harder materials systems, performing a wide range of experimentations, encompassing a large range of tool geometries and/or joint configurations, for example, becomes economically much more affordable.

Despite the above mentioned scientific, technical and economic interest of Al-Cu FSW, the investigation in this field remained almost unexplored until a few years ago. In fact, prior to 2009, investigation on Al-Cu joining by FSW was restricted to a very small number of published works, which essentially highlighted the extreme difficulty in obtaining welds free of defects as well as the extensive formation of brittle intermetallic phases during welding (Murr et al., 1998a, 1998b; Okamura and Aota, 2004; Ouyang et al., 2006; Abdollah-zadeh et al., 2008; Liu et al., 2008). Most of the core issues on Al-Cu friction stir weldability remained only incipiently characterised. A detailed and comprehensive investigation on the material flow mechanisms, the phenomena governing the formation and distribution of intermetallic phases during Al-Cu FSW, their relations with the welding parameters and their impact on the morphological, structural and mechanical properties of the welds, was absolutely required.

In this context, current investigation, conducted from September 2009 to June 2014, in the *Centro de Engenharia Mecânica da Universidade de Coimbra* (Coimbra, Portugal), had the global objective of analysing the friction stir weldability of aluminium to copper. In order to reach the research global aim, the following specific objectives were defined: To characterise the material flow mechanisms occurring during Al-Cu FSW, emphasising their relations with two particular welding variables, the relative positioning of the base material plates and the shoulder geometry; To study the influence of the rotation (ω) and traverse (v) speeds on the formation and distribution of intermetallic phases during Al-Cu FSW as well as their impact on the morphological and structural properties of the welds; To study the influence of the shoulder geometry on the formation and distribution of intermetallic phases during Al-Cu FSW as well as their impact on the morphological and structural properties of the welds; To characterise by torque-sensitivity analysis the thermomechanical conditions experienced inside the stirring volume in Al-Cu FSW, emphasising their relations with the rotation and traverse speeds, base materials properties and relative positioning of the dissimilar plates; To analyse the influence of the tool offset on the morphological, structural and mechanical properties of Al-Cu friction stir welds; To analyse the influence of the aluminium alloy type on the morphological, structural and mechanical properties of Al-Cu friction stir welds.

A deep experimental study of large number of Al-Cu friction stir butt and lap welds, produced using a wide range of welding conditions, was conducted by

performing a broad spectrum of experimental analyses and tests. The welds were carried out at the *Instituto Superior Técnico* (Lisbon, Portugal) and the *Centro Tecnológico AIMEN* (O Porriño, Spain), using three distinct base materials - non-heat-treatable AA 5083-H111 and heat-treatable AA 6082-T6 aluminium alloys plates and deoxidised high-phosphorous copper (copper-DHP) plates.

The research conducted in this work enabled the publication of six papers in high impact *Science Citation Index* journals (Galvão et al., 2010, 2011, 2012a, 2012b, 2012c, 2013). Each paper reports a particular stage of the overall investigation, addressing one of the specific objectives of the global research. All the papers published under the scope of current investigation are presented in Annexes I to VI. In order to include the published versions of the papers in the work, licenses for papers print and electronic reuse were provided by the publishers, copyright holders and journals.

The work is divided into three parts. A global overview on the research is presented in the first part, entitled *Investigation Overview*. This section is aimed to integrate all the stages of the investigation, individually presented in the published papers, highlighting the coherence and the relevance of the research project as a whole. The motivations, the most representative results and the main conclusions reached in the different stages of the research are reported in this section. The second part illustrates the *Scientific Evidence on Aluminium-to-Copper Friction Stir Welding*. This section, where a global literature review was conducted, has the purpose of presenting the state-of-the-art of Al-Cu joining by FSW, highlighting the original contribution of this study to the current knowledge. The pioneer character of some findings reached in this work was stressed by providing a chronological perspective of the evolution in Al-Cu FSW research. Finally, the main conclusions drawn from the global research problem as well as directions for future investigation on Al-Cu friction stir weldability are reported in *Investigation Outputs and Future Research*.

2 - INVESTIGATION OVERVIEW

In order to achieve the global aim of the work, partial research stages, with specific objectives, were developed, which resulted in the publication of six papers in high impact *Science Citation Index* journals, as displayed in **Table 1**. This section provides a brief description of the investigations presented in the papers published under the scope of current work, highlighting the relevance of the study as a whole. So, the motivations on the basis of each research stage as well as its most relevant results and conclusions are reported in six distinct items. The scientific background, the laboratorial procedures, detailed interpretations of the experimental results and their discussion, in light of the knowledge available in literature, when the researches were conducted, can be found in the papers (Annexes I to VI).

Table 1 - Papers published, under the scope of current work, in *Science Citation Index* journals.

Authors	Title	Journal	Year	Annex
Galvão et al.	Material flow in heterogeneous friction stir welding of aluminium and copper thin sheets.	<i>Sci. Technol. Weld. Joi.</i>	2010	I
Galvão et al.	Formation and distribution of brittle structures in friction stir welding of aluminium and copper: Influence of process parameters.	<i>Sci. Technol. Weld. Joi.</i>	2011	II
Galvão et al.	Formation and distribution of brittle structures in friction stir welding of aluminium and copper: Influence of shoulder geometry.	<i>Intermetallics</i>	2012a	III
Galvão et al.	Study of the welding conditions during similar and dissimilar aluminium and copper welding based on torque sensitivity analysis.	<i>Mater. Des.</i>	2012b	IV
Galvão et al.	Influence of tool offsetting on the structure and morphology of dissimilar aluminium to copper friction-stir welds.	<i>Metall. Mater. Trans. A</i>	2012c	V
Galvão et al.	Influence of aluminium alloy type on dissimilar friction stir lap welding of aluminium to copper.	<i>J. Mater. Process. Technol.</i>	2013	VI

2.1 - MATERIAL FLOW IN HETEROGENEOUS FRICTION STIR WELDING OF ALUMINIUM AND COPPER THIN SHEETS

Material flow is a core issue in FSW, determining the whole properties of the welds. Although important research on material flow in FSW of aluminium and its alloys has been conducted since the very initial stage of process's development (Reynolds, 2000, 2008; Guerra et al., 2002; Krishnan, 2002; Schneider et al., 2006; Arbegast, 2008), the flow mechanisms in FSW of dissimilar materials with strong differences in physical and mechanical properties as well as high chemical affinity, such as aluminium and copper, were totally unexplored when current work was launched. So, the first stage of the investigation, reported in Galvão et al. (2010) (Annex I), was aimed to characterise the material flow mechanisms during friction stir butt welding of 1 mm-thick plates of AA 5083-H111 to copper-DHP. The influence of two welding variables, i.e. the relative positioning of the base material plates and the shoulder geometry, on the flow mechanisms, and consequently, on the final structure and morphology of the welds, was investigated. Some representative results as well as an overview of the main conclusions reached in this study are displayed in **Figure 1**.

Two distinct shoulder designs, conducting to different material stirring and dragging actions during welding (Leal et al., 2008), were used in this investigation. The shoulder geometries were conventional conical and scrolled. The conjugated analysis of horizontal and transverse cross-sections of the welds, as well as their surface finishing, enabled to observe that, although the main flow principles were independent of the shoulder geometry, the amount of material dragged by the tool and the periodicity of material deposition at its trailing side were heavily influenced by the shoulder design, which seriously impacted on the final structure and morphology of the welds. In fact, whereas the dragging action of the scrolled tool was found to extend deep through the thickness of the plates, encompassing the full tool perimeter, the dragging action of the conical shoulder was restricted to the top of the sheets, at the back of the tool. As a result of this, the scrolled tool enabled the incorporation of significantly larger amounts of material, specially the retreating side material, into the shear layer surrounding the pin, where both base metals were mixed by intense plastic deformation. Moreover, the helical flutes of the shoulder forced the material flow downward around the pin, promoting through-thickness material mixing and periodic material deposition at the

rear of the tool. As illustrated in **Figure 1a**, improved surface finishing and homogeneous intermetallic structures, distributed throughout the thickness of the nugget, were noticed in the welds produced with this tool. Unlike to this, for the welds produced with the conical tool, base materials mixing occurred exclusively in the upper half of the plates' thickness, as shown in **Figure 1b**. Effectively, in these welds, an intermetallic-rich bulk was found to form around the tool, from which part adhered to the tool, avoiding material mixing through the entire plates' thickness, and the other part was expelled after some revolutions over the surface of the joints. So, instead of the improved surface finishing and homogeneous materials mixing throughout nugget's thickness, noticed for the joints produced with the scrolled tool, rough surfaces, composed of irregularly distributed material, and intermetallic-rich structures located exclusively at the upper part of the nugget were observed for the welds produced with the conical shoulder (**Figure 1b**).

As referred above, beyond the study of the influence of the shoulder geometry on material flow during welding, and consequently, on the final welding results, the influence of the relative positioning of the base material plates was also investigated. This analysis was restricted to the welds produced with the conical tool. The structure and morphology of welds carried out with the aluminium and copper alloys sequentially positioned at the advancing side of the joint were interpreted in light of the flow mechanisms occurring during the process. As illustrated in **Figures 1c and 1d**, substantial differences in the way both metals interact under the action of the welding tool were identified between the welds produced with reverse plates' positioning. In fact, whereas strong Al-Cu interaction was found to occur during welding with the copper plate positioned at the advancing side of the joint (**Figure 1c**), resulting in extensive formation of intermetallic-rich structures in the welds, significant material expulsion from the joint and incipient Al-Cu mixing occurred during welding with the reverse positioning of the plates, promoting the formation of joints with very irregular morphology, important thinning and massive aluminium flash (**Figure 1d**).

The analysis of the flow mechanisms imposed by the conical shoulder enabled to conclude that base materials interaction was avoided in the welds produced with the aluminium alloy at the advancing side. Actually, the harder copper, which was dragged by the shoulder from the retreating to the advancing side of the joint, at the trailing side of the tool, expelled the softer aluminium from the shoulder influence zone. On the other hand, for the welds produced with the reverse positioning of the plates, the very

soft aluminium alloy, which was not able to expel the copper from the under shoulder area, remained constrained inside the conical shaped cavity of the shoulder, flowing downward in the vicinity of the pin and being mixed with copper under the rotating action of the tool. It should be noted that, although strong Al-Cu interaction occurring during welding with copper at the advancing side resulted in welds with rough surface finishing and extensive intermetallic-rich structures in the nugget, much less proper welding conditions were achieved by reversing the positioning of the base material plates (**Figures 1c and 1d**).



Figure 1 - Influence of shoulder geometry (a, b) and base materials positioning (c, d) on the material flow mechanisms during Al-Cu FSW (adapted from Galvão et al., 2010).

2.2 - FORMATION AND DISTRIBUTION OF BRITTLE STRUCTURES IN FRICTION STIR WELDING OF ALUMINIUM AND COPPER: INFLUENCE OF PROCESS PARAMETERS

Excluding the welds produced with the aluminium alloy positioned at the advancing side of the tool, strong base materials mixing was noticed for all the remaining conditions studied in Galvão et al. (2010), which resulted in extensive formation of intermetallic phases in the welds. The following stages of the investigation, which are reported in Galvão et al. (2011) (Annex II) and Galvão et al. (2012a) (Annex III), were aimed to study the formation and distribution of intermetallic phases during Al-Cu FSW, as well as their repercussions on the structural and morphological properties of the welds. Current item is devoted to the research presented in Galvão et al. (2011), which was restricted to 1 mm-thick AA 5083-H111/copper-DHP butt welding with the conventional conical tool. The influence of the tool rotation and traverse speeds on the intermetallic content of the welds was particularly emphasised in this research. Some of its representative results as well as an overview of its main conclusions are displayed in **Figure 2**.

Welds produced under three distinct welding conditions, which were achieved by varying the rotation and traverse speeds of the tool, were studied. From the analysis of the welding results, which were interpreted in light of the rotation to traverse speed ratio (ω/v), a parameter extensively used in literature to infer the heat-input conditions during FSW (Seidel and Reynolds, 2001; Peel et al., 2006; Nandan et al., 2008), it was observed that, independently of the welding conditions, a rough layer of irregularly distributed material composed the surface of all welds. In fact, as displayed in **Figure 2a**, areas with significant accumulation of material and zones with severe material absence were identified all over the surface of the welds. The strong intermetallic content of the top layers, which, as illustrated in **Figure 2b**, were composed of a matrix very rich in Al and CuAl_2 , with few fine Cu and Cu_9Al_4 particles scattered over it, was found to be the main factor promoting welds poor surface finishing.

Similar to the analysis conducted in the weld surface, a detailed study of the nugget was carried out. However, unlike to that observed for the top layers, significant differences were noticed in nugget morphology and intermetallic content by varying the rotation and traverse speeds, as shown in **Figures 2c and 2d**. Although Al-Cu

intermetallic features were formed in the nugget under all welding conditions, base materials interaction patterns with larger dimension, higher intermetallic content and increased homogeneity, both in morphology and phase content, were found to be formed for increasing values of ω/v ratio, i.e. under increased heat-input and stronger mixing. In fact, whereas the formation of intermetallic features was restricted to the base materials interface in the welds produced under lower ω/v , larger and intermetallic-rich mixing structures, consisting of Al, Cu, CuAl_2 and Cu_9Al_4 , were formed by increasing the ω/v ratio (**Figure 2c**). In turn, these patterns were found to evolve to intermetallic structures exclusively composed of Cu_9Al_4 and Cu(Al) solid-solution by further increasing the heat-input and material mixing (**Figure 2d**).

In order to understand the different intermetallic content of the weld surface and nugget, as well as their distinct evolutions with the rotation and traverse speeds, the phenomenon governing intermetallic phases' formation and its relation with the material flow mechanisms imposed by the tool were studied. As the formation temperature of the Cu_9Al_4 intermetallic phase by solidification is much higher than the temperatures usually noticed in Al-Cu FSW (ASM International, 1992; Ouyang et al., 2006; Savolainen et al, 2006) and no solidified structures were identified over both the Cu_9Al_4 and CuAl_2 -rich layers of the welds, a thermomechanically induced solid-state diffusion phenomenon, promoting the formation of CuAl_2 and Cu_9Al_4 (and Cu(Al) solid-solution) in aluminium-richer and copper-richer mixing volumes, respectively, was pointed to be the mechanism governing Al-Cu phases generation during welding. The extensive formation of both intermetallic phases at the fairly low temperatures usually reached during FSW was explained by enhanced interatomic diffusion under extremely intense plastic deformation. Specifically, a close relation between the amounts of Cu_9Al_4 intermetallic phase and Cu(Al) solid-solution was found to exist (fitting analysis of the X-ray diffraction patterns), which further supported the formation of this phase by mechanical integration of aluminium in copper.

In Al-Cu FSW with conical tools, the flow mechanisms imposed by the shoulder at the surface of the welds, which, as discussed in Galvão et al. (2010), consist of dragging large amounts of aluminium from the retreating to the advancing side of the joint, provide the formation of an aluminium-rich mixing volume inside the conical shaped cavity of the tool, independently of the welding conditions. As referred above, the solid-state diffusion phenomenon, activated by the coupled action of temperature and plastic deformation, promote extensive formation of CuAl_2 layers in this region,

which are irregularly distributed at the trailing side of the tool during welding, giving rise to the poor surface finishing noticed for all the welds.

As opposed to that occurring at the surface of the welds, in the shear layer surrounding the pin, significant amounts of copper dragged by the pin from the advancing side are mixed with some aluminium or aluminium-rich material, which is forced to flow downwards from the conical cavity into this layer. This mechanism, which is also discussed in detail in Galvão et al. (2010), promotes the formation of a copper-rich mixing volume, where proper conditions for Cu_9Al_4 (and $\text{Cu}(\text{Al})$ solid-solution) formation exist. Actually, beyond the copper-rich content of the shear layer, the increased temperature and plastic deformation reached in this zone also favour the formation of Cu_9Al_4 , whose nucleation is less favourable from a thermodynamic-kinetic viewpoint than CuAl_2 (Guo et al., 2011). The occurrence of chemical and thermomechanical conditions favouring the formation of Cu_9Al_4 at the shear layer around the pin explains the larger amounts of this phase being detected in the nugget than in the surface of the welds. Moreover, for increasing values of ω/v , increasing amounts of copper as well as aluminium and aluminium-rich material are incorporated into the copper-rich mixing volume of the shear layer, where, as a result of the higher heat-input conditions and increased plastic deformation, larger amounts of Cu_9Al_4 are formed. In fact, the stronger the mixing around the pin the larger is the formation of copper-rich phases through the consumption of copper, aluminium and aluminium-rich phases.

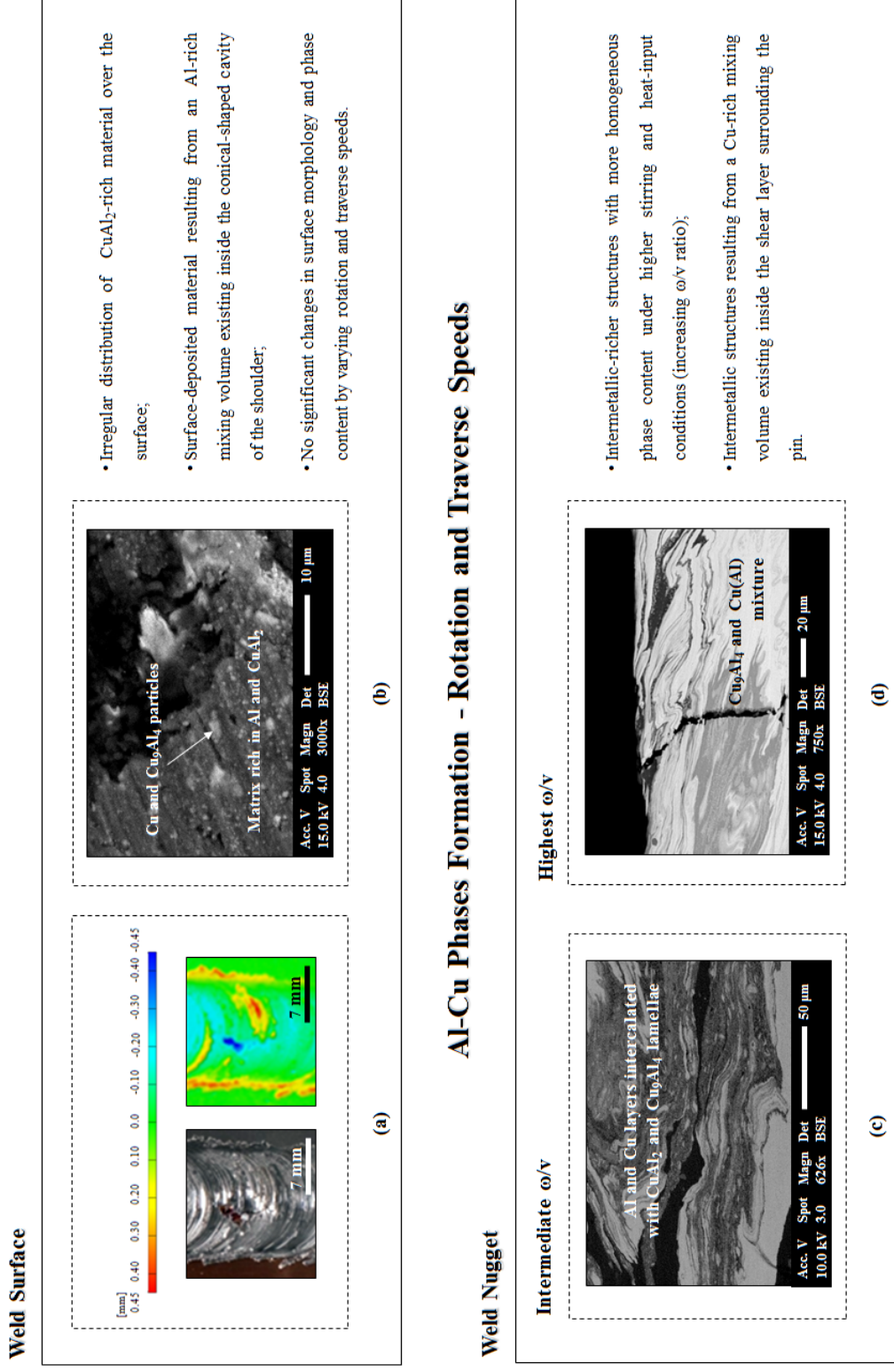


Figure 2 - Influence of rotation and traverse speeds on the formation and distribution of intermetallic phases in the surface (a, b) and nugget (c, d) of Al-Cu friction stir welds (adapted from Galvão et al., 2011).

2.3 - FORMATION AND DISTRIBUTION OF BRITTLE STRUCTURES IN FRICTION STIR WELDING OF ALUMINIUM AND COPPER: INFLUENCE OF SHOULDER GEOMETRY

A strong influence of the material flow mechanisms on the formation and distribution of intermetallic phases during Al-Cu FSW was noticed in Galvão et al. (2011). As referred before, the analysis conducted in this study was restricted to welds produced with a single tool geometry, i.e. the conical-shouldered tool. However, according to that concluded in Galvão et al. (2010), significant differences in material flow mechanisms are promoted by varying the shoulder design, pointing to important dissimilarities in the intermetallic content of the welds as well. So, a research aimed to study the influence of the shoulder geometry on intermetallic phases' formation and distribution during Al-Cu FSW is presented in Galvão et al. (2012a) (Annex III). The intermetallic content of 1 mm-thick AA 5083-H111/copper-DHP friction stir butt welds produced with the well-characterised conical and the scrolled shoulder tools, as well as its impact on welds' structural and morphological properties, were analysed. An overview of the most representative results and conclusions reached in this research are displayed in **Figure 3**.

Significant differences in the structure and morphology of weld surface and nugget were found by comparing the joints produced with different tool designs, as shown in **Figure 3**. Regarding the weld surface finishing, whereas, in good agreement with that discussed in Galvão et al. (2011), irregularly distributed CuAl_2 -rich layers were found to compose the surface of the welds carried out with the conical-shaped tool (**Figure 3a**), improved surfaces with incipient intermetallic content were noticed for the welds produced with the scrolled shoulder (**Figure 3b**). On the other hand, intermetallic-rich structures were identified in the nugget of both kinds of welds. Even so, Al-Cu mixing patterns with higher intermetallic content and increased homogeneity, both in morphology and phase content, were found to compose the nugget of welds produced with the scrolled shoulder tool. In fact, whereas Al-Cu patterns composed of overlapping lamellae of both base materials and CuAl_2 and Cu_9Al_4 intermetallic phases were identified in the nugget of the welds obtained by using the conical shoulder (**Figure 3c**), morphologically homogeneous tongue-shaped interaction features, consisting almost exclusively of CuAl_2 , were formed in the nugget of the welds

produced with the scrolled tool (**Figure 3d**). It should be stressed that the higher intermetallic content of the tongue-shaped features resulted in important brittleness in these structures, which displayed long cracks running over them (**Figure 3d**).

The structural and morphological dissimilarities between the welds produced with the different tools were interpreted in light of the intermetallic phases' formation mechanisms, identified in Galvão et al. (2011), and the material flow mechanisms, identified in Galvão et al. (2010). As discussed before, the ability of the scrolled shoulder to drag the retreating side material, i.e. the aluminium alloy, into the shear layer surrounding the pin is much higher than that of the conical shoulder. Moreover, since the incorporation of the advancing side material into the shear layer is promoted almost exclusively by the pin, being restricted to a small volume surrounding it, the amount of copper dragged into that region by the conical and scrolled tools, whose pins had similar diameter and shape, is not significantly different. This way, whereas, for the conical tool, a copper-richer mixing volume is formed inside the shear layer surrounding the pin, for the scrolled tool, an aluminium-richer mixing volume is formed in the same zone. In addition, it was well-established by Leal et al. (2008) that the plastic deformation imposed by the scrolled tool in the material to be welded is much more intense than that imposed by the other tool. As a result of this, the thermomechanically induced solid-state diffusion phenomenon governing intermetallic phases' generation during FSW gives rise to the formation a homogeneous CuAl_2 -rich intermetallic mixture inside the scrolled tool's shear layer and to a heterogeneous mixture, consisting of Al, Cu, CuAl_2 and Cu_9Al_4 intercalated lamellae, inside the shear layer of the conical tool. It is important to stress that the CuAl_2 intermetallic phase generated in the conical tool's shear layer was formed in some localised aluminium-richer zones of a mixing volume which was globally richer in copper. For both tools, the deposition of the shear layer material in the wake of the tool during its travel motion provides the formation of the nugget Al-Cu patterns discussed above (**Figures 3c and 3d**).

Regarding the surface of the welds, the lower intermetallic content noticed over the top layer of the joints produced with the scrolled shoulder, which provided improved surface finishing, also resulted from the stronger dragging ability of this tool. The helical flutes of the shoulder exerted an intense dragging action over the surface of the plates, pushing all the surface material into the shear layer surrounding the pin, preventing under-shoulder material accumulation, and consequently, the deposition of

intermetallic-rich mixtures at the top layer. On the other hand, as discussed in Galvão et al. (2011), the large amounts of CuAl_2 identified at the top layer of the welds produced with the conical tool resulted from the irregular deposition of the aluminium-rich mixture formed inside the conical-shaped cavity of this shoulder.

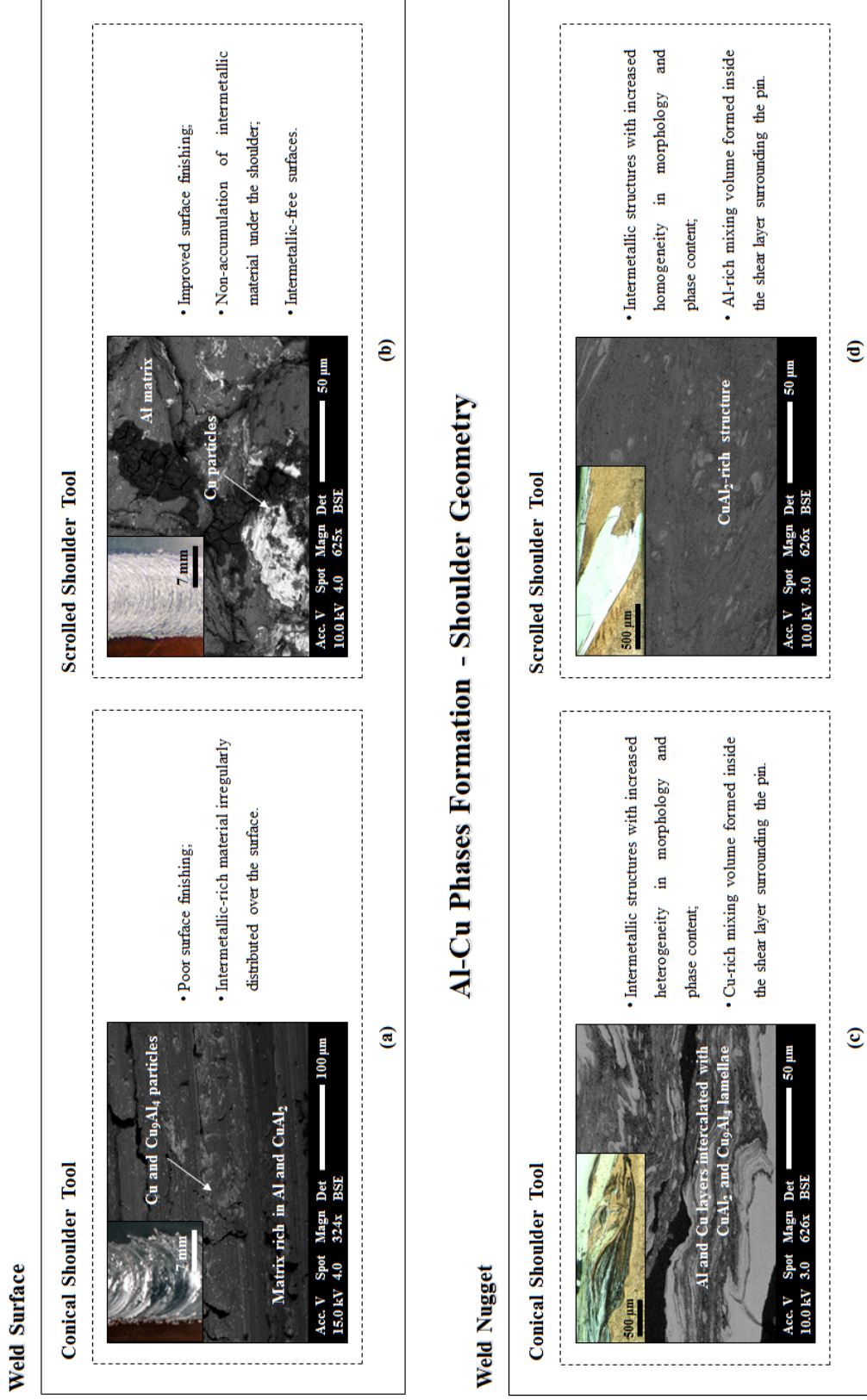


Figure 3 - Influence of the shoulder geometry on the formation and distribution of intermetallic phases in the surface (a, b) and nugget (c, d) of Al-Cu friction stir welds (adapted from Galvão et al., 2012a).

2.4 - STUDY OF THE WELDING CONDITIONS DURING SIMILAR AND DISSIMILAR ALUMINIUM AND COPPER WELDING BASED ON TORQUE SENSITIVITY ANALYSIS

The material flow mechanisms, the intermetallic phases' formation and distribution and their consequences on the structure and morphology of the welds were addressed in Galvão et al. (2010, 2011, 2012a). The influence of the base materials positioning, shoulder design and tool rotation and traverse speeds on these phenomena was deeply explored. However, the analysis was restricted to the interpretation of welds micro and macrostructure, not providing a physical understanding on the thermomechanical conditions experienced inside the Al-Cu welding volume. So, as the torque registered during welding is a physical quantity highly sensitive to the thermomechanical conditions inside the stirred volume, a torque sensitivity analysis was conducted in similar and dissimilar FSW of 1 mm-thick plates of AA 5083-H111 aluminium alloy and copper-DHP. In this research, which is presented in Galvão et al. (2012b) (Annex IV), the sensitivity of the spindle torque to the rotation and traverse speeds, base material properties and relative positioning of the dissimilar plates was interpreted in light of the material flow mechanisms, the metallurgical and thermomechanical phenomena occurring during welding and the final structure and morphology of the welds.

The spindle torque study was conducted by evaluating both the average values and the instantaneous evolution of this physical quantity during welding. More precisely, the effect of the rotation and traverse speeds on the torque registered during welding was studied by analysing the average torque variation for six distinct welding conditions, characterised by different combinations of rotation and traverse speeds. The influence of the materials to be welded and the plates positioning (exclusively in dissimilar welding) was investigated by comparing, for each condition, both the average torque and the instantaneous torque evolution in Al-Al, Cu-Cu and Al-Cu (both plates positioning) FSW. Some representative results of this study as well as an overview of the main conclusions are displayed in **Figure 4**.

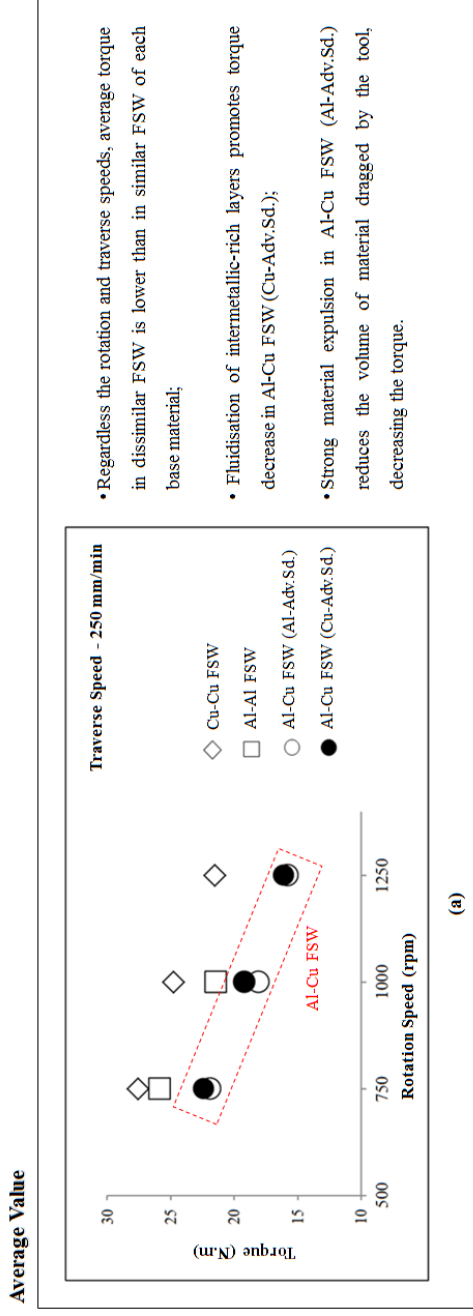
Concerning the influence of the rotation and traverse speeds on the spindle torque, it was observed that, independently of the materials to be welded or the relative positioning of the plates, the sensitivity of the average torque to the variation of these

parameters was the same. Actually, whereas an important decrease in torque value was registered for increasing rotation speed (**Figure 4a**), no significant variations in average torque were observed by varying the traverse speed. As it is well-established in literature (Peel et al., 2006; Arora et al., 2009), the increased temperature achieved during the process by increasing the rotation speed was found to promote additional material softening, which reduced the material flow stresses, and consequently, the torque registered during welding. On the other hand, as the traverse speed has much lesser influence on the temperature reached under the tool than the rotation speed (Peel et al., 2006; Arora et al., 2009), slighter changes in average torque value were noticed by varying this parameter.

Beyond the rotation speed, the combination of materials to be welded was also found to have a strong influence on the average torque evolution. As shown in **Figure 4a**, it was observed that, independently of the testing conditions, the spindle torque registered in Al-Cu welding was lower than that registered in similar joining of each base metal. As reported in Galvão et al. (2010, 2011, 2012a), strong base materials interaction occurs during Al-Cu FSW when the copper plate is positioned at the advancing side of the joint, which promotes the formation of Cu_9Al_4 -rich and CuAl_2 -rich mixtures in the pin and shoulder-governed mixing volumes. Because the CuAl_2 intermetallic phase has a melting temperature close to the peak temperatures registered by some authors in Al-Cu FSW (Ouyang et al., 2006), it can be assumed that fluidisation (not melting) of some intermetallic-rich layers occurs, inducing tool slippage during welding, which results in a significant decrease in the average torque. On the other hand, as discussed in Galvão et al. (2010), no intermetallic phases' formation occurs in dissimilar Al-Cu welding with the reverse positioning of the plates, since the expulsion of large amounts of aluminium from the under shoulder area avoids base materials mixing. The large amounts of aluminium expelled from the joint gave rise to an important decrease in the volume of material being stirred by the tool, at each revolution, reducing the spindle torque.

As illustrated in **Figure 4b**, the instantaneous torque evolution was found to be strongly dependent on both the couple of materials to be welded and the relative positioning of the dissimilar plates. In fact, whereas no important torque variations, along the welding length, were registered for both similar welding and dissimilar joining with the aluminium plate positioned at the advancing side, strong fluctuations in torque values, with important peaks and drops, were registered during dissimilar

welding with the reverse positioning of the plates. Specifically, the torque drops in these welds were observed to correspond to zones where large amounts of material were accumulated on the weld surface (surface macrograph in **Figure 4b**). As discussed in Galvão et al. (2010), under these welding conditions, significant amounts of intermetallic-rich mixtures formed during welding adhere to the tool, being non-periodically expelled after some revolutions. As a result of this, an intercalation of torque peaks, when material accumulation occurs under the tool, with significant torque drops, which correspond to intermetallic material expulsion, explains the very irregular torque evolution in dissimilar Al-Cu FSW with the copper plate located at the advancing side.



Torque sensitivity in FSW of Al and Cu

Instantaneous Evolution

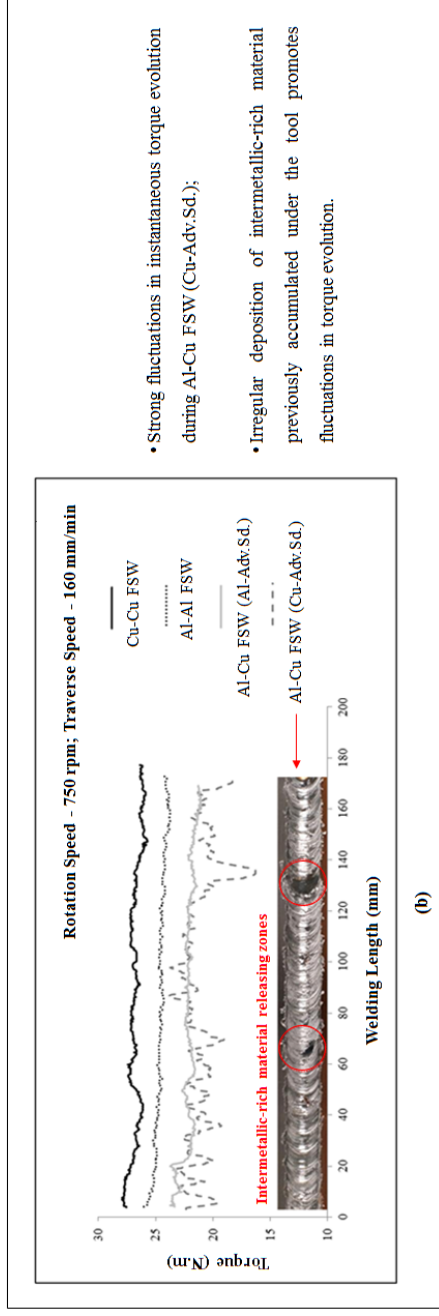


Figure 4 - Average (a) and instantaneous (b) torque evolution in Al-Al, Cu-Cu and Al-Cu FSW (adapted from Galvão et al., 2012b).

2.5 - INFLUENCE OF TOOL OFFSETTING ON THE STRUCTURE AND MORPHOLOGY OF DISSIMILAR ALUMINIUM TO COPPER FRICTION-STIR WELDS

In the previous stages of the work, presented in Galvão et al. (2010, 2011, 2012a, 2012b), the extensive formation of intermetallic phases during Al-Cu FSW was found to have a very detrimental effect on the welding conditions, affecting severely the structural and morphological properties of the welds. Some authors, such as Okamura and Aota (2004), Genevois et al. (2011) and Xue et al. (2011a), pointed tool offset, from the base materials interface towards the aluminium alloy, to be an effective solution to inhibit this phenomenon. However, the effectiveness of this strategy to achieve non-defective Al-Cu welds, with suitable surface finishing and good mechanical properties, was far from being totally supported or even consensual (Okamura and Aota, 2004; Genevois et al., 2011; Liu et al., 2011; Xue et al., 2011a; Avettand-Fenoël et al., 2012). So, a research aimed to analyse the influence of tool offset on the morphological, structural and mechanical properties of the Al-Cu friction stir welds was conducted, which is presented in Galvão et al. (2012c) (Annex V).

As opposed to the former stages of the investigation, different plate's thickness as well as aluminium alloy were used in this research, i.e. 3 mm-thick plates of AA 6082-T6 were friction stir butt welded to copper-DHP. Regarding plate's thickness, as a larger diametered-pin was required to weld the 3 mm than 1 mm-thick plates, larger range of offset values with physical representativeness was possible to be tested. In turn, concerning the aluminium alloy type, the AA 6082 alloy was used owing to its improved flowability during welding (Leitão et al., 2012). Actually, since the tool operated mostly at the aluminium side under tool offset conditions, dragging this material towards the copper plate surface, using an aluminium alloy with high flowability was essential. The most representative results and conclusions reached in this study are summarised in **Figure 5**.

Welds produced under five distinct welding conditions, achieved by varying the tool offset towards the aluminium alloy, were studied. As shown in **Figures 5a to 5c**, the structural and morphological properties of the weld surface and nugget were found to vary significantly according to the offset values, which ranged from 0 to 2.5 mm, i.e. between no offset and full offset (pin performing tangent to copper plate surface)

conditions, respectively. Regarding the weld surface properties, improved surface finishing was achieved for increasing values of tool offset. In good agreement with that concluded in Galvão et al. (2011, 2012a), the top layer of the welds produced with no/small offset was found to be composed of extensive amounts of Al-Cu intermetallic phases, which were formed in the conical shoulder cavity's mixing volume and irregularly distributed over the weld surface during tool motion (**Figures 5a and 5b**). On the other hand, no intermetallic structures or even significant amounts of copper were identified over the improved surfaces of the welds carried out with high tool offset values (**Figure 5c**). So, it was concluded that shifting the tool from base materials interface reduced significantly intermetallic phases' formation inside the shoulder-governed volume, which strongly impacted on the surface finishing of the dissimilar welds.

Similar to that reported for the weld surface, increasing values of tool offset were found to reduce strongly the amount of copper dragged from the advancing to the retreating side of the nugget, and consequently, the intermetallic content of this zone. Actually, the incorporation of copper into the shear layer, which, as discussed in Galvão et al. (2010), is promoted almost exclusively by the pin, decreased significantly by shifting the tool towards the aluminium alloy. So, as illustrated in **Figures 5a to 5c**, whereas a large volume of copper was found to be dragged to the retreating side of the welds produced without any offset (**Figure 5a**), a couple of large copper fragments (**Figure 5b**) and very small copper particles (**Figure 5c**) were dragged to the aluminium side of the nugget in welds carried out with small and large values of tool offset, respectively. Moreover, a large intermetallic-rich structure, consisting of layers of aluminium and copper alternated with CuAl_2 and Cu_9Al_4 lamellae, was found to be present in the nugget of the weld produced with no offset, as opposed to that observed for the welds carried out with increasing values of offset, in which very small amounts of intermetallic material were identified. Specifically, under full offset conditions, a composite-like structure, consisting of very small sized copper particles and residual intermetallic phases homogeneously scattered in the aluminium matrix, was observed all over the nugget of the welds.

Although tool offset was found to be an effective strategy to produce welds with improved surfaces and lower intermetallic content, no significant improvements were achieved in the mechanical strength of the joints by using this strategy. Effectively, all welds failed for very low angles during root bending testing. Even so, fracture surface

analysis revealed important differences in Al-Cu bonding structure according to the offset value, as shown in **Figures 5d to 5f**. For the welds produced with no offset, strong morphological heterogeneity was observed over the fracture surface. In fact, beyond aluminium and copper regions, in which ductile fracture-indicative features were observed, a smooth region with featureless morphology, consisting of aluminium-rich mixed material, was also noticed (**Figure 5d**). Considering the intermetallic-rich content of the nugget of this weld, significant amounts of aluminium-rich intermetallic phases, such as CuAl_2 , are expected to compose the featureless structure. The melting temperature of these phases, which, as referred in Galvão et al. (2011, 2012b), are close to the maximum temperatures registered by Ouyang et al. (2006) in Al-Cu FSW, point to the fluidisation (no melting) of some intermetallic layers being formed during welding. So, the strong differences in physical and mechanical properties between the intermetallic layers and both base materials gave rise to metallurgical discontinuities corresponding to the featureless surface, in which failure was initiated. It should be noted that no brittle cleavage failure was found to occur over the intermetallic-rich layers of the welds.

For the welds produced with small offset values, failure was found to occur along the interface between the aluminium matrix and the large copper fragments (**Figure 5e**), which, as referred above, were dragged from the advancing to the retreating side of the welds. Effectively, in the welds produced under these conditions, severe discontinuities were noticed at the interface between the large copper fragments and the aluminium matrix of the nugget. The dimension of the copper clusters, their sharp geometry and the significant differences in aluminium and copper mechanical properties hampered proper interaction of both metals. On the other hand, for high offset values, fracture was found to occur at the base materials interface, where a very smooth fracture surface, indicating absence of material joining, was observed (**Figure 5f**). The high offset values used to produce these welds promoted the formation of severe discontinuities in this region. Actually, although some localised interfacial zones presenting metallurgical continuity were identified, in which very small copper strips intercalated with aluminium-rich structures and submicron-sized intermetallic lamellae were noticed, most of the interface was found to be composed of zones with sharp Al/Cu transitions. Thermally activated interdiffusion, providing metallurgical and mechanical bonding, was not found to occur in most of the Al/Cu interfacial area.

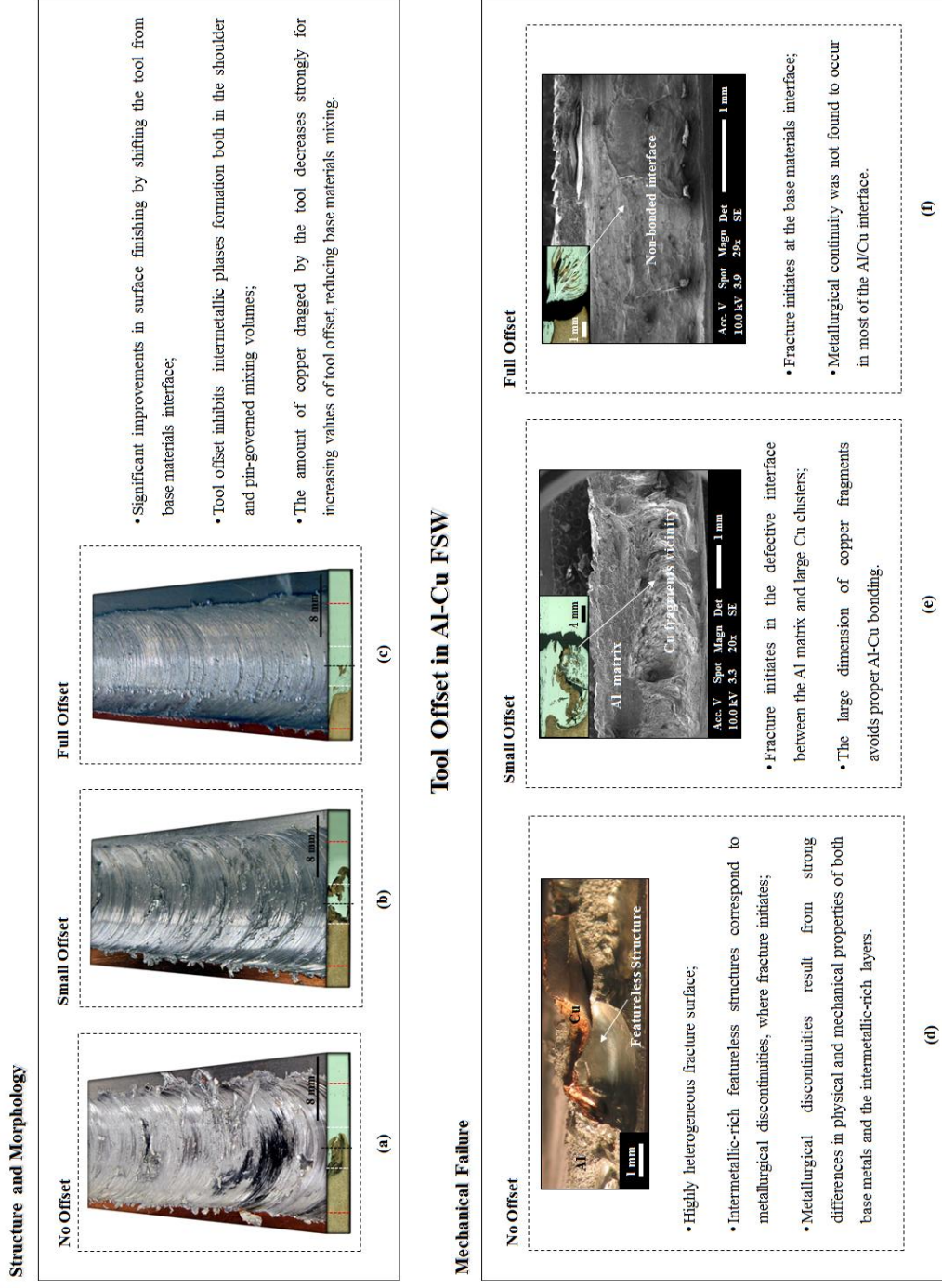


Figure 5 - Influence of tool offset on the structural/morphological (a, b, c) and mechanical (d, e, f) properties of Al-Cu friction stir welds (adapted from Galvão et al., 2012c).

2.6 - INFLUENCE OF ALUMINIUM ALLOY TYPE ON DISSIMILAR FRICTION STIR LAP WELDING OF ALUMINIUM TO COPPER

Two distinct aluminium alloys were friction stir butt welded to copper in the previous stages of this investigation, the non-heat-treatable AA 5083-H111 alloy (Galvão et al., 2010, 2011, 2012a, 2012b), and the heat-treatable AA 6082-T6 alloy (Galvão et al., 2012c). The friction stir weldability of these alloys is significantly different, as a result of their distinct mechanical behaviour under the extreme conditions of temperature and plastic deformation experienced during FSW (Leitão et al., 2012). However, the effect of the aluminium alloy on Al-Cu friction stir weldability had never been addressed. This way, a research aimed to analyse the influence of the aluminium alloy type on the morphological, structural and mechanical properties of dissimilar friction stir welds of 1 mm-thick copper-DHP plates to 6 mm-thick plates of the AA 5083-H111 and AA 6082-T6 aluminium alloys was conducted. As opposed to the previous researches, this study, which is presented in Galvão et al. (2013) (Annex VI), was focused on Al-Cu lap joining, because of its increased interest in several practical applications. Particularly, lap joining of thin copper plates to thicker aluminium alloys (copper at the top of the joint), to which current research was devoted, has high technical and economic interest by enabling, for example, copper cladding over small areas. Some representative results as well as an overview of the main conclusions reached in this research are displayed in **Figure 6**.

As shown in **Figures 6a and 6b**, the morphological properties of the weld surface were found to vary considerably according to the couple of materials being welded, although similar parameters were used to produce both types of welds. In fact, whereas a very smooth surface finishing was observed for the AA 5083/copper welds (**Figure 6a**), defects usually related to excessive heat-input during welding, such as significant tool submerging and formation of massive flash, were identified at the surface of the AA 6082/copper welds (**Figure 6b**). In good agreement with this, substantial differences were also noticed in the nugget of the welds, especially in which regards to the structure and morphology of the bonding area, as illustrated in **Figures 6c and 6d**. For the AA 5083/copper welds, evidence of material stirring by the shoulder was exclusively noticed in a very small area in the vicinity of the top copper plates' surface. As a result of this, incipient Al-Cu interaction, which was confined to the pin influence

zone, took place during welding, promoting the arising of a severe discontinuity across almost the entire Al/Cu interface (**Figure 6c**). Actually, the totally inefficient base materials mixing occurring during the process prevented the effective joining of the plates. On the other hand, a significantly larger Al-Cu interaction volume, which was found to extend beyond the pin influence zone, was registered in AA 6082/copper FSW. The shoulder, whose influence encompassed the entire thickness of the top plates, dragged larger amounts of copper, promoting strong base materials interaction during welding. This way, mixing structures consisting of aluminium and copper intercalated with intermetallic-rich lamellae (especially Cu_9Al_4) were observed all over the nugget of these joints (**Figure 6d**). However, despite the stronger interaction of both base metals, some localised discontinuities were also noticed over the nugget mixing structures, which resulted from the non-uniform materials mixing and the strong brittleness of the Al-Cu intermetallic phases formed during welding. This way, it was concluded that stronger base materials mixing in Al-Cu FSW does not necessarily mean sound joining.

A strong influence of the aluminium alloy on the welding results was noticed. Since the AA 6082 aluminium alloy experiences strong softening with plastic deformation at increasing temperatures, as opposed to the AA 5083 alloy, which presents steady flow stress behaviour at high temperatures (Leitão et al., 2012), it was concluded that the higher thermal softening experienced by the heat-treatable alloy led to further tool submerging in AA 6082/copper FSW. As a result of this, strong deepening and massive flash formation were noticed at the surface of the AA 6082/copper welds. The higher tool submerging also resulted in increased amounts of copper and aluminium being dragged by the shoulder and the pin, respectively, into the shear layer, at each tool revolution, where the strong pin-governed base materials mixing promoted the formation of the intermetallic-rich structures observed in the nugget of these welds. As opposed to this, the significantly smaller volume of copper dragged by the shoulder in AA 5083/copper FSW, as well as the less efficient material dragging promoted by the pin over the AA 5083 alloy, prevented strong base materials interaction in the shear layer, giving rise to the formation of a discontinuous Al/Cu interface.

The mechanical properties of the welds were investigated by hardness analysis. Extremely high hardness peaks were noticed in the nugget of both the AA 6082/copper and the AA 5083/copper friction stir welds. Regarding the AA 6082/copper welds,

hardness values reaching 400 HV_{0.2} were registered in the Al-Cu mixing patterns, which is in good agreement with the intermetallic-rich content of these structures. In fact, the extensive amounts of the Cu₉Al₄ intermetallic phase (and some CuAl₂) identified all over the nugget promoted the very high hardness values reached in these welds. In turn, a substantially smaller hardness peak, i.e. approximately 200 HV_{0.2}, was registered in the nugget of the AA 5083/copper welds. However, as opposed to that noticed in the AA 6082/copper welds, the hardness peak was not registered in intermetallic-rich structures, which were not formed in these welds because of the incipient materials mixing occurring during the process. Instead of it, the hardness values were surprisingly measured in a very narrow layer exclusively composed of aluminium, in the vicinity of the Al/Cu discontinuous interface (**Figure 6c**). This finding motivated a deep microstructural study of the nugget, from which it was concluded that very small grains, with some tenths of nanometres, composed the very narrow aluminium layer, which promoted the impressive hardness increase in this region by grain boundary strengthening.

The ultra-refined microstructure of the narrow AA 5083 aluminium layer was indicative of a very small growth of the recrystallized grains, resulting from low heat-input during welding. The cause promoting this phenomenon was pointed to be the very small dimension of the FSW tool, which avoided a substantial amount of heat to be generated and added during the welding process. It was concluded that the very small tool used in this work, although did not allow a suitable material flow during welding to be achieved, which resulted in the formation of important defects at the Al/Cu interface, promoted an impressive hardness increase in the aluminium alloy due to the formation of an ultra-refined microstructure.

Weld Surface

AA 5083/copper FSW



- Improved surface finishing;
- Smooth surfaces with regular and well-defined striations.

(a)

AA 6082/copper FSW



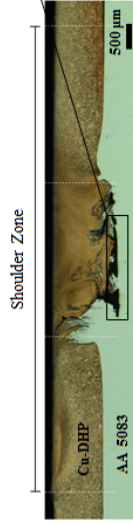
- Intense deepening and massive flash formation;
- Strong tool submerging during welding.

(b)

Al-Cu FS weldability - Aluminium Alloy Type

Weld Nugget

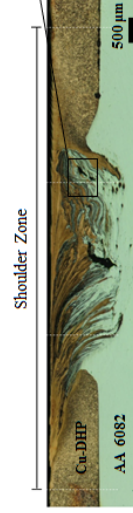
AA 5083/copper FSW



- Incipient base materials interaction;
- Lower thermal softening of the AA 5083 alloy prevents strong interaction of both base materials;
- Impressive hardness increase in a nano-structured aluminium layer in the vicinity of the discontinuity.

(c)

AA 6082/copper FSW



- Strong base materials interaction;
- Extensive formation of intermetallic phases;
- Intense thermal softening of the AA 6082 alloy promotes strong mixing of both base materials.

(d)

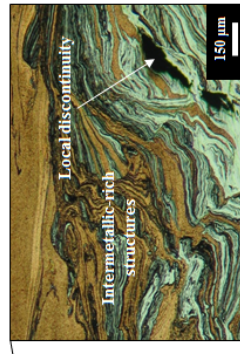
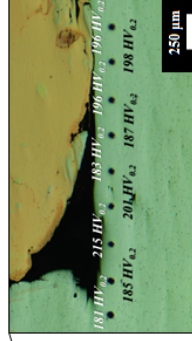


Figure 6 - Influence of the aluminium alloy type on the structural/morphological properties of the surface (a, b) and nugget (c, d) of Al-Cu friction stir lap welds (adapted from Galvão et al., 2013).

3 - SCIENTIFIC EVIDENCE ON ALUMINIUM-TO-COPPER FRICTION STIR WELDING

A large boom in dissimilar materials joining by FSW has been recently witnessed by scientific community. The number of published works on FSW of materials with very different physical and mechanical properties as well as high chemical affinity, such as aluminium and copper, has increased exponentially. This section has the purpose of presenting the state-of-the-art of Al-Cu FSW, highlighting the original and pioneer contribution of this study to the current knowledge. The scientific evidence on the macro and microstructure, defects, hardness and mechanical strength/ductility of the Al-Cu welds is reported in current section. The knowledge on the welding conditions' physical indicators and the aluminium-copper phases' formation phenomenon is also addressed. A brief synthesis highlighting the most prominent remarks is presented at the end of each item.

3.1 - WELD MACROSTRUCTURE

The macrostructure of the friction stir welds is closely related to the welding parameters and has strong influence on weld strength. Current knowledge on the influence of the tool rotation and traverse speeds, base materials positioning and properties, tool offset and tool geometry on Al-Cu welds macrostructure is resumed in this section.

3.1.1 - Tool rotation and traverse speeds

A small number of works was devoted to the study of the influence of the tool rotation and traverse speeds on Al-Cu FSW conditions. However, among the works already conducted in this field, two different approaches were adopted to study this aspect. In fact, whereas some authors varied a single parameter and kept the other constant, some

other authors varied both parameters simultaneously and discussed their results according to predefined rotation to traverse speeds ratios. The operational details and the main conclusions reached in these investigations are provided in **Tables 2 and 3**, where studies analysing the influence of tool rotation and traverse speeds on welds structure, respectively, are summarised, and in **Table 4**, where works adopting the parameters ratio to characterise the varying welding parameters are resumed.

From **Table 2**, in which two butt and one lap joining-focused investigations are displayed, it can be inferred that consensus was reached, for both joint configurations, on the effect of the rotation speed on the internal structure of the welds. In fact, all the works, i.e. Xue et al. (2011a) and Liu et al. (2011), both in Al-Cu butt welding, and Abdollah-zadeh et al. (2008), in lap welding, noticed increased base materials interaction for increasing values of tool rotation speed, which resulted in welds with less defective internal structures and increased formation of brittle intermetallic phases. Contrary to that, no consensus was reached regarding the influence of the rotation speed on the surface finishing of the butt welds. In fact, whereas significant worsening of weld surface was noticed by Xue et al. (2011a) for increasing values of tool rotation speed, improved surface finishing was reported by Liu et al. (2011) in welds produced with high tool rotation. Moreover, contrary to the previous study, an irregular evolution of the surface appearance with varying tool rotation speed was noticed by Liu et al. (2011). It should also be noted that, although some improvements on weld surface finishing were noticed in both works by varying the rotation speed, excellent surfaces, displaying smooth and regular appearance were not noticed in any of these studies. Surface finishing was not addressed by Abdollah-zadeh et al. (2008) in Al-Cu lap welding.

Table 2 - Studies addressing the effect of the rotation speed on Al-Cu weld macrostructure.

Study	Base Materials		Joint Conf.	Rotation (rpm)	Key Highlights
	Thickn.	Alloys			
<i>Xue et al. (2011a)</i>	5 mm	AA 1060 Pure copper	Butt	400 - 1000	Improved surfaces for lower rotation speed; Sounder internal structures for higher rotation speed; Increased formation of intermetallic phases for higher rotation speed.
<i>Liu et al. (2011)</i>	3 mm	AA 5052-O Pure copper	Butt	400 - 1000	Irregular evolution of surface quality with the rotation speed; Sounder internal structures for higher rotation speed; Increased formation of intermetallic phases for higher rotation speed.
<i>Abdollah-zadeh et al. (2008)</i>	4 mm 3 mm	AA 1060 Pure copper	Lap	750 - 1500	Incipient interaction for lower rotation speed; Increased formation of intermetallic phases for higher rotation speed.

As illustrated in **Table 3**, the effect of the traverse speed on the final structure and morphology of the Al-Cu welds was only addressed in two lap and one butt welding-focused studies. Abdollah-zadeh et al. (2008), in lap joining, noticed that decreasing the traverse speed, at constant rotation, promoted a similar effect on weld structure to increasing the rotation, at constant traverse speed, i.e. the increase of base materials interaction. In turn, Saeid et al. (2010), also in Al-Cu lap welding, pointed intermediate traverse speed values to provide the most suitable welding conditions by avoiding structural concerns resulting from both very low and very high base materials interaction. More recently, Tan et al. (2013), in butt joining, noticed more proper welding conditions by decreasing the traverse speed. Additionally, the decrease of the traverse speed was also reported to improve the surface finishing of the joints. Even so, excellent surface finishing, like that usually noticed in Al-Al or Cu-Cu similar FSW, was not achieved in this study.

Table 3 - Studies addressing the effect of the traverse speed on Al-Cu weld macrostructure.

Study	Base Materials		Joint Conf.	Trv. Speed (mm/min)	Key Highlights
	Thickn.	Alloys			
<i>Abdollah-zadeh et al. (2008)</i>	4 mm 3 mm	AA 1060 Pure copper	Lap	30 - 375	Incipient interaction for higher traverse speed; Increased formation of intermetallic phases for lower traverse speed.
<i>Saeid et al. (2010)</i>	4 mm 3 mm	AA 1060 Pure copper	Lap	30 - 375	Intermediate traverse speed provides more proper welding conditions.
<i>Tan et al. (2013)</i>	3 mm	5A02 alum. Pure copper	Butt	20 - 40	Better surfaces for lower traverse speed; Sounder internal structures for lower traverse speed.

As displayed in **Table 4**, Galvão et al. (2011) and Bisadi et al. (2013) were the only authors addressing the influence of varying simultaneously both the rotation and traverse speeds on Al-Cu friction stir butt and lap weldability, respectively. However, it should be noted that whereas the former authors analysed the welding results according to the rotation to traverse speeds ratio (ω/v) corresponding to each welding condition, the latter authors interpreted their results considering the rotation's square to traverse speed ratio (ω^2/v). An important effect of the ω/v ratio on the internal structure of the welds was noticed by Galvão et al. (2011). Actually, stronger base materials interaction and higher intermetallic content were noticed in welds produced with increasing ω/v ratio. However, contrary to the studies reported in **Tables 2 and 3**, no significant changes on weld surface quality were noticed by varying the rotation and traverse speeds. The surface finishing of the butt welds was found to be adversely influenced by the intermetallic content of the joints' top layer. This was a very innovative conclusion, which had never been reported in the studies conducted before, representing an important advance in the understanding of Al-Cu welds surface properties. In turn, Bisadi et al. (2013) noticed lap welds with poorer surfaces for increasing values of ω^2/v ratio. Regarding the internal structure of the joints, the authors found that intermediate values of the ω^2/v ratio provided more proper welding conditions, which is in good agreement with that reported by Saeid et al. (2010).

Table 4 - Studies addressing the effect of the rotation to traverse speeds ratio on Al-Cu weld macrostructure.

Study	Base Materials		Joint Conf.	Ratio's Range	Key Highlights
	Thickn.	Alloys			
<i>Rotation to traverse speed ratio - ω/v (rev/mm)</i>					
<i>Galvão et al. (2011)</i>	1 mm	AA 5083 Copper-DHP	Butt	$\frac{1000}{250}$; $\frac{750}{160}$; $\frac{1000}{160}$	Increased intermetallic phases formation for increasing ω/v ratio; Surface finishing independent on the ω/v ratio; Intermetallic content of the surface affects adversely the surface finishing.
<i>Rotation's square to traverse speed ratio - ω^2/v (rev²/mm)</i>					
<i>Bisadi et al. (2013)</i>	2.5 mm 3 mm	AA 5083 Pure copper	Lap	$\frac{600^2}{32}$ to $\frac{1550^2}{16}$	Improved surfaces for lower ω^2/v ratio; Intermediate ω^2/v ratio promotes sounder welding conditions.

From the analysis conducted in the previous paragraphs, it can be concluded that if, on the one hand, unanimity was reached regarding the influence of the rotation and traverse speeds on particular aspects of the welds, on the other hand, some issues still remain non-consensual. In fact, it is well-established that increased interaction of both base materials occurs under higher heat-input conditions, i.e. for lower values of traverse speed and higher values of rotation speed (or higher ω/v and ω^2/v ratios). However, the influence of the rotation and traverse speeds on the surface appearance of the Al-Cu welds does not generate unanimity. Although some authors noticed better surface finishing to be achieved under lower values of traverse speed or higher rotation speed, these findings were not corroborated by some other authors, who noticed precisely the reverse, or even, no influence of these parameters on weld surface properties. Even so, the relation found to exist between the surface appearance of the welds and its intermetallic content was an important progress in Al-Cu FSW.

3.1.2 - Base Materials Positioning

The relative positioning of the base material plates in the welding joint, defining the advancing and retreating side material, in butt joining, or the top and bottom material, in

lap joining, is a very important parameter in dissimilar FSW, which has a critical influence on the weldability of several materials (DebRoy and Bhadeshia, 2010). The operational details and main conclusions of the studies addressing the effect of base materials positioning on Al-Cu friction stir butt and lap weldability are resumed in **Tables 5 and 6**, respectively.

According to the works displayed in **Table 5**, there is no unanimity regarding the most suitable positioning of the aluminium and copper base materials in butt joining. Nevertheless, a remarkable influence of this parameter on the final welding results was noticed in all the works, even in the most preliminary investigations, such as those conducted by Murr et al. (1998a, 1998b). These authors, without mentioning the advancing and/or retreating sides of the tool, or even pointing the reasons for the phenomenon they noticed, reported considerable differences in structural soundness of the welds by changing the positioning of the aluminium and copper plates, while all other welding variables were kept constant. More than one decade later, Galvão et al. (2010) were the first authors to conduct an in-depth investigation on this aspect. Accordingly to the previous authors, significant differences in the welding results were noticed by reversing the positioning of the base material plates. Effectively, welds with much more irregular morphology were produced when the aluminium alloy was positioned at the advancing side of the joint. Significant material expulsion from the joint, and incipient Al-Cu mixing, were found to occur during welding, which resulted in the production of welds with important thinning and massive aluminium flash. The strong influence of base materials positioning on the welding results was interpreted in light of the material flow mechanisms occurring during Al-Cu FSW and the differences in physical and mechanical properties of both metals. The findings reached in this work were corroborated, one year later, by both Xue et al. (2011a) and Liu et al. (2011), who also reported improper welding conditions by positioning the aluminium plate at the advancing side of the joint.

More recently, unlike to the previous authors, Tan et al. (2013) noticed sounder Al-Cu FSW conditions by positioning the aluminium plate at the advancing side of the joint. However, the influence of base materials positioning on Al-Cu friction stir weldability was not explicitly addressed in this work.

Table 5 - Studies addressing the effect of the base materials positioning on Al-Cu butt weld macrostructure.

Study	Base Materials		Key Highlights	
	Thickn.	Alloys	Aluminium - Adv. Sd.	Copper - Adv. Sd.
<i>Murr et al. (1998a, 1998b)</i>	6 mm	AA 6061 Pure copper	Important differences in welding results by changing the base materials positioning.	
<i>Galvão et al. (2010)</i>	1 mm	AA 5083 Copper-DHP	Improper welding conditions; No Al-Cu interaction.	Sounder welding conditions; Increased Al-Cu interaction.
<i>Xue et al. (2011a)</i>	5 mm	AA 1060 Pure copper	Improper welding conditions.	Sounder welding conditions.
<i>Liu et al. (2011)</i>	3 mm	AA 5052 Pure copper	Improper welding conditions.	Sounder welding conditions.
<i>Tan et al. (2013)</i>	3 mm	5A02 alum. Pure copper	Sounder welding conditions.	Improper welding conditions.

As displayed in **Table 6**, Akbari et al. (2012) investigated the effect of base materials positioning on Al-Cu friction stir lap weldability. Keeping all the other welding variables constant, the authors observed important differences in structural soundness of the welds by varying the base materials positioning. Whereas improper welding conditions were noticed by positioning the copper plate at the top of the joint, sounder structures were achieved for the welds produced with the reverse positioning of the plates. This finding is in good agreement with the positioning adopted by most of the researchers working in Al-Cu friction stir lap welding (Abdollah-zadeh et al., 2008; Saeid et al., 2010; Xue et al., 2011b; Bisadi et al., 2013), who exclusively studied welds produced with the aluminium alloy located at the top of the joint. Galvão et al. (2013) were the only authors adopting the reverse positioning of the base material plates, which, according to them, has great interest to some practical applications, such as copper cladding over thick aluminium substrates.

Table 6 - Study addressing the effect of the base materials positioning on Al-Cu lap weld macrostructure.

Study	Base Materials		Key Highlights	
	Thickn.	Alloys	Aluminium - Top	Copper - Top
<i>Akbari et al. (2012)</i>	2 mm	AA 7070 Pure copper	Sounder structures.	Improper welding conditions.

3.1.3 - Tool Offset

Tool offset from the plates interface towards one of the base materials has been extensively reported in literature since the very initial stage of dissimilar friction stir butt welding. In fact, a large range of studies point this procedure as a possible solution for achieving proper welding conditions, since it enables to reduce, or even to avoid, the wear of the tool, formation of brittle intermetallic phases and unsuitable material flow (Watanabe et al., 2006; Lee et al., 2006; Dressler et al., 2009).

The operational details and main conclusions of the studies addressing the influence of tool offset on Al-Cu friction stir butt weldability are displayed in **Table 7**. From the table it can be concluded that one of the first works addressing this issue was conducted by Okamura and Aota (2004). Welds with less defects and better surface finishing were noticed by full shifting the tool from the base materials interface towards the aluminium alloy. According to the authors, tool offset avoided strong Al-Cu mixing, and consequently, the formation of large amount of harmful intermetallic phases. They stressed that the aluminium was exclusively extruded against the harder copper, providing welding by diffusion bonding. The achievement of defect-free welds by full shifting the tool towards the aluminium alloy was also reported by Genevois et al. (2011). In good agreement with Okamura and Aota (2004), the authors named this FSW procedure “Friction Stir Diffusion Bonding”. However, although production of non-defective welds was claimed by Genevois et al. (2011), no results concerning welds’ internal macrostructure, surface finishing, or even, strength were presented, which avoids more supported conclusions to be reached.

Unlike to the previous works, in which a single tool offset condition was analysed, Xue et al. (2011a) and Galvão et al. (2012c) studied the evolution of weld structure and morphology for varying values of tool offset towards the aluminium alloy. Significantly smaller amounts of copper dragged from the advancing to the retreating side of the joints, and consequently, lower formation of brittle intermetallic phases, was noticed in both works for increasing values of tool offset. Moreover, better surface appearance was also reported in both investigations for welds produced with high offset values. Particularly, Galvão et al. (2012c) noticed significant differences in surface intermetallic content, i.e. significantly intermetallic-richer surfaces were reported for small offset values. On the other hand, very smooth and regular surfaces, exclusively composed of aluminium, were observed for the welds produced with the tool mostly

shifted towards the aluminium alloy. Nevertheless, despite the significant improvements observed in the surface properties of the welds produced with high offset values, tool offset was considered by Galvão et al. (2012c) to be an ineffective way of improving Al-Cu friction stir weldability. Actually, metallurgical discontinuities were observed in all the welds, regardless of the offset values.

As displayed in **Table 7**, tool offset towards either the aluminium and copper alloys was tested by Liu et al. (2011) and Avettand-Fenoël et al. (2012). According to Liu et al. (2011), significant worsening in weld structure and morphology was promoted by shifting the tool from the materials interface, pointing to the ineffective contribution of tool offset to achieve proper Al-Cu FSW conditions. In good agreement with this, improper welding conditions were also noticed by Avettand-Fenoël et al. (2012) regardless of the tested tool offset. Moreover, unlike to that reported in most of the previous works, the intermetallic content of the welds produced with tool offset was found to be higher than that of the welds carried out with the tool centred at the materials interface. The authors inferred that, as opposed to a stirring volume made of equivalent fractions of ductile materials with distinct malleability, mechanical mixing is facilitated in the cases of a predominant volume fraction of one metal, resulting in increased formation of intermetallic phases.

From all the works reported above, it can be concluded that no unanimity exists in literature regarding the influence of tool offset on Al-Cu weldability. In fact, although most of the works conducted in this field pointed to significant improvements in weld surface finishing by welding with the tool shifted from the interface towards the aluminium alloy side, important divergence exists regarding the evolution of the internal structure of the welds. Several factors may contribute to this discrepancy, such as the differences in the alloys to be welded, the thickness of the base materials, the rotation and traverse speeds used to produce the welds and the geometry of the tool.

Table 7 - Studies addressing the effect of tool offset on Al-Cu butt weld macrostructure.

Study	Base Materials	Tool Offset (pct. value) ^a	Key Highlights	
			Cu Sd. Off.	Al Sd. Off.
<i>Okamura and Aota (2004)</i>	AA 6061 O-free copper	100 %	NT	Reduced formation of intermetallic phases; Less defective welds with improved surface finishing.
<i>Genevois et al. (2011)</i>	AA 1050 Pure copper	100 %	NT	Reduced Al-Cu mixing; Abolishment of several defects.
<i>Xue et al. (2011a)</i>	AA 1060 Pure copper	33 %, 67 %, 83 %, 100 %	NT	Reduced formation of intermetallic phases for higher offset values; Higher values of tool offset provide better surface finishing.
<i>Liu et al. (2011)</i>	AA 5052 Pure copper	100 %		Globally defective welds achieved by shifting the tool either to the aluminium or copper sides of the joint.
<i>Galvão et al. (2012c)</i>	AA 6082 Copper-DHP	25 %, 50 %, 75 %, 100 %	NT	Sound surfaces without intermetallic content for higher offset values; No materials mixing for high offset values; Formation of metallurgical discontinuities, regardless of the offset value.
<i>Avettand-Fenoël et al. (2012)</i>	AA 6082 Pure copper	~ 30 %		Defective internal structures; Increased formation of intermetallic phases achieved by shifting the tool either to the aluminium or copper sides of the joint.

a - Pct. offset value corresponds to the offset value to the pin radius ratio (in percentage).

NT - Non-tested.

O-free copper - Oxygen-free copper.

3.1.4 - Tool Geometry

The tool, which governs the heat generation and plastic deformation, influencing all the metallurgical and thermomechanical phenomena occurring during the process, is the core element in FSW. Particularly in Al-Cu FSW, in which sound welding conditions are very difficult to be reached, a suitable tool design is crucial to achieve proper interaction of both base materials. This issue was deeply addressed in two published works, whose operational details and main conclusions are displayed in **Table 8**.

As shown in **Table 8**, welds produced with two distinct tool designs, i.e. conical and scrolled shoulder tools, were investigated by Galvão et al. (2010, 2012a), who were pioneers in studying the influence of the tool geometry on the Al-Cu friction stir weldability. Important relations between the tool geometry, the material flow mechanisms, which remained totally uncharacterised until the development of these works, and the final welding results were established. In fact, significant differences in material flow mechanisms were noticed by varying the tool design, which seriously impacted on the final structure and morphology of the joints. In terms of surface finishing, the welds produced with the conical tool presented surfaces with higher intermetallic content and much more irregular morphology than the welds produced with the scrolled tool, for which excellent surface finishing was noticed. On the other hand, the intermetallic content inside the welds (in the nugget) produced with the scrolled tool was higher than that of the welds produced with the conical tool. Moreover, accumulation of intermetallic-rich material under the tool, which was noticed to be one of the most serious concerns in Al-Cu FSW, severely affecting the material flow and deposition processes, was registered exclusively in the welds obtained with the conventional conical shoulder tool.

Table 8 - Studies addressing the effect of the tool geometry on Al-Cu weld macrostructure.

Study	Base Materials		Joint Conf.	Key Highlights	
	Thickn.	Alloys		Conical Shoulder Tool	Scrolled Shoulder Tool
<i>Galvão et al. (2010)</i>	1 mm	AA 5083 Copper-DHP	Butt	Irregular surfaces; Upper half-plate's materials mixing; Accumulation of intermetallic material under the tool.	Excellent surfaces; Through-thickness material mixing; No accumulation of material under the tool.
<i>Galvão et al. (2012a)</i>	1 mm	AA 5083 Copper-DHP	Butt	Intermetallic-rich surfaces; Lower intermetallic content inside the welds (in the nugget).	Aluminium-rich surfaces; Higher intermetallic content inside the welds (in the nugget).

3.1.5 - Base Materials

Both the aluminium and copper alloys systems comprise a large number of alloys. Remarkable dissimilarities in structural properties exist among the several alloys of each system. This way, significant differences in Al-Cu friction stir weldability are

expected to exist according to the aluminium and copper alloys being welded. However, most of the works conducted in Al-Cu FSW are aimed to study a single welding couple, which obviously prevents the influence of base materials properties on the final welding results to be evaluated. Contrary to this, a very innovative work, whose operational details and main conclusions are displayed in **Table 9**, was conducted by Galvão et al. (2013) with the aim of investigating this issue.

The influence of the aluminium alloy type on Al-Cu welding results was studied by comparing the weldability of a heat-treatable (AA 6082) and a non-heat-treatable (AA 5083) aluminium alloy to copper in lap joining. The authors noticed important differences in the weldability of each aluminium alloy to copper, and consequently, in the final structure and morphology of both types of welds. In fact, whereas improved surface finishing and very incipient base materials interaction was noticed for the AA 5083/copper joints, surface deepening and strong materials mixing, which resulted in extensive formation of Al-Cu intermetallic phases, was observed for the AA 6082/copper friction stir welds. The different mechanical behaviour of each aluminium alloy under the extreme conditions of temperature and plastic deformation occurring during welding was found to be on the basis of the different welding results.

Table 9 - Study addressing the effect of the base materials on Al-Cu weld macrostructure.

Study	Base Materials		Joint Conf.	Key Highlights	
	Thickn.	Alloys		AA 5083/copper FSW	AA 6082/copper FSW
Galvão et al. (2013)	6 mm	AA 5083	Lap	Smooth and regular surfaces;	Deepening at the surface;
	6 mm	AA 6082		Incipient Al-Cu interaction;	Strong Al-Cu mixing;
	1 mm	Copper-DHP		Reduced formation of intermetallic phases.	Extensive formation of intermetallic phases.

Overall remarks on weld macrostructure

Important progresses have been achieved in Al-Cu FSW literature regarding the effect of the welding parameters on the weld macrostructure. It is well-established that the rotation and traverse speeds, the relative positioning of the base materials, the tool geometry, the tool offset and the type of the welded alloys have strong influence on the final structure and morphology of the welds. Important developments were also reached concerning the causes promoting the poor surface finishing of the joints. Moreover, even the non-unanimity on some issues should be regarded as a consequence of growing

knowledge. Effectively, some concepts, well-accepted in literature some years ago, such as the effectiveness of tool offset in improving the Al-Cu friction stir weldability, are currently being questioned.

3.2 - WELD DEFECTS

It is well-established that proper welding conditions are very difficult to be achieved in Al-Cu FSW, which often results in the production of defective welds. **Table 10** shows a literature-based overview of the most reported defects in Al-Cu welding, i.e. internal discontinuities (**Figure 7**), cracking (**Figure 8**) and poor surface finishing (**Figure 9**), as well as the factors promoting their formation. According to the table, the formation of internal discontinuities is predominantly noticed in Al/Cu interfacial regions (**Figure 7**), as a result of improper interaction of both base materials during welding (Abdollahzadeh et al., 2008; Saeid et al., 2010; Liu et al., 2011; Xue et al., 2011a; Akbari et al., 2012; Firouzdor and Kou, 2012; Galvão et al., 2012c, 2013; Bisadi et al., 2013; Tan et al., 2013). However, **Table 10** also shows that, as opposed to most authors, Galvão et al. (2012c) did not notice internal discontinuities exclusively in Al/Cu interfacial zones, but also at the interface of the intermetallic-rich layers and the aluminium and copper volumes. The important differences in physical and mechanical properties of the base materials and the Al-Cu phases were claimed to promote their formation.

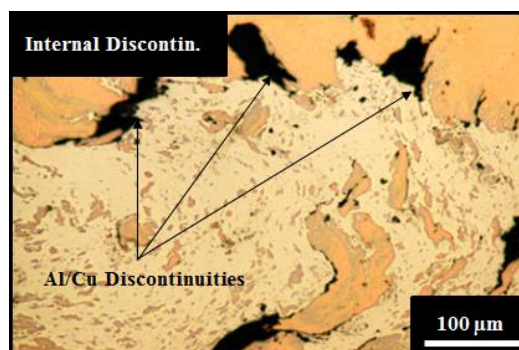


Figure 7 - Internal discontinuities formed in AA 6061/copper friction stir lap welds (adapted from Firouzdor and Kou, 2012).

Cracking is essentially noticed over the intermetallic-rich structures of the welds (**Figure 8**). As displayed in **Table 10**, the brittle nature of the Al-Cu intermetallic

phases is unanimously pointed to be the cause governing extensive cracking incidence in the Al-Cu friction stir welds (Ouyang et al., 2006; Akinlabi et al., 2010; Galvão et al., 2010, 2011, 2012a, 2013; Xue et al., 2011a; Avettand-Fenoël et al., 2012; Liu et al., 2012). In good agreement with this, it is well-established that the higher the intermetallic content of the welds, the more intense and severe is cracking (Ouyang et al., 2006; Galvão et al., 2011, 2012a).

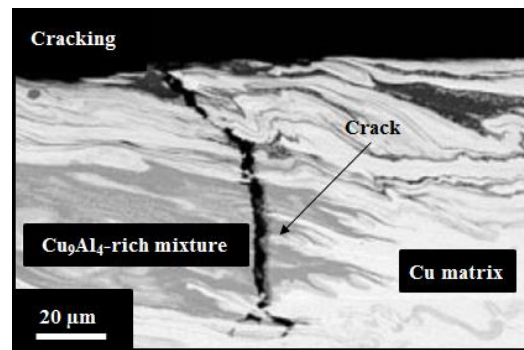


Figure 8 - Cracking in AA 5083/copper friction stir butt welds (adapted from Galvão et al., 2011).

Poor surface finishing is a concern particularly noticed in Al-Cu butt joining. As displayed in **Table 10**, rough layers of irregularly distributed material are extensively noticed at the surface of the Al-Cu butt welds (Galvão et al., 2010, 2011, 2012a, 2012c; Liu et al., 2011; Xue et al., 2011a). However, Galvão et al. (2011, 2012a, 2012c) were the only authors analysing this issue in-depth, pointing the poor surface finishing of the welds to result from the intermetallic-rich content of the top layers, which prevents a regular material deposition over the surface, promoting the formation of zones with strong material accumulation and areas with significant material absence (**Figure 9**).

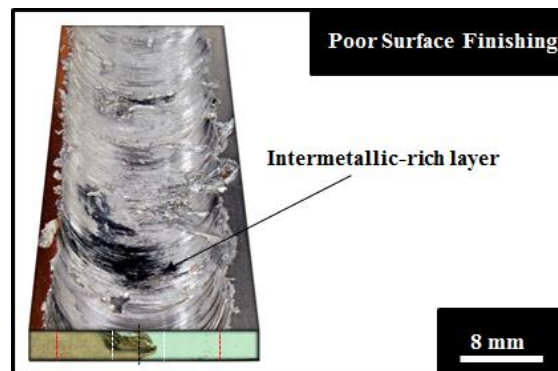


Figure 9 - Poor surface finishing in AA 6082/copper friction stir butt welding (adapted from Galvão et al., 2012c).

Table 10 - Literature-based overview of the most reported defects in Al-Cu FSW and the causes promoting their formation.

Al-Cu Welds Defects	Cause	Reports
	Base materials interface - Improper interaction of both base materials.	Abdollah-zadeh et al. (2008), Saeid et al. (2010), Liu et al. (2011), Xue et al. (2011a), Akbari et al. (2012), Firouzdor and Kou (2012), Galvão et al. (2012c, 2013), Bisadi et al. (2013), Tan et al. (2013).
Internal Discontinuities	Intermetallic layers/base materials interface - Strong differences in physical and mechanical properties.	Galvão et al. (2012c).
Cracking	Extreme brittleness of Al-Cu intermetallic phases.	Ouyang et al. (2006), Akinlabi et al. (2010), Galvão et al. (2010, 2011, 2012a, 2013), Xue et al. (2011a), Avettand-Fenoël et al. (2012), Liu et al. (2012).
Poor Surface Finishing	Intermetallic-rich layers irregularly distributed over the surface. ^a	Galvão et al. (2010, 2011, 2012a, 2012c), Liu et al. (2011), Xue et al. (2011a).

a - The intermetallic content of the top layers was exclusively concluded in the works conducted by Galvão and co-workers.

Overall remarks on weld defects

The main types of defects in Al-Cu FSW are identified in literature as well as the causes governing their formation. Improper interaction of both base materials and extensive formation of intermetallic phases are established to be the main factors promoting the production of defective welds.

3.3 - WELDING CONDITIONS' PHYSICAL INDICATORS

Physical quantities, such as temperature, traverse force, torque and power, are important indicators of the evolution in FSW conditions, whose study has increased interest in process's control. However, in Al-Cu joining, investigation has been essentially focused on the analysis of the welding temperature and torque. The knowledge on these physical quantities in Al-Cu FSW is addressed in current section.

3.3.1 - Welding Temperature

Temperature is an important aspect in FSW, which influences the whole structure of the welds. This issue was addressed in some Al-Cu FSW works, which are displayed in **Table 11**. The peak temperature, tool rotation and traverse speeds, base materials and temperature-measuring procedures used in each of these studies are shown in the table.

Temperature in Al-Cu butt welding was addressed by Savolainen et al. (2006), Ouyang et al. (2006) and Liu et al. (2011). According to **Table 11**, the peak temperatures registered in each study are significantly different, ranging between 422 °C and 580 °C. In good agreement with this, Ouyang et al. (2006) and Liu et al. (2011) also noticed very different holding times at high temperature. In fact, whereas Ouyang et al. (2006) reported temperatures above 500 °C to be achieved for 24 seconds, the temperature registered by Liu et al. (2011) did not reach this value at any instant and it was above 100 °C for only 32 seconds. It should be noted that the rotation and traverse speeds, the type and thickness of the welded alloys and the temperature-measuring

zones varied significantly among the Al-Cu butt welding works, which easily explains the differences in the reported temperatures.

Akbari et al. (2012) studied the temperature in Al-Cu lap welding (**Table 11**). The effect of the base materials positioning on the maximum temperature reached during the process was particularly emphasised in this work. According to the authors, the peak temperature varies significantly according to the material positioned at the top of the joint. In fact, whereas a maximum peak of 472.2 °C was registered in the welds produced with aluminium plate located at the top of the joint, 373 °C was found to be the maximum temperature reached in the welds achieved with the reverse base materials positioning. The authors claimed that the higher thermal conductivity of the copper provided a faster distribution of the heat through the nearby regions of the sheet, which prevented the heat to be concentrated in the welding zone.

Table 11 - Welding temperature reported in Al-Cu FSW literature.

Study	Base Materials		Welding Parameters		Measuring Procedure	Maximum Welding Temperature Measuring Zone	Value
	Alloys	Thickn.	Rotation	Trav. Speed			
Butt Joining							
<i>Savolainen et al. (2006)</i>	AA 6060 O-free copper	10 mm	750 rpm	150 mm/min	K-type thermocouples	Into the pin; 2 mm in-depth from the top surface.	500-520 °C
<i>Quyang et al. (2006)</i>	AA 6061 Pure copper	12.7 mm	914 rpm	95 mm/min	K-type thermocouples	8 mm away from butt interface (Al side); 2 mm in-depth from the top surface.	580 °C
<i>Liu et al. (2011)</i>	AA 5052 Pure copper	3 mm	1000 rpm	100 mm/min	K-type thermocouples	1.5 mm away from butt interface (Cu side); 2 mm in-depth from the top surface.	422 °C
Lap Joining							
<i>Akbari et al. (2012)</i>	AA 7070 Pure copper	2 mm 2 mm	1400 rpm	25 mm/min	Infrared thermometer	Joint's centreline; Top surface.	373 °C (Cu-top) 472.2°C (Al-top)

O-free copper - Oxygen-free copper.

3.3.2 - Welding Torque

The spindle torque is a physical quantity closely related to the energy spent during FSW. A pioneer study on the Al-Cu FSW conditions based on torque sensitivity analysis was recently conducted by Galvão et al. (2012b). The operational details and main conclusions of this investigation are displayed in **Table 12**.

For similar testing conditions, Galvão et al. (2012b) noticed significantly lower torque values in Al-Cu FSW than in similar welding of each base material. The factors promoting torque decrease in dissimilar FSW were found to vary according to the relative positioning of the base material plates. Strong material expulsion from the joint, which heavily reduced the volume of material dragged by the tool at each revolution, was pointed to be the cause on the basis of torque decrease during welding with the aluminium plate positioned at the advancing side. In turn, tool slippage promoted by fluidisation of low melting temperature intermetallic phases was claimed to reduce the spindle torque during welding with the reverse positioning of the plates. Moreover, strong fluctuations in instantaneous torque evolution were also noticed during welding with the copper plate positioned at the advancing side. According to the authors, the accumulation of intermetallic-rich material under the tool and its subsequent expulsion after some revolutions promoted important torque peaks and drops, respectively, resulting in a very irregular torque evolution.

Table 12 - Study addressing the welding conditions in Al-Cu FSW by torque sensitivity analysis.

Study	Base Materials		Joint Conf.	Key Highlights
	Thickn.	Alloys		
<i>Galvão et al. (2012b)</i>	1 mm	AA 5083 Copper-DHP	Butt	<p>Torque in Al-Cu FSW is lower than in similar FSW of each base material;</p> <p>Fluidisation of intermetallic layers promoted tool slippage during dissimilar welding with Cu plate on the advancing side;</p> <p>Material expulsion reduced the volume of material dragged by the tool during dissimilar welding with Al plate on the advancing side.</p>

Overall remarks on welding conditions' physical indicators

The knowledge on the Al-Cu FSW temperature and torque has increased in recent years. Regarding the temperature, research has been essentially focused on the peak values achieved during welding. In turn, deeper conclusions were reached on the welding torque. This quantity was established to be strongly influenced by the intermetallic phases' formation and the volume of material dragged by the tool at each revolution.

3.4 - WELD MICROSTRUCTURE

Complex thermal, mechanical and metallurgical phenomena occurring during welding govern the microstructure of the Al-Cu friction stir welds, which is explored in current section in light of the knowledge available in literature. The distinct microstructural zones of the welds are characterised, being given particular emphasis to the structure and morphology of the nugget, by describing the Al-Cu interaction patterns, resulting from base materials mixing, and the bonding features at the base materials non-mixed interface.

3.4.1 - Weld Microstructural Zones

The microstructural regions commonly identified in the transverse and horizontal sections of any weld produced by FSW are the thermomechanically-affected zone (TMAZ), which comprises the non-recrystallized TMAZ and the nugget, and the heat-affected zone (HAZ). However, in Al-Cu FSW, microstructural evidence of the HAZ is very scarcely reported in literature. In fact, this zone was noticed by a small number of authors, such as Abdollah-zadeh et al. (2008), Xia-wei et al. (2012) and Bisadi et al. (2013), who observed some increase in aluminium and/or copper grain size, and Sarrafi et al. (2011), who reported a significant loss in microstructural rolling directionality. Both phenomena were claimed to result from the thermal annealing experienced by the base materials in the HAZ.

The non-recrystallized TMAZ, which bounds the nugget at both the aluminium and copper sides of the welds, is characterised by a plastically deformed grain structure. This zone is extensively reported in Al-Cu FSW literature, independently of the alloys to be welded, the welding parameters or the joint configuration. A transmission electron microscopy (TEM)-based analysis of aluminium and copper TMAZ microstructure can be found in Genevois et al. (2011), for AA 1050/pure copper FSW.

Regarding the nugget of the welds, important grain refinement is often noticed in both the aluminium and copper sides, as a result of the dynamic recrystallization experienced by the materials during welding. Nevertheless, few researches have been focused on characterising in-depth nugget grain structure. From the works addressing this aspect, some scattering is noticed regarding the grain size, which is easily explained based on the different base materials and welding parameters used to produce the welds. Micron-sized grain structures were noticed by Genevois et al. (2011) and Goran et al. (2012) in the nugget of AA1050/pure copper and AA6082/pure copper friction stir butt welds, respectively. In turn, Xue et al. (2011b) and Galvão et al. (2013), in AA 1060/pure copper and AA 5083/copper-DHP friction stir lap welding, respectively, reported the formation of much more refined microstructures, especially for the aluminium alloy. Deep TEM and electron backscatter diffraction (EBSD)-based analyses enabled Galvão et al. (2013) to notice the formation of a nano-structured aluminium region. The impressive grain refinement reported in this work is a very important advance in Al-Cu FSW, which may contribute to the achievement of lap welds with very high strength. The small dimensions of the tool were pointed by Galvão et al. (2013) to be the cause promoting very low heat-input during welding, and consequently, the incipient growth of the recrystallized grains.

3.4.2 - Al-Cu Interaction Patterns

Important features resulting from aluminium and copper interaction during FSW are often noticed in Al-Cu welds, specifically in the nugget. As displayed in **Table 13**, significant research has been devoted to the characterisation of these interaction-promoted patterns, especially in which regards to their morphology and phase content. According to the morphology, the Al-Cu interaction structures can be grouped into three different classes, i.e. lamellar intercalated features (**Figure 10**), homogeneous mixtures (**Figure 11**) and composite-like structures (**Figure 12**). The intermetallic content of the

structures varies significantly according to their morphology, increasing from the composite-like structures to the homogeneous mixtures. Moreover, it should be noted that interaction patterns with different morphologies can coexist in the nugget. In fact, few studies reported nuggets in which a single Al-Cu interaction morphology was noticed.

The lamellar intercalated morphology was first reported in two very preliminary investigations conducted by Murr et al. (1998a, 1998b) in Al-Cu butt joining. Structures consisting of swirl and vortex-shaped intercalated lamellae were observed by these authors (**Figure 10**). Despite their fluid-like morphology, the interaction patterns resulted, according to Murr et al. (1998b), from intense solid-state plastic flow, since no evidence of melting was noticed. More recently, patterns with similar morphology and solid-state nature were noticed by several other authors, such as Ouyang et al. (2006), Galvão et al. (2011, 2012a, 2012c), Liu et al. (2011, 2012) and Tan et al. (2013), in Al-Cu butt welding, and Xue et al. (2011b), Firouzdor and Kou (2012) and Galvão et al. (2013), in Al-Cu lap joining. However, as can be observed in **Table 13**, some scattering exists in the complexity of the interaction features reported in literature. In fact, whereas Ouyang et al. (2006) and Xue et al. (2011b) noticed simpler structures, consisting exclusively of two phases, other authors, such as Galvão et al. (2011, 2012a, 2012c, 2013), Liu et al. (2011, 2012), Firouzdor and Kou (2012) and Tan et al. (2013), reported the formation of very complex features, composed of several layers of different phases.

According to Galvão et al. (2011, 2012a), the Al-Cu lamellar structures result from heterogeneous mixtures formed inside the shear layer surrounding the pin, which are deposited in the nugget during the travel motion of the tool. The initial phase content of the pin-governed mixing volume and the heat-input/stirring conditions, which were found to depend strongly on both the rotation and traverse speeds and the tool geometry, are advocated to be the factors governing the morphology of the nugget interaction patterns. In good agreement with this, Liu et al. (2012) concluded that the morphology of the lamellar structures is significantly influenced by some welding parameters, especially the rotation speed and tool offset. Important variations in the thickness, density and orientation of the intercalated lamellae were noticed by these authors when varying these parameters. More recently, a model aimed to explain the phenomena promoting the formation of the Al-Cu lamellar structures was proposed by Tan et al. (2013). Strong influence of tool axial and traverse loads as well as tool rotation direction on the final morphology of the interaction structures was noticed by these

authors. Considering the conclusions reached in these recent works, the aforementioned dissimilarities existing in literature regarding patterns complexity (**Table 13**) are easily explained by the different interaction conditions occurring in the nugget of the welds, which were produced with varied welding parameters.

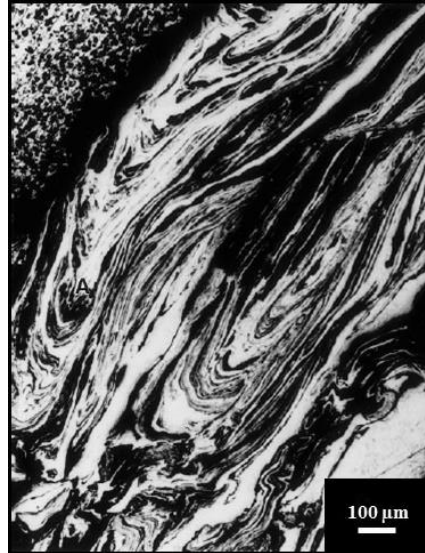


Figure 10 - Lamellar intercalated structure formed in the nugget of AA 6061-T6/copper friction stir welds (adapted from Murr et al., 1998b).

The second morphological class of Al-Cu interaction patterns, i.e. the homogeneous mixtures, is much less reported in literature than the previous morphology (**Table 13**). These patterns, which were characterised in detail by Galvão et al. (2011, 2012a), in Al-Cu butt welding, consist of a fairly homogenous volume of intermetallic-rich material (**Figure 11**). According to the authors, the formation of these features only occurs when the mixing volumes in the shear layer are very rich in one of the base material phases (aluminium or copper) and very intense stirring and heat-input conditions are experienced. Specifically, Galvão et al. (2011) stressed that the heterogeneous lamellar structures described above may evolve to homogenous mixtures under increased stirring and heat-input. Moreover, from **Table 13**, it can be observed that whereas a Cu_9Al_4 -rich structure was noticed by Galvão et al. (2011), a CuAl_2 -rich structure was reported by Galvão et al. (2012a). Significant differences in tool geometry, and consequently, in the initial content of the pin-governed mixing volumes, were on the basis of this dissimilarity. It should be noted that, similarly to that reported to the lamellar patterns, no signs of melting were noticed over the homogeneous intermetallic-rich structures.



Figure 11 - Homogeneous mixture formed in the nugget of AA 5083/copper friction stir welds (adapted from Galvão et al., 2012a).

The composite-like structures, i.e. the third morphological class of Al-Cu interaction patterns, consist of small copper, copper-rich or intermetallic particles scattered over an aluminium or aluminium-rich matrix (**Figure 12**). These structures can be observed over the entire nugget, with this zone fully assuming an aluminium-matrix composite structure, or just in some localised regions. Composite-like structures confined to localised areas of the nugget were reported by Liu et al. (2011) and Tan et al. (2013), in Al-Cu butt welding, and by Xue et al. (2011b) and Firouzdor and Kou (2012), in Al-Cu lap joining. In turn, nuggets fully assuming aluminium-matrix composite structures were reported by Xue et al. (2010, 2011a) and Galvão et al. (2012c), in Al-Cu butt welding. However, these were exclusively noticed in welds produced with high values of tool offset towards the aluminium alloy side. According to Galvão et al. (2012c), since the incorporation of copper, i.e. the advancing side material, into the shear layer is predominantly promoted by the pin, the high offset provides significant decrease in the amount of this material dragged towards the aluminium side. In turn, Xue et al. (2010, 2011a) emphasised that the copper pieces which are scraped by the pin from the bulk copper plate are fragmented in particles with non-uniform shapes/sizes and non-homogeneously distributed over the aluminium matrix. Owing to the reaction of the smallest copper particles with the aluminium matrix, small amounts of intermetallic phases are formed. Xue et al. (2011a) also reported that a minimum value of rotation speed is required to promote interfacial reaction of the copper particles with the aluminium matrix. As observed in **Table 13**, some differences exist in the phase content of the composite-like structures noticed in literature, which is in good agreement with that referred for the previous morphological classes. Again, no signs of melting were reported in these structures.

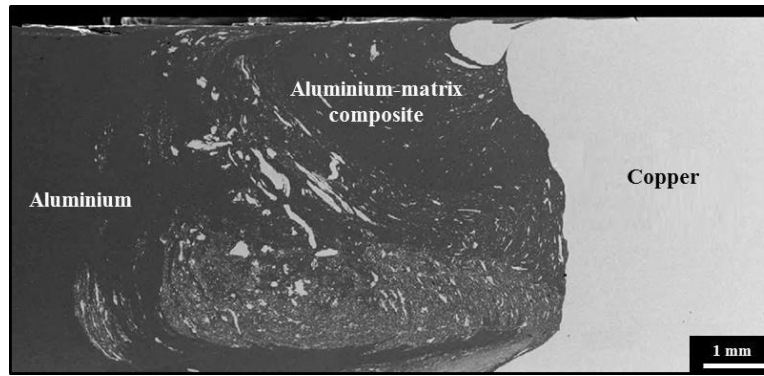


Figure 12 - Composite-like structure formed in the nugget of AA 1060/copper friction stir welds (adapted from Xue et al., 2010).

All the structures described above were found to have a common characteristic, i.e. no signs of melting. However, an exception was noticed by Ouyang et al. (2006) in Al-Cu butt welding (**Table 13**). As illustrated in **Figure 13**, which displays the intermetallic structures' gradient registered over the nugget, solidification indicative features, namely dendritic structures, grains with oriented growth over long distances and eutectic structures, were noticed for aluminium-rich phases (Al/CuAl_2 eutectics, CuAl_2 and CuAl). These melting structures were not included in any of the morphological classes referred above, since no details concerning the interaction patterns in which they were noticed were provided in this work.

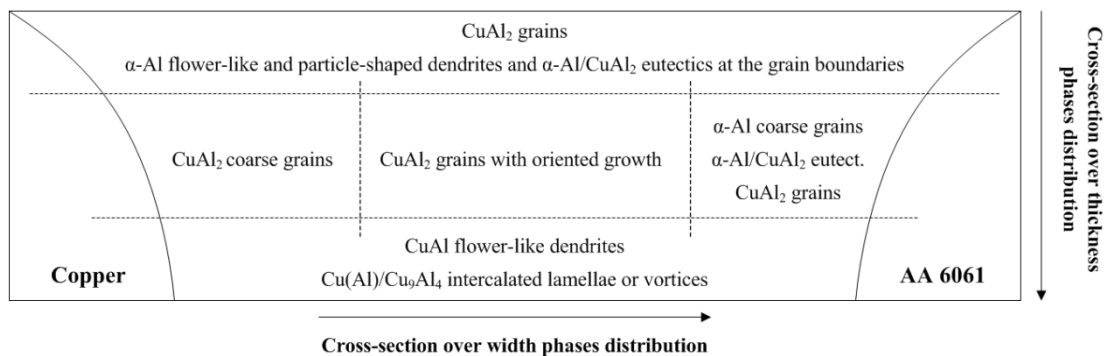


Figure 13 - Intermetallic phases distribution over the nugget of AA 6061/pure copper friction stir welds (adapted from Ouyang et al., 2006).

Table 13 - Nugget interaction features noticed in Al-Cu FSW literature.

Study	Base Materials	Interact. pattern	Phase content	Key highlights
Butt joining				
<i>Murr et al. (1998a, 1998b)</i>	AA 6061 Copper	Intercal. lamellae.	Al, Cu	Phenomenon resulting from extreme plastic flow in solid-state.
<i>Ouyang et al. (2006)</i>	AA 6061 Copper	Intercal. lamellae; Solidif. structures.	Cu(Al), Cu ₉ Al ₄ Al/CuAl ₂ , CuAl ₂ , CuAl	Constitutional liquation of Al-rich phases.
<i>Xue et al. (2010)</i>	AA 1060 Pure copper	Composite-like.	Al, Cu, CuAl ₂ , Cu ₉ Al ₄ , CuAl	Composite-like structure formed over the whole nugget of welds produced with very high offset.
<i>Galvão et al. (2011)</i>	AA 5083 Copper-DHP	Intercal. lamellae; Homog. mixtures.	Al, Cu, CuAl ₂ , Cu ₉ Al ₄ Cu(Al), Cu ₉ Al ₄	Patterns morphology depends on the homogeneity of mixing volumes; Homogeneity of mixing volumes depends on the rotation and traverse speeds.
<i>Liu et al. (2011)</i>	AA 5052 Pure copper	Intercal. lamellae; Composite-like.	Al, Cu(Al), CuAl ₂ , CuAl, Cu ₉ Al ₄ Al, Cu(Al), CuAl ₂	Intercalation model: $CuAl + Cu_9Al_4 - Cu(Al) - Al + CuAl_2 + Cu(Al)$.
<i>Xue et al. (2011a)</i>	AA 1060 Pure copper	Composite-like.	Al, Cu, CuAl ₂ , Cu ₉ Al ₄ , CuAl	Composite-like structure formed over the whole nugget of welds produced with very high tool offset values; Minimum rotation speed is required to the formation of a composite.
<i>Galvão et al. (2012a)</i>	AA 5083 Copper-DHP	Intercal. lamellae; Homog. mixtures.	Al, Cu, CuAl ₂ , Cu ₉ Al ₄ CuAl ₂ , residual phases	Homogeneity of mixing volumes depends on tool geometry.
<i>Liu et al. (2012)</i>	AA 5052 Pure copper	Intercal. lamellae.	Al, Cu, CuAl ₂ , CuAl, Cu ₉ Al ₄	Rotation speed and tool offset have strong impact on the morphology of the intercalated lamellae.
<i>Galvão et al. (2012c)</i>	AA 6082 Copper-DHP	Intercal. lamellae; Composite-like.	Al, Cu, CuAl ₂ , Cu ₉ Al ₄ Al, Cu, CuAl ₂ , Cu ₉ Al ₄	Full tool offset strongly reduces the amount of copper dragged into the shear layer.
<i>Tan et al. (2013)</i>	5A02 alum. Pure copper	Intercal. lamellae; Composite-like.	Cu(Al), CuAl ₂ , CuAl, Cu ₃ Al ₂ , Cu ₉ Al ₄ Al, Cu	Model relating tool axial and traverse loads and tool rotation direction with the final morphology of the Al-Cu patterns.
Lap joining				
<i>Xue et al. (2011b)</i>	AA 1060 Pure copper	Intercal. lamellae; Composite-like.	Cu, Cu ₉ Al ₄ Al, Cu, CuAl ₂	Intercalated lamellae formed inside large copper particles scattered over the nugget.
<i>Firouzdor and Kou (2012)</i>	AA 6061 Pure copper	Intercal. lamellae; Composite-like.	Al, Cu, CuAl ₂ , Cu ₉ Al ₄ Al, Cu	Composite-like morphology formed at the aluminium side of the nugget; Intercalated lamellae formed at the copper side of the nugget.
<i>Galvão et al. (2013)</i>	AA 6082 Copper-DHP	Intercal. lamellae.	Al, Cu, CuAl ₂ , Cu ₉ Al ₄	Intercalated lamellae encompass the whole nugget.

3.4.3 - Al/Cu Interface

The Al/Cu interface corresponds to the portion of the faying surfaces of both base materials that remains non-mixed after welding, especially in butt joining. This zone of the nugget is assuming an increasing relevance in literature, being considered one of the most crucial characteristics defining the global soundness of the welds. As displayed in **Table 14**, the phase content, thickness and continuity/uniformity of this zone have been explored in some recent investigations. The formation of a single intermetallic layer at the Al/Cu interface was noticed in most of the works reported in the table. Nevertheless, the phase content of the interfacial layer is not consensual. Xue et al. (2010, 2011a), Genevois et al. (2011) and Avettand-Fenoël et al. (2012) noticed two sublayers at the interface, specifically a CuAl_2 sublayer at the aluminium side and a Cu_9Al_4 sublayer at the copper side (**Figure 14a**). More recently, Tan et al. (2013) noticed three sublayers, i.e. the same CuAl_2 and Cu_9Al_4 sublayers reported by the previous authors and a sublayer of Cu_3Al_2 between them. Moreover, important differences in the thickness and continuity/uniformity of the interfacial layers are also reported in **Table 14**, which is associated with significant differences in the welding conditions studied in each investigation. Actually, Xue et al. (2011a) found an important relation between interfacial layer properties and tool rotation speed. According to them, increasing the tool rotation speed promoted the formation of thicker and less uniform layers. It should be noted that the continuity/uniformity of the intermetallic layer is advocated to govern the Al-Cu bonding at the whole interface, ensuring proper weld strength. Nevertheless, continuous and uniform layers were not noticed in most of these works.

According to **Table 14**, a significantly different Al/Cu interface microstructure was noticed by Galvão et al. (2012c). Instead of a single interfacial layer (composed of two or three distinct intermetallic sublayers), very small copper strips intercalated with aluminium-rich structures and submicron-sized intermetallic lamellae were observed by these authors at the Al/Cu interface (**Figure 14b**). However, as in some of the works referred above, this microstructure was found to be non-uniform all along the interface, ensuring metallurgical continuity only in some localised regions. In fact, several zones of the interface consisted of sharp Al/Cu transitions, with no signs of base materials interaction. An innovative conclusion was taken by the authors, who stressed that, under the complex material flow and deposition phenomena taking place during FSW, it is of

extreme difficulty to control the formation of a uniform and continuous thin intermetallic layer all along Al/Cu interface.

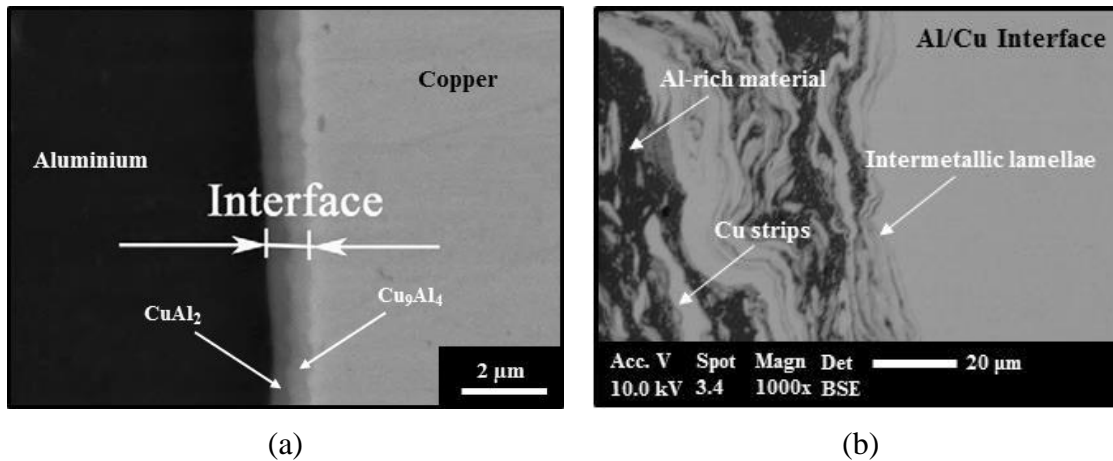


Figure 14 - Base materials interface. (a) Single intermetallic layer-type microstructure noticed in AA 1060/pure copper friction stir welds (adapted from Xue et al., 2010). (b) Multiple layers-type microstructure noticed in AA 6082/copper-DHP friction stir welds (adapted from Galvão et al., 2012c).

Table 14 - Microstructural properties of base materials interface reported in Al-Cu FSW literature.

Study	Base Materials	Al-Cu base materials interface		
		Thickn.	Phase content	Morphological Details
Xue et al. (2010)	AA 1060 Copper	1 μm	CuAl_2 , Cu_9Al_4	Intermetallic layer at the interface; Continuous and uniform layer.
Xue et al. (2011a)	AA 1060 Copper	0.3-3 μm	CuAl_2 , Cu_9Al_4	Intermetallic layer at the interface; Increasing rotation speeds promote the formation of thicker and less uniform interfacial layers.
Genevois et al. (2011)	AA 1050 Pure copper	0.2 μm	CuAl_2 , Cu_9Al_4	Intermetallic layer at the interface; Discontinuous layer - Fragmentation at the bottom region.
Galvão et al. (2012c)	AA 6082 Copper-DHP	-----	Al, Cu, CuAl_2 , Cu_9Al_4	Copper strips intercalated with Al-rich material and submicron-sized intermetallic lamellae; Discontinuous metallurgical bonding at the whole interface.
Avettand-Fenoël et al. (2012)	AA 6082 Pure copper	~3 μm	CuAl_2 , Cu_9Al_4	Intermetallic layer at the interface; No details regarding uniformity and continuity of the intermetallic layer.
Tan et al. (2013)	5A02 alum. Pure copper	1 μm	CuAl_2 , Cu_3Al_2 , Cu_9Al_4	Intermetallic layer at the interface; Non-uniform metallurgical bonding at the whole interface.

Overall remarks on weld microstructure

Significant body of knowledge has been built over the last years on the microstructural properties of Al-Cu friction stir welds. The detection of ultra-refined microstructures in the nugget of the welds was an important achievement. Solid advances have also been made regarding the characterisation of the nugget Al-Cu interaction patterns. In fact, supported relations were established between the morphology and phase content of the interaction features and the mechanisms promoting their formation, which, in turn, were found to depend on the welding conditions. The non-mixed Al/Cu interface has also been characterised in detail. The high difficulty in controlling the demanding characteristics of the interfacial layers, in order to achieve good metallurgical bonding at the whole interface, has been highlighted.

3.5 - ALUMINIUM-COPPER PHASES' FORMATION PHENOMENON

Formation of intermetallic phases during Al-Cu FSW is a phenomenon with major impact on the final structure and morphology of the welds. Current section is aimed to characterise, in light of the existing knowledge, the Al-Cu phases' formation mechanisms and kinetics of growth during FSW. Before addressing in detail the Al-Cu phases' formation in FSW, a brief contextualisation on Al-Cu phase system is presented.

3.5.1 - Al-Cu Phase System

According to the Al-Cu phase diagram, which is shown in **Figure 15**, seven equilibrium phases coexist in the Al-Cu system at temperatures below 300 °C, specifically α -Al solid-solution, θ -CuAl₂, η_2 -CuAl, ζ_2 -Cu₄Al₃, δ -Cu₃Al₂ and γ_2 -Cu₉Al₄ intermetallic phases and α -Cu solid-solution. These phases, which were enumerated in ascending order of copper to aluminium ratio, have important differences in the extent of their compositional ranges. Particularly, among the five intermetallic phases, which are

identified by different colours in the Al-Cu diagram, the γ_2 -Cu₉Al₄ phase has the widest compositional range, whereas the θ -CuAl₂ and ζ_2 -Cu₄Al₃ phases have the narrowest.

Three of the equilibrium intermetallic phases, the θ -CuAl₂, η_2 -CuAl and γ_2 -Cu₉Al₄, are more widely reported to be the aluminium and copper reaction products in Al-Cu FSW. Although it is important to keep in mind that the equilibrium phase diagram is not totally adequate to represent some of the rapid thermal changes taking place during FSW (Ouyang et al., 2006), from **Figure 15**, it can be observed that the θ -CuAl₂ and η_2 -CuAl phases result from the peritectic reactions $L + \eta_1$ -CuAl \rightarrow θ -CuAl₂ and $L + \epsilon_1 \rightarrow \eta_1$ -CuAl, which occur at the temperatures of 591 °C and 620 °C, respectively. During the equilibrium cooling, the phase η_1 -CuAl, formed at 620 °C, gives rise to the low temperature equilibrium phase η_2 -CuAl. Regarding the γ_2 -Cu₉Al₄, this phase is formed through a peritectoid reaction occurring at 870 °C. It is also important to stress that an eutectic phase can be formed at the aluminium-rich zone of the Al-Cu diagram at a significantly lower temperature than any of those referred above, as a result of the eutectic reaction $L \rightarrow \alpha$ -Al + θ -CuAl₂, which occurs at approximately 548 °C.

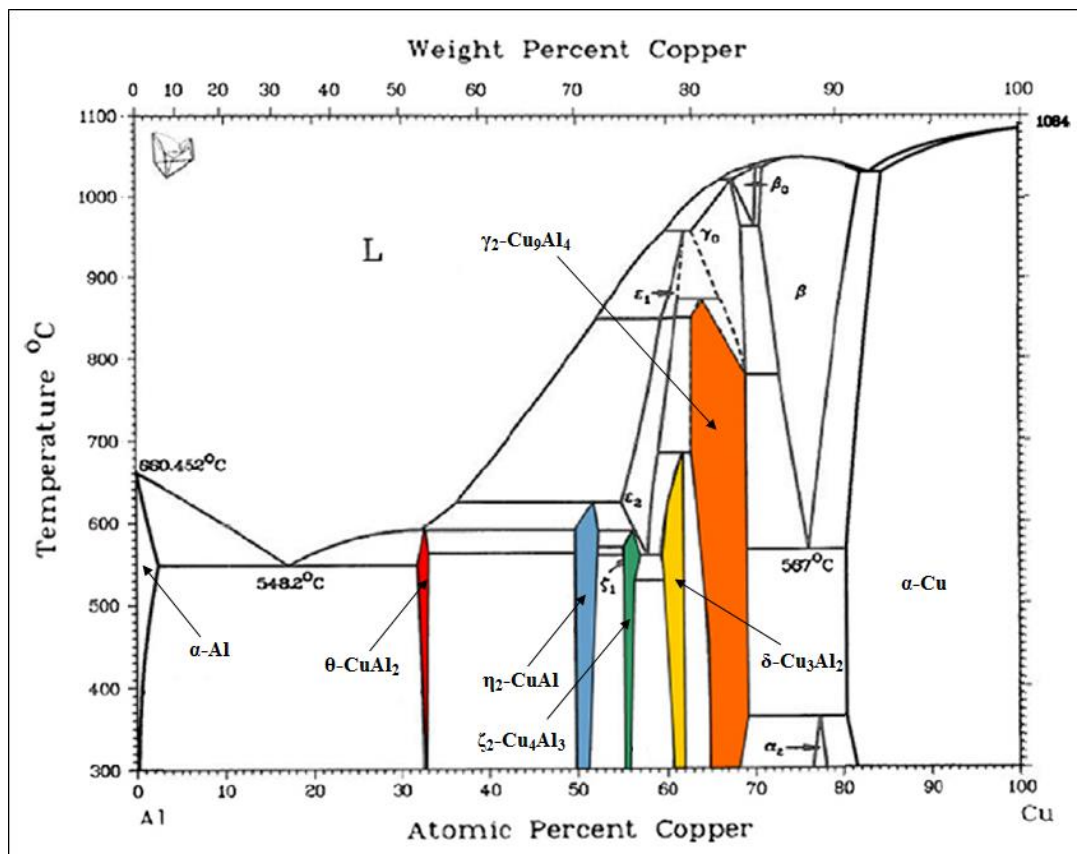


Figure 15 - Al-Cu phase diagram (adapted from Kouters et al., 2013).

The Al-Cu reaction can also be interpreted based on thermodynamic concepts. The effective heat of formation (EHF) of the different Al-Cu phases, which were calculated by Guo et al. (2011) based on Pretorius et al. (1991) model, are displayed in **Table 15**. It should be stressed that, in this model, the EHF is calculated as a function of the standard heat of formation and the effective concentration of the elements at the reaction interface. So, EHF model links standard thermodynamic concepts (heat of formation) with kinetics (effective concentration) and evaluates phase formation from a thermodynamic-kinetic viewpoint. According to it, the first intermetallic phase to nucleate is the one with the most negative EHF at the composition of the lowest liquidus temperature, which, in this case, is the θ -CuAl₂.

Table 15 - Effective heat of formation of the Al-Cu equilibrium phases.

Phase	α -Al	θ -CuAl ₂	η_2 -CuAl	ζ_2 -Cu ₄ Al ₃	δ -Cu ₃ Al ₂	γ_2 -Cu ₉ Al ₄	α -Cu
EHF (kJ/mol)	-----	-6.76	-6.68	-6.29	-5.84	-5.61	-----

Source: Guo et al. (2011).

3.5.2 - Intermetallic Phases' Formation Mechanisms in Al-Cu FSW

Important research has already been conducted on intermetallic phases' formation mechanisms during Al-Cu FSW. Published works addressing this issue are resumed in **Table 16**. From the table, it can be observed that two different phenomena were claimed by Ouyang et al. (2006) to govern the formation of Al-Cu intermetallic phases during FSW. The aluminium-rich phases, i.e. Al/CuAl₂ eutectics, CuAl₂ and CuAl, were pointed to be formed by constitutional liquation, which was supported by their solidified morphology and low melting temperature. On the other hand, as no signs of melting were noticed over the copper-rich intermetallic structures formed in the welds, i.e. intercalated lamellae of Cu(Al) and Cu₉Al₄, a solid-state diffusion phenomenon, consisting of the mechanical integration of aluminium into copper, was pointed to govern the formation of Cu₉Al₄. In fact, the melting temperature of this phase is much higher than the temperatures registered by Ouyang et al. (2006) during Al-Cu FSW, which prevented its formation by solidification. The arising of mixing regions in the welds with a similar compositional range to Cu₉Al₄ was stressed to be a key factor for the formation of this phase.

Some years later, a thermomechanically-activated solid-state diffusion phenomenon was pointed by Galvão et al. (2011) to govern the formation of both the aluminium (CuAl_2) and copper-rich (Cu_9Al_4) intermetallic phases during FSW. As no solidification structures were noticed all over the intermetallic-rich structures, the Al-Cu phases were claimed to be formed by solid-state diffusion, which was facilitated by the extremely high strain rates reached during the process. A close relation between the amounts of Cu_9Al_4 intermetallic phase and Cu(Al) solid-solution was found to exist (fitting analysis of the X-ray diffraction patterns), which supported the formation of Cu_9Al_4 by mechanical integration of aluminium in copper. In good agreement with these authors, solid-state diffusion governing the formation of Al-Cu intermetallic phases during FSW was also claimed by Liu et al. (2011), Genevois et al. (2011) and Avettand-Fenoël et al. (2012). Specifically, the maximum welding temperature registered by Liu et al. (2011) was found to be well below the lowest temperature of liquidus in the Al-Cu system (eutectic temperature), which corroborated the absence of liquation. Beyond the extreme plastic deformation, whose effect was reported by all the authors mentioned above, the thinness of the aluminium and copper mixing lamellae and the grain refinement experienced in the nugget were also pointed by Liu et al. (2011) to further facilitate the Al-Cu interatomic diffusion, increasing the kinetics of intermetallic phases' formation under fairly low temperatures and short holding times at high temperature.

Table 16 - Studies addressing intermetallic phases' formation phenomenon in Al-Cu FSW.

Study	Base Materials	Phases Formation Phenomenon	Key highlights
<i>Ouyang et al. (2006)</i>	AA 6061 Pure copper	Constitut. liquation; Solid-state diffusion.	Formation of low melting temperature aluminium-rich phases by constitutional liquation; Copper-rich Cu_9Al_4 phase formed by a solid-state mechanical mixing-based phenomenon; Arising of localised regions with increased potential for the formation of intermetallic phases.
<i>Galvão et al. (2011)</i>	AA 5083 Copper-DHP	Solid-state diffusion.	Formation of both the Al and Cu-rich intermetallic phases governed by a thermomechanically-activated solid-state diffusion phenomenon; Close relation in the amounts of Cu_9Al_4 intermetallic phase and Cu(Al) solid-solution supporting the formation of Cu_9Al_4 by mechanical integration of aluminium in copper.
<i>Liu et al. (2011)</i>	AA 5052 Pure copper	Solid-state diffusion.	High strain rates reached during welding facilitate the interatomic diffusion, under low temperature and short holding times at high temperature; Thin Al-Cu laminae and the fine grain structure formed in the nugget further facilitate the interatomic diffusion.
<i>Genevois et al. (2011)</i>	AA 1050 Pure copper	Solid-state diffusion.	Strong plastic deformation imposed on copper and aluminium facilitates atomic interdiffusion even under low Al-Cu mixing conditions.
<i>Avettand-Fenoël et al. (2012)</i>	AA 6082 Pure copper	Solid-state diffusion.	Increased influence of material flow on intermetallic phases' formation.

3.5.3 - Weld's Intermetallic Content and Phases' Kinetics of Growth

Some recent investigations have been focused on understanding the intermetallic content of the Al-Cu friction stir welds in light of the kinetics of growth of the intermetallic phases during the process. The preferential nucleation of some intermetallic phases in specific zones of the welds, or under particular welding

conditions, has been particularly emphasised. Published works addressing this issue are resumed in **Table 17**.

According to Galvão et al. (2011, 2012a) works, both in Al-Cu butt welding, the preferential nucleation of a specific intermetallic phase is governed by three factors, i.e. the primary chemical composition of the mixing volume (aluminium-rich or copper-rich), the stirring action of the tool and heat-input conditions experienced during welding, which, in turn, were found to depend strongly on the tool design and the rotation and traverse speeds. Specifically, in these works, the intermetallic phase CuAl_2 was predominantly detected over the surface and in the nugget of welds produced with conical and scrolled tools, respectively. In light of the flow mechanisms characterised by Galvão et al. (2010), the formation of this phase was inferred to occur inside the under-shoulder mixing volume, during welding with the conical tool, and inside the shear layer surrounding the pin, during welding with the scrolled tool. Both mixing volumes were found to have a common characteristic, i.e. their aluminium-rich primary composition. On the other hand, the Cu_9Al_4 intermetallic phase, which was predominantly identified in the nugget of welds produced with the conical tool, was inferred to be exclusively formed into the copper-rich shear layer of these welds. The increased temperature and plastic deformation reached in the shear layer were also found to agree well with the exclusive formation of this phase, whose nucleation is less favourable from a thermodynamic-kinetic viewpoint than CuAl_2 , inside this zone. Moreover, much larger amounts of Cu_9Al_4 were found to compose the nugget of welds produced under higher stirring and heat-input conditions, which resulted from increased formation of this phase through the consumption of copper, aluminium and aluminium-rich phases.

Contrary to the previous authors, Avettand-Fenoël et al. (2012), in Al-Cu butt joining, did not notice formation of Cu_9Al_4 intermetallic phase only inside the copper-rich mixing volumes. The formation of this phase was also found to occur in some aluminium-rich volumes, although the primitive chemical composition of the mixing volumes and the thermodynamic-kinetic driving forces for precipitation favoured the formation of CuAl_2 . According to the authors, two factors governed the preferential nucleation of Cu_9Al_4 , i.e. the higher relaxation of local residual stresses promoted by the formation of this phase and its wider solubility range (the kinetics of growth of an intermetallic phase increases with its composition range).

The factors governing the preferential formation of Cu_9Al_4 in the copper-rich mixing volumes, instead of other copper-rich intermetallic phases, such as CuAl , Cu_4Al_3 , whose formation was favoured by the thermodynamic-kinetic driving forces for precipitation, was also investigated by Avettand-Fenoël et al. (2012). The nucleation of CuAl and Cu_4Al_3 was claimed to be hampered by both their higher aluminium content and, similar to that referred above, their narrower compositional range. A brief reference to this aspect had also been previously made by Genevois et al. (2011), in Al-Cu butt welding. However, as opposed to that argued by Avettand-Fenoël et al. (2012), these authors advocated the first nucleation of CuAl and its subsequent transformation into Cu_9Al_4 during cooling.

Table 17 - Studies addressing phases' kinetics of growth in Al-Cu FSW.

Study	Base Materials	Joint Conf.	Key highlights
<i>Galvão et al. (2011)</i>	AA 5083 Copper-DHP	Butt	<p>Preferential nucleation of an intermetallic phase governed by the primary chemical composition of the mixing volume and the stirring/heat-input conditions experienced inside it;</p> <p>CuAl_2 phase formed inside the Al-rich mixing volume at the under-shoulder cavity of conical shoulder tools;</p> <p>Cu_9Al_4 phase formed inside the Cu-rich shear layer surrounding the pin of conical shoulder tools;</p> <p>Increasing formation of Cu_9Al_4 under increasing stirring/heat-input conditions by the consumption of copper, aluminium and aluminium-rich phases.</p>
<i>Genevois et al. (2011)</i>	AA 1050 Pure copper	Butt	<p>Transformation of CuAl into Cu_9Al_4 during the temperature decrease.</p>
<i>Galvão et al. (2012a)</i>	AA 5083 Copper-DHP	Butt	<p>Preferential nucleation of an intermetallic phase governed by the primary chemical composition of the mixing volume and the stirring/heat-input conditions experienced inside it;</p> <p>CuAl_2 phase formed inside the Al-rich shear layer surrounding the pin of scrolled shoulder tools.</p>
<i>Avettand-Fenoël et al. (2012)</i>	AA 6082 Pure copper	Butt	<p>Cu_9Al_4 intermetallic phase formed inside both the Cu-rich and some localised Al-rich mixing volumes;</p> <p>Relaxation of local residual stresses and wide compositional range of Cu_9Al_4 favour the formation of this phase in Al-rich volumes;</p> <p>Formation of CuAl and Cu_4Al_3 in copper-rich volumes hampered by their high aluminium content and narrow compositional range.</p>

Overall remarks on aluminium-copper phases' formation phenomenon

The formation of intermetallic phases in Al-Cu FSW is being increasingly more explored. Important conclusions have been reached on the mechanisms governing the formation of these phases, especially in which concerns to their thermomechanical nature. The intermetallic content of the welds, which is established to depend on the material flow mechanisms, the thermomechanical conditions experienced during the process and the structural properties of the Al-Cu phases, is also becoming better characterised.

3.6 - WELD HARDNESS

Hardness measurements may provide important information concerning the metallurgical and thermomechanical phenomena occurring during welding. The main aim of current section is to conduct an in-depth literature-based characterisation of hardness in Al-Cu FSW. The relation between weld hardness and microstructure is particularly emphasised.

The major phenomena governing hardness in Al-Cu friction stir welds vary significantly according to the microstructural zones of the joints, i.e. the HAZ and TMAZ. Although no deep investigations have been conducted on the microstructure of Al-Cu welds HAZ, the factors governing the hardness in this zone are well-established in light of the extensive research conducted in similar FSW of aluminium and copper. Thermal-imposed variations in grain structure and substructure (recovery and/or grain growth), for non-heat-treatable aluminium alloys and pure copper, and changes in structure and density of strengthening precipitates (coarsening and/or dissolution), for heat-treatable aluminium alloys, are the microstructural phenomena governing the hardness of Al-Cu welds HAZ, for which softening is extensively noticed (Ouyang et al., 2006; Xue et al., 2010, 2011b; Sarrafi et al., 2011; Bisadi et al., 2013; Tan et al., 2013). Even so, some reports of hardness even-match in the HAZ also exist, which is easily explained by the strong scattering existing in the welding conditions studied in Al-Cu FSW literature (Genevois et al., 2011; Liu et al., 2011; Akbari et al., 2013).

As opposed to the HAZ, the hardness in Al-Cu welds TMAZ is not predominantly governed by changes in aluminium and copper microstructure. TMAZ hardness, specifically in the nugget, is essentially governed by the formation of Al-Cu intermetallic phases, whose hardness far exceeds that of the welded materials (Rabkin et al., 1970; Wulff et al., 2004). Actually, from **Table 18**, which displays a compilation of TMAZ hardness peaks reported in Al-Cu FSW literature, it can be observed that the maximum hardness values noticed in the TMAZ were predominantly registered in the Al-Cu interaction patterns with intermetallic content. Nevertheless, few exceptions are also displayed in the table, which correspond to welds in which very incipient formation of intermetallic phases was found to occur. In these particular cases, the effect of the hard intermetallic phases on TMAZ hardness was prevented.

Regarding the most common scenario, TMAZ maximum hardness is found to vary strongly according to the structural properties of the Al-Cu interaction patterns. From the table it can be observed that the interaction features with higher intermetallic content, such as the solidified intermetallic structures noticed by Ouyang et al. (2006) and the homogeneous mixtures registered by Galvão et al. (2010), display much higher hardness values than the Al-Cu patterns with increased heterogeneity and lower intermetallic content, such as the lamellar intercalated features noticed by Ouyang et al. (2006), Liu et al. (2011), Galvão et al. (2012c) and Tan et al. (2013) and the composite-like structures noticed by Xue et al. (2010, 2011b). Even so, it should be noted that the lowest hardness peaks were registered in the composite-like structures, which agrees well with both the lower amounts, and increased scattering, of intermetallic phases in these structures. It can be concluded that the homogeneity and the intermetallic-content of the interaction patterns have strong influence on the maximum hardness reached in the Al-Cu welds.

Unlike to most authors, the maximum hardness values reported by Genevois et al. (2011), Xia-wei et al. (2012) and Galvão et al. (2013) were not registered in Al-Cu interaction patterns. According to **Table 18**, the values noticed by Genevois et al. (2011) and Xia-wei et al. (2012), which were registered in deformed and refined copper zones, respectively, are slightly lower than those registered by Xue et al. (2010, 2011b) in the composite-like structures, which agrees well with the absence of noticeable amounts of intermetallic phases in the TMAZ of these welds. On the other hand, much higher hardness values were noticed by Galvão et al. (2013) in the stirred aluminium region of AA 5083/copper welds. The impressive hardness overmatch reported by these

authors, which was significantly higher than that usually reported in aluminium FSW or friction stir processing (FSP), resulted from the formation of nano-structured aluminium layers during welding, representing an important result aiming the production of high-strength welds.

Table 18 - TMAZ hardness peaks in Al-Cu FSW literature.

Study	Base Materials	Joint Conf.	TMAZ Maximum Hardness	
			Peak Value (HV)	Measuring Zone's Microstructure
<i>Ouyang et al. (2006)</i>	AA 6061 Pure copper	Butt	760	Solidified intermetallic phases (CuAl dendrites).
<i>Galvão et al. (2010)</i>	AA 5083 Copper-DHP	Butt	701 ^a	Homog. mixtures (Cu ₉ Al ₄ -rich).
			518 ^a	Homog. mixtures (CuAl ₂ -rich).
<i>Ouyang et al. (2006)</i>	AA 6061 Pure copper	Butt	178	Intercalated lamellae.
<i>Liu et al. (2011)</i>	AA 5052 Pure copper	Butt	135	Intercalated lamellae.
<i>Galvão et al. (2012c)</i>	AA 6082 Copper-DHP	Butt	312	Intercalated lamellae.
<i>Tan et al. (2013)</i>	5A02 alum. Pure copper	Butt	195	Intercalated lamellae.
<i>Xue et al. (2010)</i>	AA 1060 Pure copper	Butt	126	Composite-like structures.
<i>Xue et al. (2011b)</i>	AA 1060 Pure copper	Lap	130	Composite-like structures.
<i>Genevois et al. (2011)</i>	AA 1050 Pure copper	Butt	125	Deformed copper layer.
<i>Xia-wei et al. (2012)</i>	AA 1350 Pure copper	Butt	120	Refined copper region.
<i>Galvão et al. (2013)</i>	AA 5083 Copper-DHP	Lap	215	Nano-structured aluminium layer.

a - The hardness values were registered in the TMAZ of two welds achieved with distinct welding conditions.

Overall remarks on weld hardness

The hardness of the Al-Cu friction stir welds has been significantly explored in literature. Important relations between weld hardness and microstructure have been established. The intermetallic content and the homogeneity of the Al-Cu interaction structures are well-supported to be the major factors governing the hardness values reached in the welds. The strong overmatch recently achieved in intermetallic-free welds by ultra-refining the microstructure of the welded materials is a prominent result, which will surely impact on Al-Cu FSW development.

3.7 - WELD MECHANICAL STRENGTH AND DUCTILITY

The effectiveness of FSW in aluminium to copper joining is strongly dependent on its ability to provide welds with increased strength and ductility. A literature-based overview of Al-Cu friction stir welds behaviour in tensile and bending testing is displayed in **Table 19**. According to the table, failure in the TMAZ was noticed in most of the studies. Severe material discontinuities and/or extensive amounts of intermetallic phases were reported by the authors, such as Abdollah-zadeh et al. (2008), Firouzdor and Kou (2012) and Bisadi et al. (2013), in Al-Cu lap welding, and Avettand-Fenoël et al. (2010), Liu et al. (2011), Xue et al. (2011a), Galvão et al. (2012c) and Tan et al. (2013), in Al-Cu butt welding, to be the causes governing the premature failure of the welds, both in tensile and bending testing. Additionally, hook-promoted thinning was also pointed by some authors, such as Bisadi et al. (2013), to further limit the mechanical behaviour of Al-Cu lap welds.

Two distinct fracture modes were predominantly noticed in literature for the TMAZ-failed welds, i.e. brittle and decohesive fracture (**Table 19**). Brittle fracture was essentially reported for welds with high intermetallic content (Liu et al., 2011; Firouzdor and Kou, 2012; Bisadi et al., 2013). In turn, decohesive failure was predominantly reported for welds in which incipient base materials interaction was noticed, and consequently, severe metallurgical discontinuities were formed (Avettand-Fenoël et al., 2010; Galvão et al., 2012c; Tan et al., 2013). However, as opposed to most authors, Galvão et al. (2012c) also reported decohesive failure for welds in which

extensive base materials mixing and brittle phases' formation were found to take place. According to them, failure was promoted by metallurgical discontinuities identified at the interface of the intermetallic-rich and the base material layers, which resulted from the strong differences in physical and mechanical properties of the base metals and the Al-Cu phases. This was a very innovative finding, which evidences that the harmful effect of intermetallic phases' formation on the mechanical performance of the Al-Cu welds is not restricted to their brittleness. It is also important to note that, although decohesive and brittle fracture were the prevalent failure modes in the welds, ductile features were noticed by some authors, such as Galvão et al. (2012c), Bisadi et al. (2013) and Tan et al. (2013), in the fracture surfaces of some welds, which resulted from the propagation of the failure over some localised regions of aluminium and copper.

Table 19 also shows that mechanical failure outside TMAZ, specifically in the HAZ or in the base material (BM), was very occasionally noticed in tensile testing. In fact, it was exclusively reported by a small number of authors, such as Abdollah-zadeh et al. (2008), Xue et al. (2011b), Firouzdor and Kou (2012), in Al-Cu lap welding, and Xue et al. (2011a), in Al-Cu butt joining, for a very limited range of welding conditions. Moreover, no relations with base material strength and ductility (efficiency values) were provided by most of these authors, which prevents more supported conclusions regarding the mechanical performance of the welds to be drawn. According to Abdollah-zadeh et al. (2008), the key factor to improve the performance of the welds was to prevent both the severe discontinuities and the extensive amounts of Al-Cu phases formed under very low and very high heat input conditions, respectively. In turn, TMAZs with intermetallic-reinforced microstructures and good metallurgical bonding at the Al/Cu interfacial zones were claimed by Xue et al. (2011a, 2011b) to be an essential requirement to achieve welds with increased strength. Finally, according to Firouzdor and Kou (2012), mechanical performance of Al-Cu lap welds was possible to be improved by welding with a non-conventional joint configuration, which maximised similar bonding and minimised Al-Cu interaction.

Table 19 - Literature-based overview of tensile and bending testing in Al-Cu FSW.

Study	Base Materials	Joint Conf.	Zone	Fracture Characteristics	
				Initiation Site	Mode
Tensile Testing					
<i>Abdollah-zadeh et al. (2008)</i>	AA 1060 Pure copper	Lap	TMAZ	Intermetallic layers; Material discontinuities.	NR
			BM	-----	-----
<i>Avettand-Fenoël et al. (2010)</i>	AA 6082 Pure copper	Butt	TMAZ	Material discontinuities.	Decohesive
<i>Liu et al. (2011)</i>	AA 5052 Pure copper	Butt	TMAZ	Intermetallic layers.	Brittle
<i>Xue et al. (2011a)</i>	AA 1060 Pure copper	Butt	TMAZ	Intermetallic layers; Material discontinuities.	NR
			HAZ	-----	-----
<i>Xue et al. (2011b)</i>	AA 1060 Pure copper	Lap	HAZ	-----	-----
<i>Firouzdor and Kou (2012)</i>	AA 6061 Pure copper	Lap	TMAZ	Intermetallic layers.	Brittle
			HAZ	-----	-----
<i>Tan et al. (2013)</i>	5A02 Al Pure copper	Butt	TMAZ	Material discontinuities.	Decohesive (Ductile)
<i>Bisadi et al. (2013)</i>	AA 5083 Pure copper	Lap	TMAZ	Intermetallic layers; Material discontinuities; Hook structure.	Brittle (Ductile)
Bending Testing					
<i>Xue et al. (2011a)</i>	AA 1060 Pure copper	Butt	TMAZ ^a	Intermetallic layers; Material discontinuities.	NR
<i>Galvão et al. (2012c)</i>	AA 6082 Copper-DHP	Butt	TMAZ	Intermetallic layers; Material discontinuities.	Decohesive (Ductile)

NR - Non-referred.

a - Most of the welds failed at the TMAZ during bending testing.

Overall remarks on weld mechanical strength and ductility

Substantial research has been devoted to the study of the mechanical properties of the Al-Cu friction stir welds. It is well-established that the mechanical success of the welds, which is still far from being achieved consistently, is mostly conditioned by the formation of material discontinuities and extensive amounts of intermetallic phases in the TMAZ. Specifically, the detrimental effect of Al-Cu phases on weld mechanical properties was recently found to go beyond the brittle nature of these compounds, which represents an important advance in this field.

4 - INVESTIGATION OUTPUTS AND FUTURE RESEARCH

Current section has the purpose of presenting the conclusions drawn from the global research as well as directions for future investigation on Al-Cu friction stir weldability.

4.1 - INVESTIGATION OUTPUTS

A detailed and comprehensive investigation, aimed to analyse the friction stir weldability of aluminium to copper, was conducted in this work. The following conclusions were reached:

- The material flow mechanisms in Al-Cu FSW are strongly influenced by the shoulder geometry and the relative positioning of the base material plates.
 - Through-thickness materials mixing and periodic material deposition at the trailing side of the tool occurs during welding with scrolled shoulder tools. On the other hand, during welding with conical shoulder tools, the formation of an intermetallic-rich bulk around the tool constrains base materials mixing to the upper half of the plates' thickness and prevents a regular deposition of the material.
 - Strong base materials interaction, and consequently, extensive formation of intermetallic phases, is promoted by placing the copper alloy at the advancing side of the tool. In turn, significant material expulsion from the joint and incipient Al-Cu mixing occurs during welding with the reverse positioning of the plates, resulting in welds with very irregular morphology.
- The intermetallic content of the Al-Cu weld surface is the key factor affecting surface finishing, being strongly dependent on the shoulder geometry, but insensitive to the tool rotation and traverse speeds. Actually, regardless of the rotation and

traverse speeds, irregular surfaces, with high intermetallic content, are formed in the welds produced with conical shoulder tools. As opposed to this, the surfaces of the welds produced with scrolled shoulder tools are very smooth, regular and intermetallic-free.

- The structural and morphological properties of the Al-Cu weld nugget are strongly influenced by the shoulder geometry and the tool rotation and traverse speeds.
 - The Al-Cu interaction patterns formed in the nugget of the welds produced with scrolled shoulder tools display higher intermetallic content and higher homogeneity, both in morphology and phase content, than those formed in the nugget of the welds produced with conical shoulder tools.
 - Patterns with larger dimension, higher intermetallic content and increased homogeneity are formed, in the nugget of the welds produced with the conical tools, for increasing values of rotation to traverse speed ratio.
- A thermomechanically induced solid-state diffusion phenomenon governs intermetallic phases' formation during Al-Cu FSW.
- The preferential nucleation of a specific intermetallic phase during Al-Cu FSW is governed by three factors - the primary chemical composition of the mixing volume, the stirring action of the tool and the heat-input conditions experienced during welding. These factors are strongly dependent on the shoulder geometry and tool rotation and traverse speeds.
 - The formation of CuAl_2 occurs predominantly inside the aluminium-rich under-shoulder mixing volume, during welding with conical tools, and inside the aluminium-rich shear layer surrounding the pin, during welding with scrolled tools. Thus, this phase is predominantly found over the surface of the welds produced with conical shoulder tools and in the nugget of the welds produced with scrolled shoulder tools.
 - The formation of Cu_9Al_4 intermetallic phase essentially occurs inside the copper-rich shear layer of the welds produced with conical tools. Accordingly, Cu_9Al_4 is predominantly found in the nugget of these welds. For increasing

values of rotation to traverse speeds ratio, much larger amounts of Cu_9Al_4 are formed.

- The spindle torque registered in Al-Cu FSW is highly sensitive to the formation of intermetallic phases and to the volume of material dragged by the tool at each revolution. Specifically, the formation of intermetallic phases has increased influence on the torque registered during dissimilar welding with the copper plate positioned at the advancing side of the tool. In turn, the volume of material dragged by the tool has strong effect on the torque registered during welding with the reverse positioning of the plates.
- Tool offset towards the aluminium side is a very suitable strategy to achieve excellent surface finished Al-Cu welds since it contributes for reducing the intermetallic content of the weld surface. However, this strategy is not effective to improve Al-Cu friction stir weldability, because it does not enable the achievement of desirable weld strength.
- The harmful effect of intermetallic phases' formation on the mechanical performance of the Al-Cu welds is not restricted to their brittleness. Actually, severe metallurgical discontinuities are formed at the interface of the intermetallic-rich layers and the aluminium and copper volumes, resulting from the strong differences in physical and mechanical properties of the base metals and the Al-Cu phases.
- The aluminium alloy type has strong influence on the Al-Cu friction stir weldability. The mechanical behaviour of the aluminium alloys, under the extreme conditions of temperature and plastic deformation occurring during welding, is a factor with major impact on the Al-Cu FSW results.
- Nano-structured aluminium regions are possible to be formed in the nugget of AA 5083/copper friction stir lap welds by using low heat-input conditions during welding. Impressive hardness increase is reached in these structures.

4.2 - FUTURE RESEARCH

Sound Al-Cu friction stir welds, with excellent surface finishing and good mechanical properties, are still far from being achieved consistently. As evidenced in current work, the important differences in physical and mechanical properties of both base metals, as well as their high chemical affinity, hamper the achievement of a suitable window of welding parameters, which enables proper material flow around the tool and, simultaneously, avoids the formation of extensive amounts of intermetallic phases during welding. Actually, aluminium to copper joining by FSW remains a demanding challenge, still requiring extensive research. Future works on Al-Cu friction stir weldability should essentially be focused on non-conventional FSW strategies, such as:

- Development and testing of innovative joint configurations, such as step and wedge-shaped joint geometries, in order to reduce the shoulder-governed Al-Cu mixing, providing intermetallic-free weld surfaces, and to enable proper pin-governed base materials interaction, avoiding the formation of severe discontinuities in the pin influence zone;
- Optimization and testing of stationary shoulder tools, enabling the minimisation of the shoulder-governed heat generation and base materials interaction;
- Testing the use of base materials interlayers, acting as intermetallic phases' formation inhibitors and material flow facilitators.

REFERENCES

- Abdollah-Zadeh, A.; Saeid, T.; Sazgari, B. Microstructural and mechanical properties of friction stir welded aluminum/copper lap joints. *J. Alloys Compd.* **2008**, *460* (1-2), 535–538.
- Akbari, M.; Behnagh, R. A.; Dadvand, A. Effect of materials position on friction stir lap welding of Al to Cu. *Sci. Technol. Weld. Joining* **2012**, *17* (7), 581–588.
- Akbari, M.; Bahemmat, P.; Haghpanahi, M.; Givi, M. -K. B. Enhancing metallurgical and mechanical properties of friction stir lap welding of Al-Cu using intermediate layer. *Sci. Technol. Weld. Joining* **2013**, *18* (6), 518–524.
- Akinlabi, E.; Els-Botes, A.; Lombard, H. Effect of tool displacement on defect formation in friction stir welding of aluminium and copper. In *8th International Symposium on Friction Stir Welding*, Timmendorfer Strand, Lübeck, Germany, May 18–20, 2010 [CD-ROM]; The Welding Institute: Cambridge, 2010.
- Arbegast, W. J. A flow-partitioned deformation zone model for defect formation during friction stir welding. *Scr. Mater.* **2008**, *58* (5), 372–376.
- Arora, A.; Nandan, R.; Reynolds, A. P.; DebRoy, T. Torque, power requirement and stir zone geometry in friction stir welding through modeling and experiments. *Scr. Mater.* **2009**, *60* (1), 13–16.
- ASM International. *Alloy Phase Diagrams*, ASM Handbook series; ASM International: United States of America, 1992.
- Avettand-Fènoël, M. -N.; Taillard, R.; Herbelot, C.; Imad, A. Structure and mechanical properties of friction stirred beads of 6082-T6 Al alloy and pure copper. *Mater. Sci. Forum* **2010**, *638-642*, 1209–1214.

- Avettand-Fenoël, M. -N.; Taillard, R.; Ji, G.; Goran, D. Multiscale study of interfacial intermetallic compounds in a dissimilar Al 6082-T6/Cu friction-stir weld. *Metall. Mater. Trans. A* **2012**, *43* (12), 4655–4666.
- Bisadi, H.; Tavakoli, A.; Sangsaraki, M. T.; Sangsaraki, K. T. The influences of rotational and welding speeds on microstructures and mechanical properties of friction stir welded Al5083 and commercially pure copper sheets lap joints. *Mater. Des.* **2013**, *43*, 80–88.
- Çam, G. Friction stir welded structural materials: beyond Al-alloys. *Int. Mater. Rev.* **2011**, *56* (1), 1–48.
- DebRoy, T.; Bhadeshia, H. K. D. H. Friction stir welding of dissimilar alloys - a perspective. *Sci. Technol. Weld. Joining* **2010**, *15* (4), 266–270.
- Dressler, U.; Biallas, G.; Mercado, U. A. Friction stir welding of titanium alloy TiAl6V4 to aluminium alloy AA2024-T3. *Mater. Sci. Eng., A* **2009**, *526* (1-2), 113–117.
- Firouzdor, V.; Kou, S. Al-to-Cu friction stir lap welding. *Metall. Mater. Trans. A* **2012**, *43* (1), 303–315.
- Galvão, I.; Leal, R. M.; Loureiro, A.; Rodrigues, D. M. Material flow in heterogeneous friction stir welding of aluminium and copper thin sheets. *Sci. Technol. Weld. Joining* **2010**, *15* (8), 654–660.
- Galvão, I.; Oliveira, J. C.; Loureiro, A.; Rodrigues, D. M. Formation and distribution of brittle structures in friction stir welding of aluminium and copper: influence of process parameters. *Sci. Technol. Weld. Joining* **2011**, *16* (8), 681–689.
- Galvão, I.; Oliveira, J. C.; Loureiro, A.; Rodrigues, D. M. Formation and distribution of brittle structures in friction stir welding of aluminium and copper: Influence of shoulder geometry. *Intermetallics* **2012a**, *22*, 122–128.

Galvão, I.; Leitão, C.; Loureiro, A.; Rodrigues, D. M. Study of the welding conditions during similar and dissimilar aluminium and copper welding based on torque sensitivity analysis. *Mater. Des.* **2012b**, *42*, 259–264.

Galvão, I.; Loureiro, A.; Verdera, D.; Gesto, D.; Rodrigues, D. M. Influence of tool offsetting on the structure and morphology of dissimilar aluminum to copper friction-stir welds. *Metall. Mater. Trans. A* **2012c**, *43* (13), 5096–5105.

Galvão, I.; Verdera, D.; Gesto, D.; Loureiro, A.; Rodrigues, D. M. Influence of aluminium alloy type on dissimilar friction stir lap welding of aluminium to copper. *J. Mater. Process. Technol.* **2013**, *213* (11), 1920–1928.

Genevois, C.; Girard, M.; Huneau, B.; Sauvage, X.; Racineux, G. Interfacial reaction during friction stir welding of Al and Cu. *Metall. Mater. Trans. A* **2011**, *42* (8), 2290–2295.

Goran, D.; Ji, G.; Avettand-Fènoël, M. -N.; Taillard, R. Texture and microstructure evolution in friction stir welded Cu-Al sheets characterized by EBSD. *Mater. Sci. Forum* **2012**, *702-703*, 574–577.

Guerra, M.; Schmidt, C.; McClure, J. C.; Murr, L. E.; Nunes, A. C. Flow patterns during friction stir welding. *Mater. Charact.* **2002**, *49* (2), 95–101.

Guo, Y.; Liu, G.; Jin, H.; Shi, Z.; Qiao, G. Intermetallic phase formation in diffusion-bonded Cu/Al laminates. *J. Mater. Sci.* **2011**, *46* (8), 2467–2473.

Kouters, M. H. M.; Gubbels, G. H. M.; Ferreira, O. D. S. Characterization of intermetallic compounds in Cu-Al ball bonds: Mechanical properties, interface delamination and thermal conductivity. *Microelectron. Reliab.* **2013**, *53* (8), 1068–1075.

Krishnan, K. N. On the formation of onion rings in friction stir welds. *Mater. Sci. Eng., A* **2002**, *327* (2), 246–251.

- Leal, R. M.; Leitão, C.; Loureiro, A.; Rodrigues, D. M.; Vilaça, P. Material flow in heterogeneous friction stir welding of thin aluminium sheets: Effect of shoulder geometry. *Mater. Sci. Eng., A* **2008**, *498* (1-2), 384–391.
- Lee, W. -B.; Schmuecker, M.; Mercardo, U. A.; Biallas, G.; Jung, S. -B. Interfacial reaction in steel-aluminum joints made by friction stir welding. *Scr. Mater.* **2006**, *55* (4), 355–358.
- Leitão, C.; Louro, R.; Rodrigues, D. M. Analysis of high temperature plastic behaviour and its relation with weldability in friction stir welding for aluminium alloys AA5083-H111 and AA6082-T6. *Mater. Des.* **2012**, *37*, 402–409.
- Liu, H. J.; Shen, J. J.; Zhou, L.; Zhao, Y. Q.; Liu, C.; Kuang, L. Y. Microstructural characterisation and mechanical properties of friction stir welded joints of aluminium alloy to copper. *Sci. Technol. Weld. Joining* **2011**, *16* (1), 92–99.
- Liu, H. J.; Shen, J. J.; Xie, S.; Huang, Y. X.; Cui, F.; Liu, C.; Kuang, L. Y. Weld appearance and microstructural characteristics of friction stir butt barrier welded joints of aluminium alloy to copper. *Sci. Technol. Weld. Joining* **2012**, *17* (2), 104–110.
- Liu, P.; Shi, Q.; Wang, W.; Wang, X.; Zhang, Z. Microstructure and XRD analysis of FSW joints for copper T2/aluminium 5A06 dissimilar materials. *Mater. Lett.* **2008**, *62* (25), 4106–4108.
- Murr, L. E.; Flores, R. D.; Flores, O. V.; McClure, J. C.; Liu, G.; Brown, D. Friction-stir welding: microstructural characterization. *Mater. Res. Innovations* **1998a**, *1* (4), 211–223.
- Murr, L. E.; Li, Y.; Flores, R. D.; Trillo, E. A.; McClure, J. C. Intercalation vortices and related microstructural features in the friction-stir welding of dissimilar metals. *Mater. Res. Innovations* **1998b**, *2* (3), 150–163.

- Nandan, R.; DebRoy, T.; Bhadeshia, H. K. D. H. Recent advances in friction-stir welding - Process, weldment structure and properties. *Prog. Mater. Sci.* **2008**, *53* (6), 980–1023.
- Okamura, H.; Aota, K. Joining of dissimilar materials with friction stir welding. *Welding International* **2004**, *18* (11), 852–860.
- Ouyang, J.; Yarrapareddy, E.; Kovacevic, R. Microstructural evolution in the friction stir welded 6061 aluminum alloy (T6-temper condition) to copper. *J. Mater. Process. Technol.* **2006**, *172* (1), 110–122.
- Peel, M. J.; Steuwer, A.; Withers, P. J.; Dickerson, T.; Shi, Q.; Shercliff, H. Dissimilar friction stir welds in AA5083-AA6082. Part I: Process parameter effects on thermal history and weld properties. *Metall. Mater. Trans. A* **2006**, *37* (7), 2183–2193.
- Pretorius, R.; Vredenberg, A. M.; Saris, F. W.; Dereus, R. Prediction of phase formation sequence and phase-stability in binary metal-aluminum thin-film systems using the effective heat of formation rule. *J. Appl. Phys.* **1991**, *70* (7), 3636–3646.
- Rabkin, D. M.; Ryabov, V. R.; Lozovskaya, A. V.; Dovzhenko, V. A. Preparation and properties of copper-aluminum intermetallic compounds. *Soviet Powder Metall. Met. Ceram.* **1970**, *9* (8), 695–700.
- Reynolds, A. P. Visualisation of material flow in autogenous friction stir welds. *Sci. Technol. Weld. Joining* **2000**, *5* (2), 120–124.
- Reynolds, A. P. Flow visualization and simulation in FSW. *Scr. Mater.* **2008**, *58* (5), 338–342.
- Saeid, T.; Abdollah-zadeh, A.; Sazgari, B. Weldability and mechanical properties of dissimilar aluminum-copper lap joints made by friction stir welding. *J. Alloys Compd.* **2010**, *490* (1-2), 652–655.

- Sarrafi, R.; Kokabi, A. H.; Gharacheh, M. A.; Shalchi, B. Evaluation of microstructure and mechanical properties of aluminum to copper friction stir butt welds. In *Friction Stir Welding and Processing VI*, Proceedings of the TMS 140th Annual Meeting & Exhibition, San Diego, CA, USA, Feb 27-Mar 3, 2011; Mishra, R. S., Mahoney, M. W., Sato, Y., Hovanski, Y., Verma, R., Eds.; John Wiley & Sons: Hoboken, NJ, 2011; pp 253–264.
- Savolainen, K.; Mononen, J.; Saukkonen, T.; Hänninen, H. A preliminary study on friction stir welding of dissimilar metal joints of copper and aluminium. In *6th International Symposium on Friction Stir Welding*, Saint-Sauveur, Quebec, Canada, Oct 10–13, 2006 [CD-ROM]; The Welding Institute: Cambridge, 2006.
- Schneider, J.; Beshears, R.; Nunes, A. C., Jr. Interfacial sticking and slipping in the friction stir welding process. *Mater. Sci. Eng., A* **2006**, 435-436, 297–304.
- Seidel, T. U.; Reynolds, A. P. Visualization of the material flow in AA2195 friction-stir welds using a marker insert technique. *Metall. Mater. Trans. A* **2001**, 32 (11), 2879–2884.
- Tan, C. W.; Jiang, Z. G.; Li, L. Q.; Chen, Y. B.; Chen, X. Y. Microstructural evolution and mechanical properties of dissimilar Al-Cu joints produced by friction stir welding. *Mater. Des.* **2013**, 51, 466–473.
- Watanabe, T.; Takayama, H.; Yanagisawa, A. Joining of aluminum alloy to steel by friction stir welding. *J. Mater. Process. Technol.* **2006**, 178 (1-3), 342–349.
- Wulff, F. W.; Breach, C. D.; Stephan, D.; Saraswati, T.; Dittmer, K. J. Characterisation of intermetallic growth in copper and gold ball bonds on aluminium metallization. In *6th Electronics Packaging Technology Conference*, Singapore, Dec 8-10, 2004 [CD-ROM]; IEEE: 2004.
- Xia-wei, L.; Da-tong, Z.; Cheng, Q.; Wen, Z. Microstructure and mechanical properties of dissimilar pure copper/1350 aluminum alloy butt joints by friction stir welding. *Trans. Nonferrous Met. Soc. China* **2012**, 22 (6), 1298–1306.

Xue, P.; Xiao, B. L.; Ni, D. R.; Ma, Z. Y. Enhanced mechanical properties of friction stir welded dissimilar Al-Cu joint by intermetallic compounds. *Mater. Sci. Eng., A* **2010**, 527 (21-22), 5723–5727.

Xue, P.; Ni, D. R.; Wang, D.; Xiao, B. L.; Ma, Z. Y. Effect of friction stir welding parameters on the microstructure and mechanical properties of the dissimilar Al-Cu joints. *Mater. Sci. Eng., A* **2011a**, 528 (13-14), 4683–4689.

Xue, P.; Xiao, B. L.; Wang, D.; Ma, Z. Y. Achieving high property friction stir welded aluminium/copper lap joint at low heat input. *Sci. Technol. Weld. Joining* **2011b**, 16 (8), 657–661.

ANNEXES

ANNEX I - Galvão, I.; Leal, R. M.; Loureiro, A.; Rodrigues, D. M. Material flow in heterogeneous friction stir welding of aluminium and copper thin sheets. *Sci. Technol. Weld. Joining* **2010**, *15* (8), 654–660.

<http://dx.doi.org/10.1179/136217110X12785889550109>

The author acknowledges the permission provided by the Institute of Materials, Minerals and Mining, the Maney Publishing and the Science and Technology of Welding and Joining journal for the print and electronic reuse of this paper in current work.

Material flow in heterogeneous friction stir welding of aluminium and copper thin sheets

I. Galvão*, R. M. Leal, A. Loureiro and D. M. Rodrigues

The aim of this investigation was to study material flow during dissimilar friction stir welding of AA 5083-H111 to deoxidised high phosphorus copper plates of 1 mm thickness. The welds were performed using different tool geometries and welding parameters. The positions of the copper and aluminium plates, relative to the advancing and retreating sides of the tool, were also changed. It was found that the tool geometry and relative position of the plates deeply influence the morphology of the aluminium and copper flow interaction zones, influencing the distribution of both materials in the weld and the formation of intermetallic compounds. The material accumulated under the tool during welding was found as another important aspect determining weld morphology.

Keywords: Aluminium, Copper, Welding tool, Material flow

Introduction

Joining dissimilar materials, such as aluminium and copper (Al/Cu) or aluminium and steel (Al/Fe–C), is of great interest in engineering and design applications. Nevertheless, fusion welding of materials with very different melting temperatures and high chemical affinity at elevated temperatures, which gives rise to the formation of brittle intermetallic compounds, makes such joining very difficult and the quality of the welds very poor. In this context, friction stir welding (FSW), which enables the joining of materials at temperatures lower than their melting temperatures, is a promising technology for joining metals with very different chemical and physical properties.¹ However, the use of the process in this type of application is not fully explored, and there are several issues that still require extensive research, such as the development of accurate welding procedures and, for the case of Al/Fe–C joining, the development of adequate FSW tool materials.² Since the main issues regarding the weldability of Al/Cu and Al/Fe–C systems, such as the mixture of both base materials in the solid state and the formation of brittle intermetallic compounds, are common to both dissimilar systems and because the joining of aluminium to copper does not require the production of tools from very expensive materials, this system is considered very interesting for research purposes. However, the limited data already published concerning FSW of aluminium to copper highlight the extremely high difficulty in obtaining welds absent of defects and the scarcity of results regarding the joining of very thin plates.^{3–7} As a matter of fact, obtaining non-defective welds in very thin plates, with

excellent surface finishing and plastic properties, which makes them able to be processed by plastic deformation, represents an additional challenge in the application of this process.

In FSW research, the study of metal flow around the tool during welding is very important to improve process productivity and weld properties. Flow visualisation studies have already been conducted by several authors using different techniques: introducing marker materials into the weld line, using etching contrast to enhance the flow patterns in the weld, welding dissimilar materials and performing numerical simulation studies.^{8–11} Despite the limitations associated with all the techniques used, which are well documented in the literature, the main metal flow mechanisms have already been established, being found that vertical, straight through and rotational flows of plasticised material take place in the vicinity and around the tool, dragging the bulk of the stirred material to a final position behind its original position. In the wake of the weld, behind the travelling tool, material deposition takes place layer by layer, resulting in the formation of the banded structure of the nugget. Variations in tool geometry and/or plate thickness do not change the main flow mechanisms, but greatly influence the amount of material dragged by the shoulder or by the pin, from the retreating and advancing sides of the tool, as well as the periodicity of the deposition at the trailing side of the tool, which, in turn, influences the final morphology of the weld. These aspects can be deduced by comparing the results from Leal *et al.*,¹¹ which studied the influence of the shoulder geometry on material flow in dissimilar FSW of very thin aluminium plates, with those from previous authors working on FSW of thick plates.

Leal *et al.*¹¹ compared the material flow during FSW using scrolled and conical shoulder tools. They reported that, in FSW of very thin AA 5182/AA 6016 plates (1 mm thick), the shoulder influence area extends

CEMUC, Department of Mechanical Engineering, University of Coimbra, Coimbra, Portugal

*Corresponding author, email ivan.galvao@dem.uc.pt

through the entire plate thickness, for both types of tools. They also observed material transported by the shoulder from the advancing to the retreating side, all around the tool, when using the scrolled geometry. For the conical geometry, they observed that the shoulder action depth was different at the leading and trailing sides of the tool. Ahead of the pin, the shoulder influence area extends throughout the thickness, encompassing the pin influence area and causing, at each rotation, layers of the advancing side material to enter a shear layer surrounding the pin. At the rear of the probe, the shoulder influence area is restricted to the top of the weld, promoting the transport of the retreating side material to the advancing side of the tool, where it also enters in the inner shear layer surrounding the pin.

An analysis similar to that performed by Leal *et al.*¹¹ was conducted during the present study, in order to characterise the material flow mechanisms during joining of materials with very different chemical, mechanical and physical properties. Namely, the influence of the tool geometry and welding parameters on material flow during dissimilar FSW of 1 mm thick plates of 5083-H111 aluminium alloy to deoxidised high phosphorus (DHP) copper was analysed.

Experimental

Materials and welding process

In the present study, 1 mm thick plates of oxygen free copper with high phosphorous content (Cu-DHP, R240) and 5083-H111 aluminium alloy (AA 5083-H111) were friction stir butt welded. Four types of welds were performed between the base metals using tools with two different shoulder geometries [conical and scrolled (Fig. 1)] and varying welding parameters (traverse and rotation speeds) in an ESAB LEGIO FSW 3U apparatus. Henceforth, in the text, the welds will be labelled C (conical series) or S (scrolled series) according to the tool used in their production. In the C series of welds, a 14 mm diameter conical tool with a 3° shoulder cavity and a 3 mm diameter cylindrical probe was used. In the S series welds, a tool with a 14 mm diameter scrolled shoulder and a 3 mm diameter cylindrical probe was used. The tilt angles were 2° for the conical tool and 0.5° for the scrolled shoulder tool. The C series welds were performed under load control (700 kg), and the S series welds were carried out under position control, with 0.05 mm penetration depth.

Table 1 displays the full set of welding conditions considered in this study. With reference to the testing conditions, the nomenclature adopted in the text to classify the welds of each series will identify the rotational and welding speeds used, as well as the material positioned at the advancing side of the tool. Thus, the C_1000_16_Cu weld is a C series weld performed with the conical tool, having rotational and welding speeds of 1000 rev min⁻¹ and 160 mm min⁻¹ respectively and with the copper plate positioned at the advancing side of the tool. When the aluminium alloy was positioned at the advancing side of the tool, the last two alphabets in the nomenclature will be Al, as shown in Table 1.

Equipments, techniques and methods

After welding, qualitative and quantitative macroscopic inspections of the weld surfaces were performed by



1 Scrolled tool

means of visual inspection and image data acquisition respectively using ARAMIS optical analysis equipment. Transverse and horizontal cross-sectioning of the welds was also performed for metallographic analysis. The samples were prepared according to standard metallographic practice and differentially etched in order to enable the identification of the different materials in the weld. ‘Modified Poulton’s reagent’ was used to enhance the aluminium and a solution of 5 mL H₂O₂ in 50 mL NH₄OH to enhance the copper. Metallographic analysis was performed using a Zeiss HD 100 optical microscope (Carl Zeiss Inc., Jena, Germany) and a Zeiss magnifier. Microhardness measurements were performed using a Shimadzu microhardness tester (Shimadzu Corp., Kyoto, Japan), with 200 g load and 15 s holding time. The elementary chemical composition (Al/Cu) was determined using electron probe microanalysis in a Cameca Camebax SX50 apparatus (Cameca, Gennevilliers, France). Finally, XRD analysis was performed using a PANalytical X’Pert PRO X-ray diffractometer (PANalytical, Almelo, The Netherlands).

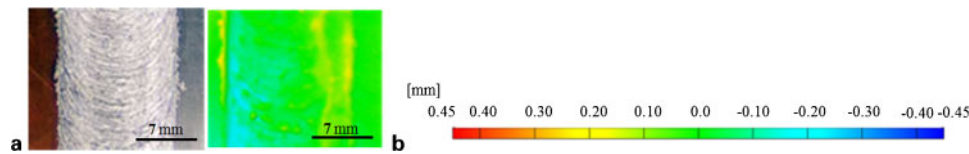
Results

Scrolled weld series

Results of the macroscopic inspection of the S-750_16_Cu weld are shown in Fig. 2. Specifically, Fig. 2a shows a picture of the weld crown, and Fig. 2b shows an image of the same surface, but acquired with an image system that enables the variations in depth inside the weld to be determined. Thus, on the scale at the right side of Fig. 2b, $z=0$ corresponds to the base material plate surface, the negative values in the scale correspond to points inside the weld from which material was removed and the positive values correspond to points inside the weld where material was accumulated. As illustrated in Fig. 2a and b, the S-750_16_Cu weld

Table 1 Welding parameters used to produce the welds

Weld	w, rev min ⁻¹	v, mm min ⁻¹	Advancing side metal
S_750_16_Cu	750	160	Cu-DHP
C_1000_16_Cu	1000	160	Cu-DHP
C_750_16_Al	750	160	AA 5083
C_1000_25_Al	1000	250	AA 5083



2 a crown appearance and b thickness spectrum of S weld

displayed good appearance with highly localised surface irregularities, not exceeding 0.2 mm in depth, which indicates some homogeneity in material deposition at the weld surface.

Figure 3 shows a transverse cross-section of the S-750_16_Cu weld in which the pin and shoulder influence zones are identified. A tongue of grey material going upwards through the advancing side of the weld is clearly visible in this cross-section. A similar weld feature was observed by Leal *et al.*¹¹ in AA 6016/AA 5182 dissimilar welds performed with the same type of tool. Magnifications of the weld features indicated in Fig. 3 by two red rectangles are shown in Fig. 4. These pictures show that the grey tongue in the Al/Cu weld is surrounded by copper and that inside the pin influence area, at the right side of the tongue, there is a clear interface between the two base materials. The very high hardness values displayed in Fig. 4a show the extreme brittleness of the grey tongue.

Chemical analysis, followed by XRD, indicated that the tongue resulted from intense Al/Cu mixture, which led to the formation of large amounts of intermetallic compounds, namely, large amount of CuAl_2 and some Cu_9Al_4 . On the other hand, the chemical and XRD analysis also showed that no material mixing or intermetallic formation occurred at the base material interface displayed in Fig. 4b.

Figure 5 shows macrographs of four horizontal cross-sections of the weld, sampling the zone near the final hole left by the tool at 0.80, 0.71, 0.54 and 0.45 mm from the weld root. The positioning of these sampling planes relative to the weld thickness is indicated in Fig. 4a. Analysing the 0.54 and 0.45 mm cross-sections, as shown in Fig. 5c and d, it is possible to observe a layer of grey material surrounding the hole left by the pin, with deep cracks, which shows its extreme brittleness. This inner layer is surrounded by copper, which, according to the pictures, was dragged by the shoulder from the advancing side of the weld, around the tool, and it was extruded against the inner shear layer at the back of the tool.

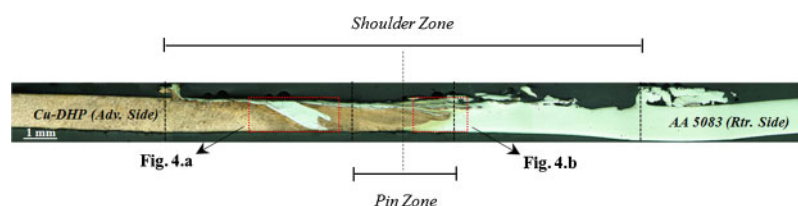
The aluminium alloy, which is the retreating side material, is only dragged into the inner grey layer at the top of the weld, as shown in Fig. 5a and b. In these pictures, it is possible to observe that the aluminium alloy has been pushed towards the advancing side of the weld, at the back of the tool, where materials from all

the layers are pushed into the inner shear layer (1 in Fig. 5a and b). These materials are mixed around the pin and flow, from the top to the bottom of the weld, where the mixture sloughs off in the wake of the weld after one or more rotations, giving rise to the grey tongue visible in the transverse section (2 in Fig. 5a and c). The copper layer, which is dragged by the shoulder around the tool, is extruded against the inner layer at the trailing side of the tool (3 in Fig. 5c). Finally, the aluminium, from the retreating side (4 in Fig. 5c), is extruded against the copper layer giving rise to the interface shown in Fig. 4b. It is important to emphasise that these flow mechanisms are similar to those reported by Leal *et al.*¹¹ in dissimilar joining of very thin aluminium plates.

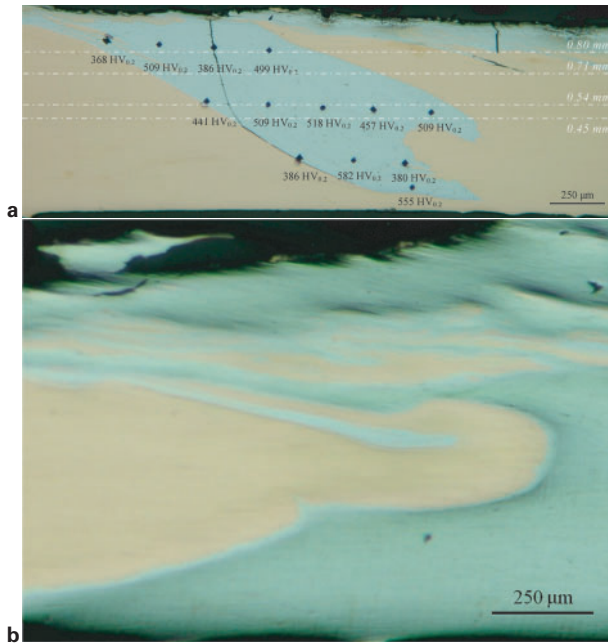
Conical weld series

Figure 6 shows results of the macroscopic inspection of C welds, demonstrating that all the weld crowns are formed of a thick layer of irregularly distributed material. From Fig. 6b, it is possible to observe that for the welds performed with the aluminium on the advancing side (C-750_16_Al and C-1000_25_Al) large amounts of material were dragged from the retreating side (blue areas, 0.45 mm deep) to the advancing side of the tool, where it is accumulated (red areas). Figure 7 shows transverse cross-sections of these welds, which demonstrate that, independent of the welding parameters, the copper is pushed from the retreating to the advancing side of the weld, and the aluminium is expelled from the under shoulder area, giving rise to massive aluminium flash. The onion ring structure characteristic of the welds performed with conical shoulder tools was not formed in these cases. However, under the upper copper layer, at the advancing side of the weld, a very small area of aluminium lamellae with small copper particles embedded on it is formed. XRD analysis indicated that no material mixing or intermetallic formation occurred in this lamellar structure.

Figure 8 illustrates a transverse cross-section of the C-1000_16_Cu weld performed with the copper plate at the advancing side of the tool. As for the previous welds, the weld nugget does not exhibit the classical onion ring structure. The most important features of these welds, outlined in the picture by red rectangles, are the presence of an aluminium layer, which was pushed from the retreating to the advancing side of the weld (1), a clear boundary between the aluminium and copper at the retreating side (2), inside the pin influence area, and



3 Transverse cross-section of S-750_16_Cu weld



a material tongue; b Al/Cu interface

4 Magnifications of zones signalled in Fig. 3

finally, the presence of a dark region extending from the pin influence area to the advancing side of the weld (3).

Figure 9 shows a magnification of the dark region (3) in Fig. 8. Since this picture was taken from the weld without etching, the region displays grey and yellow tones. The hardness measurements presented in the figure and the presence of a crack in the region where the highest hardness values were registered (700 HV0.2) are indicative of great brittleness. A quantitative chemical analysis inside the area indicated in Fig. 9 by a red rectangle identified the presence of both copper and aluminium, which indicates that this area resulted from intense material mixing during welding. XRD analysis identified Cu_9Al_4 in this weld zone.

Macrographs of four weld horizontal cross-sections were registered after polishing, sampling the zone near the final hole left by the tool at 0.74, 0.66, 0.61 and

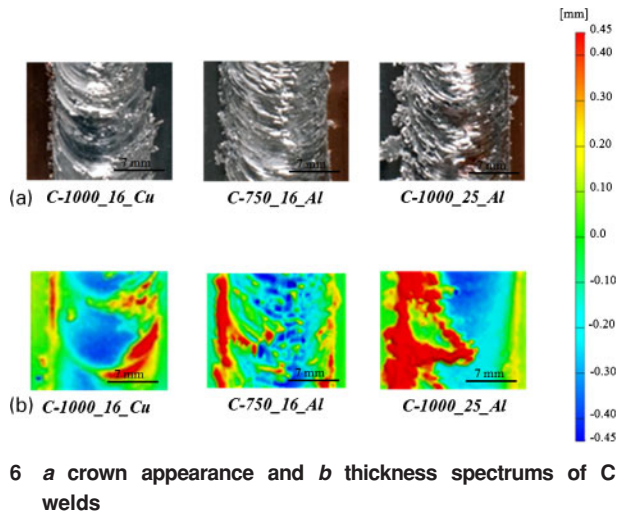
0.41 mm from the weld root. These are shown in Fig. 10. The positioning of these sampling planes relative to the weld thickness is indicated in Fig. 9. From the pictures, it can be concluded that the shoulder influence area was restricted to the top surface of the weld, at the rear of the tool, where it promotes the transport of aluminium from the retreating to the advancing side of the tool. In fact, in the 0.74 and 0.66 mm horizontal sections (Fig. 10a and b), at the rear of the tool, mixed and intercalated layers of aluminium and copper are visible all across the shoulder influence area. On the other hand, in front of the weld, only a very thin layer of copper is visible, which was dragged from the advancing to the retreating side of the weld, inside the pin influence area. In the 0.61 mm horizontal section (Fig. 10c), the quantity of aluminium dragged to the advancing side diminishes drastically. In the lower plane, at 0.41 mm (Fig. 10d), the probe is completely surrounded by copper, and no signs of mixing are visible. Therefore, the mixing of both base materials occurs in the upper half of the plate thickness, in the under shoulder area, giving rise to the dark region shown in Fig. 8. There is also no onion ring structure discernible in this Al/Cu weld.

The Al–Cu mixing area, at the upper middle thickness, displays morphology with fluid-like patterns, as can be seen by analysing Fig. 9. The analysis of the material accumulated in the under shoulder cavity during the process, which was collected at the end of the welding operation (Fig. 11a), also showed fluid-like patterns, as can be observed in Fig. 11b. High hardness values, of the order of those registered in the intermetallic structure of the welds (Fig. 9), were measured for this material, as displayed in Fig. 11b. XRD analysis detected the presence of Cu_9Al_4 . The presence of this intermetallic compound, which has a melting temperature of 1030°C ,^{4,12,13} much higher than the usual FSW temperatures, suggests that an accumulation of solid intermetallic occurs under the shoulder, with detrimental effects on weld surface finishing, as shown in Fig. 6.

XRD analysis also showed that the upper weld layer, as shown in Fig. 6a, has large amounts of Cu_9Al_4 and CuAl_2 . Since the CuAl_2 intermetallic phase has a lower



5 Horizontal cross-sections of S-750_16_Cu weld at a 0.80 mm, b 0.71 mm, c 0.54 mm and d 0.45 mm from root



melting temperature than the FSW process temperatures ($\approx 660^\circ\text{C}$),^{4,12,13} it is possible to assume that this intermetallic will be in a fluidised or extremely plasticised state during the welding operation. The accumulation of intermetallic rich material in the under shoulder cavity and the formation of a fluidised intermetallic layer at the interface between the tool and the base materials will prevent the formation of the solid intercalated onion ring structure characteristic of the conical shoulder welds.

Conclusions

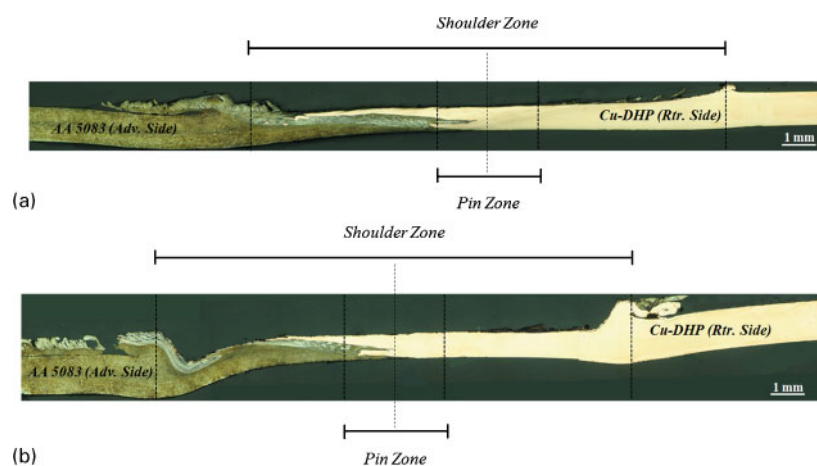
This research showed that material flow mechanisms during Al/Cu FSW are similar to those reported in dissimilar aluminium welding, being strongly conditioned by the shoulder geometry. However, in the particular case of the Al–Cu welds performed with the conical shoulder, a strong influence of base material positioning, relative to the tool rotation direction, in the final weld morphology, was also depicted. Namely, the welds performed with the aluminium placed at the advancing side of the tool were morphologically very irregular, being significantly thinner and exhibiting flash formation due to the expulsion of the aluminium from the weld area. According to the flow mechanisms identified in the paper, during welding, the retreating side material is dragged to the advancing side by the shoulder, at the trailing side of the tool. This

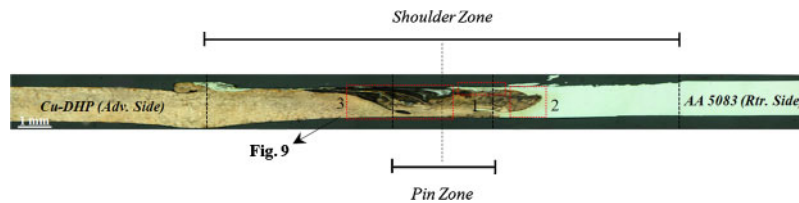
material transport occurs at the top of the plates. Therefore, when the copper alloy is located at the retreating side of the tool, it will be transported by the shoulder to the advancing side, where the aluminium alloy is located.

Mechanical characterisation of the base materials revealed that the aluminium alloy is much softer than the copper alloy. Simultaneously, since the thermal conductivity of the AA 5083 alloy is less than half of that of the Cu-DHP, it is possible to assume that thermal softening will be stronger for this material. Therefore, under the temperature and loading conditions developed in the process, the extremely soft aluminium alloy will be pushed away from the under shoulder area by the copper entering there at each rotation. The aluminium, which is expelled, gives rise to the flash displayed in Fig. 7 for the welds performed with aluminium at the advancing side. No Al/Cu mixing or intermetallic formation takes place under these welding conditions.

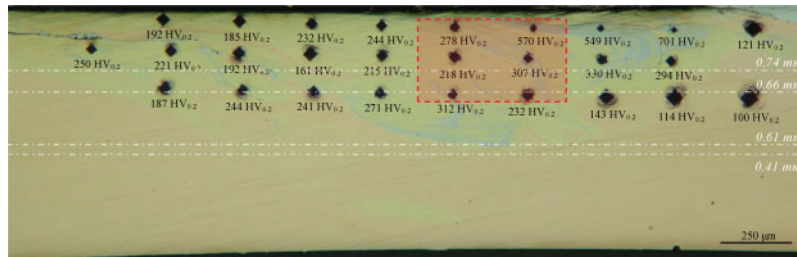
On the other hand, when the aluminium is located at the retreating side of the tool, it will be dragged by the shoulder to the advancing side, where the harder copper plate is located. The very soft aluminium alloy, which is not able to push away the copper from the under shoulder area, will be constrained inside the conical shaped cavity under the shoulder, flowing downward, in the vicinity of the pin, through the cavity, which is formed due to tool traverse motion. Owing to tool rotation, the aluminium is mechanically mixed in the copper matrix giving rise to the intermetallic structures detected in the XRD analysis, at the upper part of the weld. Part of the Al/Cu mixture adheres to the tool, and another part is expelled after some revolutions, giving rise to the very irregular weld crowns displayed in Fig. 6 for the welds performed with the conical tool. The formation of intermetallic structures in the under shoulder area also avoids material mixing through the entire plate thickness and the formation of the typical onion ring structure.

In the case of the scrolled shoulder tool, the two helical flutes (Fig. 1) force the material flow downwards, around the pin, giving rise to through thickness material mixing and periodic material deposition at the rear of the tool, and consequently, very good internal and surface weld morphology. However, the formation of a

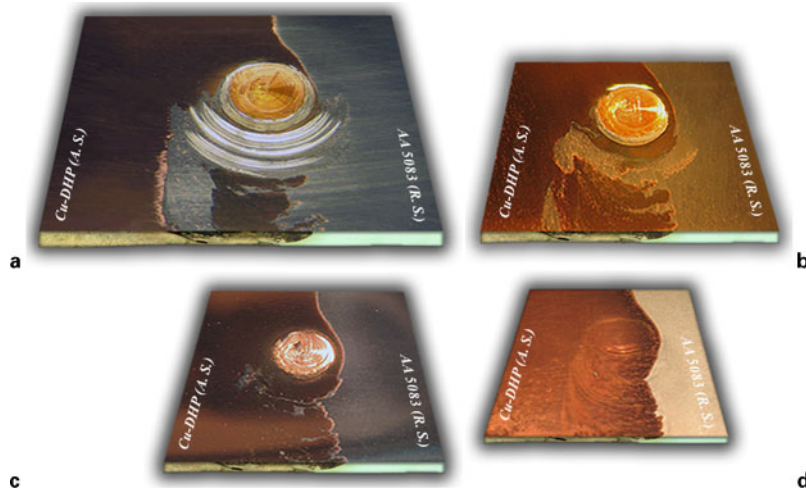




8 Transverse cross-section of C-1000_16_Cu weld



9 Magnification of dark zone signalled in Fig. 8

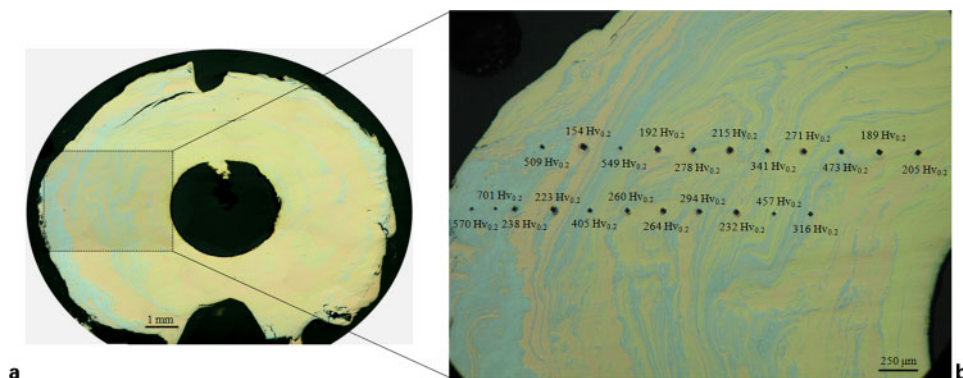


10 Horizontal cross-sections of C-1000_16_Cu weld at a 0.74 mm, b 0.66 mm, c 0.61 mm and d 0.41 mm from root

large volume of material with very brittle intermetallic structures has a very detrimental effect on final weld strength, especially for very thin plates joining.

During the present study, it was also found that the nature of the intermetallics formed during the process

was different for both types of welds, namely, the presence of large amounts of Cu_3Al_4 was detected for the C welds, and CuAl_2 was detected for the S welds, which shows a deep relationship between material flow mechanisms and the formation of intermetallics.



11 a macroscopy and b microscopy of weld material accumulated under tool

Acknowledgement

The authors are indebted to the Portuguese Foundation for the Science and Technology through COMPETE Program from QREN and to FEDER for the financial support.

References

1. T. DebRoy and H. K. D. H. Bhadeshia: 'Friction stir welding of dissimilar alloys – a perspective', *Sci. Technol. Weld. Join.*, 2010, **15**, (4), 266–270.
2. H. K. D. H. Bhadeshia and T. DebRoy: 'Critical assessment: friction stir welding of steels', *Sci. Technol. Weld. Join.*, 2009, **14**, (3), 193–196.
3. A. Abdollah-Zadeh, T. Saeid and B. Sazgari: 'Microstructural and mechanical properties of friction stir welded aluminum/copper lap joints', *J. Alloys Compd.*, 2008, **460**, 535–538.
4. J. Ouyang, E. Yarrapareddy and R. Kovacevic: 'Microstructural evolution in the friction stir welded 6061 aluminum alloy (T6-temper condition) to copper', *J. Mater. Process. Technol.*, 2006, **172**, 110–122.
5. P. Liu, Q. Shi, W. Wang, X. Wang and Z. Zhang: 'Microstructure and XRD analysis of FSW joints for copper T2/aluminium 5A06 dissimilar materials', *Mater. Lett.*, 2008, **62**, 4106–4108.
6. P. Xue, B. L. Xiao, D. R. Ni and Z. Y. Ma: 'Enhanced mechanical properties of friction stir welded dissimilar Al–Cu joint by intermetallic compounds', *Mater. Sci. Eng. A*, 2010, **527**, 5723–5727.
7. H. Okamura and K. Aota: 'Joining of dissimilar materials with friction stir welding', *Weld. Int.*, 2004, **18**, (11), 852–860.
8. R. Nandan, G. G. Roy, T. J. Lienert and T. Debroy: 'Three-dimensional heat and material flow during friction stir welding of mild steel', *Acta Mater.*, 2007, **55**, 883–895.
9. L. Fratini, G. Buffa, D. Palmeri, J. Hua and R. Shivpuri: 'Material flow in FSW of AA7075–T6 butt joints: numerical simulations and experimental verifications', *Sci. Technol. Weld. Join.*, 2006, **11**, (4), 412–421.
10. S. Muthukumar and S. K. Mukherjee: 'Two modes of metal flow phenomenon in friction stir welding process', *Sci. Technol. Weld. Join.*, 2006, **11**, (3), 337–340.
11. R. M. Leal, C. Leitão, A. Loureiro, D. M. Rodrigues and P. Vilaça: 'Material flow in heterogeneous friction stir welding of thin aluminium sheets: effect of shoulder geometry', *Mater. Sci. Eng. A*, 2008, **A498**, 384–391.
12. ASM International: 'ASM handbook', Vol. 3, 'Alloy phase diagram'; 1992, Materials Park, OH, ASM International.
13. D. M. Rabkin, V. R. Ryabov, A. V. Lozovskaya and V. A. Dovzhenko: 'Preparation and properties of copper–aluminum intermetallic compounds', *Poroshk. Metall.*, 1970, **8**, (92), 101–107.

ANNEX II - Galvão, I.; Oliveira, J. C.; Loureiro, A.; Rodrigues, D. M. Formation and distribution of brittle structures in friction stir welding of aluminium and copper: influence of process parameters. *Sci. Technol. Weld. Joining* **2011**, *16* (8), 681–689.

<http://dx.doi.org/10.1179/1362171811Y.0000000057>

The author acknowledges the permission provided by the Institute of Materials, Minerals and Mining, the Maney Publishing and the Science and Technology of Welding and Joining journal for the print and electronic reuse of this paper in current work.

Formation and distribution of brittle structures in friction stir welding of aluminium and copper: influence of process parameters

I. Galvão, J. C. Oliveira, A. Loureiro and D. M. Rodrigues*

Morphological, metallographic and structural analyses of aluminium–copper dissimilar welds produced under different friction stir welding conditions were conducted in order to analyse the mechanisms of intermetallic phases formation, its relation with welding conditions and its consequences in the weld structure and morphology. Under lower heat input conditions, only a thin intermetallic layer distributed along the aluminium/copper interface was depicted inside the nugget. Increasing the heat input promoted material mixing and formation of increasing amounts of intermetallic rich structures. The intermetallic phase content and the homogeneity of the mixed area increased with increasing heat input, evolving from structures containing Al, Cu, CuAl_2 and Cu_9Al_4 to structures predominantly composed of Cu_9Al_4 and $\text{Cu}(\text{Al})$. In order to explain these results, the mechanisms of intermetallic phases formation are discussed, taking into account the process parameters and material flow mechanisms in friction stir welding. Important relations between intermetallic formation and weld surface morphology were also found.

Keywords: Friction stir welding, Aluminium–copper, Welding parameters, Intermetallic phases

Introduction

The industrial application of the friction stir welding (FSW) technology has been driven by its potential for joining materials hardly weldable by traditional fusion processes as well as for dissimilar welding of materials with very different properties, such as aluminium to copper.¹ Although some experiments in the FSW of aluminium to copper have already been reported, successful joining of these metals has not been achieved yet, and several issues still require extensive research.

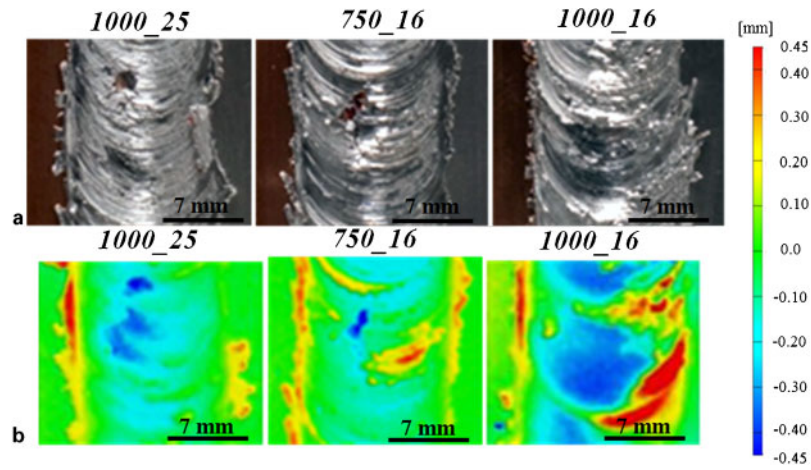
The different physical and mechanical properties of the base materials as well as its chemical affinity make mandatory the optimisation of the welding parameters in order to provide adequate metal flow around the tool and, simultaneously, to prevent the formation of a large amount of brittle Al–Cu intermetallic compounds. Murr *et al.*,² who were the first to analyse Al–Cu friction stir welds, focused their work on the study of the microstructure and metal flow during dissimilar welding of 6 mm thick copper (99.9%) to 6061-T6 aluminium. Their microstructural analysis allowed observing complex intercalated microstructures, with vortices throughout the weld zone, resulting from welded metals overlapping. Some years later, Ouyang *et al.*³ studied the microstructure of 12.7 mm thick copper (99.9%) to 6061-T6 aluminium friction stir welds, detecting the

presence of a mixed region with several intermetallic compounds, such as CuAl_2 , CuAl and Cu_9Al_4 . Ouyang *et al.*³ also observed a high disparity of mechanical properties in the nugget of the welds, specifically the hardness, which varied between 136 and 760 HV0.2. More recently, Xue *et al.*⁴ analysed 5 mm thick copper (99.9%) to 1060 aluminium friction stir welds. The authors observed in the nugget of the welds a bottom zone with a composite structure, which was formed by particles with different sizes dispersed in the aluminium matrix. The particles, mainly composed of CuAl_2 , Cu_9Al_4 and low amounts of CuAl , formed a local composite structure with higher mechanical properties than the aluminium base material. The formation of a continuous, thin and uniform intermetallic layer at the Al/Cu interface was also reported. This layer was predominantly formed of CuAl_2 at the aluminium side and Cu_9Al_4 at the copper side. Finally, Galvão *et al.*,⁵ Xue *et al.*⁶ and Liu *et al.*⁷ reported the extremely high difficulty in producing non-defective Al–Cu welds with suitable surface finishing by comparing welds produced under different FSW conditions.

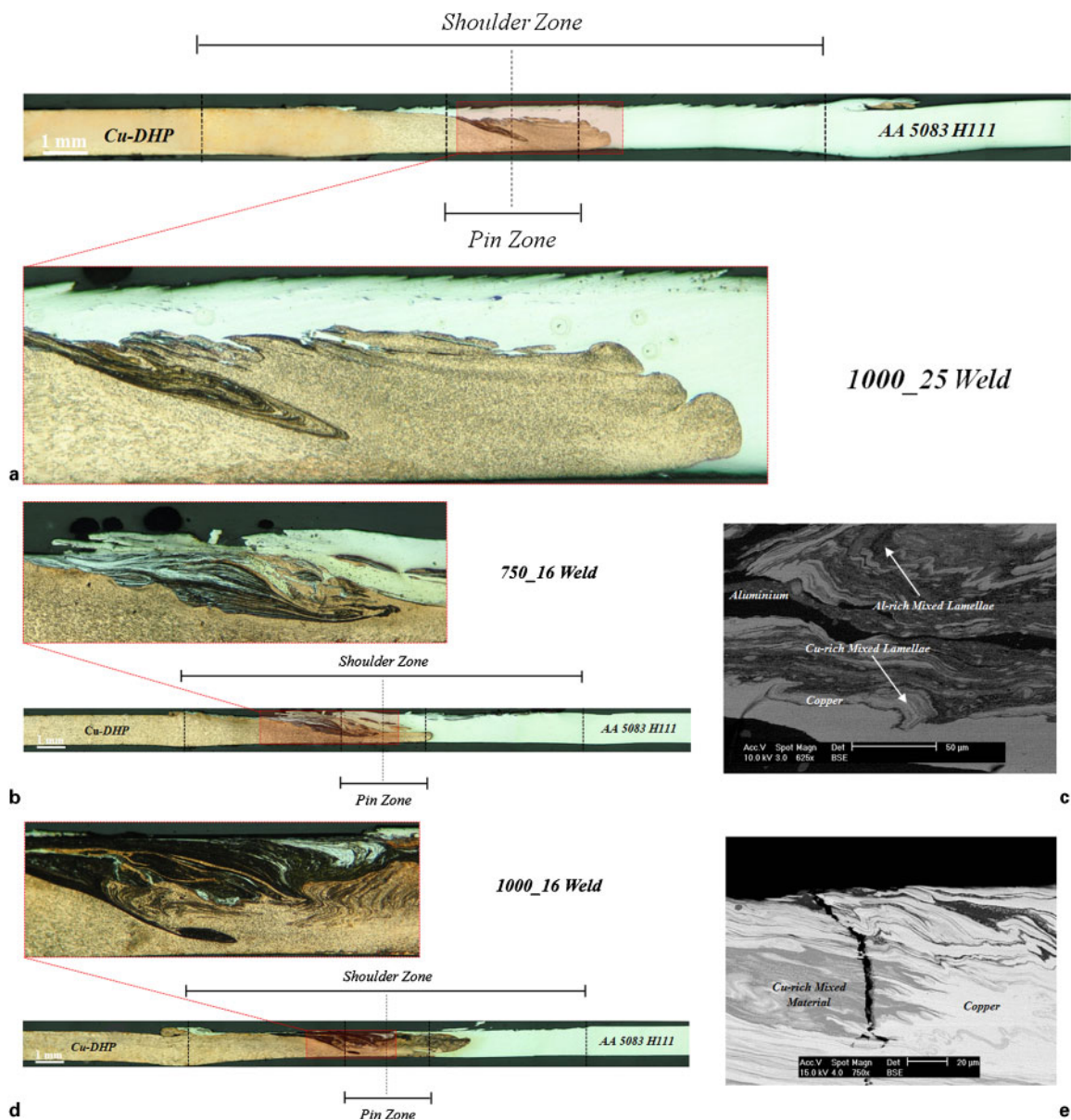
According to previous authors, the occurrence of important flow defects, the poor surface finishing and the formation of large amounts of brittle intermetallic structures in the nugget are the main problems in Al–Cu friction stir weldability. Comparing the data already published concerning the FSW of aluminium to copper also highlights the large scatter in welding results and the lack of information concerning the influence of the process parameters in intermetallic phase formation and

CEMUC, Department of Mechanical Engineering, University of Coimbra, Rua Luís Reis Santos, Coimbra 3030-788, Portugal

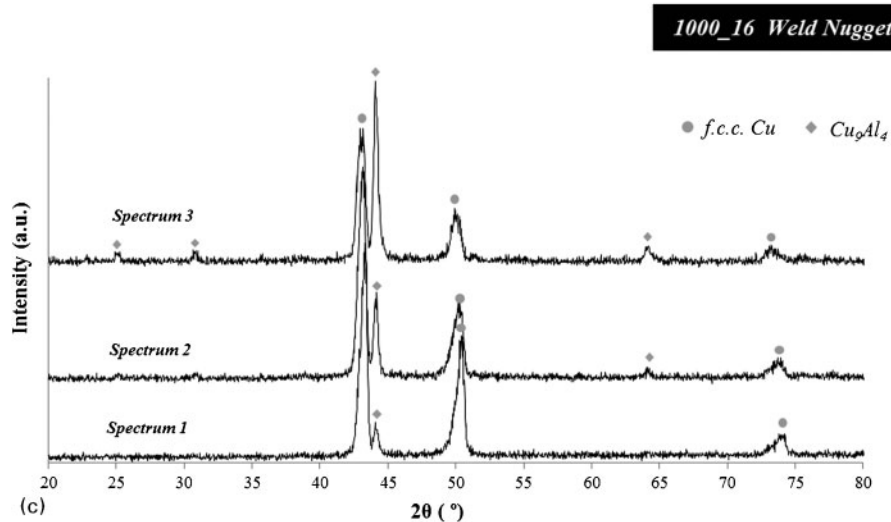
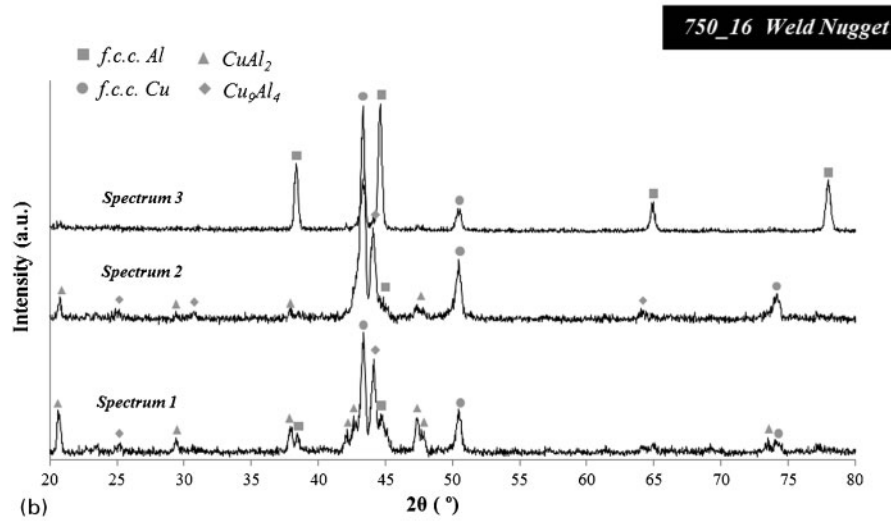
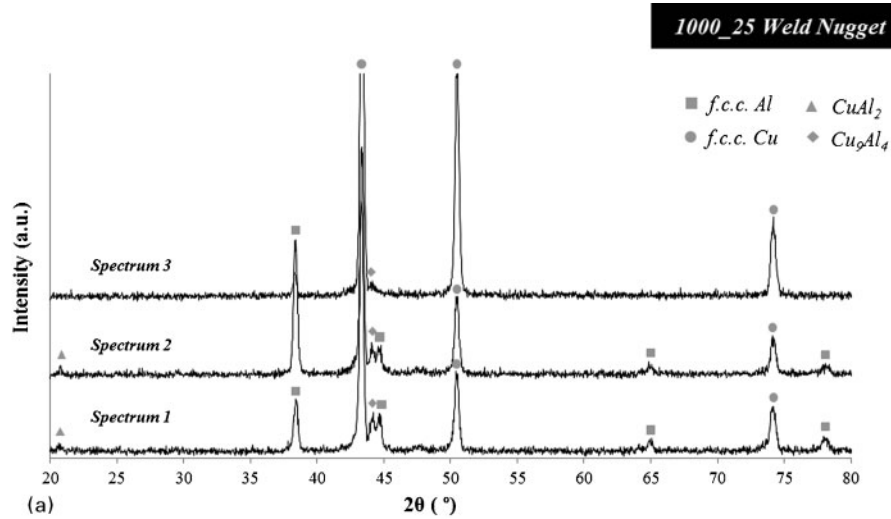
*Corresponding author, email dulce.rodrigues@dem.uc.pt



1 a images and b thickness spectra of weld crowns



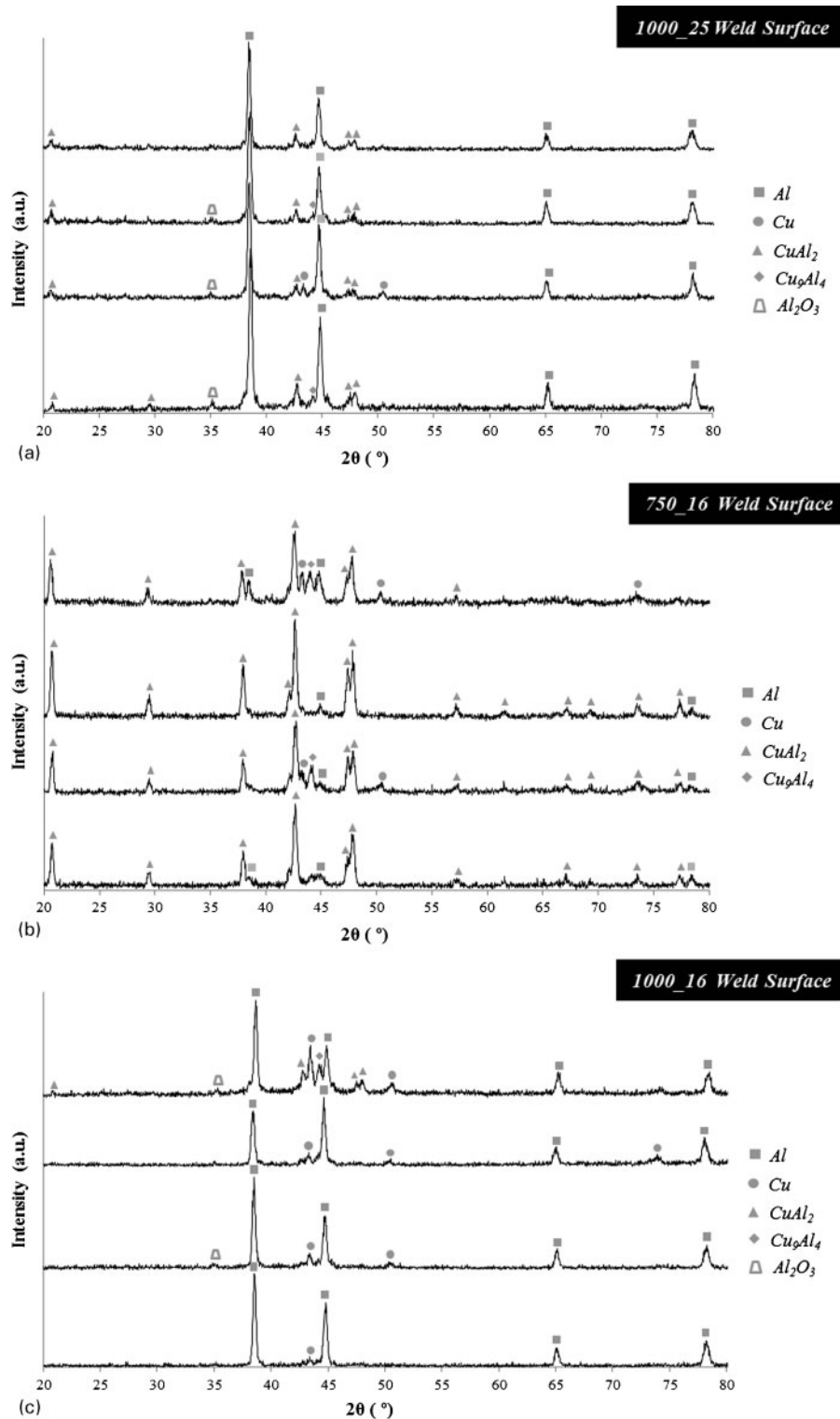
2 Macrographs of traverse cross-sections of a 1000_25, b 750_16 and d 1000_16 welds and backscattered electron (BSE) images of mixing zone of c 750_16 and e 1000_16 welds



3 Results of XRD analysis performed in nugget of a 1000_25, b 750_16 and c 1000_16 welds

Table 1 Welding parameters used to carry out welds

Weld	Rotational speed/rev min ⁻¹	Traverse speed/mm min ⁻¹	ω/v ratio/rev mm ⁻¹
1000_25	1000	250	4.0
750_16	750	160	4.7
1000_16	1000	160	6.3



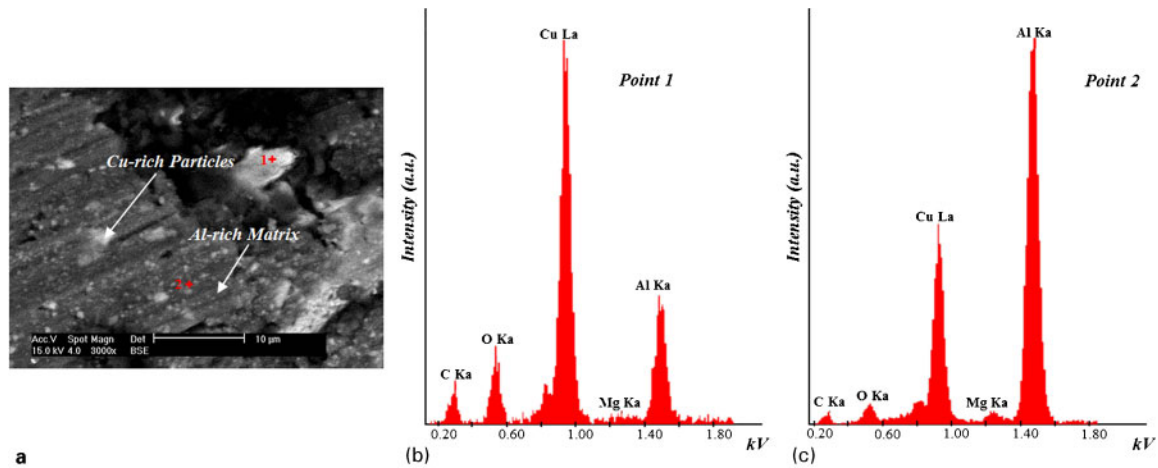
4 Results of XRD analysis performed on surface of a 1000_25, b 750_16 and c 1000_16 welds

its consequences in weld microstructure and morphology. This was the main objective of the current study, in which dissimilar friction stir welds of 1 mm thick plates of Cu-DHP and AA 5083-H111 were analysed.

Experimental

In the present work, 1 mm thick plates of oxygen free copper with high phosphorous content (Cu-DHP, R 240) and 5083-H111 aluminium alloy (AA 5083-H111) were friction stir butt welded. The welds were performed

between the base materials using different processing parameters (varying traverse and rotation speeds) in an ESAB LEGIO FSW 3U equipment. A 14 mm diameter H13 steel tool with a 3° shoulder conical cavity and a 3 mm diameter cylindrical probe was used. The welds were produced with no tool's horizontal offset, under load control (700 kg) and using a tool tilt angle of 2°. Based on a previous study⁵ and in order to obtain the most adequate metal flow around the tool, the harder Cu-DHP plate was positioned at the advancing side of the tool in all the welds.



5 Image (BSE) registered on surface of a 1000_25 weld and EDS spectra acquired in b copper rich and c aluminium rich zones

Table 1 displays the welding conditions used in this study. With reference to the testing conditions, the nomenclature adopted in the text to classify the welds identifies the rotational and welding speeds used. Thus, weld 750_16 is a weld performed with the rotational and welding speeds of 750 rev min^{-1} and 160 mm min^{-1} respectively. The tool rotation/tool traverse speed ratio ω/v , which is usually assumed as proportional to the heat input during the welding process,⁸⁻¹² is also presented in Table 1. The 1000_25 welding conditions ($\omega/v=4.0 \text{ rev mm}^{-1}$) will conduct to the lowest heat input during welding and the 1000_16 to the highest heat input ($\omega/v=6.3 \text{ rev mm}^{-1}$).

After welding, qualitative and quantitative macroscopic inspections of the weld surface were performed by visual inspection and image data acquisition using the ARAMIS optical analysis equipment respectively. The ARAMIS equipment enables to determine the variations in depth, inside the weld, relative to the base materials' plate surfaces. Transverse cross-sectioning of the welds was performed for metallographic analysis. The samples were prepared according to standard metallographic practice. Metallographic analysis was performed using optical microscopy in a Zeiss HD 100 equipment. Scanning electron microscopy/energy dispersive X-ray spectroscopy (SEM/EDS) and micro-X-ray diffraction (XRD) were performed in the cross-section and on the surface of all the welds using a Philips XL30 SE microscope and a PANalytical X'Pert PRO microdiffractometer respectively. Fittings of the XRD patterns were performed with the PROFIT V1c software from Philips Electronics using pseudo-Voigt functions.

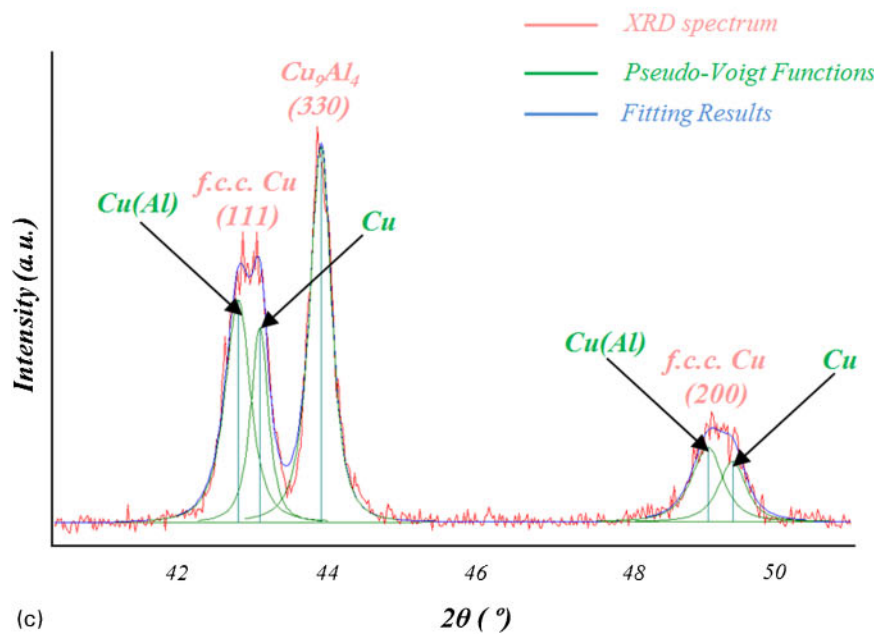
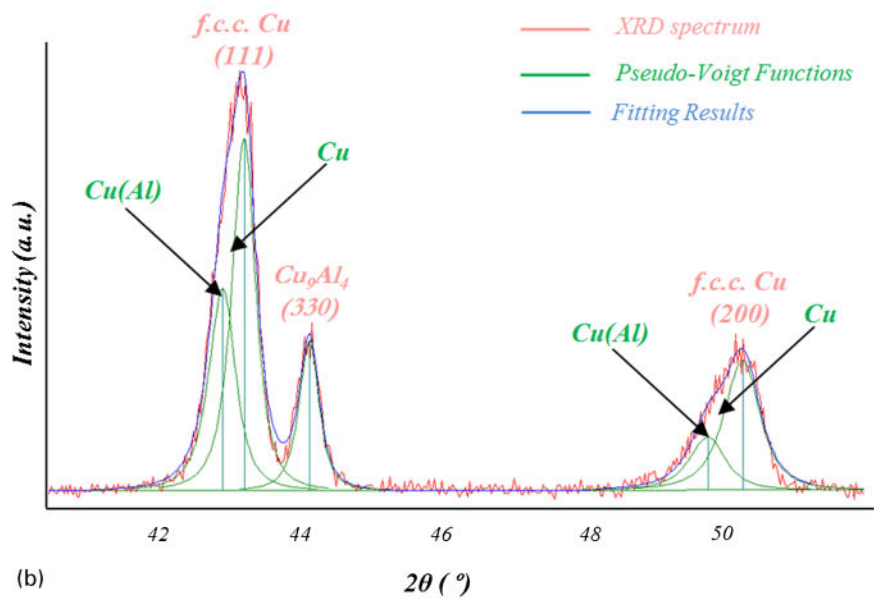
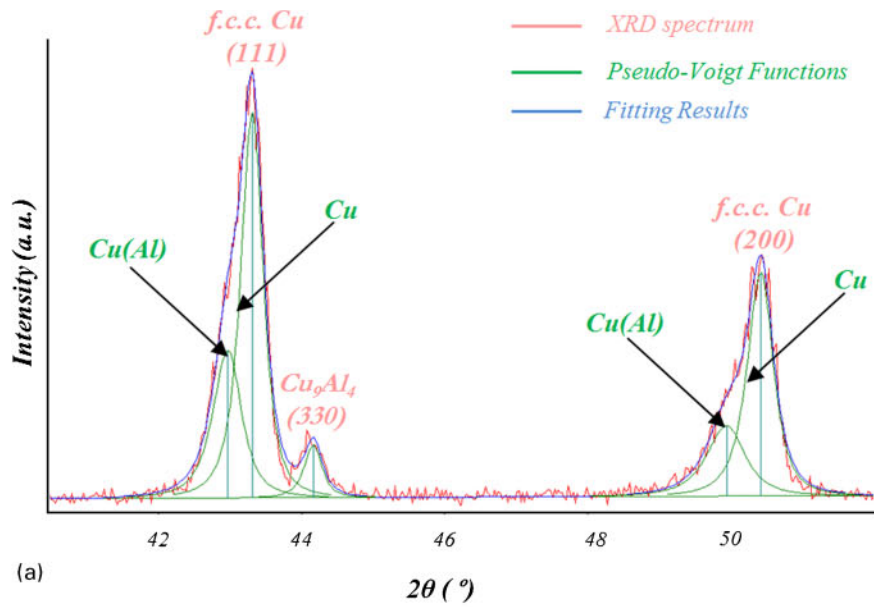
Weld morphology and structure

Results of the visual inspection of the weld surface are shown in Fig. 1. From Fig. 1a, it is possible to conclude that all the weld crowns are formed by a silver layer of irregularly distributed material. Figure 1b shows areas with significant accumulation of material (red areas) and areas with severe material absence (blue areas), which emphasises the strong discontinuity in material deposition during the process. This type of surface finishing, which is usual in dissimilar aluminium to copper friction stir welds^{5-7,13} but never observed in Al-Al or Cu-Cu

similar welds, constitutes one of the main concerns in Al-Cu joining due to its detrimental effect in both weld appearance and resistance.

Figure 2 displays optical macrographs of the transverse cross-sections of the welds and SEM images, acquired in backscattered electron (BSE) mode, of the selected weld areas. In order to facilitate the analysis, the pin and shoulder influence areas are indicated in each cross-section using vertical lines. Comparing all the macrographs, two common features can be observed: the presence of an aluminium layer at the top of all the welds, which was pushed from the retreating to the advancing side of the tool, and the presence of copper at the bottom of the welds. Despite these similarities, significant differences can also be observed by comparing the different nugget morphologies.

As shown in Fig. 2a, in the 1000_25 weld, which was obtained under the lowest heat input conditions ($\omega/v=4.0 \text{ rev mm}^{-1}$), the base materials are completely separated by a sharp and well defined interface at the weld nugget. The low heat input did not provide enough energy for material mixing, which resulted in an interface morphology similar to that obtained by other authors when performing friction diffusion bonding.¹⁴ In the 750_16 weld ($\omega/v=4.7 \text{ rev mm}^{-1}$), shown in Fig. 2b, a mixed region is observed, composed of bright and dark zones, extending to the copper side of the pin zone. The BSE image in Fig. 2c, which was acquired inside this area, displays complex mixing patterns composed of layers of copper and aluminium alternated with copper or aluminium rich mixed lamellae. In the weld produced under the highest heat input conditions ($\omega/v=6.3 \text{ rev mm}^{-1}$), i.e. the 1000_16 weld (Fig. 2d), the top aluminium layer is only visible in the upper right part of the pin zone and is much thinner than in the previous welds. In this weld, a large mixing area, embedded in a copper matrix, is observed. The mixing zone is much larger than in the previous welds, extending out of the pin zone through both the aluminium and copper sides of the weld. Furthermore, the BSE image in Fig. 2e, which was acquired in this mixing area, shows an almost homogeneous mixture, in which only copper and copper rich mixed structures are discernible. It is important to note the presence of a crack, which propagates along the mixing patterns,



6 Magnification and fitting analysis of strongest Cu_9Al_4 and fcc Cu peaks of XRD spectra a 1, b 2 and c 3, acquired in nugget of 1000_16 weld

indicating the extreme brittleness of these structures. Comparing all the welds in Fig. 2, it is possible to conclude that increasing the heat input resulted in the formation of mixed material zones with increasing dimension and homogeneity.

The results of the XRD analysis performed in three different locations of the weld nugget are shown in Fig. 3. All the XRD patterns obtained in the 1000_25 weld nugget (Fig. 3a) show intense fcc Al and fcc Cu peaks corresponding to the aluminium and copper parts of the nugget. Low intensity XRD peaks indexed to the intermetallic compounds Cu_9Al_4 and CuAl_2 are also detected (spectrum 2 in Fig. 3a). Although no important Al–Cu mixing area has been depicted in the cross-section of the nugget (Fig. 2a), Al was extruded against the Cu at the top of the weld, giving rise to the formation of small amounts of these intermetallic phases at the interface. Once again, these results are very similar to that obtained by other authors using friction diffusion bonding.¹⁴

For the 750_16 weld (Fig. 3b), zones with base material composition, mixing regions with significant amounts of fcc Cu, fcc Al, Cu_9Al_4 and CuAl_2 and mixing areas only composed of fcc Cu and Cu_9Al_4 were identified. This complex distribution of phases is in accordance with the heterogeneous morphology of the mixing structures already depicted in Fig. 2c. Finally, for the 1000_16 weld, which has the most homogeneous mixing area in the nugget (Fig. 2e), only fcc Cu and Cu_9Al_4 were detected in the nugget by XRD (Fig. 3c).

Comparing all the spectra in Fig. 3, it is possible to conclude that the composition of the nugget, similar to the nugget morphology, evolves with heat input, since increasing the ω/v ratio increases the amount of intermetallic phases and the homogeneity in composition of the nugget. In fact, whereas for the 750_16 weld both CuAl_2 and Cu_9Al_4 were detected, for the 1000_16 weld, corresponding to the highest heat input welding conditions, only Cu_9Al_4 was detected.

Figure 4 shows the results of the XRD structural analysis of the silver layer on top of the welds, which is shown in Fig. 1. From the spectra, it is possible to conclude that fcc Al is the predominant phase on the top layer of all the welds. Significant amounts of CuAl_2 and residual amounts of Cu_9Al_4 and fcc Cu are also discernible in the diffractograms. In addition to the Cu–Al system phases, the formation of minor amounts of cubic Al_2O_3 was also observed, which indicates that surface oxidation occurred during or after the FSW process. A BSE image and EDS spectra registered for the 1000_25 weld crown are shown in Fig. 5, where it is possible to see that the top layer of this weld has copper rich particles (Fig. 5b) embedded in an Al–Cu mixed matrix (Fig. 5c). The Al–Cu matrix consists of a mixture of CuAl_2 and Al, and the Cu richer particles correspond to the Cu and/or Cu_9Al_4 phases detected by XRD. The same type of morphology was registered for the other two welds. Therefore, the thick and irregular surface of the welds results from the deposition of an intermetallic rich layer, with physical and mechanical properties quite different from those of both base materials. The differences in the amount of the different phases, which can be depicted by comparing the diffractograms in Fig. 4, can be attributed to the strong irregularity of the material deposition process at the top of the weld, which was already discussed when analysing Fig. 1.

Another important aspect to retain from previous analysis is that whereas in the nugget the structure and composition clearly evolve by changing process parameters (compare Figs. 2 and 3), at the weld surface, the structure and composition are very similar, independent of the welding conditions (compare Figs. 1 and 4). This has to be a consequence of the concurrent effect of material flow in the FSW and the mechanisms of intermetallic phase formation, as will be analysed in the next section.

Analysis of intermetallic phase formation

According to Ouyang *et al.*,³ the formation of intermetallic phases cannot be exclusively understood based on the Al–Cu phase diagram,¹⁵ since the chemical reactions occurring under the thermal cycles imposed by the FSW process are far from the equilibrium conditions. Furthermore, the melting temperature of the Cu_9Al_4 intermetallic phase (1030°C)¹⁶ is quite higher than the peak temperatures registered during Al–Cu FSW.^{3,7} Therefore, only a thermomechanically induced solid state diffusion process can justify the formation of this high melting temperature intermetallic phase under FSW thermal conditions.

In this work, the highest amount of Cu_9Al_4 was detected in the 1000_16 weld nugget. Figure 6 shows the (111) and (200) fcc Cu peaks and the (330) Cu_9Al_4 peak of the diffractograms of Fig. 3c. In addition to the XRD patterns (in red), the results of the fitting with pseudo-Voigt functions (in blue and green) are also presented in the figure. Analysing the figure, it is possible to conclude that the (111) and (200) Cu diffraction peaks in Fig. 6a are highly asymmetrical, presenting a shoulder at lower diffraction angles. Both peaks can be fitted with two contributions, one with 2θ value corresponding to the Cu base material, and another with lower intensity and centred at lower diffraction angles, which corresponds to a solid solution of Cu(Al). Both phases are also present in the diffraction patterns of Fig. 6b and c, although the intensity of the diffraction peaks indexed to the Cu(Al) solid solution in Fig. 6c is higher than that indexed to the Cu base material. It is also important to observe that despite the fact that the relative intensities of the Cu and Cu(Al) contributions differ from figure to figure, the amounts of Cu_9Al_4 and Cu(Al) formed in the different zones of the nugget are closely related. Higher amounts of Cu(Al) correspond to higher amounts of Cu_9Al_4 and vice versa.

Since the formation of the Cu(Al) solid solution results from the incorporation of Al atoms in the Cu structure,³ it can be argued that Cu_9Al_4 formation follows the same mechanism. During FSW, the incorporation of Al atoms in the Cu matrix can be assumed as a mechanical process, which results from the stirring action of the tool, pushing aluminium from its retreating side and copper from its advancing side into the inner shear layer surrounding the pin. This assumption is based on the results of a deep analysis of the material flow mechanisms during dissimilar Al–Cu FSW, which can be found in Ref. 5. The shear layer materials, which complete one or more revolutions around the pin before being extruded against the retreating side at the back of the tool, are subjected to extremely intense plastic

deformation, which, according to some authors, enhances the solid state diffusion rates in solid state joining processes.^{17–24} Increased atomic diffusion rates enable achieving a suitable atomic concentration for Cu_9Al_4 formation even at low FSW temperatures. The occurrence of favourable conditions for Cu_9Al_4 formation, mainly at the shear layer surrounding the pin, with a copper rich composition, is the reason why this intermetallic compound was detected in large amounts when analysing the weld cross-section, but only in small amounts at the weld surface. Once again, the FSW material flow mechanisms analysed by Galvão *et al.*⁵ are on the basis of current assumption.

Concerning the CuAl_2 phase, previous studies reported that this compound has an enthalpy of formation significantly lower than the Cu_9Al_4 .^{25,26} Effectively, from the Al–Cu equilibrium diagram, it is possible to observe that the formation of this phase results from a peritectic reaction, which occurs at 590°C .^{3,15} However, during FSW, the formation of this compound should also be explained based on a thermomechanically induced solid state diffusion process, since, although its melting temperature is close to the FSW temperatures, no solidification structures such as primary dendrites of Al and CuAl_2 and/or Al– CuAl_2 eutectic structures were detected in the SEM analysis. Nevertheless, since the temperatures achieved during FSW are close to the CuAl_2 melting temperature, the formation of this intermetallic occurs wherever the suitable atomic concentrations are locally achieved, which easily occurs at the weld surface, where the shoulder drags large amounts of aluminium from the retreating side of the tool against the copper plate surface at the advancing side. This mechanism also explains the presence of large amounts of CuAl_2 at all weld surface, independent of the welding parameters in use. By increasing the heat input, increasing amounts of both Al and CuAl_2 will be dragged by the shoulder into the inner shear layer surrounding the pin, where chemical and thermomechanical conditions for the formation of Cu_9Al_4 exist. In fact, the cross-sections in Fig. 2 show that the shear layer dimensions increase with increasing heat input, while the upper aluminium layer tends to disappear.

Finally, the XRD results in Fig. 3c showed the absence of CuAl_2 in the nugget of the 1000_16 weld, produced under the highest heat input conditions, which can be explained assuming the occurrence of structural evolution of the CuAl_2 into Cu_9Al_4 , inside the shear layer. In fact, an investigation conducted by Wang *et al.*,²⁵ which was aimed to study the combustion synthesis of copper aluminides, reported that for copper rich mixtures, the formation of Cu_9Al_4 and solid solution of aluminium in copper is possible through the consumption of Cu, Al, CuAl and CuAl_2 . Since in the present study CuAl_2 was detected on the surface of all the welds, independently of nugget phase composition, it is possible to assume that CuAl_2 present at the weld surface results mainly from base material stirring under the shoulder, where large amounts of aluminium are stirred against the copper surface.⁵ In the course of the dynamic material flow process, the materials under the shoulder are incorporated in the shear layer surrounding the pin,^{5,27} where material mixing and plastic deformation are extremely intense, and conditions for Cu_9Al_4 formation will be reached under appropriate heat input conditions.

Conclusions

The influence of the welding parameters on brittle intermetallic phase formation and distribution during aluminium to copper FSW was investigated. It was observed that increasing the heat input, by performing welds under higher ω/v ratio, resulted in the formation of mixed material zones with increasing dimension and homogeneity. The morphology of the mixing zones and the type and amount of the intermetallic phases, which were found to result from a thermomechanically induced solid state process, are also strongly dependent on the welding parameters. In fact, under lower heat input conditions, no important mixing patterns were found in the nugget, indicating the formation of an interface morphology similar to that obtained by other authors when performing friction diffusion bonding. On the other hand, increasing the ω/v ratio, the weld nuggets displayed heterogeneous phase composition, with significant amounts of both base materials (Al and Cu) as well as some quantities of CuAl_2 and Cu_9Al_4 intermetallic phases. For the welds obtained under the higher ω/v ratio, only Cu, $\text{Cu}(\text{Al})$ solid solution and Cu_9Al_4 were registered. The structural evolution of the CuAl_2 intermetallic phase, under the mechanical conditions developed inside the shear layer surrounding the pin, was pointed as one of the reasons for the formation of increasing amounts of Cu_9Al_4 and $\text{Cu}(\text{Al})$ under higher heat input conditions. Finally, it was found that the rough and irregular crowns, characteristic of dissimilar aluminium to copper friction stir welds, result from the formation of a CuAl_2 rich layer under the shoulder, at the weld surface, which is irregularly distributed at the trailing side of the tool during the welding process.

Acknowledgements

The authors are indebted to the Portuguese Foundation for the Science and Technology (FCT) and FEDER for the financial support and to company Thyssen Portugal – Aços e Serviços Lda for providing the heat treatments for the FSW tools.

References

1. T. DebRoy and H. K. D. H. Bhadeshia: 'Friction stir welding of dissimilar alloys – a perspective', *Sci. Technol. Weld. Join.*, 2010, **15**, (4), 266–270.
2. L. E. Murr, Y. Li, R. D. Flores, E. A. Trillo and J. C. McClure: 'Intercalation vortices and related microstructural features in the friction-stir welding of dissimilar metals', *Mater. Res. Innov.*, 1998, **2**, 150–163.
3. J. Ouyang, E. Yarrapareddy and R. Kovacevic: 'Microstructural evolution in the friction stir welded 6061aluminum alloy (T6-temper condition) to copper', *J. Mater. Process. Technol.*, 2006, **172**, 110–122.
4. P. Xue, B. L. Xiao, D. R. Ni and Z. Y. Ma: 'Enhanced mechanical properties of friction stir welded dissimilar Al–Cu joint by intermetallic compounds', *Mater. Sci. Eng. A*, 2010, **A527**, 5723–5727.
5. I. Galvão, R. M. Leal, A. Loureiro and D. M. Rodrigues: 'Material flow in heterogeneous friction stir welding of aluminium and copper thin sheets', *Sci. Technol. Weld. Join.*, 2010, **15**, (8), 654–660.
6. P. Xue, D. R. Ni, D. Wang, B. L. Xiao and Z. Y. Ma: 'Effect of friction stir welding parameters on the microstructure and mechanical properties of the dissimilar Al–Cu joints', *Mater. Sci. Eng. A*, 2011, **A528**, 4683–4689.
7. H. J. Liu, J. J. Shen, L. Zhou, Y. Q. Zhao, C. Liu and L. Y. Kuang: 'Microstructural characterisation and mechanical properties of

- friction stir welded joints of aluminium alloy to copper', *Sci. Technol. Weld. Join.*, 2011, **16**, (1), 92–99.
8. H. Lombard, D. G. Hattingh, A. Steuwer and M. N. James: 'Optimising FSW process parameters to minimise defects and maximise fatigue life in 5083-H321 aluminium alloy', *Eng. Fract. Mech.*, 2008, **75**, 341–354.
 9. R. Nandan, T. DebRoy and H. K. D. H. Bhadeshia: 'Recent advances in friction-stir welding – process, weldment structure and properties', *Prog. Mater. Sci.*, 2008, **53**, 980–1023.
 10. M. J. Peel, A. Steuwer, P. J. Withers, T. Dickerson, Q. Shi and H. Shercliff: 'Dissimilar friction stir welds in AA5083–AA6082. Part I: process parameter effects on thermal history and weld properties', *Metall. Mater. Trans. A*, 2006, **37A**, 2183–2193.
 11. T. U. Seidel and A. P. Reynolds: 'Visualization of the material flow in AA2195 friction-stir welds using a marker insert technique', *Metall. Mater. Trans. A*, 2001, **32A**, 2879–2884.
 12. B. Yang, J. Yan, M. A. Sutton and A. P. Reynolds: 'Banded microstructure in AA2024-T351 and AA2524-T351 aluminum friction stir welds. Part I: metallurgical studies', *Mater. Sci. Eng. A*, 2004, **A364**, 55–65.
 13. E. Akinlabi, A. Els-Botes and H. Lombard: 'Effect of tool displacement on defect formation in friction stir welding of aluminium and copper', Proc. 8th Int. Symp. on 'Friction stir welding', Timmendorfer Strand, Germany, May 2010, TWI.
 14. C. Genevois, M. Girard, B. Huneau, X. Sauvage and G. Racineux: 'Interfacial reaction during friction stir welding of Al and Cu', *Metall. Mater. Trans. A*, 2011, **42A**, 2290–2295.
 15. 'Alloy phase diagrams' in 'ASM handbook', Vol. 3; 1992, Materials Park, OH, ASM International.
 16. D. M. Rabkin, V. R. Ryabov, A. V. Lozovskaya and V. A. Dovzhenko: 'Preparation and properties of copper-aluminum intermetallic compounds', *Poroshk. Metall.*, 1970, **8**, (92), 101–107.
 17. S. Bozzi, A. L. Helbert-Etter, T. Baudin, B. Criqui and J. G. Kerbiguet: 'Intermetallic compounds in Al 6016/IF-steel friction stir spot welds', *Mater. Sci. Eng. A*, 2010, **A527**, 4505–4509.
 18. G. Cao and S. Kou: 'Friction stir welding of 2219 aluminum: behavior of θ (Al_2Cu) particles', *Weld. J.*, 2005, **84**, 1-s–7-s.
 19. G. Heness, R. Wuhner and W. Y. Yeung: 'Interfacial strength development of roll-bonded aluminium/copper metal laminates', *Mater. Sci. Eng. A*, 2008, **A483–A484**, 740–742.
 20. A. Kostka, R. S. Coelho, J. dos Santos and A. R. Pyzalla: 'Microstructure of friction stir welding of aluminium alloy to magnesium alloy', *Scr. Mater.*, 2009, **60**, 953–956.
 21. W.-B. Lee, M. Schmuecker, U. A. Mercardo, G. Biallas and S.-B. Jung: 'Interfacial reaction in steel–aluminum joints made by friction stir welding', *Scr. Mater.*, 2006, **55**, 355–358.
 22. Y. S. Sato, S. H. C. Park, M. Michiuchi and H. Kokawa: 'Constitutional liquation during dissimilar friction stir welding of Al and Mg alloys', *Scr. Mater.*, 2004, **50**, 1233–1236.
 23. E. Taban, J. E. Gould and J. C. Lippold: 'Dissimilar friction welding of 6061-T6 aluminum and AISI 1018 steel: properties and microstructural characterization', *Mater. Des.*, 2010, **31**, 2305–2311.
 24. D. Yashan, S. Tsang, W. L. Johns and M. W. Doughty: 'Inertia friction welding of 1100 aluminium to type 316 stainless steel', *Weld. J.*, 1987, **66**, 27–37.
 25. L. L. Wang, Z. A. Munir and J. B. Holt: 'The combustion synthesis of copper aluminides', *Metall. Trans. B*, 1990, **21B**, 567–577.
 26. F. W. Wulff, C. Breach, D. Stephan, Saraswati, K. Dittmer and M. Garnier: 'Further characterisation of intermetallic growth in copper and gold ball bonds on aluminium metallisation', Proc. Conf. SEMICON Singapore, May 2005, SEMI.
 27. R. M. Leal, C. Leitão, A. Loureiro, D. M. Rodrigues and P. Vilaça: 'Material flow in heterogeneous friction stir welding of thin aluminium sheets: effect of shoulder geometry', *Mater. Sci. Eng. A*, 2008, **A498**, 384–391.

ANNEX III - Galvão, I.; Oliveira, J. C.; Loureiro, A.; Rodrigues, D. M. Formation and distribution of brittle structures in friction stir welding of aluminium and copper: Influence of shoulder geometry. *Intermetallics* **2012a**, 22, 122–128.

<http://dx.doi.org/10.1016/j.intermet.2011.10.014>

The author acknowledges the permission provided by Elsevier and the *Intermetallics* journal for the print and electronic reuse of this paper in current work.



Formation and distribution of brittle structures in friction stir welding of aluminium and copper: Influence of shoulder geometry

I. Galvão, J.C. Oliveira, A. Loureiro, D.M. Rodrigues*

CEMUC, Department of Mechanical Engineering, University of Coimbra, Rua Luís Reis Santos, 3030-788 Coimbra, Portugal

ARTICLE INFO

Article history:

Received 9 September 2011

Received in revised form

19 October 2011

Accepted 20 October 2011

Available online xxx

Keywords:

A. Multiphase intermetallics

B. Phase identification, Phase transformation, Surface properties

C. Welding

ABSTRACT

The aim of present study was to analyse the influence of the shoulder geometry on the formation and distribution of brittle structures during friction stir welding of aluminium and copper. With this aim, welds were produced using two different friction stir welding tools: a scrolled and a conical shoulder tool. It was observed that, welding under the same welding parameters but with different tools, the nugget of the welds had completely different intermetallic content. Whereas the scrolled tool promoted the formation of a mixing region almost exclusively composed of CuAl_2 , the conical tool gave rise to the formation of an aluminium, copper, CuAl_2 and Cu_9Al_4 mixture, with higher heterogeneity and lower intermetallic content. Moreover, it was also concluded that the tool geometry also governs the welds surface characteristics. Whereas an irregularly distributed intermetallic-rich material, with strong non-metallic characteristics, was observed on surface of the welds carried out with the conical tool, a regular surface with insignificant amounts of intermetallic material was depicted in the welds produced with the scrolled tool. In current paper, these findings are analysed and explained based on material flow mechanism in friction stir welding.

© 2011 Elsevier Ltd. All rights reserved.



1. Introduction

Friction Stir Welding (FSW) is an innovative solid-state welding technology, which according to DebRoy and Bhadeshia [1] has great potential for joining dissimilar materials with very different physical and mechanical properties, such as aluminium and copper. The production of aluminium/copper (Al/Cu) hybrid systems would have high technical and economic impact, since it would enable the creation of engineering solutions combining copper's improved mechanical, thermal and electrical properties with aluminium's low specific weight and cost. However, aluminium to copper friction stir welding is still at an embryonic stage and, so far, no sound joining of these metals was achieved. Large incidence of microstructural defects [2], related to irregular material flow during welding, strong brittleness [3], due to the formation of large amounts of brittle Al/Cu intermetallic phases, and very irregular surface finishing [4], are the most important problems associated to Al/Cu joining by friction stir welding. Nevertheless, only incipient research has been done in this area and very few studies have been carried out in order to understand the relation between the weld morphology, the mechanisms of intermetallic phases formation and the process parameters.

Ouyang et al. [5] developed a study which was aimed to investigate the microstructural evolution during friction stir welding of AA 6061-T6 to Copper (99.9%). The authors noticed the formation of a mechanically-mixed region at the weld nugget, composed of large amounts of CuAl_2 , CuAl and Cu_9Al_4 intermetallic phases. The presence of the Cu_9Al_4 phase, with melting temperature much higher than the temperatures achieved during the friction stir welding process, was specially emphasised in this study. The authors claimed that this intermetallic compound, which was predominantly detected in copper-rich zones of the nugget, intercalated with lamellae of saturated solid solution of aluminium in copper, resulted from the mechanical integration of aluminium atoms into the copper metallic matrix. Abdollah-Zadeh et al. [6] and Sarrafi et al. [7] also detected the presence of the same intermetallic phases referred by Ouyang et al. [5] in Al/Cu friction stir welds. However, no mechanisms were advanced by these authors for explaining intermetallic phases formation. It is also important to emphasise that the relation between process parameters and intermetallic phase formation, or the relation between intermetallic phases distribution and weld morphology, have never been addressed in literature. The presence of intermetallics was mainly analysed in which concerns to its influence on the welds strength, being still controversial if it is detrimental [6] or favourable [8].

* Corresponding author. Tel.: +351 239 790 700; fax: +351 239 790 701.
E-mail address: dulce.rodrigues@dem.uc.pt (D.M. Rodrigues).

Table 1
Welding conditions used to carry out the welds.

Weld	Tool		Tool positioning	Rotational speed (rev min ⁻¹)	Traverse speed (mm min ⁻¹)
	Geometry	Dimensions			
WC		Conical shoulder: 14 mm-diameter	H13 Steel	Plunge depth: 0.9 mm Tilt angle: 2°	750
		Smooth cylindrical pin: 3 mm-diameter 0.9 mm-length			
WS		Scrolled shoulder: 14 mm-diameter	H13 Steel	Plunge depth: 0.95 mm Tilt angle: 0.5°	160
		Threaded cylindrical pin: 3 mm-diameter 1 mm-length			

Galvão et al. [9] studied the material flow mechanisms taking place during Al/Cu dissimilar friction stir welding, by comparing AA 5083-H111 to copper-DHP welds produced with different tool geometries: conical and scrolled shaped shoulder tools. The authors reported significant differences in the material flow mechanisms induced by both types of tools, in intermetallic phase content inside the nugget and in weld morphology. In present study, by performing a thorough macro and microstructural analysis of welds cross-section and surface, important relations were established between material flow mechanisms, the nature of the brittle intermetallic phases and its distribution during welding. It was also found that the formation of the intermetallic phases deeply influences the weld crown morphology, which remains one of the main concerns in Al/Cu joining by friction stir welding.

2. Experimental procedure

In present work, 1 mm-thick joints of oxygen-free copper with high phosphorous content (Cu-DHP, R 240) and 5083-H111 aluminium alloy (AA 5083-H111), friction stir butt welded using conical and scrolled shoulder tools, are analysed. Table 1 displays the tools' characteristics, the welding conditions used and the nomenclature adopted in the text for identifying the welds. Thus, the WS and WC acronyms identify the welds produced with the

scrolled and the conical tools, respectively. In all welds the copper plate was placed at the advancing side of the tool, for the reasons explained in Galvão et al. [9].

After welding, the surface of the welds was photographed. Transverse cross-sectioning of the welds was performed for metallographic analysis. The samples were prepared according to standard metallographic practice and etched in order to enable the identification of the different materials in the weld. A solution of 5 ml of H₂O₂ in 50 ml of NH₄OH was used for enhancing the welds microstructure. Metallographic analysis of transverse cross-sections was performed using optical microscopy, in a ZEISS HD 100 equipment. Scanning electron microscopy/Energy dispersive X-ray spectroscopy (SEM/EDS) and micro X-ray diffraction were performed in the cross-section and on the surface of the welds, using a PHILIPS XL30 SE microscope and a PANalytical XPert PRO micro-diffractometer, respectively.

3. Results

Pictures of the welds surface, optical macrographs of the cross-sections and SEM micrographs, acquired in back scattered electrons (BSE) mode, of selected cross-section areas of the WS and WC welds, are illustrated in Figs. 1 and 2, respectively. Comparing the surface of both welds, it can be concluded that the weld produced

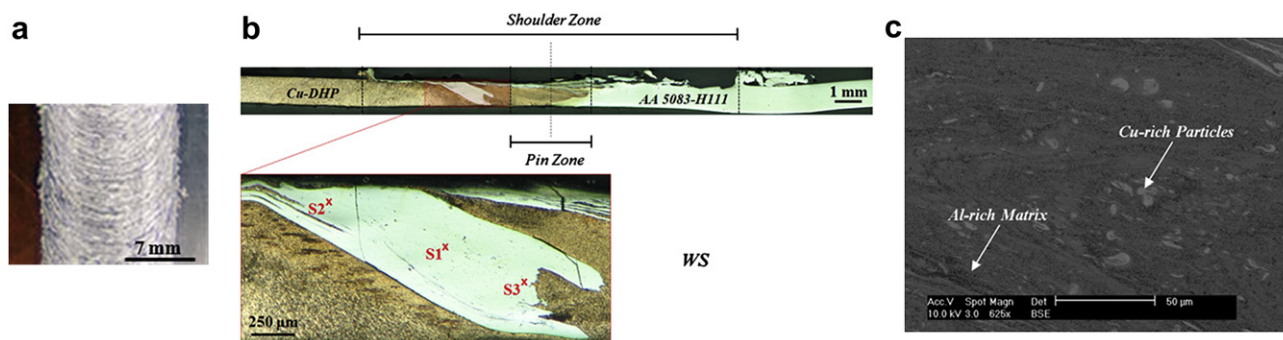


Fig. 1. Picture of the surface (a), macrograph of the transverse cross-section (b) and BSE micrograph of the mixing zone (c) of the WS weld.

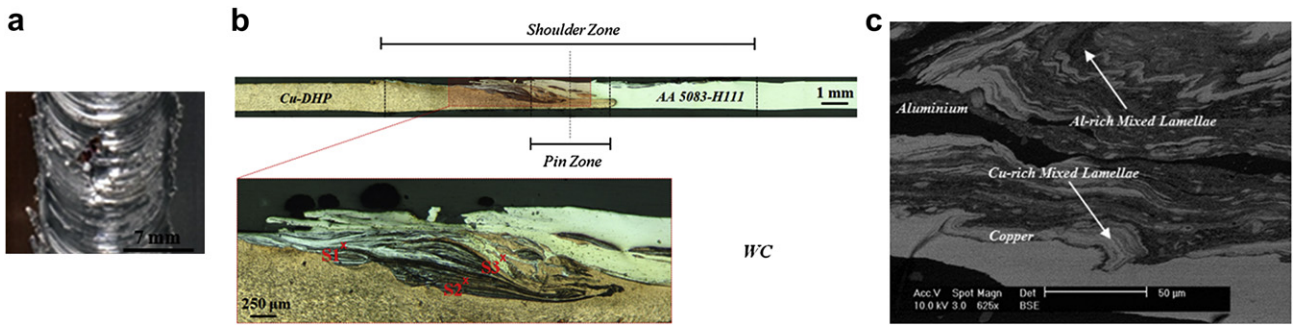


Fig. 2. Picture of the surface (a), macrograph of the transverse cross-section (b) and BSE micrograph of the mixing zone (c) of the WC weld.

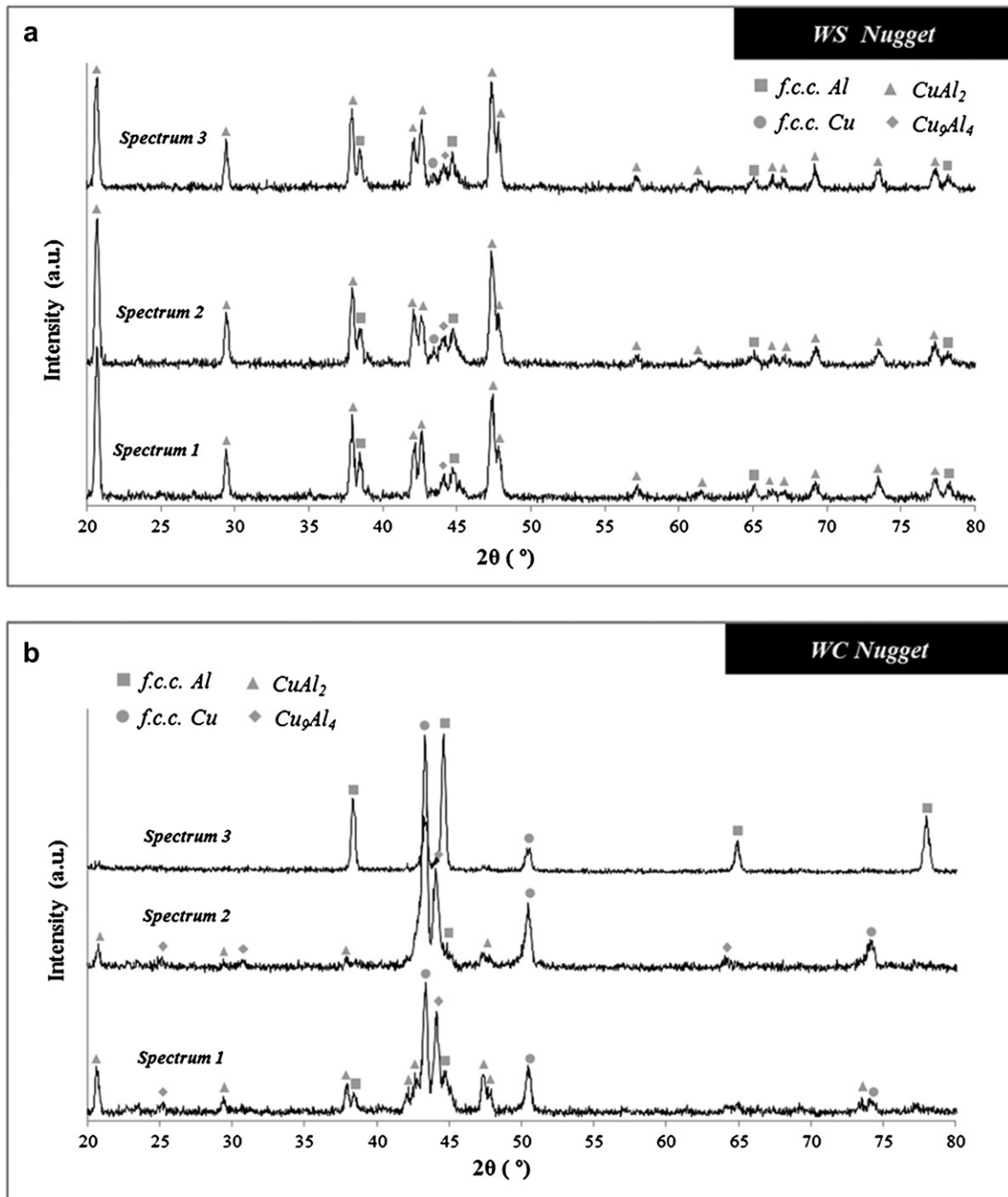


Fig. 3. Results of the XRD analysis performed in the nugget of the WS (a) and WC (b) welds.

with the scrolled tool displays a much smoother surface than the weld produced with the conical tool. Effectively, whereas the surface of the WC weld is formed by a shiny layer of irregularly distributed material, with deep voids (Fig. 2a), the surface of the WS weld displays fine and regularly distributed arc shaped striations (Fig. 1a), with characteristics similar to those observed in similar Al/Al [10] or Cu/Cu [11] friction stir welds.

Comparing the cross-section macrographs of the WS and WC welds (Figs. 1b and 2b), in which the pin and shoulder influence areas are delimited using vertical lines, two common features are observed: Aluminium at the top of both welds, which was pushed from the retreating to the advancing side of the tool in the shoulder influence zone, and copper at the bottom of the welds, which was

pushed from the advancing to the retreating side of the tool, across the pin influence zone. Despite these similarities, significant differences are also observed by comparing both nuggets morphology. Effectively, a well-defined tongue of grey material going upwards through the advancing side of the WS weld is observed in Fig. 1b. This tongue is embedded in a copper matrix and presents a quite homogeneous morphology, in which no lamellae of intercalated materials are discernible. In fact, the BSE micrograph acquired in the tongue, which is illustrated in Fig. 1c, shows a homogenous aluminium-rich material matrix, in which some copper-rich particles are dispersed. For the WC weld, a mixed region composed of bright and dark lamellae, extending through the copper side of the shoulder influenced zone is shown in Fig. 2b.

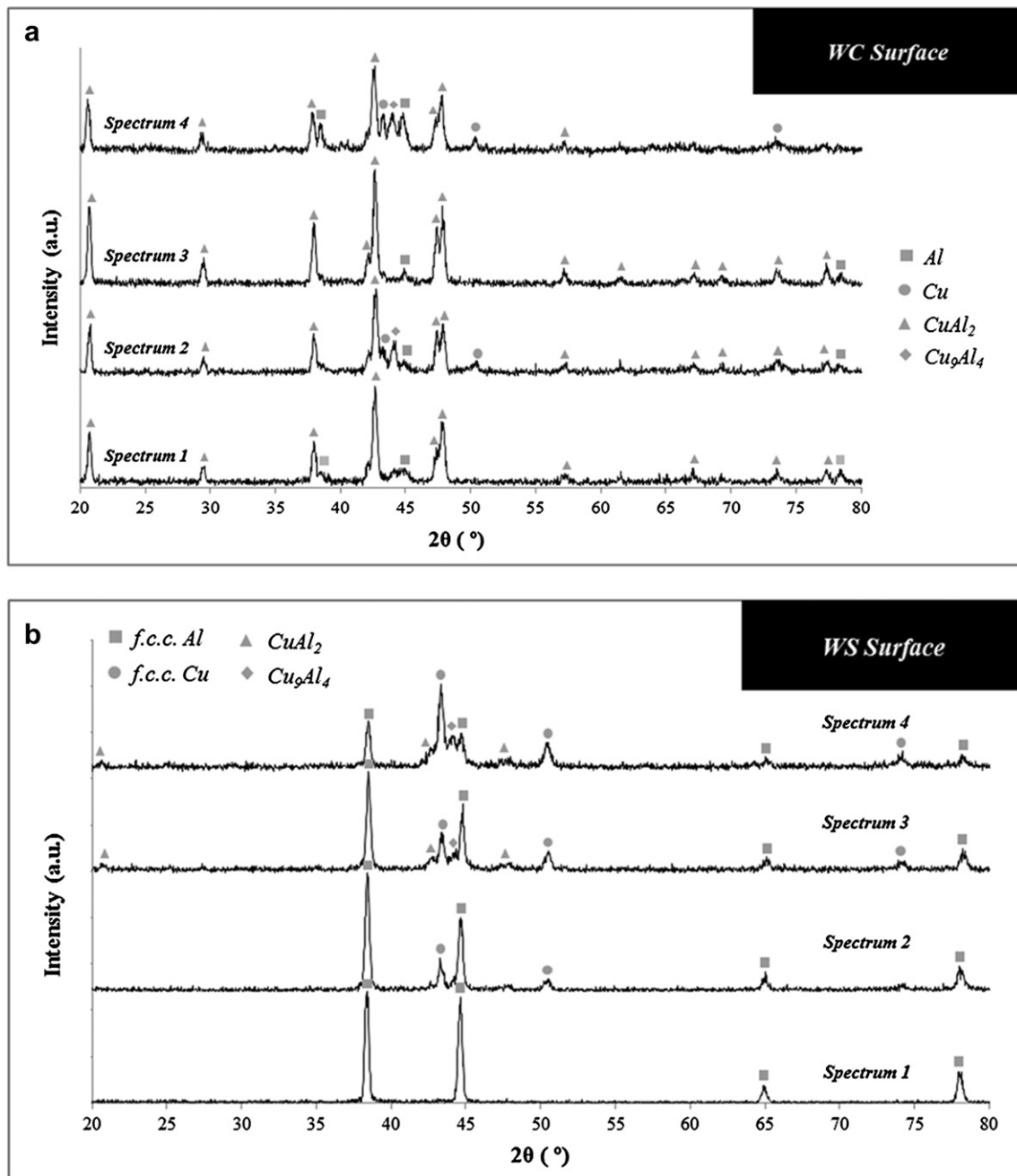


Fig. 4. Results of the XRD analysis performed on the surface of the WC (a) and WS (b) welds.

The BSE micrograph illustrated in Fig. 2c, which was acquired inside this area, displays complex mixing patterns composed of layers of copper and aluminium alternated with copper or aluminium-rich mixed lamellae.

The results of the XRD analysis performed in different zones of the nugget of the welds (S points indicated at red in the cross-section magnifications of Figs. 1b and 2b) are shown in Fig. 3. Fig. 3a shows that the material tongue formed in the nugget of the WS weld is mostly composed of CuAl_2 , which agrees well with the homogeneous morphology of this structure (Fig. 1b and c). In fact, only an almost negligible quantity of copper (f.c.c. Cu) and small amounts of aluminium (f.c.c. Al) and Cu_9Al_4 were detected in this zone. On the other hand, as shown in Fig. 3b, zones with base materials composition (f.c.c. Cu or f.c.c. Al), regions with high amounts of copper, aluminium, Cu_9Al_4 and CuAl_2 and areas only composed of copper and Cu_9Al_4 were detected in the diffractogram acquired in the nugget of the WC weld, which is also in accordance with the heterogeneous morphology observed in Fig. 2b and c.

Comparing the WC and WS welds, it can be concluded that, although both welds have been done using the same process parameters, both the morphology and the phase content of the nuggets are completely different. Effectively, whereas the scrolled tool promoted the formation of a mixed region almost exclusively composed of CuAl_2 , the conical tool gave rise to a Cu_9Al_4 -rich mixture in the nugget, with lower intermetallic content than that of the WS weld.

It was already shown that the material flow mechanisms induced by each of these tool geometries, which are deeply analysed in Leal et al. [12], for dissimilar joining of aluminium alloys, and in Galvão et al. [9], for Al/Cu welding, have a strong influence on the quantity of retreating and advancing side material that is incorporated in the shear layer surrounding the pin at each revolution of the tool. According to Galvão et al. [9], the intense dragging action of the helical flutes of the scrolled tool, which goes deep through the thickness of the plates and encompasses the full tool perimeter, enables the incorporation of large amounts of aluminium, located at the retreating side of the tool, in shear layer surrounding the pin, where both base materials are mixed by intense plastic deformation. The incorporation of copper, which is the advancing side material, in the shear layer is promoted almost exclusively by the pin, being restricted to a very small volume surrounding it, which makes that the shear layer resulting from this process has an aluminium-rich composition. The high temperatures and plastic deformation in the shear layer enhance the solid-state atomic diffusion rates [13] generating suitable conditions for the formation of aluminium-richer intermetallic phases, such as CuAl_2 . After one or more revolutions, the shear layer material is extruded against the advancing side material, at the back of the tool, giving rise to the formation of the CuAl_2 -rich material tongue observed in the cross-section macrograph of Fig. 1b. Macrographs illustrating the flow mechanism discussed in this paragraph can be found in Galvão et al. [9] and Leal et al. [12].

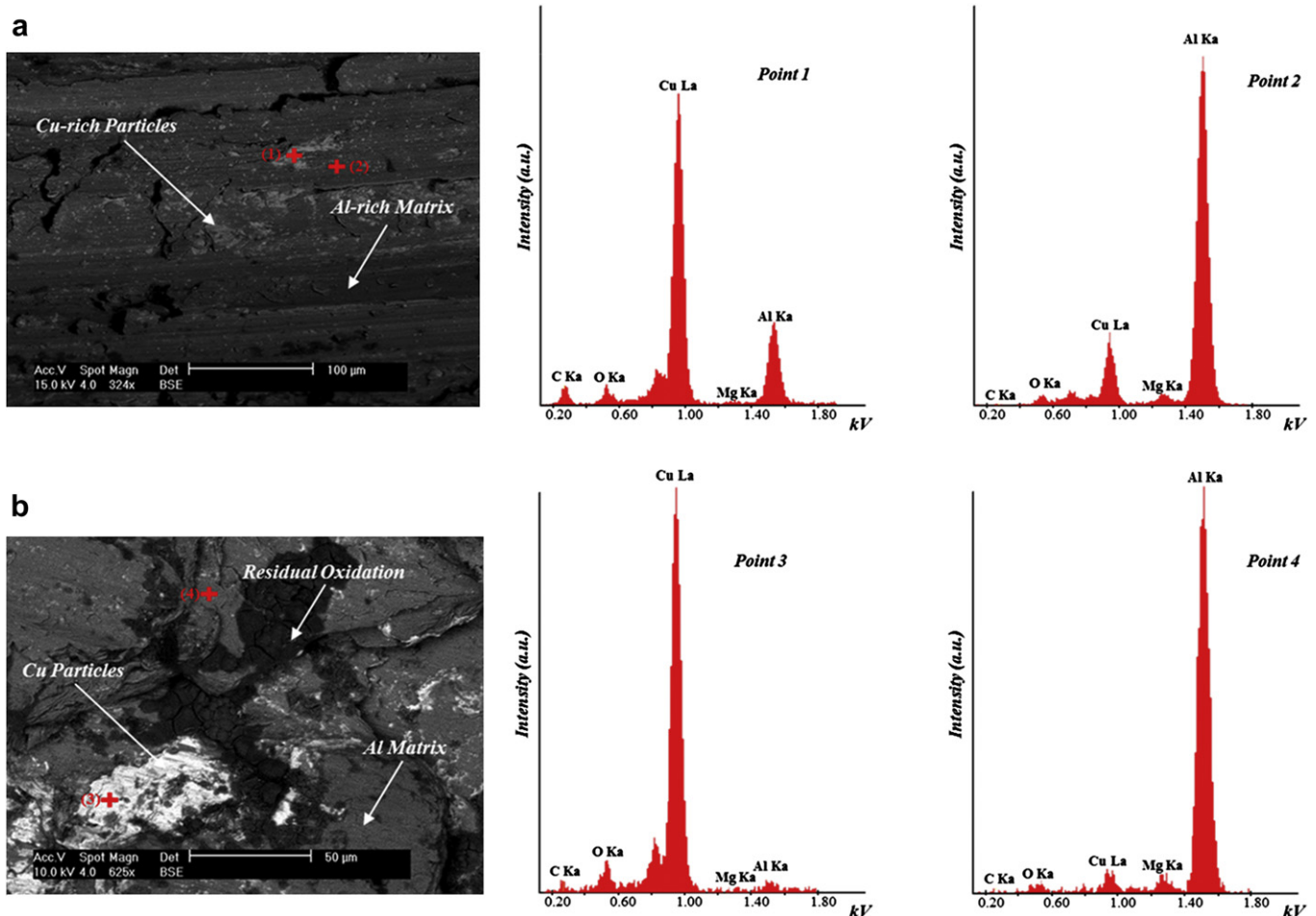


Fig. 5. BSE micrograph and EDS spectra registered on the surface of the WC (a) and the WS (b) welds.

For the conical tool, the dragging action of the shoulder is restricted to the top of the plates, at the back of the tool, where aluminium is also incorporated into the shear layer's mixing volume surrounding the pin, but in smaller quantities than for the scrolled tool, in which dragging action completely encompasses the shoulder perimeter and plate's thickness. The aluminium dragged by the conical shoulder, from the retreating side, is forced downward at the back of the tool, into the shear layer surrounding the pin, being mechanically-mixed with the copper dragged by the pin, from the advancing side, at the leading side of tool. According to Leal et al. [12], the dragging and stirring action of the conical shoulder is much less intense than for the scrolled shoulder, which makes that the shear layer composition for this tool is richer in copper and very heterogeneous, with intercalated layers of both base materials. Under the processing conditions, the Cu-rich zones of the shear layer give rise to the formation of the Cu_9Al_4 copper-rich intermetallic phase and some locally Al-rich regions of the shear layer give rise to the formation of the CuAl_2 . It is important to emphasise that both phases are formed at the same processing temperature, despite the differences in the enthalpy of formation between them [14], which points for the fact that both phases result from a mechanical stirring process as referred by Ouyang et al. [5].

The phase content of the weld crowns was also analysed in order to understand the differences in surface finishing between both welds. Figs. 4 and 5 illustrate the results of the XRD and SEM/EDS analysis, respectively, carried out on the surface of the WC and WS welds. The diffractogram in Fig. 4.a shows that high amounts of the intermetallic phase CuAl_2 are distributed over the WC weld. Small amounts of f.c.c. Al, f.c.c. Cu and Cu_9Al_4 were also detected. The distribution of these phases on the top of the weld can be understood in Fig. 5a. According to the figure, the top shiny layer irregularly distributed over the weld (Fig. 2a), is composed of an aluminium-rich mixed matrix with small particles of copper-rich material embedded in it. Galvão et al. [9] stressed that important quantities of aluminium, which is quite softer than copper, remain constrained inside the conical shaped scape volume under the shoulder where an Al-rich mixing volume is formed, which explains the presence of large amounts of CuAl_2 at the weld crowns.

For the WS weld, the same type of analysis, whose results are displayed in Fig. 4b, revealed high quantity of aluminium, some copper and very small amount of intermetallic phases at the weld surface. In fact, SEM/EDS results displayed in Fig. 5b shows that the top layer of this weld is composed of large particles of pure copper scattered in a pure aluminium matrix. Actually, as stressed before, the helical flutes of the scrolled shoulder exert an intense dragging action over the surface of the plates, pushing materials, from both retreating and advancing sides of the tool, into the inner shear layer surrounding the pin. No accumulation of material is promoted under the shoulder, and for that reason, there is no intermetallic deposition at the weld surface. The shiny layer visible on the top of the WS weld, in Fig. 1a, is mainly constituted of aluminium, and for that reason it displays morphology very similar to that of similar aluminium welds. For the WC weld, the top layer consists of an intermetallic-rich mixture, with strong non-metallic characteristics, which is irregularly distributed over the weld surface during tool traverse motion, compromising negatively weld surface finishing.

Although the WS weld displayed much more homogeneous structure and improved surface finishing, relative to the WC weld, the formation of important quantities of CuAl_2 inside the shear layer, which give rise to the through thickness intermetallic grey tongue in the weld nugget, is very detrimental in terms of weld strength. This results from the extreme brittleness of the CuAl_2 tongue, with deep cracks inside it, as can be seen in Fig. 1b.

4. Conclusion

The influence of the shoulder geometry on the formation and distribution of brittle structures in friction stir welding of aluminium and copper was investigated in present study. Important relations between material flow mechanisms, the nature of the brittle intermetallic phases and its distribution during welding were established. It was observed that the nugget of welds produced using the same process parameters, but different tool geometries, displayed completely different morphology and intermetallic content. In fact, whereas the scrolled tool promoted the formation of a tongue-shaped mixing region almost exclusively composed of CuAl_2 , the conical tool gave rise to the formation of an aluminium, copper, CuAl_2 and Cu_9Al_4 mixture, with higher heterogeneity and lower intermetallic content. This enables to conclude that material flow mechanisms induced by each shoulder geometry have a strong influence on the phase content of the mixtures.

It was also observed that the tool geometry strongly determines the surface finishing of the welds, since it has great influence on the nature of the material deposited on the top of the joints. Effectively, whereas an irregularly distributed intermetallic-rich material, with strong non-metallic characteristics, was observed on surface of the welds carried out with the conical tool, a regular surface with no significant amount of intermetallic material was depicted in the welds produced with the scrolled tool. It was inferred that the large formation of intermetallic material, specifically CuAl_2 , on the surface of the conical weld results from material mixing in the under shoulder volume, which contains large amount of aluminium that is constrained inside the conical cavity of the tool. On the other hand, since no accumulation of material is promoted under the scrolled shoulder, there is no intermetallic deposition at the weld surface.

Acknowledgements

The authors are indebted to the Portuguese Foundation for the Science and Technology (FCT) and FEDER for the financial support, and to company *Thyssen Portugal – Aços e Serviços Lda* for providing the heat treatments for the friction stir welding tools.

References

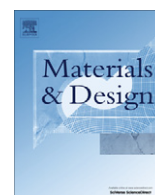
- [1] DebRoy T, Bhadeshia HKDH. Friction stir welding of dissimilar alloys - a perspective. *Sci Technol Weld Joining* 2010;15:266–70.
- [2] Xue P, Ni DR, Wang D, Xiao BL, Ma ZY. Effect of friction stir welding parameters on the microstructure and mechanical properties of the dissimilar Al–Cu joints. *Mater Sci Eng A* 2011;528:4683–9.
- [3] Saeid T, Abdollah-zadeh A, Sazgari B. Weldability and mechanical properties of dissimilar aluminum–copper lap joints made by friction stir welding. *J Alloys Compd* 2010;490:652–5.
- [4] Liu HJ, Shen JJ, Zhou L, Zhao YQ, Liu C, Kuang LY. Microstructural characterisation and mechanical properties of friction stir welded joints of aluminium alloy to copper. *Sci Technol Weld Joining* 2011;16:92–9.
- [5] Ouyang J, Yarrapareddy E, Kovacevic R. Microstructural evolution in the friction stir welded 6061aluminum alloy (T6-temper condition) to copper. *J Mater Process Technol* 2006;172:110–22.
- [6] Abdollah-zadeh A, Saeid T, Sazgari B. Microstructural and mechanical properties of friction stir welded aluminum/copper lap joints. *J Alloys Compd* 2008;460:535–8.
- [7] Sarrafi R, Kokabi AH, Gharacheh MA, Shalchi B. Evaluation of microstructure and mechanical properties of aluminium to copper friction stir butt welds. In: Mishra R, Mahoney MW, Sato Y, Hovanski Y, Verma R, editors. *Friction stir welding and processing VI*. Hoboken, New Jersey: John Wiley & Sons Inc.; 2011. p. 253–64.
- [8] Xue P, Xiao BL, Ni DR, Ma ZY. Enhanced mechanical properties of friction stir welded dissimilar Al–Cu joint by intermetallic compounds. *Mater Sci Eng A* 2010;527:5723–7.
- [9] Galvão I, Leal RM, Loureiro A, Rodrigues DM. Material flow in heterogeneous friction stir welding of aluminium and copper thin sheets. *Sci Technol Weld Joining* 2010;15:654–60.
- [10] Leitão C, Leal RM, Rodrigues DM, Loureiro A, Vilaça P. Mechanical behaviour of similar and dissimilar AA5182-H111 and AA6016-T4 thin friction stir welds. *Mater Des* 2009;30:101–8.

- [11] Leal RM, Sakharova N, Vilaça P, Rodrigues DM, Loureiro A. Effect of shoulder cavity and welding parameters on friction stir welding of thin copper sheets. *Sci Technol Weld Joining* 2011;16:146–52.
- [12] Leal RM, Leitão C, Loureiro A, Rodrigues DM, Vilaça P. Material flow in heterogeneous friction stir welding of thin aluminium sheets: effect of shoulder geometry. *Mater Sci Eng A* 2008;498:384–91.
- [13] Yashan D, Tsang S, Johns WL, Doughty MW. Inertia friction welding of 1100 aluminium to type 316 stainless Steel. *Weld J* 1987;66:27–37.
- [14] Wulff FW, Breach C, Stephan D, Saraswati, Dittmer K, Garnier M. Further characterisation of intermetallic growth in copper and gold ball bonds on aluminium metallisation. Singapore: SEMICON; 2005.

ANNEX IV - Galvão, I.; Leitão, C.; Loureiro, A.; Rodrigues, D. M. Study of the welding conditions during similar and dissimilar aluminium and copper welding based on torque sensitivity analysis. *Mater. Des.* **2012b**, 42, 259–264.

<http://dx.doi.org/10.1016/j.matdes.2012.05.058>

The author acknowledges the permission provided by Elsevier and the Materials & Design journal for the print and electronic reuse of this paper in current work.



Technical Report

Study of the welding conditions during similar and dissimilar aluminium and copper welding based on torque sensitivity analysis

I. Galvão, C. Leitão, A. Loureiro, D.M. Rodrigues*

CEMUC, Department of Mechanical Engineering, University of Coimbra, Rua Luís Reis Santos, 3030-788 Coimbra, Portugal

ARTICLE INFO

Article history:

Received 14 February 2012

Accepted 29 May 2012

Available online 7 June 2012

ABSTRACT

The aim of present study was to analyse and compare the influence of the welding conditions on torque evolution, during similar and dissimilar friction stir butt welding of 5083-H111 aluminium alloy and copper-DHP. The torque registered during welding, using different welding parameters and base materials combinations, and its relation with the morphological and structural properties of the welds were analysed. Independently of the materials to be welded and the relative plates positioning, in dissimilar friction stir welding, the sensitivity of the average torque to the process parameters was observed to be the same. It was also observed that the average torque is strongly conditioned by the materials to be welded, since, for all welding parameters, the lowest average torque values were always registered during dissimilar welding. Material flow and intermetallic-formation were found to determine this behaviour. Important differences in instantaneous torque evolution, during welding, were also observed depending on base materials combinations.

© 2012 Elsevier Ltd. All rights reserved.

1. Introduction

A key combination of excellent electrical and thermal conductivities, outstanding corrosion properties and good strength and fatigue resistance makes copper very suitable to be used in many emerging industrial sectors [1]. Nevertheless, the heavyweight and expensive cost of this material limit its wider application. So, the implementation of aluminium/copper (Al/Cu) hybrid structures, maintaining most of copper's specific properties and simultaneously allowing important weight and cost savings, is a very attractive solution in numerous industrial fields. Friction Stir Welding (FSW), traditionally pointed as a solid-state welding technology suitable for joining materials with very different physical and mechanical properties [2], is the most appropriate solution for producing Al/Cu hybrid structures. However, only incipient investigation has already been performed on Al/Cu FSW and no appropriate welding conditions, enabling to produce welds with excellent surface finishing, sound microstructures and suitable mechanical properties, have been defined yet [3–5]. Actually, further research, enabling full understanding of all metallurgical, thermal and mechanical phenomena taking place during welding, is still mandatory.

Recently, some important advances have been achieved in Al/Cu FSW understanding, mainly in which concerns the material flow during the process and the mechanisms of intermetallic phases formation/distribution, as well as their effect on the final properties of

the welds. Actually, Galvão et al. [6], in dissimilar FSW of 1 mm-thick AA 5083-H111 to copper-DHP, emphasised the influence of the base materials positioning on material flow during welding and, consequently, on the final structure and morphology of the welds. Positioning the aluminium plate at the advancing side of the tool, the authors observed that the harder copper, which was pushed from the retreating to the advancing side of the tool, expelled large amounts of the softer aluminium from the under shoulder area, preventing base materials mixing. As a result, strong thinning and massive aluminium flash were observed on the surface of these welds. On the other hand, for the welds produced with the copper plate at the advancing side of the tool, strong base materials mixing/interaction was observed. Fluid-like morphologies, composed of intercalated layers of both base materials and mixed Al/Cu lamellae, were identified in the nugget of these welds. Furthermore, Galvão et al. [6] also reported the presence of a very irregular layer over the surface of these welds. Large amounts of CuAl_2 and Cu_9Al_4 intermetallic phases were detected both in the nugget's fluid-like structures and on this irregular layer [7]. This led the authors to conclude about the existence of important mixing volumes in both the inner shear layer, surrounding the pin, and the under shoulder cavity, giving rise to the deposition of large amounts of intermetallic-rich materials on the surface of the welds.

Despite of these advances in Al/Cu FSW understanding, the influence of the welding parameters on welding conditions, which according to several authors can be inferred by a torque (N m) sensitivity analysis [8–10], is an aspect which remains totally uncharacterised in Al/Cu FSW. So, the aim of the present study was to

* Corresponding author. Tel.: +351 239 790 700; fax: +351 239 790 701.

E-mail address: dulce.rodrigues@dem.uc.pt (D.M. Rodrigues).

analyse and compare the influence of the welding conditions on torque evolution, during similar and dissimilar friction stir butt welding of AA 5083-H111 and copper-DHP. More precisely, the torque registered during welding, using different welding parameters and base materials combinations, and its relation with the morphological and structural properties of the welds will be analysed in current paper.

2. Experimental procedure

In previous works [6,11,12], similar and dissimilar friction stir butt welds of 1 mm-thick plates of oxygen-free copper, with high phosphorous content (copper-DHP, R240), and 5083-H111 aluminium alloy, were carried out in an ESAB LEGIO FSW 3U equipment, using a 14 mm-diameter conical tool with a 3° shoulder cavity and a 3 mm-diameter cylindrical probe. As illustrated in Table 1, which shows the full set of welding conditions considered in those works, the welds were performed under load control (700 kg), using a tool tilt angle of 2° and varying traverse (16 and 25 cm min⁻¹) and rotation (750, 1000 and 1250 rev min⁻¹) speeds. In dissimilar welding, the relative positioning of the base materials relative to the tool rotation direction was also alternated, which determined a set of 22 welding conditions to be analysed. Table 1 also displays the nomenclature adopted in the text for labelling the different welds, which was selected in order to identify, for each sample, the base materials and the variable welding conditions. Thus, the Al-750-16 and Cu-750-16 welds correspond, respectively, to 5083 aluminium (Al/Al) and copper-DHP (Cu/Cu) similar welds produced with the rotational and welding speeds of 750 rev min⁻¹ and 16 cm min⁻¹. In turn, the DCu-750-16 and DAl-750-16 acronyms identify Al/Cu dissimilar welds carried out with copper and aluminium plates positioned at the advancing side of the tool, respectively, and with the same welding parameters used for the previous similar welds.

All the welds performed had 175 mm in length. In each welding test, the instantaneous spindle torque was registered by the monitoring system of the FSW apparatus, which enabled to plot individually the torque evolution during welding. However, in order to avoid any influence of the initial and final unstable welding periods on the torque sensitivity analysis, average torque values were calculated considering only the acquisition period corresponding to a 50 mm central welding length. In order to characterise the plastic behaviour of the 5083 aluminium alloy and copper-DHP,

until very large values of plastic deformation, shear tests were performed using an Instron 4206 equipment. The tests were carried out, at room temperature, using a testing speed of 5 mm min⁻¹. Strain data acquisition was performed, using ARAMIS Optical 3D Deformation & Strain Measurement system, according to the procedures explained elsewhere [13].

3. Results

3.1. Spindle torque assessment

Significant dissimilarities in structure and morphology between the Cu/Cu, Al/Al and Al/Cu friction stir welds, which were well-documented in previous investigations [6,11,12], point to important differences in materials behaviour and materials flow mechanisms, and consequently, on the flow stresses developed during welding. So, the spindle torque variation, which is a quantity closely related to the energy spent during welding [9], which, in turn, varies according to base materials characteristics and welding parameters, can be used as a quantitative parameter enabling to evaluate the welding conditions [14].

The evolution of the average torque, with the rotational and traverse speeds, for similar and dissimilar aluminium and copper FSW is illustrated in Fig. 1. The welds produced with the traverse speeds of 16 and 25 cm min⁻¹ are represented, in the graphs, by black triangles and white circles, respectively. From the pictures, it can be concluded that, independently of the materials to be welded, or the relative positioning of the plates, in dissimilar FSW, the torque sensitivity to the varying process parameters was the same. Specifically, whereas an important decrease in torque values was registered when increasing the rotational speed, no significant torque variations were registered by varying the traverse speed. The same type of results has already been reported by previous authors. Arora et al. [8] stated that increasing the rotational speed, increases the temperature developed in the process, promoting additional material softening and decreasing the flow stresses associated to material stirring, which strongly contributes in decreasing the torque registered by the welding equipment. Peel et al. [10] and Arora et al. [8], who also reported small torque variations by changing the traverse speed in FSW, stated that this parameter may have small influence on the temperature field around tool pin.

In Fig. 2 is analysed the evolution of the average torque with base materials characteristics. More precisely, the diamonds,

Table 1
Welding conditions: processing parameters and base material combinations.

Similar Welds					
Base Material		Welding Conditions			
Copper-DHP	AA 5083	Rotational speed (rev min ⁻¹)	Traverse speed (cm min ⁻¹)	Axial load (kg)	Tilt angle (°)
Cu-750-25	Al-750-25	750	25	700	2
Cu-750-16	Al-750-16		16		
Cu-1000-25	Al-1000-25	1000	25		
Cu-1000-16	Al-1000-16		16		
Cu-1250-25	-----	1250	25		
Cu-1250-16	-----		16		
Dissimilar welds					
Adv. Side Material		Welding Conditions			
Copper-DHP	AA 5083	Rotational Speed (rev min ⁻¹)	Traverse Speed (cm min ⁻¹)	Axial Load (kg)	Tilt Angle (°)
DCu-750-25	DAl-750-25	750	25	700	2
DCu-750-16	DAl-750-16		16		
DCu-1000-25	DAl-1000-25	1000	25		
DCu-1000-16	DAl-1000-16		16		
DCu-1250-25	DAl-1250-25	1250	25		
DCu-1250-16	DAl-1250-16		16		

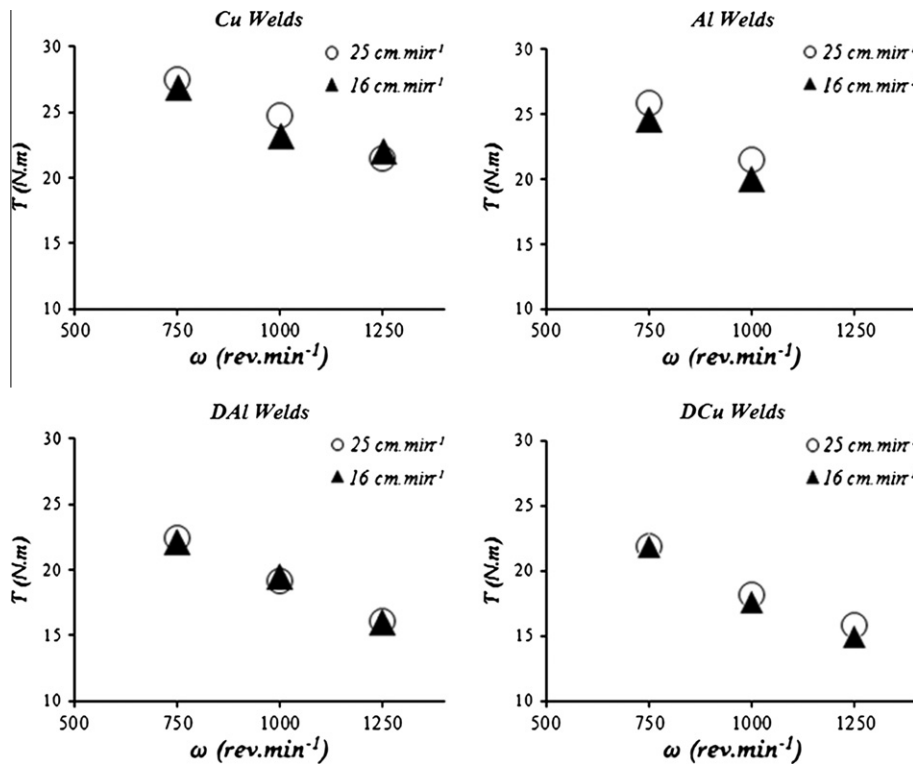


Fig. 1. Evolution of the average torque with the process parameters in similar (*Cu* and *Al* welds) and dissimilar (*DAI* and *DCu* welds) aluminium and copper FSW.

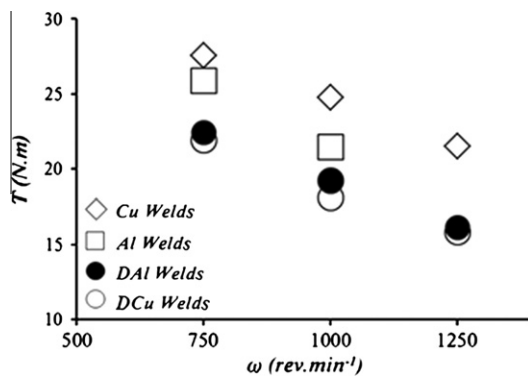


Fig. 2. Influence of the base materials on the average torque of the welds produced with a travel speed of $25 \text{ cm} \cdot \text{min}^{-1}$.

squares and circles represent the average torque for Cu/Cu, Al/Al and Al/Cu welding with a traverse speed of $25 \text{ cm} \cdot \text{min}^{-1}$ and different tool rotation rates. From the picture, it can be observed that the torque is also influenced by base materials combination. In fact, for all welding parameters, the highest and lowest torque values were registered in Cu/Cu welding and Al/Cu welding, respectively. Intermediate values of torque were registered for the Al/Al welding tests. Firouzdor and Kou [15] also registered, in dissimilar 6061 aluminium to AZ31 magnesium welding, values of torque lower than those acquired during the similar joining of both metals.

Analysing the similar welds torque, it can be observed that the values corresponding to the copper welding tests were only slightly higher than those measured for aluminium welding, despite the important differences in hardness and thermal conductivity between both base materials. In fact, since the 5083 aluminium alloy displays significantly lower hardness than that of the

copper-DHP (70 Hv vs. 90 Hv) and less than half of its thermal conductivity ($120 \text{ W/m} \cdot \text{K}$ vs. $339 \text{ W/m} \cdot \text{K}$), it is conceivable to assume that thermal softening would be stronger during Al/Al welding, and consequently, the flow stresses developed during the process would be gentler than during Cu/Cu welding, conducting to much lower torque values. However, from Fig. 3, which illustrates, for both base materials, stress–strain curves obtained in shear, at room temperature, in quasi-static conditions ($5 \text{ mm} \cdot \text{min}^{-1}$), it can be observed that the 5083 alloy, despite displaying much lower yield stress, exhibits pronounced hardening with plastic deformation, attaining shear strength values much higher than those registered for copper, at much higher plastic deformation values. As FSW involves strong plastic deformation, it is possible to assume that the more intense thermal softening experienced by the aluminium relative to the copper alloy, will be balanced by the more intense hardening behaviour of this material, which will increase the flow stresses during welding. So, as stated in a previous investigation by Leitão et al. [16], pronounced differences in plastic behaviour during welding, which justify noticeable differences in friction stir weldability, would also justify the small differences in FSW torque registered in current work for materials with significantly different physical and mechanical properties.

The instantaneous torque evolution during welding, for the 750–16 aluminium and copper similar and dissimilar welding tests, is plotted in Fig. 4, in which significant differences in torque evolution can be observed depending on the materials to be welded. In fact, whereas almost flat curves, without significant variations along the welding length, illustrate the torque evolution in similar welding, strong fluctuations in torque values, with important peaks and drops, were registered during the dissimilar welding carried out with the copper plate at the advancing side of the tool. From the top layer photograph of the *DCu*-750-16 weld, which was included in Fig. 4, it can be observed that the torque drops correspond to weld zones where large amounts of material were accumulated

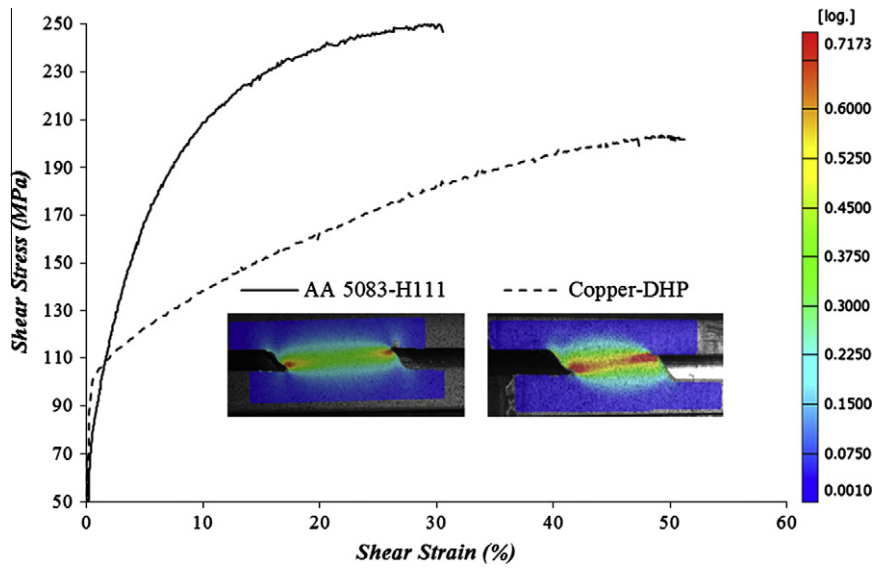


Fig. 3. Stress–strain curves and strain fields in the shear samples at maximum load ($T = 25\text{ }^{\circ}\text{C}$, 5 mm min^{-1}).

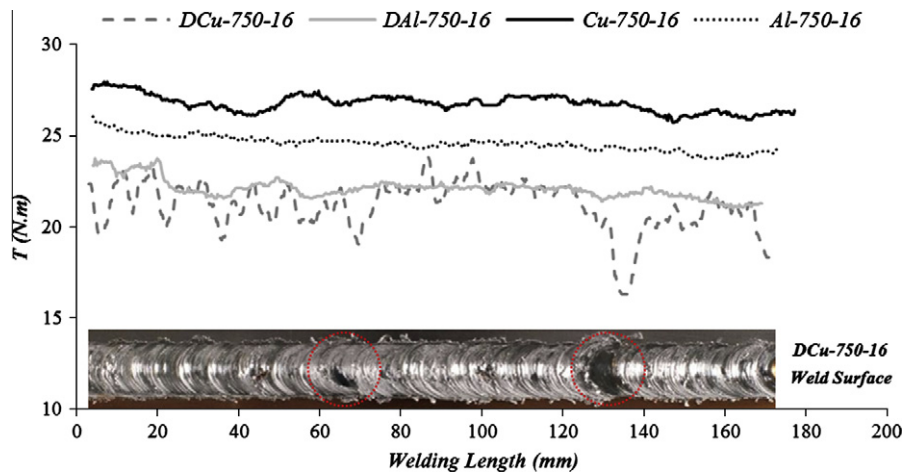


Fig. 4. Instantaneous torque evolution curves for the 750-16 aluminium and copper similar and dissimilar welds and surface macrograph of the DCu-750-16 weld.

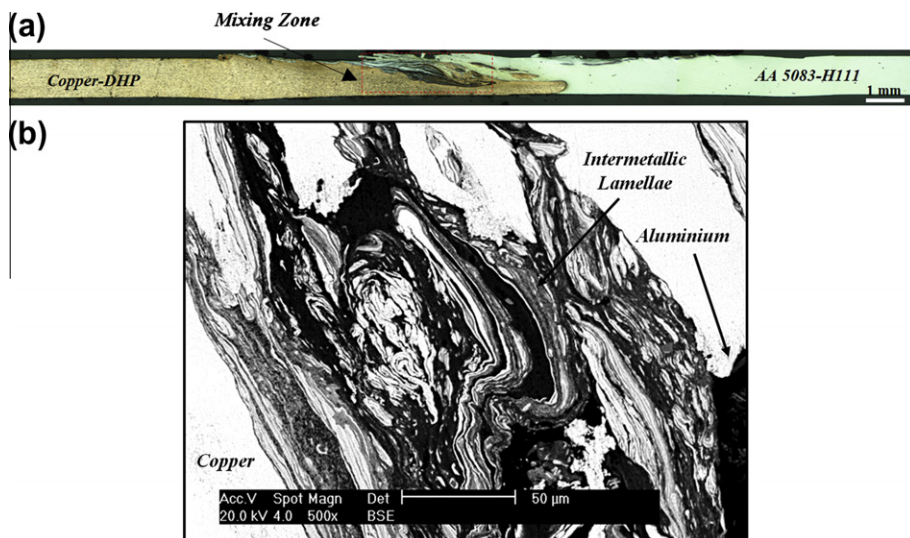


Fig. 5. Transverse cross-section (a) and BSE magnification registered in the nugget (b) of a dissimilar weld produced with copper-DHP at the advancing side.

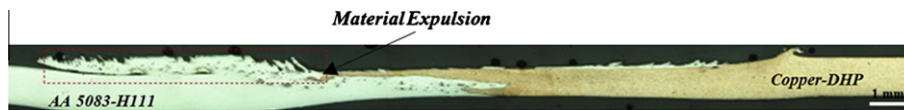


Fig. 6. Transverse cross-section of a dissimilar weld produced with AA 5083 at the advancing side.

on the weld surface (dark grey zones highlighted in the figure). Finally, Fig. 4 also shows that, similarly to that observed in similar welding, the instantaneous torque curves registered for the dissimilar Al/Cu welds produced with aluminium at the advancing side of the tool (DAI-750-16 weld) do not present significant fluctuations, which points to an important influence of plates positioning on material flow during welding, as already stated before [6].

3.2. Torque-determining factors in dissimilar Al/Cu welding

Important dissimilarities in the average torque values (Fig. 2), as well as in the instantaneous torque evolution (Fig. 4), were observed depending on the combination of materials to be welded, which indicate that the metallurgical, thermal and mechanical phenomena taking place during welding have a strong influence on the developed flow stresses. Actually, as reported in Galvão et al. [6], strong base materials interaction takes place during Al/Cu welding, when positioning the copper plate at the advancing side of the tool, as exemplified in Fig. 5a, where a transverse cross-section of one of these welds is shown. Important base materials mixing, taking place both in the shoulder and pin-governed volumes, results in the formation of Cu_9Al_4 and CuAl_2 -rich mixtures (mixing zone highlighted in Fig. 5a). The intermetallic phase CuAl_2 , in particular, has a melting temperature close to the peak temperatures measured by Ouyang et al. [17] in FSW of 6061 aluminium to copper, which promotes the fluidisation of the intermetallic-rich layers being formed during welding. The fluid-like morphology of the intermetallic-rich structures, which can be observed in the nugget of the welds and in the under-shoulder material [6], is exemplified by the back-scattered electrons (BSE) image in Fig. 5b. The formation of large amounts of CuAl_2 -rich fluidised films under the shoulder, may induce tool slippage during welding, contributing for significant decrease of the dissimilar welding average torque, relative to similar materials welding, as registered in Fig. 2.

Analysing the instantaneous torque evolution (Fig. 4), strong differences in torque behaviour were also registered for the dissimilar welds produced with copper plate at the advancing side of the tool. According to Galvão et al. [6], large accumulation of intermetallic-rich material under the tool has important consequences in the metal flow and material deposition processes. Effectively, instead of a periodic material deposition at the rear of the tool, characteristic of similar welding, significant amounts of intermetallic-rich mixtures, formed during welding, adhere to the tool, being non-periodically expelled after some revolutions. As a result, an irregular intercalation of torque peaks, when material accumulation takes place under the tool, with significant torque drops, which correspond to intermetallic material expulsion, explains the very irregular torque evolution registered in Fig. 4.

Finally, in which concerns to the dissimilar welds produced with the aluminium plate at the advancing side of the tool, different causes can be attributed to the relatively low average torque values measured during welding, in comparison to the similar materials welding results, registered in Fig. 2. In fact, as reported by Galvão et al. [6], for these dissimilar welds, large amounts of aluminium are expelled from the under shoulder area during welding, as highlighted in the cross-section of Fig. 6, and consequently, no base material mixing and/or intermetallic phases formation take place during welding. Due to the large amounts of aluminium being

expelled from the weld, the volume of material being stirred by the tool, at each revolution, becomes smaller than in similar materials welding, decreasing the torque registered during welding.

4. Conclusion

The sensitivity of the spindle torque to the welding conditions, during similar and dissimilar FSW of 5083-H111 aluminium and copper-DHP, was investigated in this study. Important relations between material flow stresses and the metallurgical, mechanical and thermal phenomena taking place during welding were established. Independently of the materials to be welded and the relative positioning of the plates, in dissimilar FSW, the sensitivity of the measured torque to the process parameters was very similar. In fact, whereas an important decrease in torque values was promoted by increasing the rotational speed, no significant torque changes were achieved by varying the traverse speed. However, it was also observed that the torque is strongly conditioned by the combination of materials to be welded, since, for all welding parameters, the lowest values were registered in dissimilar welding. A smaller volume of material dragged by the tool, at each revolution, than in similar FSW, as well as tool slippage, are pointed as the main causes for torque decrease in dissimilar welding. Finally, the strong fluctuations in instantaneous torque acquisition, registered in dissimilar welding with the copper at the advancing side, were related with the large intermetallic content of these welds.

Acknowledgements

The authors are indebted to the Portuguese Foundation for the Science and Technology (FCT) and European Regional Development Fund (ERDF) for the financial support, and to company *Thyssen Portugal – Aços e Serviços Lda* for providing the heat treatments for the friction stir welding tools.

References

- [1] Tyler DE, Black WT. Introduction to copper and copper alloys. In: ASM International Handbook Committee, editor. Properties and selection: nonferrous alloys and special-purpose materials. AMS International: United States of America; 1992. p. 216–40.
- [2] DeRoy T, Bhadeshia HKDH. Friction stir welding of dissimilar alloys – a perspective. *Sci Technol Weld Joi* 2010;15:266–70.
- [3] Galvão I, Oliveira JC, Loureiro A, Rodrigues DM. Formation and distribution of brittle structures in friction stir welding of aluminium and copper: influence of shoulder geometry. *Intermetallics* 2012;22:122–8.
- [4] Liu HJ, Shen JJ, Zhou L, Zhao YQ, Liu C, Kuang LY. Microstructural characterisation and mechanical properties of friction stir welded joints of aluminium alloy to copper. *Sci Technol Weld Joi* 2011;16:92–9.
- [5] Xue P, Ni DR, Wang D, Xiao BL, Ma ZY. Effect of friction stir welding parameters on the microstructure and mechanical properties of the dissimilar Al–Cu joints. *Mater Sci Eng A* 2011;528:4683–9.
- [6] Galvão I, Leal RM, Loureiro A, Rodrigues DM. Material flow in heterogeneous friction stir welding of aluminium and copper thin sheets. *Sci Technol Weld Joi* 2010;15:654–60.
- [7] Galvão I, Oliveira JC, Loureiro A, Rodrigues DM. Formation and distribution of brittle structures in friction stir welding of aluminium and copper: influence of process parameters. *Sci Technol Weld Joi* 2011;16:681–9.
- [8] Arora A, Nandan R, Reynolds AP, DeRoy T. Torque, power requirement and stir zone geometry in friction stir welding through modeling and experiments. *Scr Mater* 2009;60:13–6.
- [9] Cui S, Chen ZW, Robson JD. A model relating tool torque and its associated power and specific energy to rotation and forward speeds during friction stir welding/processing. *Int J Mach Tools Manu* 2010;50:1023–30.

- [10] Peel MJ, Steuwer A, Withers PJ, Dickerson T, Shi Q, Shercliff H. Dissimilar friction stir welds in AA5083-AA6082. Part I: Process parameter effects on thermal history and weld properties. *Metall Mater Trans A* 2006;37A:2183–93.
- [11] Leal RM, Sakharova N, Vilaça P, Rodrigues DM, Loureiro A. Effect of shoulder cavity and welding parameters on friction stir welding of thin copper sheets. *Sci Technol Weld Joi* 2011;16:146–52.
- [12] Tronci A, McKenzie R, Leal RM, Rodrigues DM. Microstructural and mechanical characterisation of 5XXX-H111 friction stir welded tailored blanks. *Sci Technol Weld Joi* 2011;16:433–9.
- [13] Leitão C, Galvão I, Leal RM, Rodrigues DM. Determination of local constitutive properties of aluminium friction stir welds using digital image correlation. *Mater Des* 2012;33:69–74.
- [14] Longhurst WR, Strauss AM, Cook GE, Fleming PA. Torque control of friction stir welding for manufacturing and automation. *Int J Adv Manuf Tech* 2010;51:905–13.
- [15] Firouzdor V, Kou S. Al-to-Mg friction stir welding: effect of material position, travel speed, and rotation speed. *Metall Mater Trans A* 2010;41A:2914–35.
- [16] Leitão C, Louro R, Rodrigues DM. Analysis of high temperature plastic behaviour and its relation with weldability in friction stir welding for aluminium alloys AA5083-H111 and AA6082-T6. *Mater Des* 2012;37:402–9.
- [17] Ouyang J, Yarrapareddy E, Kovacevic R. Microstructural evolution in the friction stir welded 6061 aluminum alloy (T6-temper condition) to copper. *J Mater Process Technol* 2006;172:110–22.

ANNEX V - Galvão, I.; Loureiro, A.; Verdera, D.; Gesto, D.; Rodrigues, D. M. Influence of tool offsetting on the structure and morphology of dissimilar aluminum to copper friction-stir welds. *Metall. Mater. Trans. A* **2012c**, *43* (13), 5096–5105.

<http://dx.doi.org/10.1007/s11661-012-1351-x>

The author acknowledges the permission provided by The Minerals, Metals & Materials Society, the ASM International, the Springer and the Metallurgical and Materials Transactions A journal for the print and electronic reuse of this paper in current work.

Influence of Tool Offsetting on the Structure and Morphology of Dissimilar Aluminum to Copper Friction-Stir Welds

IVAN GALVÃO, ALTINO LOUREIRO, DAVID VERDERA, DANIEL GESTO,
and DULCE MARIA RODRIGUES

In this work, a systematic analysis of the effect of tool offsetting on the morphological, structural, and mechanical properties of 6082-T6 aluminum to copper-DHP friction-stir welds was performed, enabling full understanding of Al-Cu bonding structure and failure mechanisms. Important relations between tool positioning and the thermomechanical phenomena taking place during welding were established. Tool offsetting was revealed to be an effective way of solving one of the most important concerns in Al/Cu friction-stir welding, *i.e.*, the formation of large amounts of intermetallic-rich structures, which deeply influence the final strength and surface morphology of the welds. Actually, for welds produced without tool offsetting, it was found that the formation of fluidized intermetallic-rich structures promote the formation of internal decohesion areas inside the nugget, which have a detrimental effect on weld strength. For welds carried out with tool offsetting, intermetallic formation is almost suppressed, but important metallurgical discontinuities in the vicinity of large copper fragments, dispersed over the nugget, and at the nugget/copper interface were also found to have a detrimental effect on weld strength.

DOI: 10.1007/s11661-012-1351-x

© The Minerals, Metals & Materials Society and ASM International 2012

I. INTRODUCTION

JOINING dissimilar materials with high chemical affinity and completely different physical and mechanical properties, such as aluminum and copper, has already been recognized as an additional challenge in friction-stir welding (FSW) development.^[1] In fact, the establishment of dissimilar welding parameters, enabling adequate metal flow around the tool, and simultaneously, avoiding the formation of large amount of brittle intermetallic compounds, which seriously deteriorate the strength and surface morphology of the welds,^[2] has not been achieved yet. The development of new welding strategies, such as using interlayer materials,^[3] conceiving new joint design solutions,^[4,5] or offsetting the tool from the dissimilar base materials interface, to avoid intensive mixing during welding, are currently pointed as solutions for achieving successful dissimilar joining.

Among the alternative welding strategies mentioned in the previous paragraph, tool offsetting has been the most explored technique for aluminum to copper (Al/Cu) friction-stir welding. Okamura and Aota,^[6] who were among the first to report the use of this technique in Al/Cu welding, shifted the tool pin toward the

aluminum side in FSW of 8-mm-thick plates of 6061 aluminum alloy to oxygen-free copper. Restricting the pin stirring action to the aluminum side, they avoided base materials mixing and, consequently, inhibited the formation of brittle Al/Cu intermetallic phases during welding. The authors pointed out that the diffusion bonding, which took advantage of the friction plastic flow phenomenon taking place during welding, resulted in the production of less defective welds with improved surface appearance relative to welds obtained by traditional nonoffsetted FSW procedures. However, in spite of this, the offsetted welds displayed very poor tensile properties.

Genevois *et al.*^[7] also used tool offsetting in friction-stir welding of 4-mm-thick 1050-H16 aluminum alloy to commercially pure copper plates. These authors used full offsetting, with the pin fully displaced to the aluminum side, working tangent to the copper plate. No mechanical mixing between the base materials was observed in these conditions. The authors reported that frictional heating promoted thermally activated interdiffusion at the Al/Cu interface, giving rise to the formation of a very thin layer of intermetallic compounds (about 200 nm). No results concerning the structure, surface finishing, and mechanical properties of the welds were presented, which did not allow evaluating the effectiveness of this technique in obtaining sound bonding.

Xue *et al.*^[8] also reported the effect of tool offsetting towards the aluminum side on the morphological, structural, and mechanical properties of 5-mm-thick friction-stir welds between 1060 aluminum and pure copper (99.9 pct). The authors tested several degrees of offsetting, observing that small offsetting values (from 0

IVAN GALVÃO, Ph.D. Student, and ALTINO LOUREIRO and DULCE MARIA RODRIGUES, Professors, are with the Department of Mechanical Engineering, CEMUC, University of Coimbra, Rua Luís Reis Santos, 3030-788 Coimbra, Portugal. Contact e-mail: ivan.galvao@dem.uc.pt DAVID VERDERA and DANIEL GESTO, Engineers, are with the AIMEN, Relva 27A Torneiros, 36410 Porriño, Spain.

Manuscript submitted February 11, 2012.

Article published online August 23, 2012

to 33 pct of the pin radius) gave rise to the production of defective joints with poor surface finishing. Strong cracking incidence, due to the formation of high amounts of intermetallic phases, and important macrodefects, related to unsuitable material flow during welding, were pointed as the main concerns in using small tool offset. On the other hand, they reported important improvements in welds soundness and surface finishing by using larger values of tool offset (between 67 pct and 83 pct of the pin radius). However, most of the welds failed at the aluminum/copper interface for very low bending angles.

Finally, contrary to previous works, Liu *et al.*^[9] reported a detrimental effect of tool offsetting on welding results. Actually, they reported defective weld surfaces independently of the tool positioning, to either the aluminum or copper sides of the joint, or the tool offset width.

From the previous studies, it can be concluded that the effectiveness of FSW tool offsetting in obtaining nondefective Al/Cu welds, with suitable surface finishing and good mechanical properties, is not still supported or even consensual. Effectively, although it is well accepted that offsetting the tool reduces the interaction of both base materials and, consequently, inhibits the formation of Al-Cu brittle intermetallics, no consensus exists regarding the final properties of the welds. In this work, a systematic analysis of the effect of tool offsetting on the morphological, structural, and mechanical properties of aluminum to copper friction-stir welds is performed, which enables full understanding of the Al-Cu bonding failure reported in current and previous literature.

II. EXPERIMENTAL PROCEDURE

Three-millimeters-thick plates of oxygen-free copper with high phosphorous content (copper-DHP, R 240) and 6082-T6 aluminum alloy (AA 6082-T6) were friction-stir butt welded using a MTS I-Stir PDS equipment (MTS, Eden Prairie, MN). A H13 steel tool composed of a 16-mm-diameter shoulder, with a 7° conical cavity, and a 5 mm-diameter and 2.9 mm-length cylindrical probe was used. In order to study the effect of tool shifting on morphological, structural, and mechanical properties of the welds, different tool positions were tested, with offsetting values ranging from 0 to 2.5 mm, as shown in Figure 1 and Table I. According to the

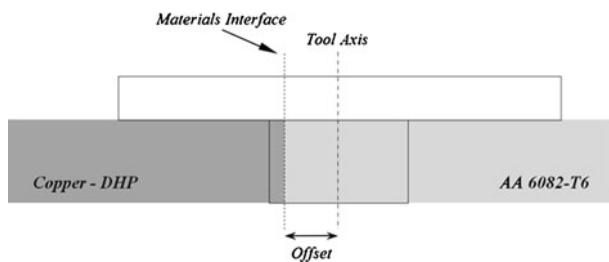


Fig. 1—Tool offset scheme.

figure, tool offset, which corresponds to the distance from the base materials interface to the tool axis, was always performed towards the aluminum side. In order to guarantee proper welding conditions, the copper-DHP plate was always positioned at the advancing side of the tool. Effectively, as reported by Galvão *et al.*^[10] no sound welding can be achieved by using the reverse base materials positioning, since under the high temperatures and strain rates experienced during FSW, the copper alloy, which is dragged by the shoulder from the retreating to the advancing side of the tool, pushes the softer aluminum alloy away from the under shoulder area, resulting in the production of welds morphologically very irregular. Tool offsetting towards the aluminum side was performed based on these same findings, as well as on Okamura and Aota^[6] recommendations, which point that by offsetting the tool from the joint interface, towards the softer retreating side material, promotes its extrusion against the harder advancing side material, resulting in welding by diffusion bonding.

The rotational and traverse speeds, as well as the axial load and tool tilt angle, were kept constant, with the values shown in Table I. This table also displays the nomenclature adopted in the text for labeling the different welds, which was selected in order to identify the only variable welding condition, *i.e.*, the tool offsetting value. Thus, the O_{2.5} weld corresponds to the weld performed with the tool shifted 2.5 mm from the base materials interface to the aluminum side. Macroscopic inspection of the weld surfaces was performed followed by transverse cross sectioning for metallographic analysis. The cross-section samples, prepared according to standard metallographic practice, were observed using optical microscopy, in a ZEISS HD 100 equipment (Carl Zeiss, Oberkochen, Germany). Scanning electron microscopy/energy dispersive X-ray spectroscopy (SEM/EDS) and micro X-ray diffraction were also performed in the cross-section and on the surface of some selected welds, using a PHILIPS XL30 SE microscope (Philips, Amsterdam, the Netherlands) and a PANalytical X'Pert PRO (PANalytical B.V., Almelo, the Netherlands) microdiffractometer, respectively. Microhardness measurements were performed using a Shimadzu Microhardness Tester (Shimadzu Corporation, Kyoto, Japan), with 200 g load and 15 seconds holding time. In order to evaluate the strength of the welds, bending specimens were taken from all welds and tested, in accordance with the ISO 5173:2009(E) stan-

Table I. Welding Parameters and Tool Offsetting Width

Weld	Rotational Speed (rev.min ⁻¹)	Traverse Speed (mm.min ⁻¹)	Axial Load (kN)	Tilt Angle (deg)	Tool Offset (mm)
O ₀					0.0
O _{0.6}					0.6
O _{1.3}	1000	200	7	3	1.3
O _{1.9}					1.9
O _{2.5}					2.5

dard, in an Instron 4206 equipment (Instron Corporation, Norwood, MA).

III. RESULTS

A. Morphological Analysis

Pictures of the weld surfaces and optical macrographs of the cross sections are illustrated in Figure 2. Pin and shoulder influence zones are indicated in each cross section using white and red vertical lines, respectively. Comparing the cross sections of the different welds, it can be observed that the amount of copper dragged by the tool, as well as base materials mixture, strongly varied by changing tool offsetting. In fact, in the pin influence zone of the O_0 weld cross section shown in Figure 2(a), a copper volume with a mass of darker material inside of it can be observed. For the welds produced with small ($O_{0.6}$ and $O_{1.3}$ welds) and large offsetting ($O_{1.9}$ and $O_{2.5}$ welds) values, only relatively

large copper fragments (Figures 2(b) and (c)) or smaller size copper particles (Figures 2(d) and (e)), respectively, can be observed inside the pin influence zone. It is also apparent from the figure that the dark structures observed in O_0 weld cross section were almost suppressed by increasing tool offset.

Important differences in surface finishing can also be depicted by comparing the top layer of the welds in Figure 2. In fact, whereas thick and very rough top layers, similar to those obtained by other authors in traditional non-offsetted procedures,^[8,9,11] can be observed on the surface of the welds produced with no or very low offsetting values (Figures 2(a) through (c)), very smooth surfaces, with fine and regularly distributed arc shaped striations, like those observed in similar Al/Al^[12] or Cu/Cu^[13] friction-stir welds, can be observed for the welds performed with the highest offsetting values (Figures 2(d) and (e)). According to previous studies,^[2,14] the formation and irregular distribution of intermetallic-rich structures over the weld surfaces is the

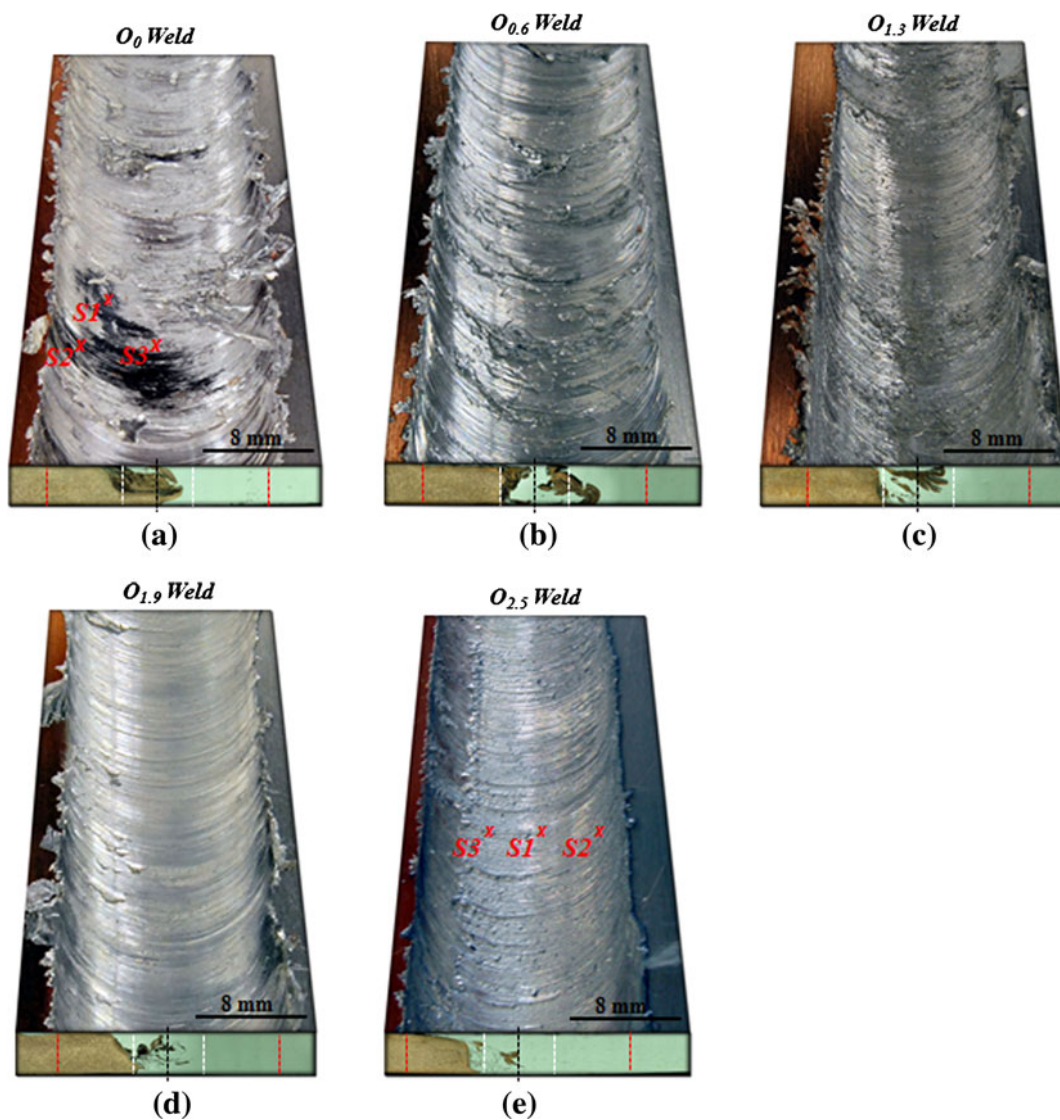


Fig. 2—Surface and transverse cross-section macrographs of the O_0 (a), $O_{0.6}$ (b), $O_{1.3}$ (c), $O_{1.9}$ (d), and $O_{2.5}$ (e) welds.

main reason for obtaining very poor surface finishing. Figure 3 shows the results of a XRD analysis performed on the surface of the welds produced with the extreme offsetting values, *i.e.*, the O_0 (S1, S2, and S3 analysis points in Figure 2(a)) and $O_{2.5}$ welds (S1, S2, and S3 analysis points in Figure 2(e)). In this figure, it can also be observed that whereas high amounts of $CuAl_2$ and Cu_9Al_4 are present on the rough and irregular top layer of the O_0 weld (Figure 3(a)), no intermetallic structures, or even significant amounts of copper, were identified on the surface of the $O_{2.5}$ weld (Figure 3(b)). These results suggest that, in addition to welding parameters,^[2] and

tool geometry,^[14] tool offsetting also has a strong influence on intermetallic phases formation, deeply influencing welds morphology and surface finishing.

B. Failure Analysis

Although tool offsetting revealed to be an effective way of solving one of the most important concerns in Al/Cu friction-stir welding, *i.e.*, the formation of very irregular intermetallic-rich surfaces, the industrial interest of this welding strategy strongly depends on its effectiveness in providing welds with acceptable

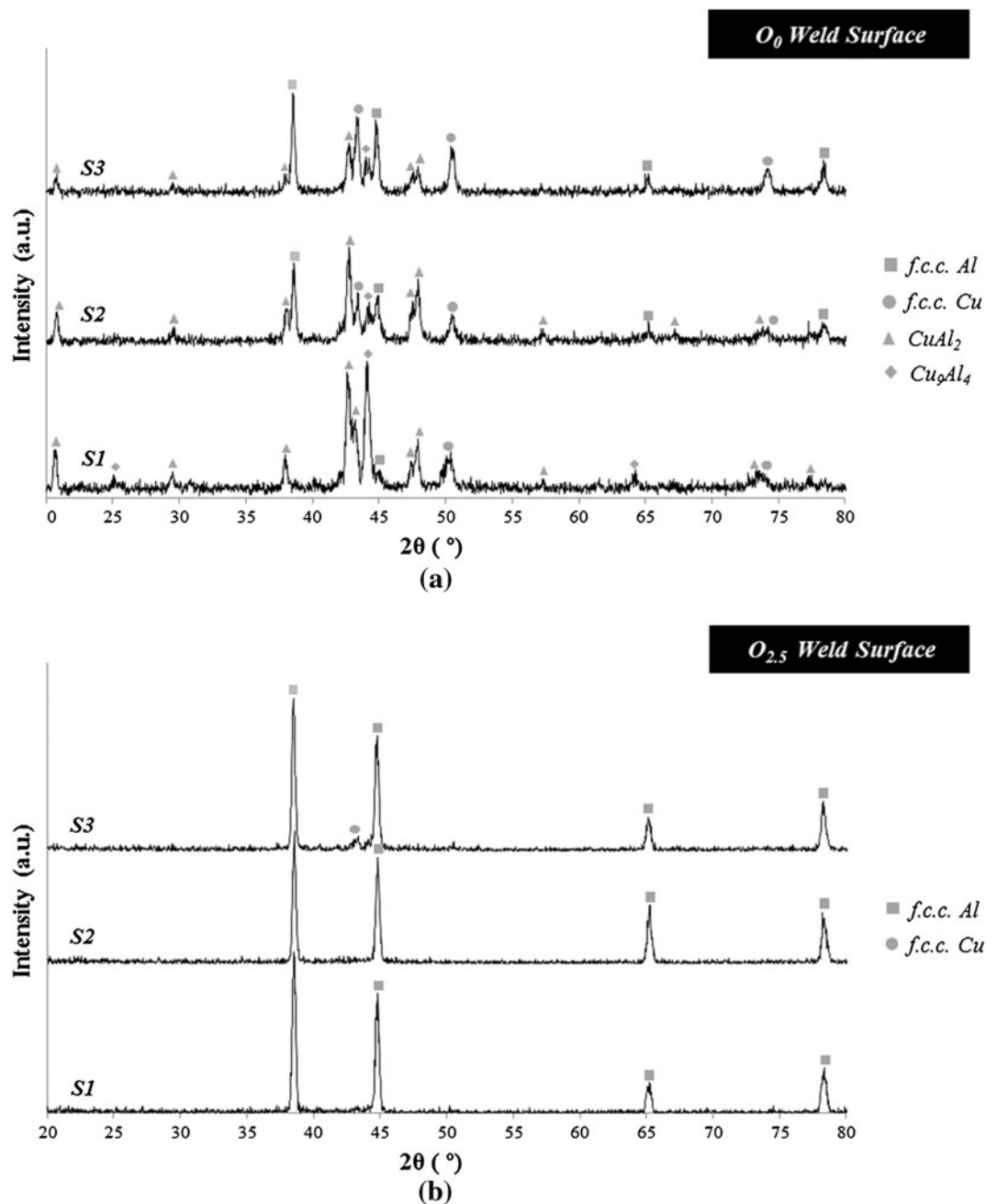


Fig. 3—X-rays diffractograms acquired on the surface of the O_0 (a) and $O_{2.5}$ (b) welds.

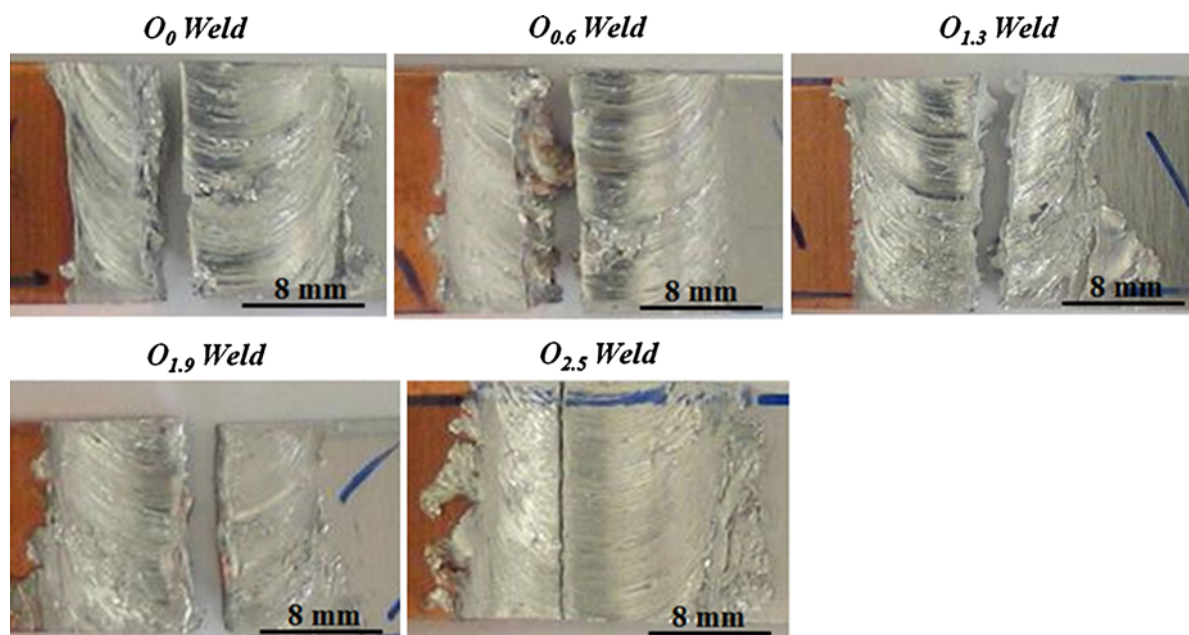


Fig. 4—Pictures of the tested bending specimens.

strength. So, root bending tests were performed using transverse specimens from all welds. Pictures of the fractured samples are shown in Figure 4, where it can be observed that all welds failed for low bending angles, *i.e.*, approximately 20 deg. Fracture surfaces analysis revealed important differences in Al-Cu bonding structure, according to tool offsetting.

Figure 5 shows a macrograph of a fracture surface of the O_0 weld and SEM micrographs of three selected areas signalized in that image. Figure 5(a) clearly illustrates the strong morphological heterogeneity of the fracture surface. In fact, besides aluminum and copper zones, with ductile fracture features, illustrated in Figures 5(b) and (c), respectively, another smooth region with featureless morphology, which cannot be associated to any mode of fracture, was identified in the fracture surface. Figures 5(d) and (e), which illustrate a backscattered electron (BSE) micrograph and EDS spectra registered in the featureless zone, show that this region is composed of aluminum-rich islands (zone 1) dispersed over an Al/Cu mixed matrix (zone 2).

Analyzing the fracture surfaces of the $O_{0.6}$ and $O_{1.3}$ welds, strong differences in fracture morphology relative to the O_0 weld were depicted. In order to illustrate these differences, a transverse cross section (Figure 6(a)) and a macrograph of the fracture surface (Figure 6(b)) of an $O_{1.3}$ bending sample are shown in Figure 6. In the transverse cross section, it can be observed that, at the bottom of the weld, the crack runs along the interface between the aluminum matrix and a large copper fragment. In the fracture surface macrograph (Figure 6(b)), which corresponds to a longitudinal view of the weld, it can also be observed large voids distributed along the bottom of the weld, where the fracture was initiated, and ductile fracture features in the aluminum matrix at the top of it. It is also important to stress that no large areas with featureless structures,

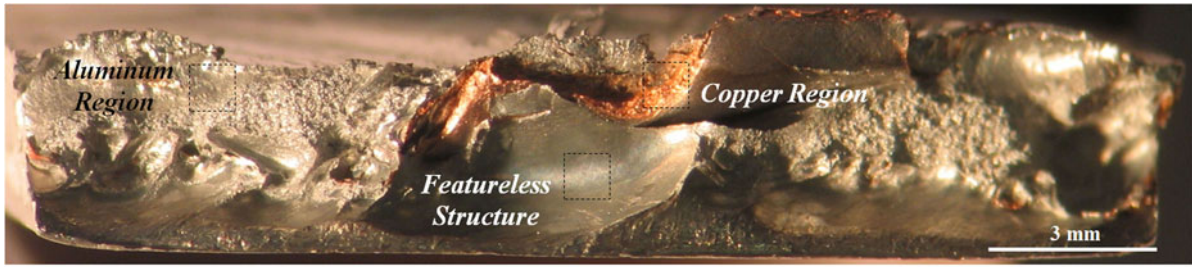
similar to those observed for the O_0 weld, were identified in the fracture surfaces of the $O_{0.6}$ or $O_{1.3}$ welds.

Finally, a transverse cross section and a fracture surface macrograph of the $O_{2.5}$ bending specimen, which are also representative of the $O_{1.9}$ weld failure mode, are illustrated in Figure 7. From the transverse cross-section macrograph (Figure 7(a)), it can be observed that the fracture took place at the advancing side of the weld, at the interface between the aluminum-rich nugget and the copper matrix. The SEM fracture surface macrograph, illustrated in Figure 7(b), shows a very smooth fracture surface, with very small evidence of ductile failure only at the top layer of the weld.

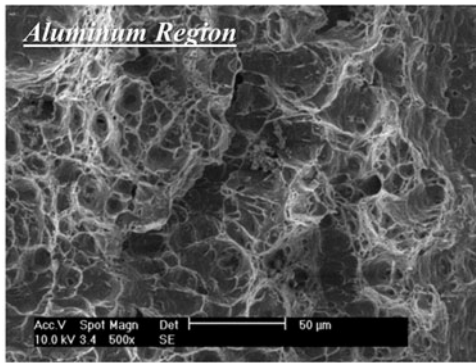
C. Discussion

From previous results, it can be concluded that offsetting the tool relative to the base materials interface deeply changed the Al/Cu welds morphologies, but it had no important effect in improving the weld strength. In fact, despite with different characteristics, severe discontinuities were detected in all weld-bending samples fractographs.

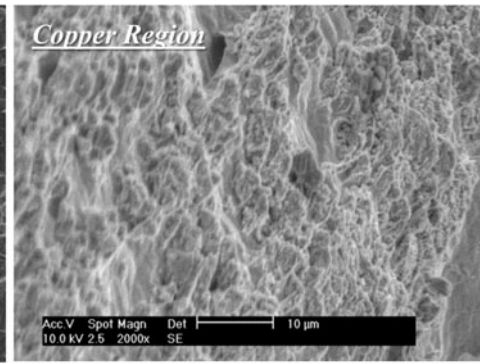
Analyzing the cross-section macrograph of the O_0 weld, which is illustrated in Figure 2(a), a dark color structure inside the nugget was found, corresponding to a large mixing region extending into the copper side of it. From Figure 8(a), in which a BSE micrograph registered in the mixing zone is illustrated, it can be observed that this region is composed of layers of copper (white) and aluminum (black) alternated with copper-rich or aluminum-rich (light and dark gray, respectively) mixed lamellae. Figure 9(a), which illustrates the results of the XRD analysis carried out in this region (see S_1 , S_2 , and S_3 analysis points in Figure 8(a)), confirms the formation of a structure with highly heterogeneous phase content: pure base materials



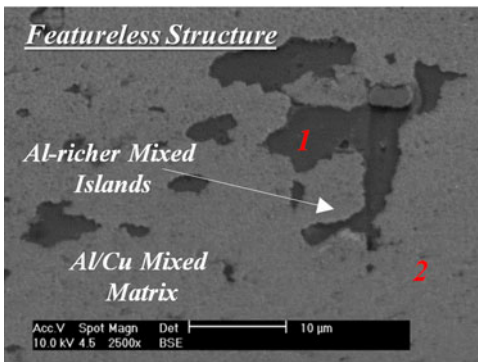
(a)



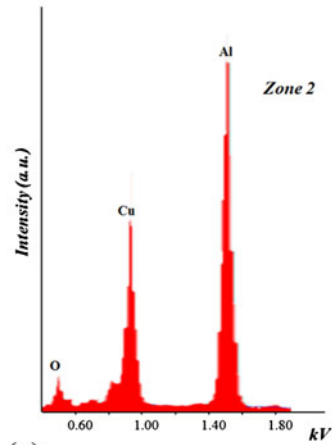
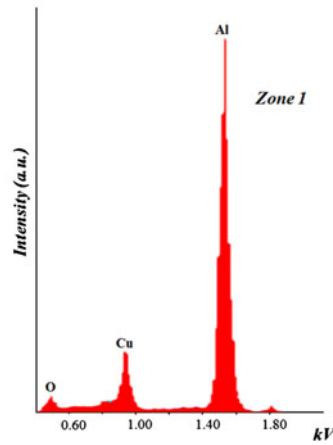
(b)



(c)

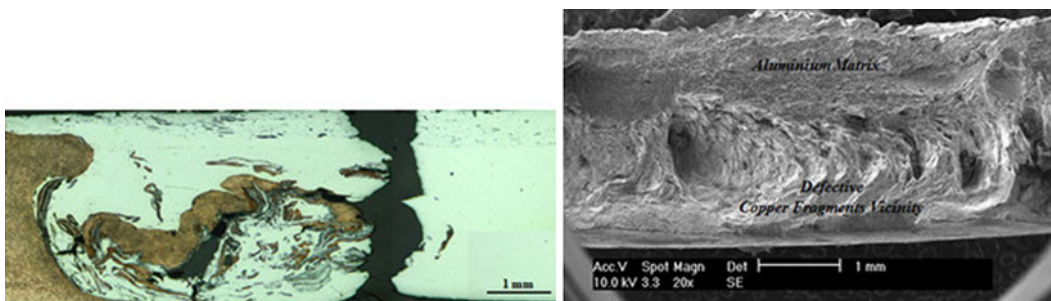


(d)



(e)

Fig. 5—Optical macrograph of the fracture surface of the O_0 weld bending specimen (a), SE micrographs of the aluminum (b) and copper (c) regions, and BSE micrograph (d) and EDS results (e) registered in the featureless structure.



(a)

(b)

Fig. 6—Optical macrograph of the transverse cross section (a) and SE micrograph of the fracture surface (b) of the $O_{1.3}$ weld-bending specimen.

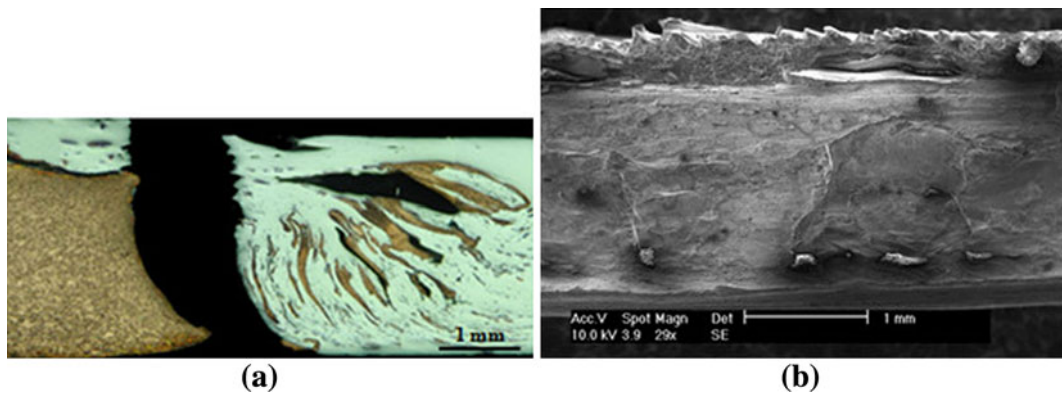


Fig. 7—Optical macrograph of the transverse cross section (a) and SE macrograph of the fracture surface (b) of the $O_{2.5}$ weld bending specimen.

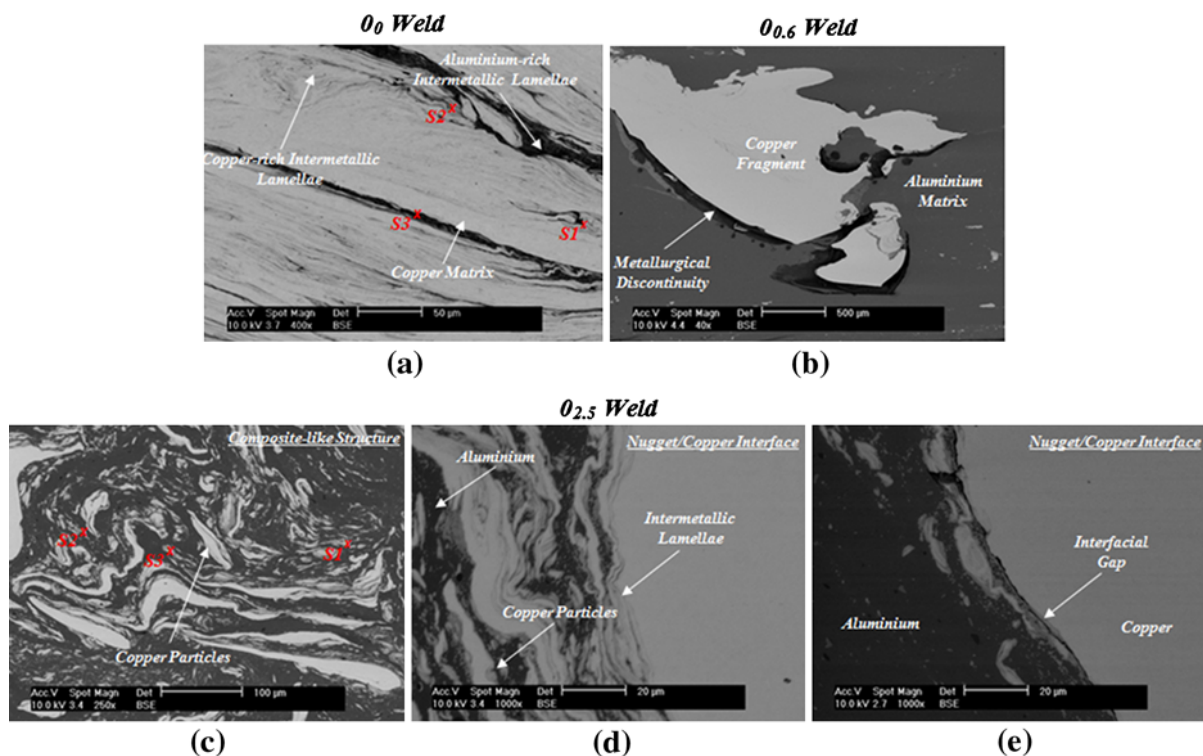


Fig. 8—BSE micrographs registered in the mixing zone of the O_0 weld (a), copper fragments vicinity of the $O_{0.6}$ weld (b), nugget's composite-like structure (c) and aluminum/copper interface zones (d, e) of the $O_{2.5}$ weld.

composition (face-centered cubic [fcc] Al and fcc Cu) and significant amounts of aluminum-rich ($CuAl_2$) and copper-rich (Cu_9Al_4) intermetallic phases. The rich intermetallic content of the nugget of the O_0 weld agrees well with the bimetallic composition of the featureless structure observed in the fractograph of this weld (Figure 5(a)). Based on the aluminum-rich chemical composition of the featureless surface (Figure 5(e)), it is expected that significant amounts of aluminum-rich phases, such as $CuAl_2$ and/or $Al/CuAl_2$, compose this structure. The low melting temperature of these phases, which, according to a previous FSW study from Ouyang *et al.*^[15] are close to the Al/Cu FSW peak temperatures, point to the fluidization of the intermetallic phases being formed during welding. The strong differences in

physical and mechanical properties between the intermetallic structures, flowing downward around the pin, and the base materials dragged by it, gave rise to metallurgical discontinuities corresponding to the smooth morphology of the featureless surface observed in the macrograph of Figure 5(a). It is also important to stress that, although extremely high hardness values have been registered in the intermetallic-rich structures present in the nugget of the O_0 weld, as illustrated in Figure 10(a), no brittle cleavage type failure was registered for this joint, contrary to that referred by previous studies on dissimilar FSW.^[9,16]

Unlike that observed for the O_0 weld, no featureless smooth surface was observed in fractographs of the welds produced with small tool offsetting values ($O_{0.6}$

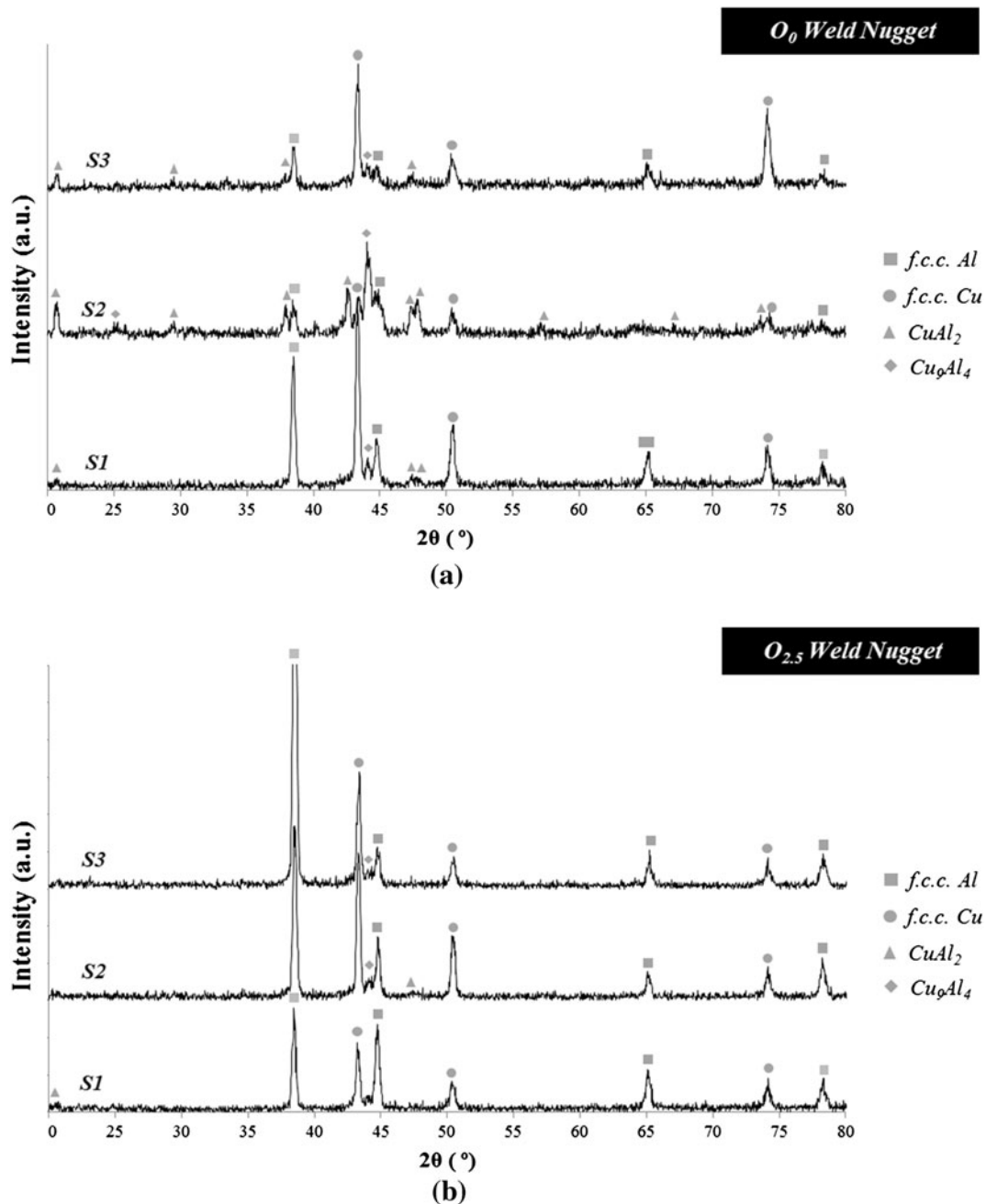


Fig. 9—X-ray diffractograms acquired in the nugget of the O_0 (a) and $O_{2.5}$ (b) welds.

and $O_{1.3}$ welds). Instead, the fracture surface analysis indicated the presence of large voids aligned with the interface of the large copper fragments dispersed inside the nugget, which can be observed in Figures 2(b) and (c). In fact, since the incorporation of copper, which was placed at the advancing side of the tool, in the shear layer is promoted almost exclusively by the pin,^[2,17] tool offsetting promotes an important decrease of the amount of copper dragged by the tool during welding. The very hard copper clusters being dragged inside the softer aluminum matrix (Figure 10(b)) also have a sharp geometry, which makes material filling around them very difficult and promotes the formation of very large

discontinuities at the interface of the copper clusters, as illustrated in Figure 8(b). Similar results have already been reported by Xue *et al.*^[8] and Esmaili *et al.*^[18] in AA 1060/copper and AA 1050/brass FSW, respectively. So, it can be concluded that although using small values of tool offsetting has reduced the interaction of both base materials, which inhibited the formation of high amounts of intermetallic phases, no improvements in Al/Cu bonding were achieved.

For the $O_{1.9}$ and $O_{2.5}$ welds, whose cross sections are illustrated in Figures 2(d) and (e), it was already concluded that the amount of copper dragged by the pin is much lower than in previous welding procedures.

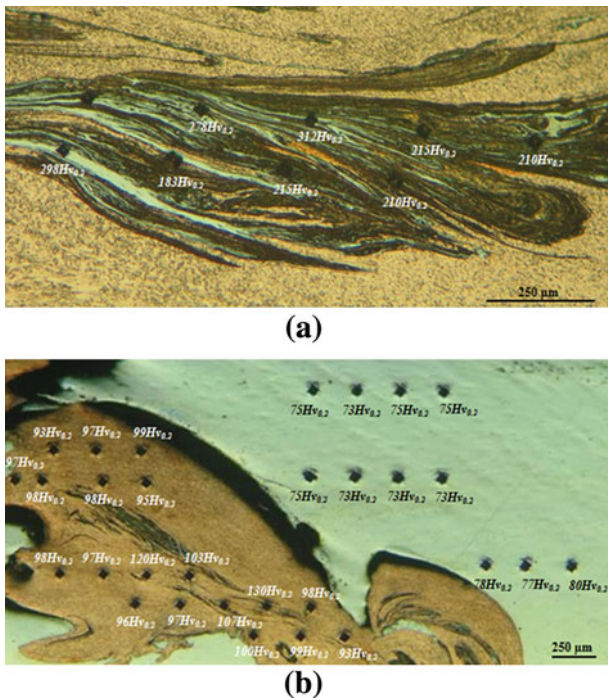


Fig. 10—Hardness measurements registered in cross-section structures of the O_0 (a) and $O_{0.6}$ (b) welds.

Specifically, a composite-like structure, composed of very small-sized copper particles homogeneously scattered in the aluminum matrix side of the nugget/copper interface, was detected in the nugget of the $O_{2.5}$ weld, as illustrated in Figure 8(c). This figure shows that large tool offsetting avoided dragging of large copper particles. Figure 9(b) illustrates the results of the XRD analysis carried out in the nugget of the $O_{2.5}$ weld (see S1, S2, and S3 analysis points in Figure 8(c)). From the diffractogram, it can be observed that in good agreement with that registered for the weld surface (Figure 3(b)), very low intensity $CuAl_2$ and Cu_9Al_4 diffraction peaks were registered in the nugget of this weld. In fact, tool offsetting avoided intense material interaction and the generation of large mixing volumes with atomic concentrations suitable for the formation of aluminum or copper-rich intermetallic phases.^[2,15]

Finally, Figures 8(d) and (e) illustrate, for both the $O_{1.9}$ and $O_{2.5}$ welds, the nugget/copper interface characteristics. It can be observed that no thin and continuous intermetallic layer, indicating the metallurgical continuity suggested by Xue *et al.*^[19] and Genevois *et al.*^[7] was observed all along the nugget/copper interface. In fact, although some localized interfacial zones presenting metallurgical continuity have been identified, in which very small copper particles were intercalated with aluminum-rich material and nanosized intermetallic lamellae (Figure 8(d)), most of nugget/copper interfacial region is composed of zones with sharp Al/Cu transitions, with no signs of base materials interaction (Figure 8(e)). Actually, important interfacial gaps were often observed in the sharp Al/Cu transition zones,

pointing to metallurgical discontinuity between both base materials. This enables to conclude that thermally activated interdiffusion referred by several authors did not occur in most of aluminum/copper interfacial area. As a result, no joining took place between both base materials, which gave rise to the smooth fracture interface shown in Figure 7. Effectively, under the complex material flow and deposition phenomena taking place during FSW, it will be of extreme difficulty to control the formation of a uniform and continuous thin intermetallic layer all along Al/Cu interface.

Several welding conditions have already been tested, by the authors, in aluminum to copper FSW, in order to better understand the material flow mechanisms and the metallurgical phenomena taking place during the joining of these metals. Effectively, the authors intend to achieve a suitable window of welding conditions for joining aluminum to copper by FSW. These study results intend to illustrate the influence of a particular “process parameter,” the tool offsetting, on aluminum to copper friction-stir welding results. For that reason, all other process parameters were set constant.

IV. CONCLUSIONS

From the current study, it can be concluded that offsetting the tool from base materials interface inhibits the formation of Al/Cu intermetallic phases during welding, which have strong influence on surface morphology and mechanical properties of the welds. As a result, welds with excellent surface finishing were produced. Nevertheless, no significant improvements in mechanical properties of the welds were achieved. In fact, independently of tool offsetting, the formation of important metallurgical discontinuities seriously compromised the strength of all welds.

ACKNOWLEDGMENTS

The authors are indebted to the Portuguese Foundation for the Science and Technology (FCT) and European Regional Development Fund (ERDF) for the financial support and to the company *Thyssen Portugal—Aços e Serviços Lda* for providing the heat treatments for the friction-stir welding tools.

REFERENCES

1. T. DebRoy and H.K.D.H. Bhadeshia: *Sci. Technol. Weld. J.*, 2010, vol. 15 (4), pp. 266–70.
2. I. Galvão, J.C. Oliveira, A. Loureiro, and D.M. Rodrigues: *Sci. Technol. Weld. J.*, 2011, vol. 16 (8), pp. 681–89.
3. D.J. Blosmo, T. Curtis, T. Johnson, N. Prociwe, C.A. Widener, B. Carlson, R. Szymanski, and M.K. West: *Friction Stir Welding and Processing VI*, R. Mishra, M.W. Mahoney, Y. Sato, Y. Hovanski, and R. Verma, eds., Wiley, Hoboken, NJ, 2011, pp. 409–16.
4. M. Geiger, F. Micari, M. Merklein, L. Fratini, D. Contorno, A. Giera, and D. Staud: *Int. J. Mach. Tools Manu.*, 2008, vol. 48, pp. 515–21.

5. H.J. Liu, J.J. Shen, S. Xie, Y.X. Huang, F. Cui, C. Liu, and L.Y. Kuang: *Sci. Technol. Weld. J.*, 2012, vol. 17 (2), pp. 104–10.
6. H. Okamura and K. Aota: *Weld. Int.*, 2004, vol. 18 (11), pp. 852–60.
7. C. Genevois, M. Girard, B. Huneau, X. Sauvage, and G. Racineux: *Metall. Mater. Trans. A*, 2011, vol. 42A, pp. 2290–95.
8. P. Xue, D.R. Ni, D. Wang, B.L. Xiao, and Z.Y. Ma: *Mater. Sci. Eng. A*, 2011, vol. 528, pp. 4683–89.
9. H.J. Liu, J.J. Shen, L. Zhou, Y.Q. Zhao, C. Liu, and L.Y. Kuang: *Sci. Technol. Weld. J.*, 2011, vol. 16 (1), pp. 92–99.
10. I. Galvão, R.M. Leal, A. Loureiro, and D.M. Rodrigues: *Sci. Technol. Weld. J.*, 2010, vol. 15 (8), pp. 654–60.
11. E. Akinlabi, A. Els-Botes, and H. Lombard: *8th International Symposium on Friction Stir Welding*, Timmendorfer Strand, Germany, 2010.
12. C. Leitão, R.M. Leal, D.M. Rodrigues, A. Loureiro, and P. Vilaça: *Mater. Des.*, 2009, vol. 30, pp. 101–08.
13. R.M. Leal, N. Sakharova, P. Vilaça, D.M. Rodrigues, and A. Loureiro: *Sci. Technol. Weld. J.*, 2011, vol. 16 (2), pp. 146–52.
14. I. Galvão, J.C. Oliveira, A. Loureiro, and D.M. Rodrigues: *Intermetallics*, 2012, vol. 22, pp. 122–28.
15. J. Ouyang, E. Yarrapareddy, and R. Kovacevic: *J. Mater. Process. Technol.*, 2006, vol. 172, pp. 110–22.
16. V. Firouzdor and S. Kou: *Metall. Mater. Trans. A*, 2011, vol. 43A, pp. 303–15.
17. R.M. Leal, C. Leitão, A. Loureiro, D.M. Rodrigues, and P. Vilaça: *Mater. Sci. Eng. A*, 2008, vol. 498, pp. 384–91.
18. A. Esmaili, M.K.B. Givi, and H.R.Z. Rajani: *Mater. Sci. Eng. A*, 2011, vol. 528, pp. 7093–7102.
19. P. Xue, B.L. Xiao, D.R. Ni, and Z.Y. Ma: *Mater. Sci. Eng. A*, 2010, vol. 527, pp. 5723–27.

ANNEX VI - Galvão, I.; Verdera, D.; Gesto, D.; Loureiro, A.; Rodrigues, D. M. Influence of aluminium alloy type on dissimilar friction stir lap welding of aluminium to copper. *J. Mater. Process. Technol.* **2013**, 213 (11), 1920–1928.

<http://dx.doi.org/10.1016/j.jmatprotec.2013.05.004>

The author acknowledges the permission provided by Elsevier and the Journal of Materials Processing Technology for the print and electronic reuse of this paper in current work.



Influence of aluminium alloy type on dissimilar friction stir lap welding of aluminium to copper

I. Galvão^a, D. Verdera^b, D. Gesto^b, A. Loureiro^a, D.M. Rodrigues^{a,*}

^a CEMUC, University of Coimbra, Rua Luís Reis Santos, 3030-788 Coimbra, Portugal

^b AIMEN, Relva 27A Torneiros, 36410 Porriño, Spain

ARTICLE INFO

Article history:

Received 11 February 2013

Received in revised form 5 May 2013

Accepted 7 May 2013

Available online xxx

Keywords:

Friction stir lap welding

AA 6082/copper

AA 5083/copper

Microstructure

ABSTRACT

A heat-treatable (AA 6082) and a non-heat treatable (AA 5083) aluminium alloys were friction stir lap welded to copper using the same welding parameters. Macro and microscopic analysis of the welds enabled to detect important differences in welding results, according to the aluminium alloy type. Whereas important internal defects, resulting from ineffective materials mixing, were detected for the AA 5083/copper welds, a relatively uniform material mixing was detected in the AA 6082/copper welds. Micro-hardness testing and XRD analysis also showed important differences in microstructural evolution for both types of welds. TEM and EBSD-based study of the AA 5083/copper welds revealed the formation of submicron-sized microstructures in the stirred aluminium region, for which untypically high hardness values were registered.

© 2013 Elsevier B.V. All rights reserved.

1. Introduction

Despite the large number of potential industrial applications of aluminium/copper (Al/Cu) hybrid components, in practice, the use of this metallic couple remains limited. The different physical and mechanical properties of both metals, as well as its chemical affinity at temperatures higher than 120 °C, which often results in extensive brittle intermetallic phases formation during welding, make the joining of these two materials very difficult. Although some success in Al/Cu joining has already been achieved by friction and explosion welding, strong restrictions in the thickness of the welded plates and joint geometry limit the wider application of these processes.

Friction stir welding (FSW), a welding technology, which, although has initially been developed for Al-alloys, soon spread to many other materials and materials combinations, renewed the hope of joining aluminium to copper for a large range of plate thicknesses and varied joint geometries (Çam, 2011). In this technology, a stirring tool composed of suitable designed shoulder and pin, which protrudes from the base of the tool shoulder, is pressed against plates to be welded and moves along them. The heat caused by the friction between the tool and the workpiece results in intense local heating that does not melt the plates to be joined, but severely deforms the material around the tool. The production of welds by plastic deformation, at temperatures below the melting temperature of the base materials, is viewed as an interesting way for

reducing the formation of brittle intermetallic phases during Al/Cu welding and, consequently, cracking in the joints. Actually, several works have already addressed dissimilar friction stir welding of these materials, in both butt and lap joint configurations. However, Al/Cu friction stir butt welding has been much more explored than lap joining, for which, so far, only a small number of studies was conducted.

Elrefaey et al. (2004) were one of the first investigating the feasibility of lap joining of 2 mm-thick AA1100 H24 plates to 1 mm-thick copper plates. They found that the joint strength strongly depended on the penetration depth of the pin tip into the copper surface. The authors observed that the joints showed very weak fracture loads when the pin did not penetrate in the copper surface. On the other hand, slight penetration of the pin tip into the copper surface increased the joint strength significantly. Although the level of bond strength was quite low, it exhibited a general tendency to increase with a rise in the rotation speed.

Some years later, Abdollah-Zadeh et al. (2008) and Saeid et al. (2010), in friction stir lap welding of 4 mm-thick AA 1060 to 3 mm-thick commercially pure copper, pointed out two factors affecting the welding results, i.e., the amount of brittle and hard intermetallic compounds and the “cold weld” condition. Whereas the welds produced under very high heat input conditions (high rotation speed and low traverse speed) presented formation of brittle intermetallic layers, in which strong micro-cracking takes place, the welds carried out under low heat input conditions (low rotation speed and high traverse speed) displayed incompletely welded interfaces. According to the authors, the optimum welding results should be achieved by adjusting rotational and traverse speed values. In 2011,

* Corresponding author. Tel.: +351 239 790 700; fax: +351 239 790 701.
E-mail address: dulce.rodrigues@dem.uc.pt (D.M. Rodrigues).

Xue et al. (2011) reported the beneficial effect of using a large pin diameter for friction stir welding AA 1060 aluminium alloy to commercially pure copper plates, both of 3 mm-thick. According to the authors, a larger diameter pin gives rise to a larger bonding area, which inhibits more effectively the cracks propagation during mechanical testing, enhancing the bonding strength of the Al/Cu interface.

More recently, Akbari et al. (2012) analysed the effect of base materials positioning on friction stir lap welding of 2 mm-thick plates of AA 7070 aluminium alloy to commercially pure copper. Welds produced with the aluminium alloy located on the top of joint and the copper at the bottom, as well as welds carried out with the reverse base materials positioning, were studied by the authors. It was observed that, under similar welding conditions, the strength of the joints produced with the aluminium plate on the top was higher than that of the welds carried out with the reverse materials positioning. According to Akbari et al. (2012), the influence of the base materials positioning on the mechanical properties of the joints is closely related with the way how it affects the heat input during welding. Effectively, the authors concluded that the higher strength of the welds produced with the aluminium plate on the top of the joint is mainly influenced by the higher peak temperatures reached during welding with this plates' positioning.

In the same year, Firouzdor and Kou (2012) compared the results of AA 6061/commercially pure copper friction stir lap welding carried out by using two different welding procedures, which were called "conventional" and "modified" friction stir lap welding. In conventional welding, the 1.6 mm-thick AA 6061 aluminium alloy plate was placed at the top of the lap joint and the copper plate, with the same thickness, was placed at the bottom. On the other hand, in modified lap welding, the 1.6 mm-thick plates were positioned in the reverse way, i.e., the copper plate was placed at the top and the aluminium plate at the bottom. Furthermore, a smaller AA 6061 aluminium alloy plate was butt welded to the copper at the top of the joint, with a slight pin penetration into the bottom sheet. In butt welding, the pin was shifted into aluminium plate, which was positioned at the advancing side of the tool. As a result of their study, the authors found that modified lap FSW significantly improved the quality of the Al/Cu friction stir lap welds. In fact, for specific values of rotation and traverse speed, the joint strength and the ductility of the "modified" welds was about twice and five to nine times higher, respectively, than those of the "conventional welds". Firouzdor and Kou (2012) also observed that voids were no longer present along the Al–Cu interface as in conventional lap welds, which shifted the location of fracture in tensile testing from along the interface to through Cu.

This year, Bisadi et al. (2013), in friction stir lap welding of 2.5 mm-thick AA 5083 to 3 mm-thick commercially pure copper sheets, claimed, in good agreement with Abdollah-Zadeh et al. (2008) and Saeid et al. (2010), that extreme welding temperatures give rise to defective joints. The authors observed channel-like defects near the sheets interface, for very low temperatures, and cavities at the interface of stirred aluminium particles and the copper, for high welding temperatures. According to the authors, high welding temperatures lead to higher aluminium diffusion to the copper sheet, which makes that aluminium particles are forced into the copper sheet and, after quenching, some cavities are formed at the interface of the particles and the copper matrix. Besides the high temperatures, the different melting temperatures and contraction coefficients of both materials are pointed by the authors as the main factors on the basis of this type of defect. It was also reported that, for the range of welds tested, the hardness values of the stirred aluminium alloy were considerably lower than that of the aluminium base material, contrary to the stirred copper hardness, which was in over-match relative to the base material.

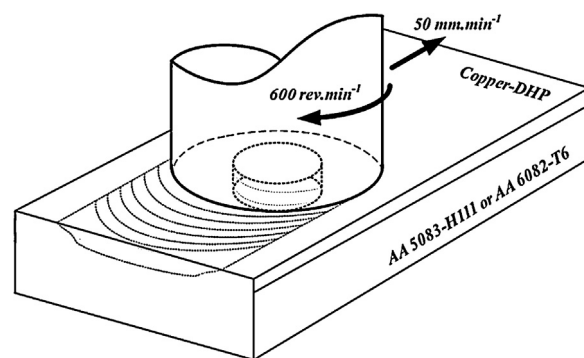


Fig. 1. Schematic representation of Al/Cu friction stir welding.

Excepting the works conducted by Akbari et al. (2012) and Firouzdor and Kou (2012), in all other studies presented above, the aluminium plates were positioned at the top of the Al/Cu lap joint and the copper plates at the bottom. Aluminium to copper friction stir lap welding with reverse plates positioning, enabling the joining of very thin copper plates to thicker aluminium plates remains deeply unexplored. This joint configuration, which, for example, enables copper cladding over small areas, has high technical and economic interest. Furthermore, most of the reported works were focused on welding of copper to commercially pure aluminium (1xxx aluminium series). Effectively, so far, only few works have already addressed friction stir lap welding of copper and aluminium alloys of other series with high industrial applicability, such as 6xxx and 5xxx aluminium series. In this context, dissimilar friction stir welding of 1 mm-thick copper-DHP plates to 6 mm-thick AA 5083-H111 and AA 6082-T6 aluminium alloys plates, with the copper plate located at the top of the joint, was carried out in present work. The influence of the base materials intrinsic properties on Al/Cu friction stir weldability, which has never been investigated, was studied by performing a deep structural and mechanical characterisation of the welds.

2. Experimental

Copper-DHP (R240) was friction stir lap welded to two different aluminium alloys, the heat treatable AA 6082-T6 and the non-heat treatable AA 5083-H111 alloy, in a MTS I-Stir PDS equipment. As illustrated in Fig. 1, the 1 mm-thick copper-DHP plates were placed at the top of 6 mm-thick plates of each aluminium alloy, being clamped against it. Welding was carried out with a tool composed of a 9.5 mm-diameter conical shoulder, with an 8° cavity, and a 3 mm-diameter and 1 mm-long cylindrical probe, which is schematically represented in Fig. 2. In order to study the effect of the aluminium

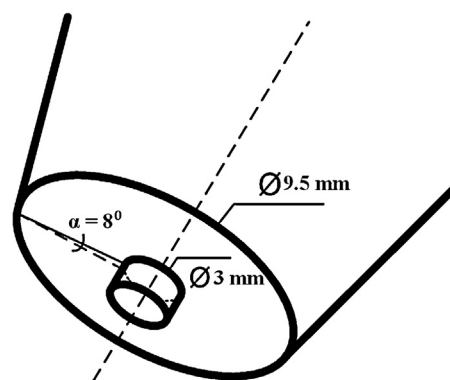


Fig. 2. Friction stir welding tool.

alloy type on welding results, all welds were conducted using the same welding parameters, namely, rotational and traverse speeds of 600 rpm and 50 mm min^{-1} , respectively, tool tilt angle of 0° and tool axial load of 4.5 kN. In this way, the nomenclature adopted in the text for labelling the different welds will identify the only variable welding condition, i.e., the aluminium alloy. So, copper-DHP/AA 5083-H111 and copper-DHP/AA 6082-T6 welds will be identified by the acronyms W5 and W6, respectively.

After welding, a qualitative macroscopic inspection of the weld surfaces was performed by means of visual inspection. Transverse cross-sectioning of the welds was performed for metallographic analysis. The samples were prepared according to standard metallographic practice and differentially etched in order to enable the analysis of the microstructural transformation induced by welding. Metallographic analysis was performed using optical microscopy, in a ZEISS 100 HD equipment. The microstructure of some selected welds was also analysed by transmission electron microscopy (TEM) and electron backscatter diffraction (EBSD) in a FEI Tecnai G² S-Twin and a FEI Quanta 400FEG ESEM/EDAX Genesis X4M microscopes, respectively. Microhardness measurements were performed using a Shimadzu Microhardness Tester, with 200 g load and 15 s holding time. Micro X-ray diffraction and electron probe micro analysis (EPMA) were performed in the cross-section of the welds using a PANalytical X'Pert PRO micro-diffractometer and a Cameca Camebax SX50 apparatus, respectively.

3. Results

3.1. Welds structure and morphology

Images of the surfaces, cross-section macrographs and micrographs registered in some selected cross-section areas of W5 and

W6 welds are illustrated in Figs. 3 and 4, respectively. Significant differences in surface finishing can be observed by comparing the surface photographs in Figs. 3a and 4a. In fact, whereas the W5 weld presents a very smooth surface composed of regular and well-defined striations, similar to those obtained in similar copper friction stir welding by Galvão et al. (2013), signs of significant tool submerging and formation of massive flash are observed at the surface of the W6 weld. It is important to stress that, although both welds have been carried out under the same welding conditions, the W6 weld surface presents defects usually associated to excessive heat input during friction stir welding. This result is in good agreement with Leitão et al. (2011), who studied the influence of base materials properties on defect formation during AA 5083 and AA6082 aluminium alloys FSW.

Comparing the cross-section macrographs of both welds, displayed in Figs. 3b and 4b, for copper etching, and in Figs. 3c and 4c, for aluminium etching, important differences in the structure and morphology of the bonding area, where the top and bottom materials interact, can also be observed. Fig. 3b and c, which display the cross-section of the W5 weld, show that the Al–Cu interaction zone of this weld is restricted to the pin influence zone, where a very fine recrystallized grain structure is discernible for both base materials. Very small evidence of material stirred by the shoulder can be observed at the top of the weld in Fig. 3b, indicating that the shoulder influence zone was restricted to the top surface of the copper plate. The totally inefficient mixing, between aluminium and copper, gave rise to a large discontinuity between both base materials, preventing the effective joining of the plates. Actually, according to Fig. 3, coupling between the two materials only occurred at the advancing side of the tool where the aluminium was pushed upward, into the copper plate.

The cross-section macrographs of the W6 weld are shown in Fig. 4b and c. From the pictures, it can be concluded that the Cu/Al

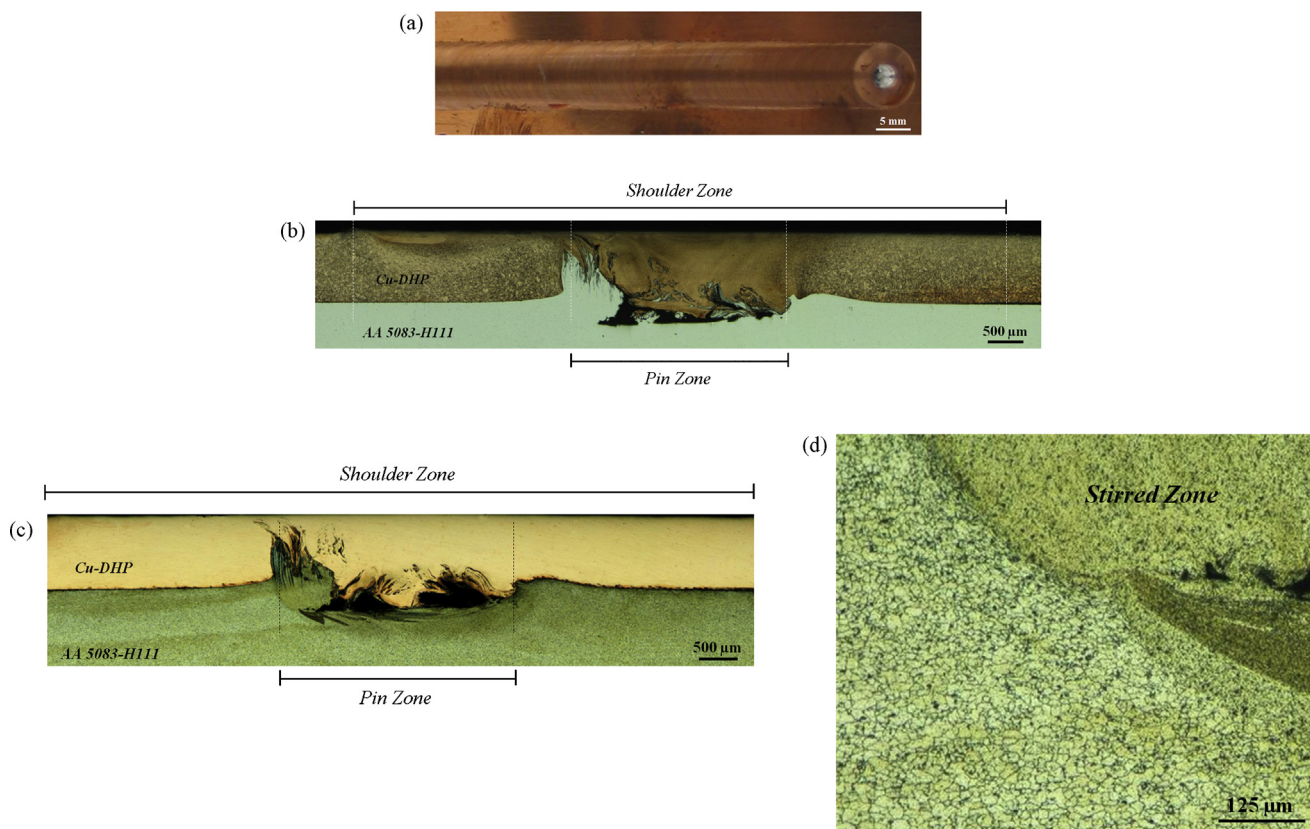


Fig. 3. Surface photograph (a); copper (b) and aluminium (c) etched cross-section macrographs and micrograph of the aluminium stirred zone (d) of the W5 weld.

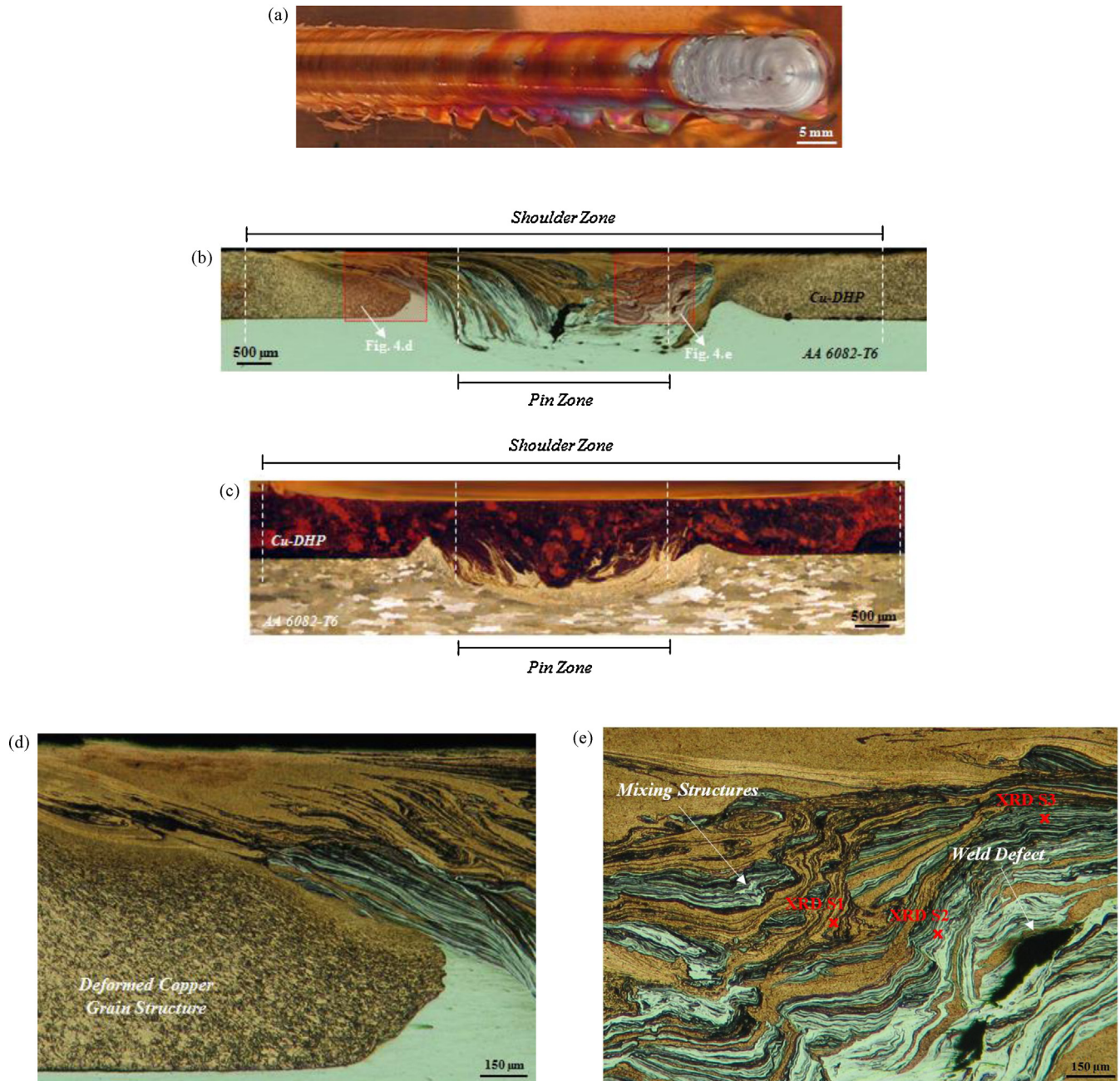


Fig. 4. Surface photograph (a); copper (b) and aluminium (c) etched cross-section macrographs and micrographs of the under shoulder copper structure (d) and of the mixing structures (e) of the W6 weld.

interaction volume for the W6 weld is significantly larger than that observed for the W5 weld. The picture in Fig. 4b also shows the presence of a well-defined shoulder influenced zone, encompassing the entire copper plate's thickness. This is also enhanced in Fig. 4d where deformed copper grains are discernible across the entire plate thickness. This enables to conclude that, under the same axial loading conditions, a larger amount of copper was dragged by the shoulder for the W6 weld than for the W5 weld. In good agreement with this, as illustrated in Fig. 4e, strong base materials interaction took place during W6 welding, resulting in the formation of mixing structures with morphology similar to those observed by Galvão et al. (2011) and Galvão et al. (2012) in Al–Cu friction stir butt welding. In fact, a complex mixing structure composed of copper and aluminium intercalated with lamellae of material morphologically

different of both base materials, which, according to these authors, have intermetallic-rich phase composition, is discernible in Fig. 4e.

However, in spite of a more efficient base materials mixing than in W5 welding, which points to a stronger interaction between both base materials, some internal defects were also observed for the W6 weld, specifically, micro-discontinuities embedded in the mixing structures of Fig. 4e. It is important to stress that these defects, besides presenting different morphology, are significantly smaller than those observed for the W5 weld. Non-uniform base materials mixing, which should result in the appearance of small discontinuities, as well as the strong brittleness of new Al–Cu phases, formed during welding, should have some influence on material flow, giving rise to this type of defects. According to Abdollah-Zadeh et al. (2008) and Saeid et al. (2010), cracking incidence in

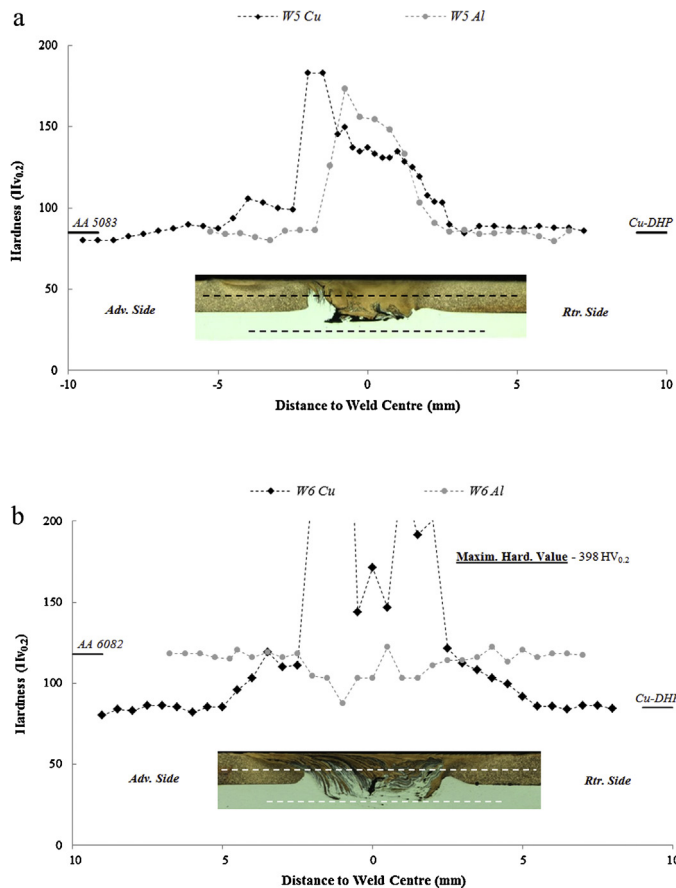


Fig. 5. Hardness profiles registered across the transverse cross-section of the W5 (a) and W6 (b) welds.

intermetallic-rich zones is one of the main causes for the premature failure of dissimilar Al–Cu friction stir welds. This way, it can be concluded that stronger base materials mixing during dissimilar Al–Cu welding does not necessarily mean sound joining.

Fig. 5 shows hardness profiles registered across the transverse sections of W5 (Fig. 5a) and W6 (Fig. 5b) welds. Each graph shows the results of hardness measurements performed along horizontal planes located in the top (copper) and bottom (aluminium) plates, as illustrated by the horizontal lines plotted in the cross-section pictures included in the figure. The average hardness of the base materials is also indicated in the graphs by short lines, located at each side of the hardness profiles. According to the figures, whereas for the W5 weld an important increase in hardness was registered for both the AA 5083 (W5 Al) and copper (W5 Cu) stirred zones, for

the W6 weld, the hardness increase was restricted to the upper copper layer (W6 Cu), being registered a smooth hardness decrease in the stirred AA 6082 aluminium alloy (W6 Al). For the W5 weld, further hardness measurements, performed closer to the stirred Al–Cu interface ($\sim 125 \mu\text{m}$ from the bonding discontinuity), as illustrated in Fig. 6, allowed observing the existence of an important hardness gradient inside the AA 5083 stirred volume. The hardness values measured in this zone, which range from $158 \text{ HV}_{0.2}$ to $215 \text{ HV}_{0.2}$, are higher than those of the W5 Al hardness profile in Fig. 5a and much higher than the hardness values reported by Hirata et al. (2007), El-Danaf et al. (2010) and Tronci et al. (2011), in similar AA 5083 friction stir welding/processing, and by Bisadi et al. (2013), in dissimilar AA 5083/copper FSW.

Two main factors can be related to the very important, and non-expectable, hardness increase inside the stirred volume of the W5 weld: one is the intense grain refinement which can be noticed inside the stirred volumes displayed in Fig. 3b–d, the other is the formation of new Al–Cu phases, either solid solution phases or intermetallic compounds, inside the stirred volume, as previously reported by Ouyang et al. (2006) and Galvão et al. (2011). The same phenomena should be associated with the hardness increase registered in the upper copper layer of the W6 weld. In opposition to this, the hardness decrease registered inside the AA 6082 stirred volume is undoubtedly related to the heat-treatable nature of this alloy. As well-documented in previous studies, such as in Svensson et al. (2000), the hardness of this material is determined by the size and dispersion of strengthening precipitates rather than by the grain size. The dissolution of strengthening phases in the stirred zone and coarsening of strengthening particles in the heat affected zone are the main causes for the hardness losses in this alloy.

In order to understand the sharp hardness increase inside the stirred volumes of the W5 and W6 welds, XRD analyses were accomplished enabling to determine the phase content in the highest hardness zones of both welds. For the W5 weld, the area analysed corresponded to the refined aluminium layer, in the vicinity of the Al–Cu interface (see S1, S2 and S3 points in Fig. 6). For the W6 weld, the area analysed was located inside the stirred/mixing material region (see S1, S2 and S3 points in Fig. 4e). The diffractograms obtained for the W5 and W6 welds are displayed in Fig. 7. According to the diffractogram corresponding to the W5 weld (Fig. 7a), the only phase detected in the area analysed was f.c.c. Al. In order to complement the XRD results for the W5 weld, the elemental chemical composition of the refined aluminium layer was also investigated by performing electron probe microanalysis (see EPMA analysis zone in Fig. 6). From Fig. 8, where the results of this analysis are displayed, it can be concluded that only Al and small amounts of Mg and Mn, which are the main alloy elements of the AA 5083 alloy, were identified in this zone, which is in good agreement with the XRD results. In this way, it is possible to conclude that the formation of new Al–Cu intermetallic phases during welding is not on the

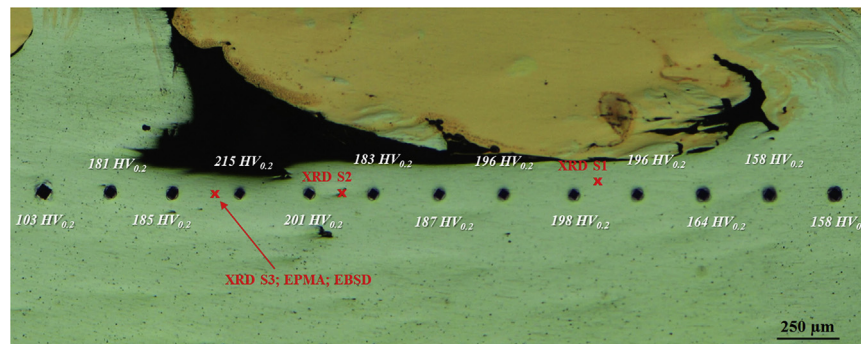


Fig. 6. Hardness values registered in the aluminium stirred region of the W5 weld, in the vicinity of the Al–Cu interface.

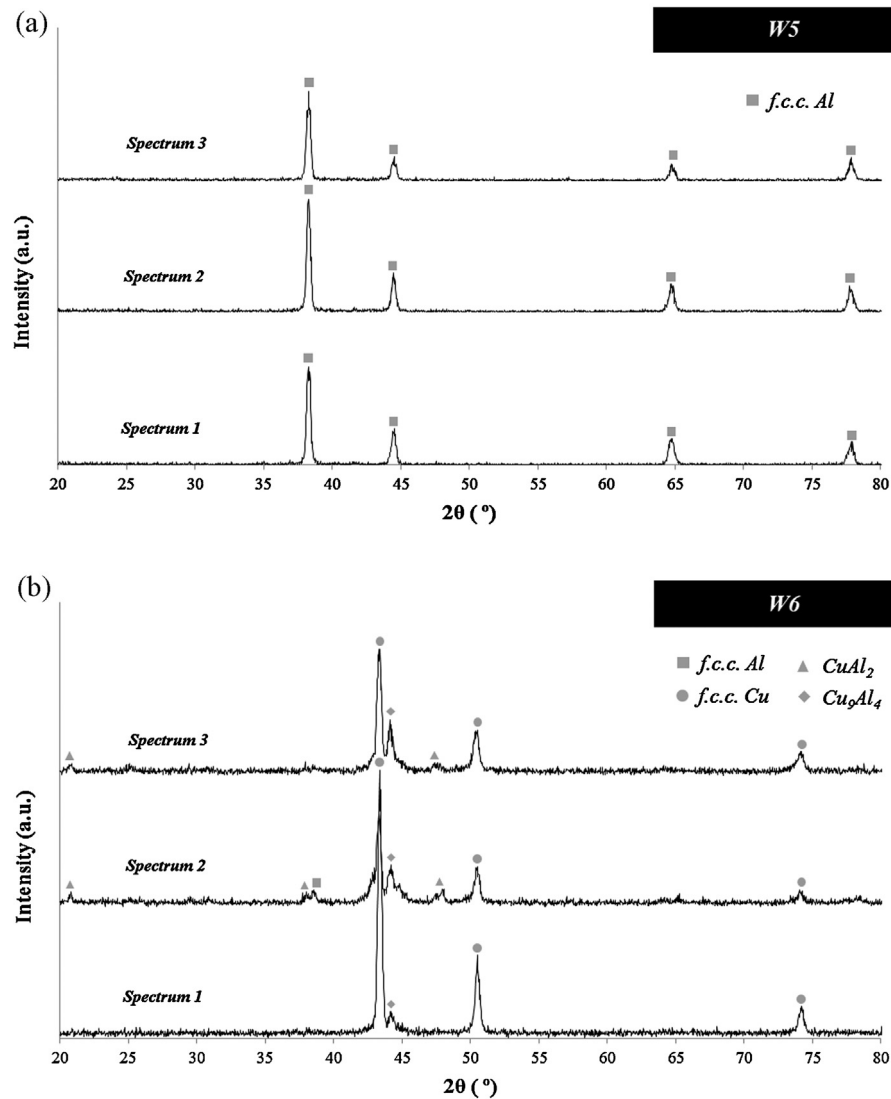


Fig. 7. Results of the XRD inspection carried out in the stirred zone of the W5 (a) and W6 (b) welds.

basis of the strong hardness increase (from 85 HV_{0.2} to 215 HV_{0.2}) registered in the refined aluminium layer. On the other hand, for the W6 weld (Fig. 7b), for which intense material mixing inside the stirred volume can be observed in Fig. 4, and very high hardness values were also registered (~400 HV_{0.2}), the XRD analysis enabled to identify the presence of important amounts of Cu₉Al₄ and small amounts of CuAl₂, which are responsible for the hardness increase.

4. Discussion

4.1. Influence of the aluminium alloy type on the welding results

Since both weld types analysed in this work were carried out under the same welding conditions, a strong influence of aluminium alloys type on welding results has to be pointed. Actually, Leitão et al. (2012a,b) have already addressed the influence of the markedly different mechanical behaviours of the AA 5083 and the AA 6082 aluminium alloys, at high temperature and strain rates, on the friction stir weldability of both alloys. According to these authors, whereas the AA 6082 aluminium alloy experiences strong softening with plastic deformation at increasing temperatures, which is traduced by a strong decrease of the flow stresses of the material with plastic deformation, the AA 5083 alloy presents,

at high temperatures, steady flow stress behaviour. As a result of this, under the same axial load during FSW, the higher thermal softening experienced by the AA 6082 alloy led to further submerging of the tool during welding, relative to the 5083 alloy, which resulted in the strong deepening and massive flash formation observed at the surface of the W6 weld (Fig. 4a). The higher tool submerging during AA 6082/copper-DHP welding also resulted in increased amounts of copper and aluminium being dragged by the shoulder and the pin, respectively, into the shear layer at each tool revolution. The strong pin-governed base materials mixing at the shear layer resulted in the formation of the mixing structures observed in the stirred zone of the W6 weld (Fig. 4e). As opposed to this, for the W5 weld, the significantly smaller volume of copper dragged by the tool, at each revolution, as well as the less efficient material dragging promoted by the pin in the AA 5083 alloy, prevented strong base materials interaction in the shear layer, which resulted in the formation of a discontinuous aluminium/copper interface in the stirred zone.

4.2. Microstructural evolution of the AA 5083 aluminium alloy during welding

Hardness values in the range of 200 HV_{0.2} were registered in the refined aluminium region of the W5 weld. Taking into account

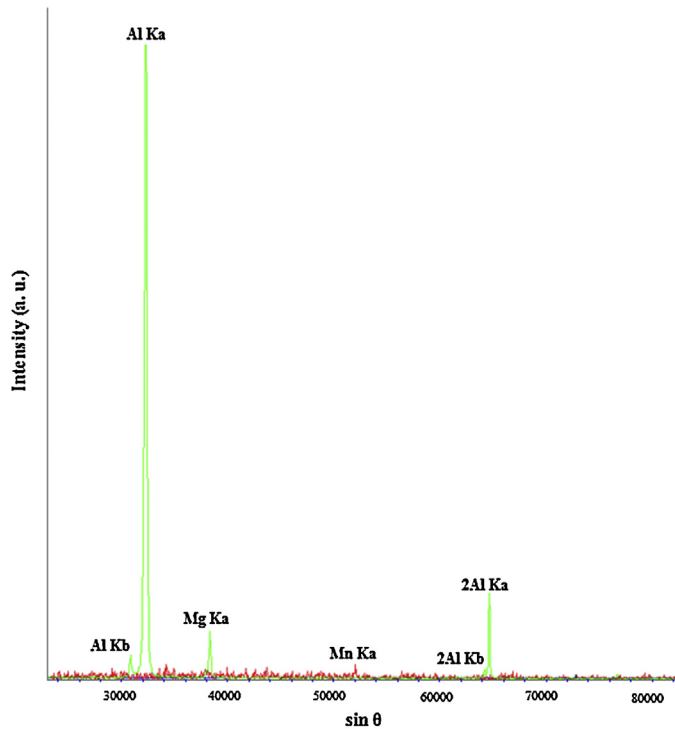


Fig. 8. Qualitative chemical analysis (EPMA) carried out in the stirred aluminium region of the W5 weld, in the vicinity of the Al–Cu interface.

that, according to Figs. 7a and 8, no Al–Cu phases were formed in that zone, this hardness increase may be considered surprisingly high. In order to understand this phenomenon, a deep TEM and EBSD-based microstructural study of the W5 weld was performed.

Results of the TEM analysis carried out in the stirred aluminium region of the W5 weld, where the hardness profile of Fig. 5a was registered, are illustrated in Fig. 9a. It can be observed that equiaxed submicron sized grains, with well-defined grain boundaries and low dislocations density, compose the microstructure of the stirred aluminium region. A histogram representing the grain

size distribution in this zone, plotted after performing hundreds of grain measurements over several TEM micrographs, is illustrated in Fig. 9b. The histogram shows an average grain size of 325 nm (± 90 nm), with most of the grains ranging between 150 nm and 450 nm. Previous metallographic analysis (Fig. 3d) enabled to determine an average grain size of 24 μm for the AA 5083 base material. The dynamic recrystallization taking place during FSW promoted the formation of an ultrafine-grained microstructure reported in Fig. 9.

The microstructure of the stirred aluminium layer was also studied by EBSD. Fig. 10 illustrates EBSD patterns acquired in two different zones of the W5 weld, i.e., in the hard aluminium layer (Fig. 10a) and in the AA 5083 base material (Fig. 10b). Important differences can be observed by comparing both pictures. Effectively, contrary to that observed in the base material electron backscatter patterns (EBSPs), patterns overlapping can be observed in Fig. 10a, which corresponds to the analysis carried out in the stirred zone. According to Maitland and Sitzman (2007), the overlapping phenomenon takes place at grain boundaries when the electron beam diameter is large enough to produce EBSPs from two grains simultaneously. Since the achievable resolution of EBSD for aluminium is typically ~ 50 nm (Humphreys, 2004), patterns overlapping should indicate the presence of nano grains in the hard aluminium layer, with a grain size value in the range of the technique resolution. This value is about seven times lower than the TEM-based grain size. Effectively, the EBSD analysis was performed in an aluminium layer located in the vicinity of the Al/Cu discontinuity (see EBSD analysis done in Fig. 6), contrary to the TEM analysis, which was carried out at middle thickness of the aluminium stirred region. The grain size differences point to the existence of a grain size gradient across the thickness of the stirred zone, which is in good agreement with the hardness results shown in Figs. 5 and 6. The quite higher grain refinement and hardness increase in a very thin aluminium layer in the vicinity of the materials discontinuity are easily explained by the length of the tool pin used to produce the joints. In fact, during welding, the pin, whose length is 1 mm, i.e., the thickness of the top copper plate, performed tangentially to the superficial layer of the bottom aluminium plate, in which a stronger stirring action was promoted. As the rate of nucleation of new grains is proportional to the rate of plastic deformation, more nucleation points are formed

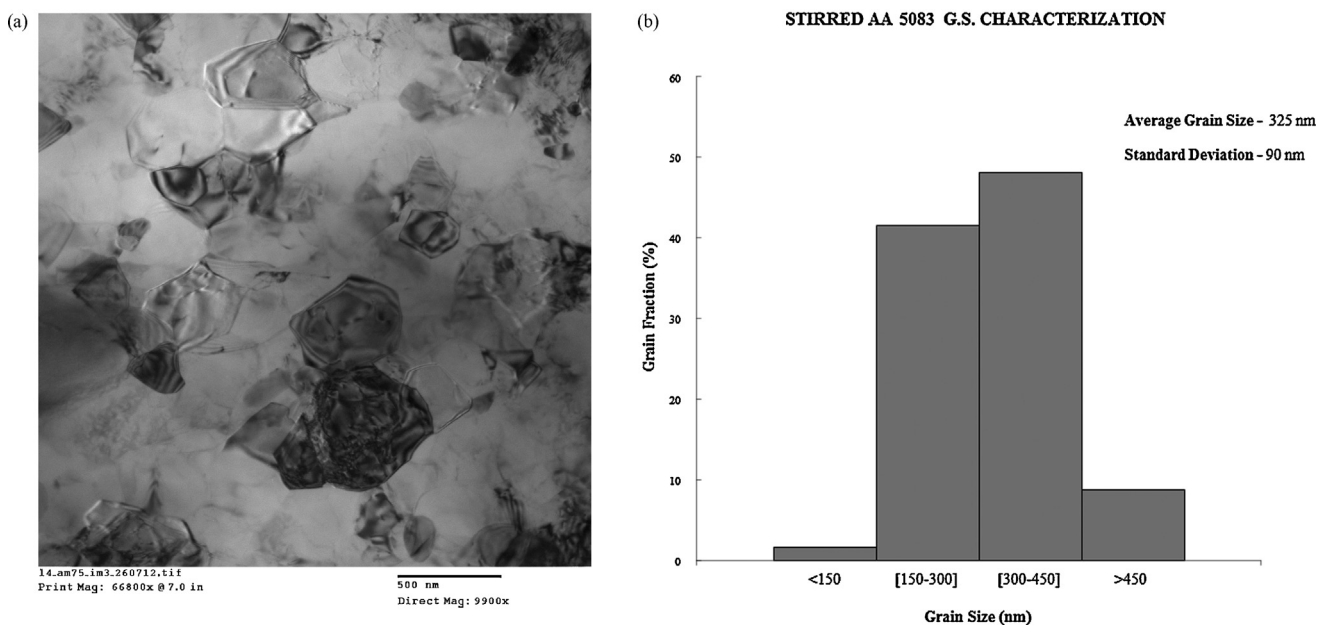


Fig. 9. TEM micrograph registered in the stirred aluminium region of the W5 weld (a) and the grain size distribution in that zone (b).

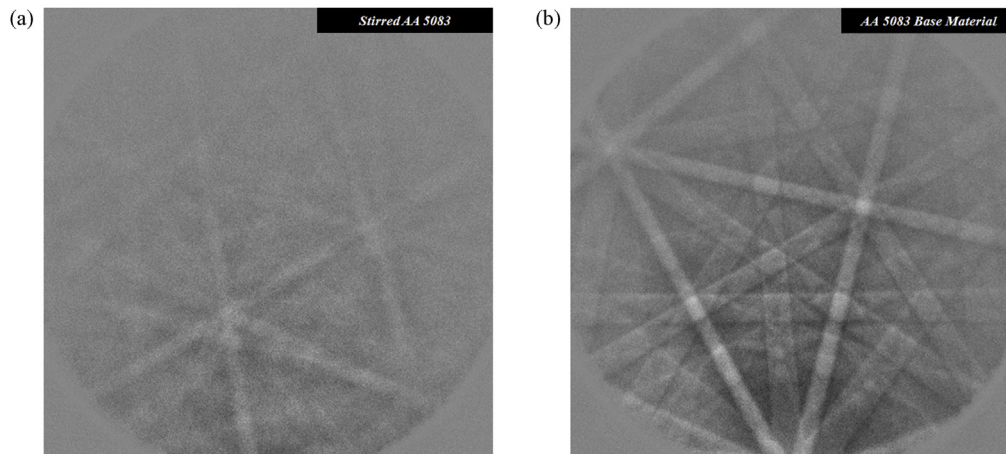


Fig. 10. EBSD patterns acquired in the stirred aluminium layer of the W5 weld, in the vicinity of the Al–Cu interface (a), and in the AA 5083 base material (b).

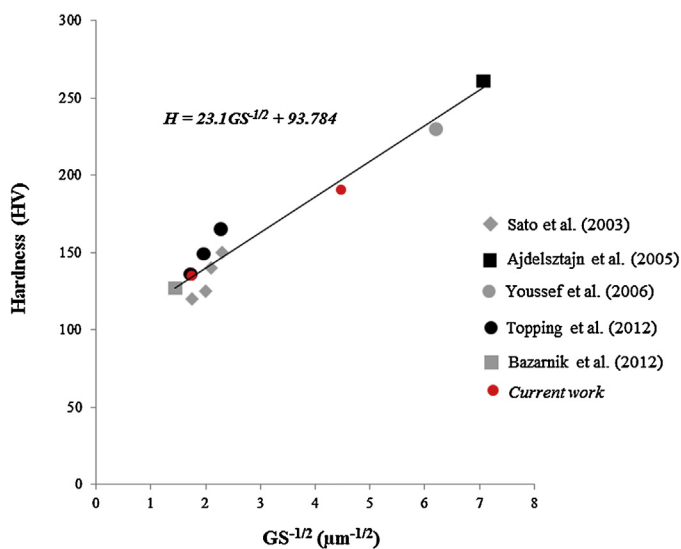


Fig. 11. Hall–Petch relationship for ultra-fine grained AA 5083 aluminium alloy. See refs. (Ajdelsztajn et al., 2005, Bazarnik et al., 2012, Sato et al., 2003, Topping et al., 2012 and Youssef et al., 2006).

and, consequently, less grain growth took place in this zone, giving rise to stronger grain refinement and hardness increase.

The improvement of the AA 5083 aluminium alloy mechanical properties, by creating submicrometer or nanometric grain structures, has already been explored in several researches from other authors who used powder metallurgy and/or severe plastic deformation techniques (combined or not with friction stir processing) to obtain fine grained structures. Results from some of these studies are resumed in Fig. 11, in which the AA 5083 hardness (HV) is plotted against the reciprocal of the square root of the grain size ($\mu\text{m}^{-1/2}$). The Hall–Petch equation was also fitted to the bibliographical results. Results from current work, namely, the average hardness values measured in the vicinity of the Al–Cu interface (190 HV_{0.2}) and some hundreds of micrometres below, across the W5 Al line displayed in Fig. 5a (135 HV_{0.2}), were also included in the graph. From the figure it can be observed that the grain size inside the AA5083 stirred volume of the W5 weld, obtained using elementary FSW procedures, is of the same magnitude of that obtained by other authors under other severe plastic deformation conditions.

The ultra-refined microstructure of the friction stir welded AA 5083 aluminium alloy, which resulted in an impressive hardness

increase in the stirred zone of the W5 weld, is indicative of a very small thermal-activated grain growth after dynamic recrystallization. According to Cui et al. (2009), tool size and rotation/travel speed ratio have great influence on the grain size of the friction stir processed microstructures, which decreases for decreasing values of these parameters as a result of the lower heat input during welding. The rotation/traverse speed ratio used in present work is not significantly lower than that tested by Hirata et al. (2007), El-Danaf et al. (2010), Tronci et al. (2011) and Bisadi et al. (2013) in AA 5083 or AA 5083/copper–DHP friction stir welding/processing studies, for which significantly coarser and softer microstructures were achieved. However, the tool used to produce the welds is significantly smaller than the tools usually reported in most of these works. According to Ma and Mishra (2005), lower values of tool shoulder and pin reduce the thermal input significantly because the decrease in the contact area between the tool and workpiece and the decrease in the linear surface velocity of the tool. This way, it can be concluded that the very small tool used in present work, although does not have allowed a suitable material flow during welding, which resulted in the formation of important defects at the Al–Cu interface, promoted an impressive hardness increase in the aluminium alloy due to the formation of ultra-refined microstructure in this material. This conclusion can be the starting point for future researches focused on the production of sound AA 5083/Cu–DHP friction stir lap welds with improved mechanical properties. Combining materials' mechanical enhancement obtained in this study with proper friction stir welding conditions, which can be achieved by studying a larger range of welding parameters, is an attractive challenge for future works. Specifically, the production of mechanically enhanced Al/Cu clad components, which combine copper's thermal and electrical properties with aluminium's low specific weight and cost, by performing parallel friction welding passes all along the workpiece surface is a very interesting topic to be investigated.

5. Conclusions

The influence of aluminium alloy properties on Al/Cu friction stir weldability was analysed in this study for a specific set of welding parameters. The following conclusions can be drawn:

- The different plastic properties of the AA 5083 and AA 6082 aluminium alloys, at high temperature and strain rates, have an important effect on the metallurgical and material flow

phenomena taking place during Al/Cu welding and, consequently, on the final properties of the welds;

- Whereas the AA 5083/copper-DHP welds presented excellent surface finishing, but highly defective Al/Cu interfaces, without any signs of base materials interaction, the AA 6082/copper-DHP welds displayed poor surface properties, but strong base materials mixing in the stirred zone;
- For the AA 5083/copper-DHP welds, an impressive hardness increase was registered in the aluminium part of the weld due to the formation of an ultra-refined microstructure;
- The very small tool used in present work played a decisive role in the microstructural evolution of the AA 5083-H111 aluminium alloy during welding.

Acknowledgements

This research is sponsored by FEDER funds through the program COMPETE and by National funds through FCT, under the project PEst-C/EME/UI0285/2011.

References

- Abdollah-Zadeh, A., Saeid, T., Sazgari, B., 2008. Microstructural and mechanical properties of friction stir welded aluminium/copper lap joints. *Journal of Alloys and Compounds* 460, 535–538.
- Ajdelsztajn, L., Jodoin, B., Kim, G.E., Schoenung, J.M., 2005. Cold spray deposition aluminium alloys. *Metallurgical and Materials Transactions A* 36A, 657–666.
- Akbari, M., Abdi Behnagh, R., Dadvand, A., 2012. Effect of materials position on friction stir lap welding of Al to Cu. *Science and Technology of Welding and Joining* 17, 581–588.
- Bazarnik, P., Lewandowska, M., Andrzejczuk, M., Kurzydowski, K.J., 2012. The strength and thermal stability of Al–5Mg alloys nano-engineered using methods of metal forming. *Materials Science and Engineering A* 556, 134–139.
- Bisadi, H., Tavakoli, A., Sangsarak, M.T., Sangsarak, K.T., 2013. The influences of rotational and welding speeds on microstructures and mechanical properties of friction stir welded Al5083 and commercially pure copper sheets lap joints. *Materials & Design* 43, 80–88.
- Çam, G., 2011. Friction stir welded structural materials: beyond Al-alloys. *International Materials Reviews* 56, 1–48.
- Cui, G.R., Ma, Z.Y., Li, S.X., 2009. The origin of non-uniform microstructure and its effects on the mechanical properties of a friction stir processed Al–Mg alloy. *Acta Materialia* 57, 5718–5729.
- El-Danaf, E.A., El-Rayes, M.M., Soliman, M.S., 2010. Friction stir processing: an effective technique to refine grain structure and enhance ductility. *Materials Design* 31, 1231–1236.
- Elrefaey, A., Takahashi, M., Ikeuchi, K., 2004. Microstructure of aluminium/copper lap joint by friction stir welding and its performance. *Journal of High Temperature Society* 30, 286–292.
- Firouzdor, V., Kou, S., 2012. Al-to-Cu friction stir lap welding. *Metallurgical and Materials Transactions A* 43A, 303–315.
- Galvão, I., Leal, R.M., Rodrigues, D.M., Loureiro, A., 2013. Influence of tool shoulder geometry on properties of friction stir welds in thin copper sheets. *Journal of Materials Processing Technology* 213, 129–135.
- Galvão, I., Oliveira, J.C., Loureiro, A., Rodrigues, D.M., 2011. Formation and distribution of brittle structures in friction stir welding of aluminium and copper: influence of process parameters. *Science and Technology of Welding and Joining* 16, 681–689.
- Galvão, I., Oliveira, J.C., Loureiro, A., Rodrigues, D.M., 2012. Formation and distribution of brittle structures in friction stir welding of aluminium and copper: influence of shoulder geometry. *Intermetallics* 22, 122–128.
- Hirata, T., Oguri, T., Hagino, H., Tanaka, T., Chung, S.W., Takigawa, Y., Higashi, K., 2007. Influence of friction stir welding parameters on grain size and formability in 5083 aluminium alloy. *Materials Science and Engineering A* 456, 344–349.
- Humphreys, F.J., 2004. Characterisation of fine-scale microstructures by electron backscatter diffraction (EBSD). *Scripta Materialia* 51, 771–776.
- Leitão, C., Loureiro, A., Rodrigues, D.M., 2011. Influence of Base Material Properties and Process Parameters on Defect Formation during FSW. In: Koçak, M. (Ed.), *Proceedings of the International Congress on Advances in Welding Science and Technology for Construction, Energy & Transportation Systems*. Antalya, Turkey, pp. 177–184.
- Leitão, C., Louro, R., Rodrigues, D.M., 2012a. Analysis of high temperature plastic behaviour and its relation with weldability in friction stir welding for aluminium alloys AA5083-H111 and AA6082-T6. *Materials Design* 37, 402–409.
- Leitão, C., Louro, R., Rodrigues, D.M., 2012b. Using torque sensitivity analysis in accessing friction stir welding/processing conditions. *Journal of Materials Processing Technology* 212, 2051–2057.
- Ma, Z.Y., Mishra, R.S., 2005. Development of ultrafine-grained microstructure and low temperature (0.48 T_m) superplasticity in friction stir processed Al–Mg–Zr. *Scripta Materialia* 53, 75–80.
- Maitland, T., Sitzman, S., 2007. Electron backscatter diffraction (EBSD) technique and materials characterization examples. In: Zhou, W., Wang, Z.L. (Eds.), *Scanning Microscopy for Nanotechnology*. Springer, New York, pp. 41–75.
- Ouyang, J., Yarrapareddy, E., Kovacevic, R., 2006. Microstructural evolution in the friction stir welded 6061 aluminium alloy (T6-temper condition) to copper. *Journal of Materials Processing Technology* 172, 110–122.
- Saeid, T., Abdollah-Zadeh, A., Sazgari, B., 2010. Weldability and mechanical properties of dissimilar aluminium – copper lap joints made by friction stir welding. *Journal of Alloys and Compounds* 490, 652–655.
- Sato, Y.S., Urata, M., Kokawa, H., Ikeda, K., 2003. Hall–Petch relationship in friction stir welds of equal channel angular-pressed aluminium alloys. *Materials Science and Engineering A* 354, 298–305.
- Svensson, L.E., Karlsson, L., Larsson, H., Karlsson, B., Fazzini, M., Karlsson, J., 2000. Microstructure and mechanical properties of friction stir welded aluminium alloys with special reference to AA 5083 and AA 6082. *Science and Technology of Welding and Joining* 5, 285–296.
- Topping, T.D., Ahn, B., Li, Y., Nutt, S.R., Lavernia, E.J., 2012. Influence of process parameters on the mechanical behavior of an ultrafine-grained Al alloy. *Metallurgical and Materials Transactions A* 43, 505–519.
- Tronci, A., McKenzie, R., Leal, R.M., Rodrigues, D.M., 2011. Microstructural and mechanical characterisation of 5XXX-H111 friction stir welded tailored blanks. *Science and Technology of Welding and Joining* 16, 433–439.
- Xue, P., Ni, D.R., Wang, D., Xiao, B.L., Ma, Z.Y., 2011. Achieving high property friction stir welded aluminium/copper lap joint at low heat input. *Science and Technology of Welding and Joining* 16, 657–661.
- Youssef, K.M., Scattergood, R.O., Murty, K.L., Koch, C.C., 2006. Nanocrystalline Al–Mg alloy with ultrahigh strength and good ductility. *Scripta Materialia* 54, 251–256.